# COMPUTATION OF THE CAPACITANCE MATRIX FOR DIELECTRIC-COATED WIRES

Joseph C. Clements, et al

Kentucky University

Prepared for:

Rome Air Development Center

March 1974

UNCLASSIFIED

SECURITY CLASSIFICATION OF THIS PAGE *(When Data Entered)*

| REPORT DOCUMENTATION PAGE | | READ INSTRUCTIONS BEFORE COMPLETING FORM |
|---|---|---|
| 1. REPORT NUMBER<br>RADC-TR-74-59 | 2. GOVT ACCESSION NO. | 3. RECIPIENT'S CATALOG NUMBER<br>AD 778948 |
| 4. TITLE *(and Subtitle)*<br>COMPUTATION OF THE CAPACITANCE MATRIX FOR DIELECTRIC-COATED WIRES | | 5. TYPE OF REPORT & PERIOD COVERED<br>Phase Report<br>6. PERFORMING ORG. REPORT NUMBER<br>N/A |
| 7. AUTHOR(s)<br>Joseph C. Clements<br>Clayton R. Paul | | 8. CONTRACT OR GRANT NUMBER(s)<br>F30602-72-C-0418 |
| 9. PERFORMING ORGANIZATION NAME AND ADDRESS<br>University of Kentucky<br>Lexington KY 40506 | | 10. PROGRAM ELEMENT, PROJECT, TASK AREA & WORK UNIT NUMBERS<br>95670002 |
| 11. CONTROLLING OFFICE NAME AND ADDRESS<br>Rome Air Development Center (RBC)<br>Griffiss Air Force Base, New York 13441 | | 12. REPORT DATE<br>March 1974<br>13. NUMBER OF PAGES<br>163 |
| 14. MONITORING AGENCY NAME & ADDRESS *(if different from Controlling Office)*<br>Same | | 15. SECURITY CLASS. *(of this report)*<br>UNCLASSIFIED<br>15a. DECLASSIFICATION DOWNGRADING SCHEDULE<br>N/A |

16. DISTRIBUTION STATEMENT *(of this Report)*

Approved for public release; distribution unlimited.

17. DISTRIBUTION STATEMENT *(of the abstract entered in Block 20, if different from Report)*

Same

18. SUPPLEMENTARY NOTES

RADC Post-doctoral Coordinator: Dr. W. W. Everett, Jr. (RBC)

19. KEY WORDS *(Continue on reverse side if necessary and identify by block number)*

Wire-Wire Coupling
Dielectric-Coated Wires-Coupling



20. ABSTRACT *(Continue on reverse side if necessary and identify by block number)*

A matrix inversion technique is presented which may be used to compute the capacitance matrix of a system of bare or dielectric-coated parallel cylindrical wires. Systems of cylindrical wires with dielectric-coating have heretofore been untreated while bare wire systems have received minimal attention. A Fourier series expansion is used to represent the charge distribution over the surfaces of the boundaries. The boundary conditions are enforced at discrete points by requiring the potential to be constant along conductor boundaries

DD FORM 1 JAN 73 1473 EDITION OF 1 NOV 65 IS OBSOLETE

UNCLASSIFIED

SECURITY CLASSIFICATION OF THIS PAGE *(When Data Entered)*

20. (Continued)

and the normal component of the displacement vector to be continuous across dielectric boundaries. A matrix equation relating to the Fourier coefficients to the boundary conditions is obtained and then inverted to yield an expression which can be reduced to the relationship defining the multiwire capacitance matrix. Emphasis is placed upon an accurate determination of the charge distribution since the fields are easily determined once the charge distribution is known. Some specific problems are solved with very accurate results being attained for widely spaced wires and good accuracy being attained for wires closely spaced. Finally, relevant applications to network problems and extra-high voltage (EHV) power transmission are cited.

# COMPUTATION OF THE CAPACITANCE MATRIX FOR DIELECTRIC-COATED WIRES

Joseph C. Clements
Clayton R. Paul

University of Kentucky

## FOREWORD

The Post-Doctoral Program at Rome Air Development Center is pursued via Project 9567 under the direction of Dr. W. W. Everett, Jr. The Post-Doctoral Program is a cooperative venture between RADC and the participating universities: Syracuse University (Department of Electrical and Computer Engineering), the U.S. Air Force Academy (Department of Electrical Engineerint), Cornell University (School of Electrical Engineering), Purdue University (School of Electrical Engineering), University of Kentucky (Department of Electrical Engineering), Georgia Institute of Technology (School of Electrical Engineering), Clarkson College of Technology (Department of Electrical Engineering), State University of New York at Buffalo (Department of Electrical Engineering), North Carolina State University (Department of Electrical Engineering), Florida Technological University (Department of Electrical Engineering), Florida Institute of Technology (College of Engineering), Air Force Institute of Technology (Department of Electrical Engineering), and the University of Adelaide (Department of Electrical Engineering) in South Australia. The Post-Doctoral Program provides, via contract, the opportunity for faculty and visiting faculty at the participating universities to spend a year full-time on exploratory development and operational problem-solving efforts with the post-doctorals splitting their time between RADC (or the ultimate customer) and the educational institutions.

The Post-Doctoral Program is totally customer-funded with current projects being undertaken for Air Defense Command (NORAD), Air Force Communications Service, Federal Aviation Administration, Defense Communications Agency, Aeronautical Systems Division (AFSC), Aero-Propulsion Laboratory (AFSC), and Rome Air Development Center (AFSC). This particular effort was

funded under Project 4540 and managed by the RADC Electromagnetic Compatibility Branch.

Joseph C. Clements received the B.S.E.E. degree (1971) and the M.S.E.E. degree (1973) both from the University of Kentucky. He served as a Graduate Instructor at the University of Kentucky (1971-1973) teaching courses and laboratories in Electronics. His research interests are in the areas of Linear System Theory and Electromagnetics with emphasis on the numerical solution of distributed parameter networks.

Clayton R. Paul received the B.S.E.E. degree from The Citadel (1963), the M.S.E.E. degree from Georgia Institute of Technology (1974), and the Ph.D. degree from Purdue University (1970). He served as a graduate assistant (1963-64) and as an instructor (1964-65) on the faculty of Georgia Institute of Technology. As a graduate instructor at Purdue University (1965-1970) he taught courses in linear system theory, electrical circuits and electronics. From 1970-1971 he was a Post Doctoral Fellow with the Rome Air Development Center, Griffiss AFB, New York, working in the area of Electromagnetic Compatibility. His areas of research interests are in linear multivariable systems and electrical network theory with emphasis on distributed parameter networks and multiconductor transmission lines.

The authors wish to give a special acknowledgement to Professor Arlon T. Adams of Syracuse University for many helpful and enlightening discussions throughout the course of this research.

This report has been reviewed by the Office of Information, RADC and approved for release to the National Technical Information Service (NTIS).

This technical report has been reviewed and is approved.

APPROVED: Woodrow W. Everett Jr.

WOODROW W. EVERETT, JR.
Project Engineer:

APPROVED: Joseph J. Naresky

JOSEPH J. NARESKY
Chief, Reliability and Compatibility Division

FOR THE COMMANDER: Carlo P. Crocetti

CARLO P. CROCETTI
Chief, Plans Office

## ABSTRACT

The unintentional coupling of energy between wires in cable bundles which connect electronic subsystems is an important source of interference on aircraft, missles, and ground systems. The models presently used for predicting this wire coupled interference are the TEM mode transmission line models and inherent in the use of these types of models is the ability to determine the per unit length capacitance and inductance parameters. The predominant method of connecting electronic subsystems for many years uses stranded conductors which are coated with a dielectric insulation and grouped together into large, densely packed cable bundles. Flexible flat pack and woven cable assemblies utilize closely coupled dielectric coated wires and are finding increased usage on modern avionics systems. It is therefore important to develop methods of computing the per unit length capacitance and inductance elements for closely coupled cylindrical wires having dielectric insulation since the transmission line models will be used in intrasystem compatibility prediction computer programs where experimental measurement of the parameters is either impractical or impossible. Formulation of these transmission line models is useless unless one can determine the per unit length parameters. A matrix inversion technique is presented for computing the capacitance matrix of a system of bare or dielectric coated parallel cylindrical wires. Systems of cylindrical wires with dielectric insulation have previously been untreated. In fact, the simplest problem of determining the per unit length capacitance of two circular conductors with dielectric insulation cannot be solved in closed form and has received no attention in the literature. A Fourier series expansion is used to represent the charge distribution over the surfaces of the boundaries. The boundary conditions are enforced at discrete points by requiring the potential to be constant along the conductor boundaries and the normal component of the displacement vector to be continuous across the dielectric boundaries. A matrix equation relating the Fourier coefficients to the boundary conditions is obtained and then inverted to yield the relationship defining the per unit length multiwire capacitance matrix.

TABLE OF CONTENTS

LIST OF FIGURES

# CHAPTER I

# INTRODUCTION

## 1.1 A Discussion of the Literature

In this text, the concepts of capacitance will be applied to systems of circular cylindrical conductors with and without dielectric coating. The existing literature on these systems is quite sparse except for the case of two infinitely long, non-insulated conductors - the capacitance of which has been known for quite some time and can be found in many undergraduate text books [1,2]. For the case of two bare

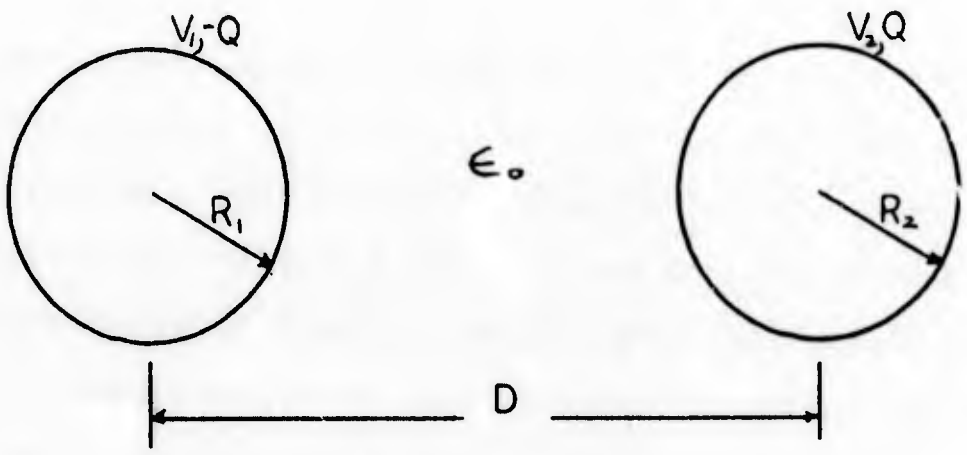


Fig. 1-1. -- Two conductor system.

wires in free space shown in Figure 1-1, Smythe [3] gives

$$C = \frac{Q}{V_1 - V_2} = \frac{2\pi\epsilon_0}{\cosh^{-1}((D^2 - R_1^2 - R_2^2/2R_1R_2))}, \qquad (1\text{-}1)$$

where C is the capacitance per unit length, $V_1$ and $V_2$ are the potentials of the conductors, and Q and -Q are the total charges on the conductors. With $R=R_1=R_2$, equation (1-1) reduces to

$$C = \frac{\pi\varepsilon_0}{\cosh^{-1}(D/2R)} \quad . \tag{1-2}$$

For more than two conductors the capacitance as defined by the ratio $Q/(V_1-V_2)$ for two wires cannot be applied. In this case the capacitance matrix is needed in order to describe the system. For three conductors the capacitance matrix cannot be obtained in closed form.

The determination of the capacitance matrix for microstrip transmission lines has received much attention in the literature [4-7]. In contrast, the determination of the capacitance matrix for parallel cylindrical wires has received only minimal attention. Recently, some papers [5,8-10] have appeared for multiple bare wire systems. However, the papers by Sarma [8,9] and Abou-Seada [10] focus upon the determination of the fields surrounding overhead transmission lines in order to predict the corona associated with extra-high voltage (EHV) power transmission. Kammler [5] briefly discussed the case of multiple bare wires between ground planes for use in microwave filters, but his emphasis is primarily upon strip line parameters. Boast [11] gives an approximate capacitance matrix for bare wires which are spaced widely enough to allow each wire to be replaced by a line charge at its center which is a very serious restriction for closely spaced wires.

This text will consider the determination of the capacitance matrix for the problems cited above [8-10], but primarily the goal here is to generalize the method obtained for bare wires to the more practical case of dielectric-coated wires which arise in the large bundled cables in missle and aircraft systems [12]. An accurate determination of this

matrix would be highly beneficial to the extensive frequency response analyses being done on these systems [13-15]. The relatively new flexible cable assemblies [16] also serve as an illustration of the application of this analysis; very few specifications have been published for these due to the lack of appropriate analytical techniques.

## 1.2 Capacitance and the Capacitance matrix

In Figure 1-2 are two infinitely long conductors, $C_1$ and $C_2$, in free space. Since the conductors are infinitely long the problem is two dimensional. Associated with $C_1$ and $C_2$ are their charges $Q_1$ and $Q_2$ and

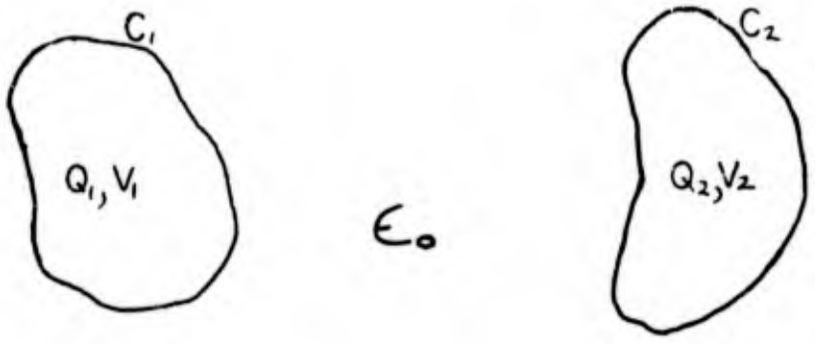


Fig. 1-2. -- Two conductors embedded in an infinite medium.

their potentials relative to infinity $V_1$ and $V_2$ respectively. In Section 1.1 where the two conductors were circular cylinders, $Q_1$ was equal in magnitude and opposite in sign to $Q_2$ and the capacitance was defined by the ratio

$$C = \frac{Q_1}{V_1 - V_2} \quad . \tag{1-3}$$

However, if $V_1$, $V_2$, $Q_1$ and $Q_2$ are considered to be aribtrary, then the system of Figure 1-2 is described by the relationship

$$\begin{bmatrix} Q_1 \\ Q_2 \end{bmatrix} = \begin{bmatrix} C_{11} & C_{12} \\ C_{12} & C_{22} \end{bmatrix} \begin{bmatrix} V_1 \\ V_2 \end{bmatrix} \tag{1-4}$$

where

$$\underline{c} = \begin{bmatrix} C_{11} & C_{12} \\ C_{12} & C_{22} \end{bmatrix} \tag{1-5}$$

is defined to be the capacitance matrix of the system. Setting $Q_1 = -Q_2$ in equation (1-4), the ratio of equation (1-3) becomes:

$$C = \frac{Q_1}{V_1 - V_2} = \frac{C_{11}C_{22} - C_{12}^2}{C_{11} + C_{22} + 2C_{12}} \quad . \tag{1-6}$$

In general, consider N conductors embedded in a medium consisting of essentially free space but having regions of linear, homogeneous, and isotropic dielectrics as shown in Figure 1-3. The solution for the

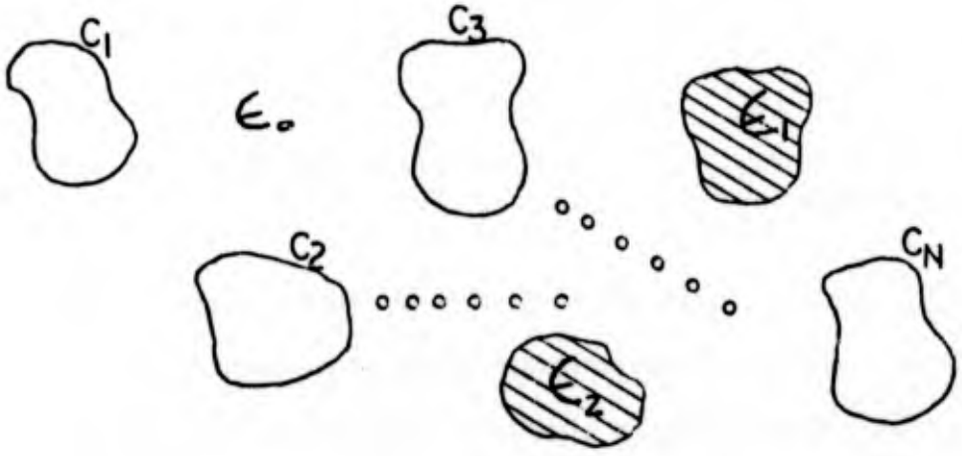


Fig. 1-3. -- N conductors in the presence of dielectric regions.

potential function $\phi$ exterior to the conductors is given by Laplace's equation $\Delta^2\phi = 0$ subject to the appropriate boundary conditions on the

conductor surfaces. The capacitance matrix for this system can be postulated from a consideration of linearity and uniqueness of the solutions of Laplace's equation. From the uniqueness theorem, two general propositions can be established [17]. These are:

(1) the field is uniquely specified everywhere from a knowledge of the potential on the surface of each conductor;

(2) the field is uniquely specified everywhere from a knowledge of the total charge on each conductor.

If, in Figure 1-3, a unit charge is placed on $C_1$ with $C_2 \rightarrow C_n$ left uncharged then by (2) the potential is everywhere specified including on the conductors; the potentials

$$p_{11}, p_{21}, \cdots p_{n1}$$

will result on $C_1 \rightarrow C_n$. Now, since Laplace's equation is linear, the property of homogeneity yields for a total charge $Q_1$ placed on $C_1$ the potentials

$$p_{11}Q_1, p_{21}Q_1, \cdots p_{n1}Q_1$$

on $C_1 \rightarrow C_n$. Similarly, if $Q_i$ is placed on $C_i$, then the potentials

$$p_{1i}Q_i, p_{2i}Q_i, \cdots p_{ni}Q_i$$

will result on $C_1 \rightarrow C_n$. Invoking the property of additivity, if $Q_1 \rightarrow Q_n$ are simultaneously placed on $C_1 \rightarrow C_n$ respectively, then the total potentials $V_1 \rightarrow V_n$ will become

$$\begin{bmatrix} V_1 \\ V_2 \\ \vdots \\ V_n \end{bmatrix} = \begin{bmatrix} p_{11} & p_{12} \cdots & p_{1n} \\ \vdots & & \\ & & \\ p_n & \cdots & p_{nn} \end{bmatrix} \begin{bmatrix} Q_1 \\ Q_2 \\ \vdots \\ Q_n \end{bmatrix} . \qquad (1\text{-}7)$$

The $p_{ij}$ terms are called the coefficients of potential and are purely geometrical quantities. Reciprocity relations [3] show that $p_{ji} = p_{ij}$, and thus, $\underset{\sim}{p}$ is a symmetric matrix.

The solution of equation (1-7) yields:

$$\begin{bmatrix} Q_1 \\ Q_2 \\ \cdot \\ \cdot \\ \cdot \\ Q_n \end{bmatrix} = \begin{bmatrix} c_{11} & c_{12} \cdots & c_{1n} \\ \cdot & & \cdot \\ \cdot & & \cdot \\ \cdot & & \cdot \\ \cdot & & \cdot \\ c_n & \cdots & c_{nn} \end{bmatrix} \begin{bmatrix} V_1 \\ V_2 \\ \cdot \\ \cdot \\ \cdot \\ V_n \end{bmatrix} \qquad (1\text{-}8)$$

where $\underset{\sim}{c} = \underset{\sim}{p}^{-1}$. $\underset{\sim}{c}$ is by definition the capacitance matrix of the system. The $c_{ij}(i=j)$ terms are called the coefficients of capacitance and the $c_{ij}(i\neq j)$ terms are called the coefficients of induction. Since $\underset{\sim}{p}$ is symmetric $\underset{\sim}{c}$ is also symmetric, and thus, $c_{ji}=c_{ij}$. As for the $p_{ij}$ terms, the $c_{ij}$ terms are also purely geometrical quantities.

## 1.3 Applications to Network Problems

In network problems [13-15] it is desirable to work with equivalent circuit representations. These can be deduced from equation (1-8). As an example consider the system of three conductors shown in Figure 1-4(a) for which the equivalent circuit representation of Figure 1-4(b) is desired. The relationship between the charges

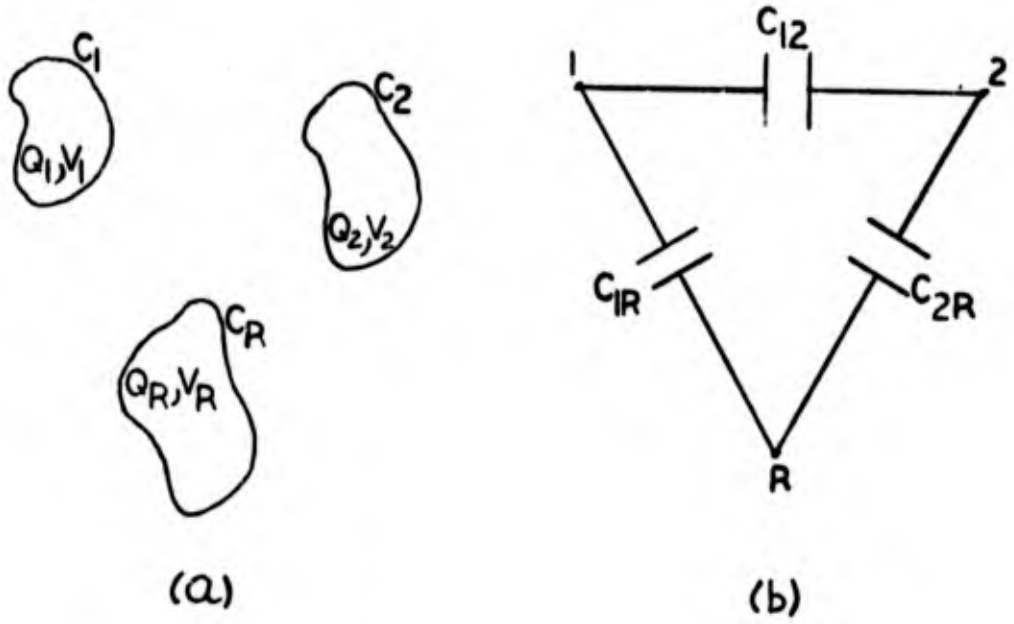


Fig. 1-4. -- (a) A three conductor system.
(b) Its equivalent circuit.

and the potentials of this system is:

$$\begin{bmatrix} Q_1 \\ Q_2 \\ Q_R \end{bmatrix} = \begin{bmatrix} c_{11} & c_{12} & c_{1R} \\ c_{12} & c_{22} & c_{2R} \\ c_{1R} & c_{2R} & c_{RR} \end{bmatrix} \begin{bmatrix} V_1 \\ V_2 \\ V_R \end{bmatrix} \qquad (1\text{-}9)$$

where $C_R$ has been randomly selected as the "0" potential reference conductor. (A practical example may have $C_R$ as a ground plane near $C_1$ and $C_2$). Rewriting equation (1-9) subject to $V_R=0$ gives

$$\begin{aligned} Q_1 &= c_{11}V_1 + c_{12}V_2 \\ Q_2 &= c_{12}V_1 + c_{22}V_2 \\ Q_3 &= c_{13}V_1 + c_{23}V_2. \end{aligned} \qquad (1\text{-}10)$$

Now, enforcing the condition appropriate to network problems that the sum of the charge in the system be equal to zero, equations (1-10) can be reduced to

$$\begin{aligned} Q_1 &= -(Q_2+Q_3) = -(c_{12}+c_{13})V_1 - (c_{22}+c_{23})V_2 \\ Q_2 &= -(Q_1+Q_3) = -(c_{11}+c_{13})V_1 - (c_{12}+c_{23})V_2 \end{aligned} \tag{1-11}$$

or

$$\begin{aligned} Q_1 &= c^*_{11}V_1 + c^*_{12}V_2 \\ Q_2 &= c^*_{12}V_1 + c^*_{22}V_2 \end{aligned} \tag{1-12}$$

where

$$\begin{aligned} c^*_{11} &= -(c_{12}+c_{13}) \\ c^*_{12} &= -(c_{22}+c_{23}) \\ c^*_{22} &= -(c_{12}+c_{23}) \,. \end{aligned} \tag{1-13}$$

As for a previous case reciprocity can be invoked to show that $c^*_{12} = c^*_{21}$. The final step is to write equation (1-12) in the form

$$\begin{aligned} Q_1 &= (c^*_{11}+c^*_{12})V_1 - c^*_{12}(V_1-V_2) \\ Q_2 &= -c^*_{12}(V_2-V_1) + (c^*_{22}+c^*_{12})V_2 . \end{aligned} \tag{1-14}$$

Letting

$$\begin{aligned} C_{1R} &= c^*_{11} + c^*_{12} \\ C_{12} &= -c^*_{12} \\ C_{2R} &= c^*_{22} + c^*_{12} \end{aligned} \tag{1-15}$$

equations (1-14) become:

$$\begin{aligned} Q_1 &= C_{1R}V_1 + C_{12}(V_1-V_2) \\ Q_2 &= C_{12}(V_2-V_1) + C_{2R}V_2 \end{aligned} \tag{1-16}$$

where $C_{1R}$, $C_{12}$, and $C_{2R}$ are the capacitances (sometimes called "direct" capacitances) shown in Figure 1-4(b).

In general, the above example can be extended to a system of N+1 conductors in which one conductor is chosen as a zero potential reference subsequent to the determination of the relationship

$$\begin{bmatrix} Q_1 \\ Q_2 \\ \vdots \\ Q_{n+1} \end{bmatrix} = \begin{bmatrix} C_{11} & \cdots & C_{1(n+1)} \\ \vdots & & \vdots \\ C_{(n+1)1} & \cdots & C_{(n+1)(n+1)} \end{bmatrix} \begin{bmatrix} V_1 \\ V_2 \\ \vdots \\ V_{n+1} \end{bmatrix} . \qquad (1\text{-}17)$$

By first using the condition appropriate to network problems that

$$\sum_{i=1}^{n+1} Q_i = 0 \qquad (1\text{-}18)$$

a set of N equations is generated by writing

$$Q_m = -\left( \sum_{\substack{j=1 \\ j \neq m}}^{n+1} \sum_{i=1}^{n} C_{ji} V_i \right) \qquad \begin{matrix} m=1,2,\ldots n+1 \\ m \neq \text{REFERENCE} \end{matrix} \qquad (1\text{-}19)$$

In matrix form

$$\begin{bmatrix} Q_1 \\ Q_2 \\ \vdots \\ Q_m \end{bmatrix} = \begin{bmatrix} C^*_{11} & \cdots & C^*_{1m} \\ \vdots & & \vdots \\ C^*_{1m} & & C^*_{mm} \end{bmatrix} \begin{bmatrix} V_1 \\ V_2 \\ \vdots \\ V_m \end{bmatrix} \qquad (1\text{-}20)$$

where the set of conductors m is exclusive of the reference conductor. Making the substitutions

$$\begin{aligned} C_{ij} &= \sum_{i=1}^{m} C^*_{ji} \qquad (j=i) \\ C_{ij} &= -C^*_{ij} \qquad (j \neq i) \end{aligned} \qquad (1\text{-}21)$$

gives the values of the capacitances to be used in an equivalent network.

## 1.4 An Outline of the Problem

As stated previously, the purpose of this text is to determine the capacitance matrix for a system of n conductors as defined by the relationship

$$\begin{bmatrix} Q_1 \\ Q_2 \\ \vdots \\ Q_n \end{bmatrix} = \begin{bmatrix} c_{11} & c_{12} & \cdots & c_{1n} \\ c_{12} & & & \vdots \\ \vdots & & & \\ c_{1n} & \cdots & & c_{nn} \end{bmatrix} \begin{bmatrix} V_1 \\ V_2 \\ \vdots \\ V_{n+1} \end{bmatrix} . \qquad (1\text{-}18)$$

The procedure is to formulate a method for two bare wires and then to compare the results obtained with the exact results which are known and have been given in Section 1.1. If the results for two bare wires are adequate, then the method will be generalized to multiconductor systems.

The methods chosen for Chapters 2 and 3 involve the application of Maxwell's "method of subareas". Higgins and Black [18] suggested this method for circular cylindrical systems in a paper published in the special March, 1955 issue of the IRE Transactions on Microwave Theory and Techniques. However, this paper was primarily concerned with strip-line parameters and the cylindrical systems were merely mentioned as an example. Their contention was that by subsectioning the conductors longitudinally either approximately (Chapter 2) or exactly (Chapter 3) and applying "the method of subareas" that any degree of accuracy desired could be obtained merely by increasing the number of subareas. Chapters 2 and 3 serve as an examination of those

beliefs. Chapter 4 deals with a technique associated with the general "method of moments" [19], suggested by Dr. Arlon T. Adams* of Syracuse University. This method is found to be quite accurate and is extended to systems of multiple bare wires. In Chapter 5, the methods of Chapter 4 are extended to systems of dielectric-coated wires with the two-wire case being worked out explicitly.

Emphasis is placed upon the charge distribution since the problems involving the determination of the potnetial and the electric fields, V and $\bar{E}$ respectively, in [8-10] can be solved using

$$V = \frac{1}{4\pi\varepsilon_0} \int_{s'} \frac{\sigma_s(r')ds'}{|\bar{r} - \bar{r}'|} \tag{1-19}$$

and

$$\bar{E} = \frac{1}{4\pi\varepsilon_0} \int_{s'} \frac{\sigma_s(r')(\bar{r} - \bar{r}')ds'}{|\bar{r} - \bar{r}'|^3} \tag{1-20}$$

once the charge distribution $\sigma_s(r')$ over the surfaces s' is known.

---

*Private communications

# CHAPTER II

# THE POLYGONAL APPROXIMATION

## 2.1 Introduction

In this chapter the two bare wire problem is treated by making a polygonal conductor approximation of the wires. The method to be described is basically one proposed by Higgins and Black [18] in 1955, the concepts of which date back to Maxwell's "method of subareas". It is an important method today in that this method has not been feasible for large systems of conductors until the advent of large storage computers capable of handling the large systems of equations involved in solving the problem. Furthermore, the technique for two circular conductors serves as a basis for the determination of the capacitance matrix currently used in multiconductor cable response analysis [12].

Briefly, the procedure is as follows. First of all, each wire is approximated by an infinitely long polygonal conductor having an arbitrary number of sides as shown in Figure 2-1. Each side is assumed to have an unknown constant surface charge density $\sigma_i$, as shown in Figure 2-2, where wire 1 has been unfolded and stretched along the x-axes. Then, a set of matrix equations is formed relating the unknown constants, the $\sigma_i$'s, to the potential boundary conditions established by the surface of the wires. Once the equations are solved, an approximate charge distribution results. Finally, the approximate capacitance is the area under the charge distribution curve for wire 1.

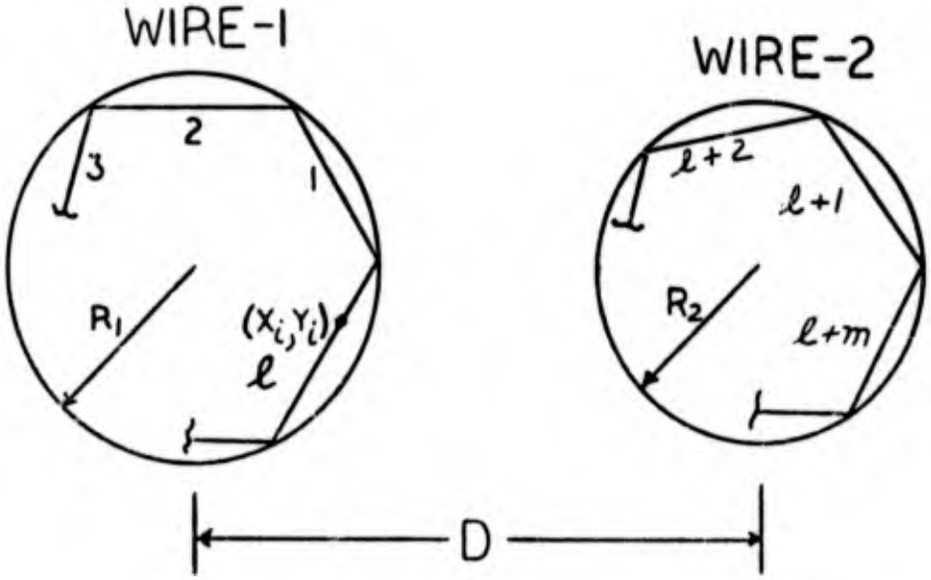


Fig. 2-1. -- Two bare wires broken up into an arbitrary number of infinitely long finite width strips.

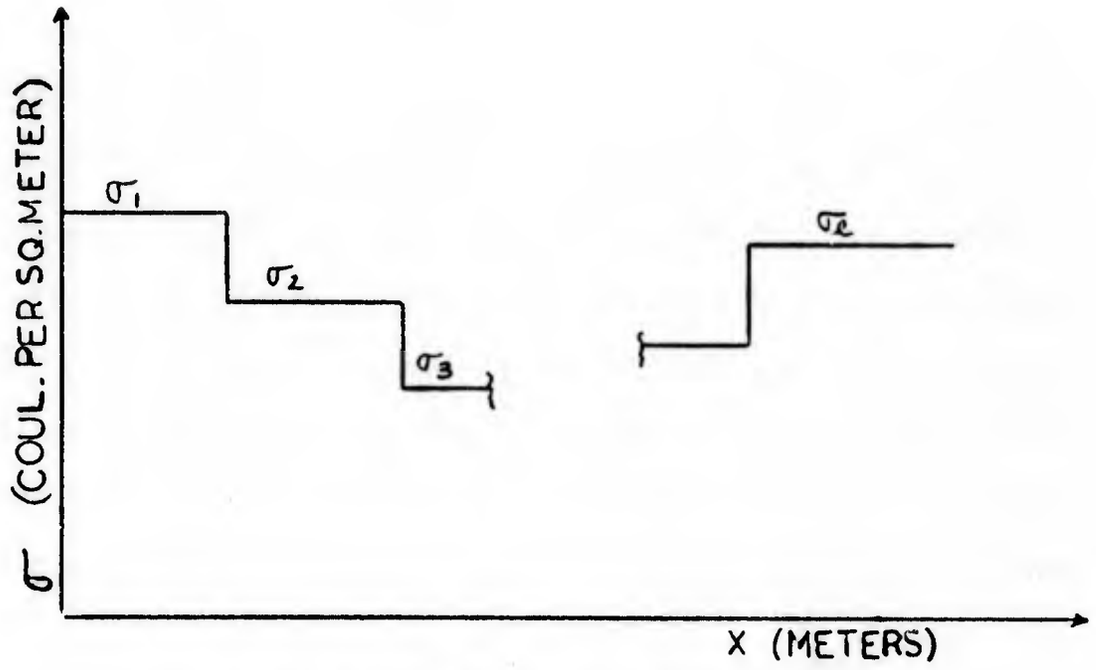


Fig. 2-2. -- Assumption of unknown charge densities on wire 1.

## 2.2 A General Development for the Two Wire Case

Since the polygonal conductors used to replace the actual conductors support several infinitesimally thin, infinitely long, and finite width strips of charge, the analysis begins by determining the potential at a field point (x,y) due to a single representative strip of charge. The surface charge density of each strip is assumed to be constant, and since the wires are infinitely long, the fields will show no dependence in the direction along the wires. Therefore, Poisson's equation can be written as

$$\phi(x,y) = \frac{1}{4\pi\varepsilon_o} \int_{s'} \frac{\sigma(x',y')ds'}{\sqrt{(x-x')^2 + (y-y')^2}}, \qquad (2\text{-}1)$$

where s' denotes that the integral is taken over area containing the charge distribution $\sigma(x',y')$. However, this integral is not valid in the strict sense in that it assumes that s' can be enclosed by some volume V. But clearly, s' cannot be enclosed by any V since it extends to infinity. Consequently a slightly different point of view will be taken here. Referring again to Figure 2-1, consider the magnification of one of the flat strips. This is shown in Figure 2-3, where each small circle represents an infinitesimal line charge of $\lambda$ coulombs per unit length. The potential at the point (x,y) due to a typical line charge at (x',y') within this strip is

$$\phi(x,y) = \frac{-\lambda}{4\pi\varepsilon_o} \ln((x-x')^2 + (y-y')^2), \qquad (2\text{-}2)$$

where a reference potential term has been omitted. (The reason for this is explained in Appendix A). If the strip is now considered to be composed of n identical line charges each existing within some width $\Delta w$, the approximate potential becomes:

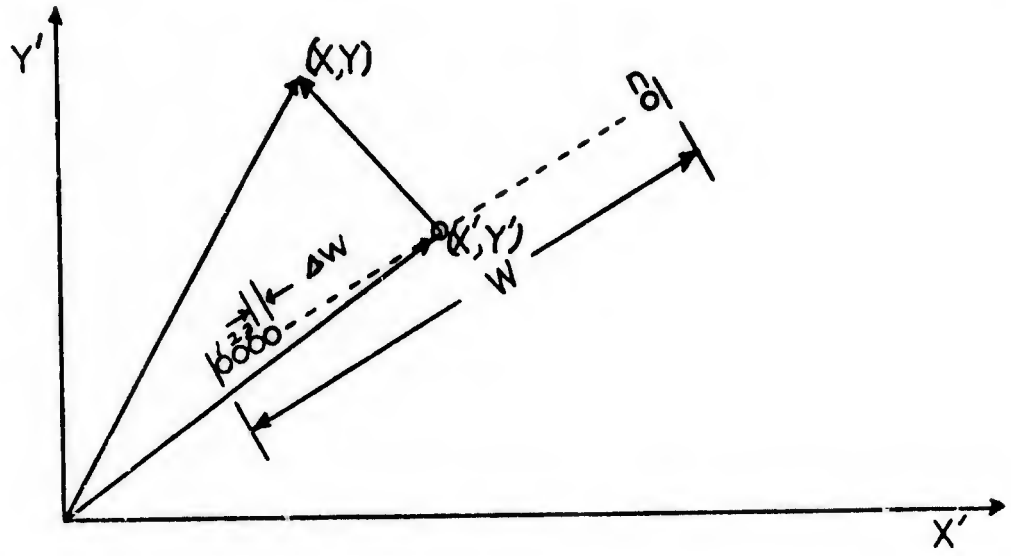


Fig. 2-3. -- A typical strip of width w from Fig.2-1consisting of n infinite line charges all of λ coulombs per unit length. Each line charge occupies a width Δw.

$$\phi(x,y) \simeq \frac{-1}{4\pi\varepsilon_o} \sum_{j=1}^{n} \lambda \, \ell n((x-x'_j)^2 + (y-y'_j)^2), \qquad (2\text{-}3)$$

where the $j^{th}$ line charge is located at $(x'_j, y'_j)$. As n becomes very large, the line charge can be considered to be uniformly distributed over the interval Δw giving $\lambda = \sigma\Delta w$. Then, as n becomes infinite equation (2-3) becomes the integral equation

$$\phi(x,y) = \frac{-\sigma}{4\pi\varepsilon_o} \int_{w'} \ell n((x-x')^2 + (y-y')^2)dw', \qquad (2\text{-}4)$$

with w' denoting the integral over the width of the strip. Thus, upon integrating equation (2-4) an expression is obtained which gives the potential at any point (x,y) due to a uniformly charged infinitesimally thin strip extending to infinity in one dimension.

The next step in the analysis is to formulate a set of matrix equations involving all of the unknown surface charge densities and the known values of the potentials on the conductor surfaces. In particular, consider a point $(x_i,y_i)$ on the polygonal boundary as shown in Figure 2-1. Since this boundary is an equipotential surface, the potential at all points on the boundary can be specified. Thus, let the potential at $(x_i,y_i)$ be equal to $V_1$ and let the two conductors be divided into a total of k strips; $\ell$ strips for wire 1 and $k-\ell$ strips for wire 2. Using superposition and equation (2-4) an expression in terms of k unknown charge densities is now

$$\phi(x_i,y_i) = V_1 = \frac{-1}{4\pi\epsilon_o} \sum_{j=1}^{k} \sigma_j \int_{w'_j} \ell n((x_i-x')^2+(y_i-y')^2)dw', \qquad (2\text{-}6)$$

which is one equation in k unknowns. Similarly, if k-1 more distinct points are selected on the boundaries of the wires and equation (2-6) is written for each of these points, then a set of k equations in k unknowns results. The equations to be solved appear in matrix form

$$\begin{bmatrix} D_{11} & \cdots & D_{1k} \\ \vdots & & \vdots \\ D_{\ell 1} & \cdots & D_{\ell k} \\ \hline D_{(\ell+1)1} & \cdots & D_{(\ell+1)k} \\ \vdots & & \vdots \\ D_{k1} & \cdots & D_{kk} \end{bmatrix} \begin{bmatrix} \sigma_1 \\ \vdots \\ \sigma_\ell \\ \hline \sigma_{\ell+1} \\ \vdots \\ \sigma_k \end{bmatrix} = \begin{bmatrix} V_1 \\ \vdots \\ V_1 \\ \hline V_2 \\ \vdots \\ V_2 \end{bmatrix} \qquad (2\text{-}7)$$

where

$$D_{ij} = \frac{-1}{4\pi\varepsilon_o} \int_{w'_j} \ln((x_i-x')^2 + (y_i-y')^2)dw'. \qquad (2\text{-}8)$$

Each $D_{ij}$ can be interpreted as the potential that would appear at point i due to the $j^{th}$ infinitely long flat strip with a uniform surface charge density of one coulomb per square meter. When j is equal to i, the integrand of $D_{ij}$ is singular; however, this presents no problem as the singularity is integrable. Note that the equations above the dashed line enforce the boundary conditions on wire 1, and those below the dashed line enforce the boundary conditions on wire 2.

Equation (2 - 7) can be solved for the unknown charge densities by any one of a variety of known methods; the method used herein is Gauss elimination with complete pivoting and is available as the subroutine DGELG in the IBM Scientific Subroutine Package. With the constant charge densities of each strip known, an approximate charge distribution over the wires results. The capacitance of the system will then be related to the area under the charge distribution curve of wire 1 thus completing the problem.

At this point it would be convenient to summarize the above procedure as a sequence of steps.

(1) Break wire 1 into $\ell$ strips and wire 2 into $k-\ell$ strips.

(2) Select a set of k points, called the "match points", along the boundaries of the conductors.

(3) For each match point i compute the potential due to each strip j assuming the $j^{th}$ strip to have a uniformly distributed surface charge density of one coulomb per square meter. These values will be the $D_{ij}$ terms.

(4) Formulate the set of matrix equations (2-7) by enforcing the boundary conditions at the match points. Set $V_1 = -V_2 = 1$ volt.

(5) Solve the set of matrix equations for the values of the unknown charge densities.

(6) Plot the charge distribution and determine the capacitance.

## 2.3 A Specific Development of the Problem Solved

In accordance with the preceding development an application is made to two identical bare wires. In this case, the capacitance in farads per meter is known to be

$$C = \frac{Q}{V_2 - V_1} = \frac{2\pi\epsilon_o}{\cosh^{-1}(D/2R)} \quad . \qquad (2\text{-}9)$$

This shows that the capacitance is dependent upon the ratio of the distance between centers D and the radius of the wires R. Usually the capacitance is considered as a function of this ratio (D/R) instead of D and R separately. Thus, R is set equal to one meter and D is varied causing no loss of generality. Each wire is divided into n equal width strips giving a total of 2n. Various values of D and n are treated with the results being plotted. A discussion of these results follows in section 2.4; however, it is convenient at this time to consider some details involved in this problem.

Figure 2-4 illustrates the setup of the two wires for n=4. The setup for all other values of n follows the same pattern as for n=4. Match point 1 and $\sigma_1$ are assigned to strip 1 and so on. The matrix equations which evolve according to section 2.2 are:

$$\begin{bmatrix} D_{11} & \cdots & D_{18} \\ D_{21} & & \vdots \\ D_{31} & & \vdots \\ D_{41} & \cdots & D_{48} \\ \hline D_{51} & \cdots & D_{58} \\ D_{61} & & \vdots \\ D_{71} & & \vdots \\ D_{81} & \cdots & D_{88} \end{bmatrix} \begin{bmatrix} \sigma_1 \\ \sigma_2 \\ \sigma_3 \\ \sigma_4 \\ \hline \sigma_5 \\ \sigma_6 \\ \sigma_7 \\ \sigma_8 \end{bmatrix} = \begin{bmatrix} +1 \\ +1 \\ +1 \\ +1 \\ \hline -1 \\ -1 \\ -1 \\ -1 \end{bmatrix}, \qquad (2\text{-}10)$$

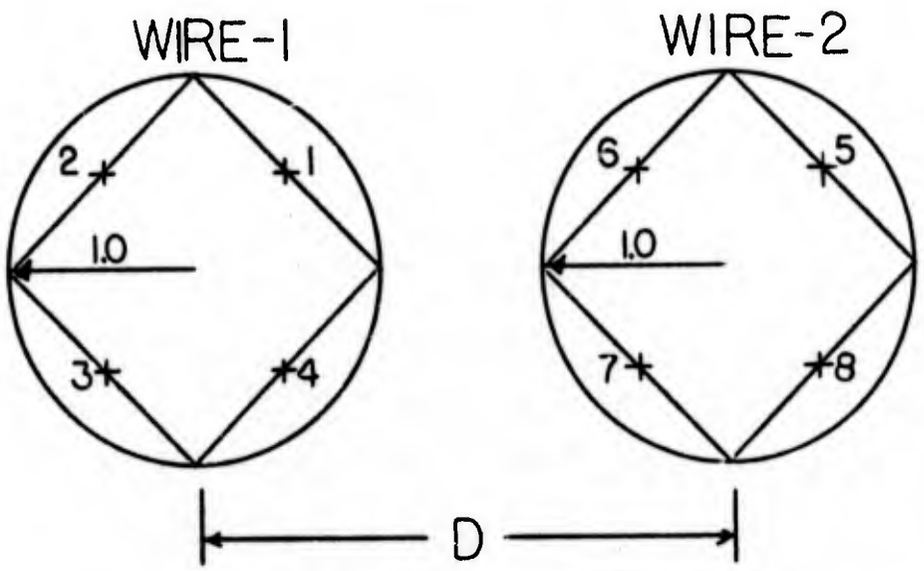


Fig. 2-4. -- The geometry for four strips per wire. "+" indicates a match point.

where the terms above the dashed line enforce the boundary conditions on wire 1 and those below enforce the boundary conditions on wire 2. Once the σ's are determined a plot of the charge distribution on wire 1 as shown in Figure 2-5 is the result. One half the area under this

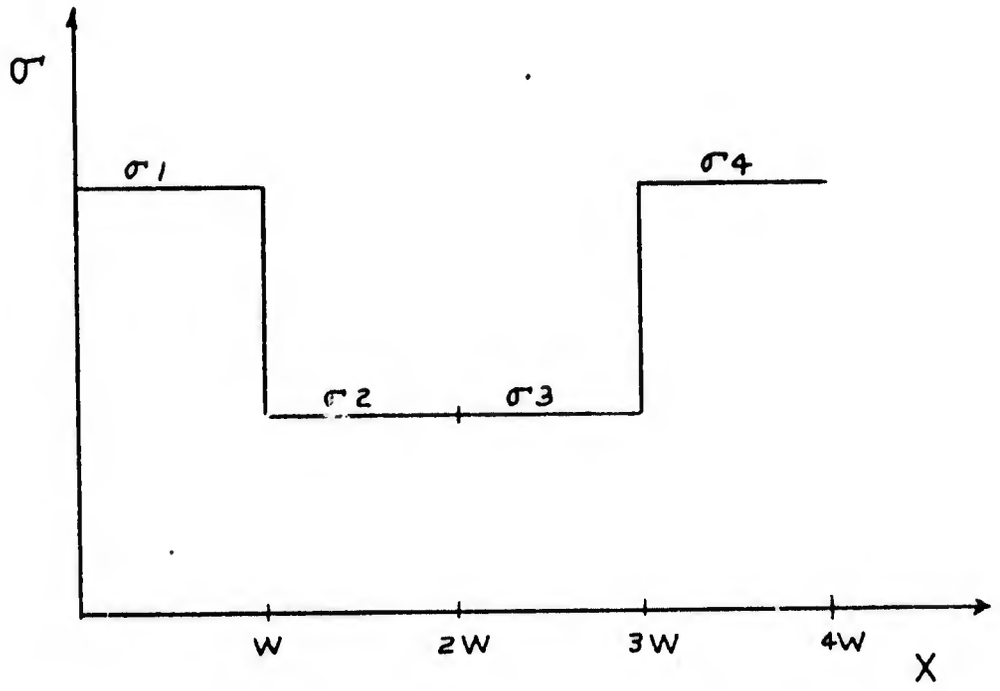


Fig. 2-5. -- The form of the plot for wire 1 resulting from the solution of the problem in Fig.2-4.

curve is the approximate capacitance of the two wires. The curve for wire 2 is the negative of the curve for wire 1 if the strips are plotted in the sequence 6,5,8,7. Note that Figure 2-5 is not directly comparable to a plot of the exact charge distribution since the polygonal approximation is plotted over a length of 4w and an exact plot would extend over $2\pi R$. However, as n becomes very large the approximate charge distribution should approach the exact. A suitable remedy to this is to use circular strips rather than flat; an approach which will be considered in a later chapter, but now, a more detailed description of the determination of the $D_{ij}$ terms is taken up.

The determination of each $D_{ij}$ requires an evaluation of equation (2-8). Letting $(x_{ij}, y_{ij})$ represent the position of the $i^{th}$ field point with respect to a coordinate system on the $j^{th}$ strip, equation (2-8) becomes:

$$D_{ij} = \frac{-1}{4\pi\varepsilon_o} \int_{w'_j} \ln((x_{ij}-x')^2 + (y_{ij}-y')^2)dw'. \qquad (2\text{-}11)$$

the integration is then accomplished very simply if the coordinate system used is arranged as shown in Figure 2-6 where a rectangular

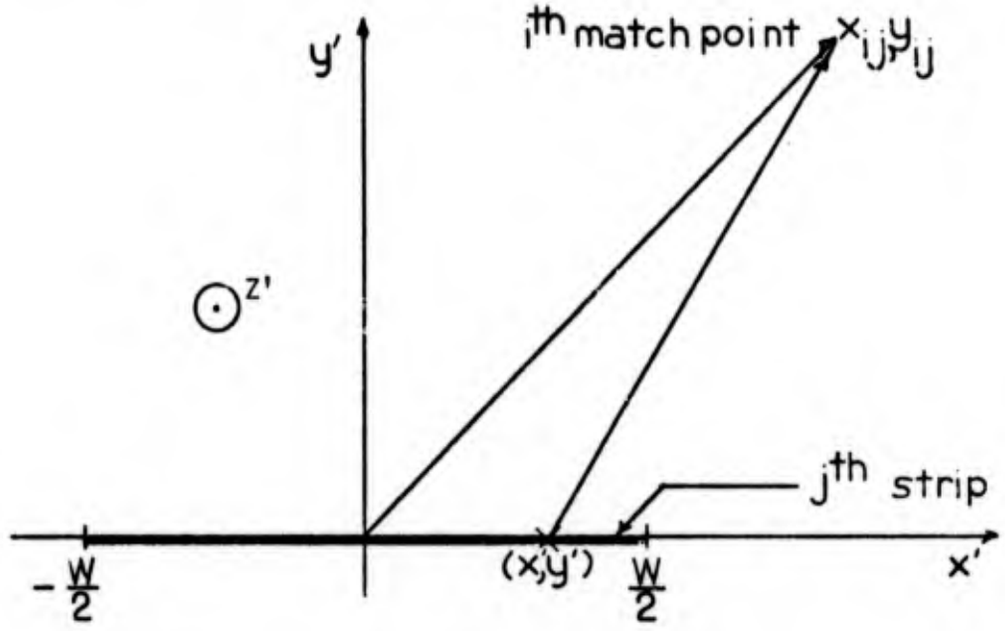


Fig. 2-6. -- The coordinate system used to determine each $D_{ij}$.

coordinate system is placed at the center of a strip of width w lying in the x'-z' plane. Equation (2-11) now simplifies to

$$D_{ij} = \frac{-1}{4\pi\varepsilon_o} \int_{-w/2}^{w/2} \ln((x_{ij}-x')^2 + y_{ij}^2)dx'. \qquad (2\text{-}12)$$

Equation (2-12) is a form which is integrable. Let $t = x-x_{ij}$,

$t'_{ij} = w/2 + x_{ij}$, and $t''_{ij} = w/2 - x_{ij}$ yielding

$$D_{ij} = \frac{-1}{4\pi\varepsilon_o} \int_{-t'_{ij}}^{t''_{ij}} \ln(t^2+y_{ij}^2)dt. \qquad (2\text{-}13)$$

Then, with the aid of Dwight [20]

$$D_{ij} = \frac{-1}{4\pi\varepsilon_o} \left(t \ln(t^2+y_{ij}^2) - 2t + 2y_{ij} \tan^{-1}(t/y_{ij})\right)\Big|_{-t'_{ij}}^{t''_{ij}}. \qquad (2\text{-}14)$$

Equation (2-14) is now readily available for computer use. The expression to be evaluated is written as a Fortran Function Subprogram in the variable $t$ and the values of $t'_{ij}$ and $t''_{ij}$ for a particular $D_{ij}$ are passed to it. For example, call equation (2-14) "FCT(t)." Then

$$D_{ij} = \frac{-1}{4\pi\varepsilon_o} \left(FCT(t''_{ij}) - FCT(t'_{ij})\right), \qquad (2\text{-}15)$$

with the values of $y_{ij}$ being pickedup through common storage. Thus, each $D_{ij}$ term can be computed by obtaining the location of the $i^{th}$ match point with respect to the center of the $j^{th}$ strip and substituting this value into equation (2-15).

The above procedure for the problem solved is now written down in a sequence of steps.

(1) Divide each wire into n equal width strips yielding a total of 2n.

(2) Assign 2n match points such that one match point occurs at the center of each strip.

(3) Select match point 1.

(4) Select strip I and determine $x_{11}$, $y_{11}$, $t'_{11}$, and $t''_{11}$.

(5) Determine $D_{11}$ by using the values from (4) in equation (2-15).

(6) Repeat (4) and (5) with strips $j = 2,3,\ldots,2n$.

(7) Repeat (3),(4),(5) and (6) with match points $2,3,4,\ldots,2n$.

(8) Set

$$\underline{V} = \begin{bmatrix} V_1 \\ \cdot \\ \cdot \\ \cdot \\ V_n \\ V_{n+1} \\ \cdot \\ \cdot \\ \cdot \\ V_{2n} \end{bmatrix} = \begin{bmatrix} +1 \\ \cdot \\ \cdot \\ \cdot \\ +1 \\ -1 \\ \cdot \\ \cdot \\ \cdot \\ -1 \end{bmatrix} .$$

(9) Solve $\underline{D}\,\underline{\sigma} = \underline{V}$

(10) Plot the charge distribution on wire I.

(11) Calculate the capacitance per unit length as $C = \sum_{i=1}^{n} \sigma_i \, \Delta w_i$.

## 2.4 Results and Discussion of the Polygonal Approximation

The procedure outlined in section 2.3 for the two bare wire polygonal approximation was programmed on an IBM 360/65 computer using standard Fortran language and programming techniques. All computations were performed using double precision arithmetic in order to minimize computational error. The results are collected in Appendix B and have been arranged according to each D/R value that was analyzed. The first page for each D/R contains a plot of the capacitance obtained by the polygonal approximation versus the number of strips per wire (NS) used. Each computed value is marked by a "Δ", and a

line is drawn through these points. As a reference, the exact capacitance is also drawn on the same plot as a straight line. Above this is a table of values plotted and the exact capacitance. On the succeeding pages are some plots of the charge distribution versus the distance along the boundary of wire 1 for some selected values of NS. The exact charge distribution appears as a reference on each plot and is identified by the "Δ" placed at various computed points. The headings on each plot identify the particular distance between centers to radius ratio (D/R) and the number of strips per wire (NS). The values of D/R that were analyzed are 2.1,2.2,2.3,3.0, and 10.0.

Consider the case represented by D/R = 2.1 in which the wires are very close together. This example serves to point out some very interesting events that occur as a result of close spacings. Referring to p. B-1, it is noted that the capacitance is converging to the exact solution; however, this convergence is quite slow. Beginning with NS = 3, the approximate capacitance is 26.2 picofarads. The addition of one strip per wire up to 13 strips per wire improves the capacitance value an average of 4.4 picofarads per step. From NS = 14 to NS = 20 the average improvement is about 1.23 picofarads per step. It is further noted that the $\underset{\sim}{D}$ matrix is becoming large (40 x 40 for NS = 20) increasing the possibility of computational error. Proceeding from a value of NS = 19 to NS = 20 the capacitance improves by only 0.76 picofarads, and if it is assumed that the capacitance continues to improve by this same amount per additional strip until one decimal place accuracy is achieved, then approximately 32 strips per wire will have to be used. In this case the $\underset{\sim}{D}$ matrix will be of order 64. Thus,

increasing the number of strips per wire becomes a futile effort as the capacitance value is still in error by 9.87% with NS = 20. (The error used here is actually the relative error expressed in per cent i.e. for C* the approximation to C, R.E. $=((|C-C^*|/|C|)\times 100.)$

The reasons for the above behavior can be established by comparing the approximating charge distribution to the exact charge distribution for some of the D/R values considered. Beginning with p. B-2, it is ascertained from the plot of the exact charge distribution that most of the charge is concentrated in the region where the two wires nearly touch i.e. from zero to 1.57 meters, and from 4.71 to 6.28 meters. The charge density in this region is changing very rapidly; whereas, from 1.57 to 4.71 meters the charge density is fairly constant. For a value of NS = 3 on p. B-2, a very poor estimation of the total charge under the exact curve is yielded by the approximate curve. For NS=4, the estimation is a little better in the region from 1.57 to 4.71 meters but still very poor outside. It is also noted that incrementing NS from 3 to 4 has lengthened the approximate curve with some additional charge being picked up in this way. This is an important, although possibly obvious, consideration. Since the boundaries have been approximated, a point by point comparison of the two curves appearing in each plot cannot be made. The approximate charge distribution serves to estimate the total charge appearing on wire 1. As NS increases, this estimate becomes better and better, but before a point by point comparison of the two charge distributions can be made, NS must become infinite. For values of NS = 5 and 6, the polygonal boundaries are becoming a closer representation of the actual boundaries, and thus, the

approximate distribution begins to move into alignment with the exact distribution. This is evidenced further on p. B-4 where the plots for values of NS = 11 and 12 are shown. With this increment, the improvement in capacitance is about 1.77 picofarads, but for NS = 12, the capacitance is still in error by almost 23%. Thus, there is still much error and the improvement made by incrementing NS by one is small. Now for values of NS = 17, 18, 19, and 20 on pp. B-5 and B-6, the approximate charge distribution has moved into fairly good alignment with the actual distribution. However, by observing these in sequence, it becomes evident why the convergence is slow. At NS = 17, the region from 1.57 to 4.71 is well approximated and thus the total charge under the actual distribution is in good agreement; however, the region from 0 to 1.57 and 4.71 to 6.28 is not well approximated and is improving very slowly with increasing NS. From a value of NS = 17 to a value of NS = 20, the charge density on strip 1 changes from slightly less than $0.12 \times 10^{-9}$ coul/m$^2$ to slightly greater than $0.12 \times 10^{-9}$ coul/m$^2$. Thus, increasing NS beyond 20 may eventually give good results but the value of NS necessary for any specific accuracy is likely to be far beyond computer capabilities.

For a value of D/R = 2.2, the overall behavior is the same as for D/R = 2.1. The capacitance curve rises a little more steeply and levels off a little sooner as shown on p. B-7. With NS = 20, the capacitance is in error by 5.27%, and each increase in NS shows little improvement. As before, this behavior is explained by looking at the charge distributions. The exact charge distribution is not as steep in the region where the wires nearly touch since the wires are not

quite as close as with D/R = 2.1. The quantity of charge appearing in the more concentrated region does not seem to be as great a fraction of the total charge as when D/R=2.1. Also the charge in the region from 1.57 to 4.71 meters is more nearly constant than in the previous case; consequently, the assumed charge distribution is better suited to this region. Observing on p. B-8, the results with NS = 9 and 10, the total charge in the 1.57 to 4.71 meters region is approximated well. After a value of NS = 10, improvement of the capacitance comes with better approximations to the highly concentrated regions as evidenced on p. B-9 for values of NS = 13 and NS = 14. Yet, the problem is still the same as before; it is very difficult to fit a steep slope with the type charge distribution assumed. For values of NS = 17, 18, 19, and 20 on pp. B-10 and B-11 it is seen that the improvement per additional value of NS is only very slight as before; and thus, the capacitance will converge very slowly after a value of NS = 20.

Spreading the wires a little more and looking at the D/R = 2.3 case, the results are a little better. This time with a value of NS = 20, the capacitance is within 3.67%, and again, the capacitance curve rises a little more quickly and levels off once the error becomes due to the inaccuracy involved in approximating the more highly concentrated region. For values of NS = 17, 18, 19, and 20 on pp. B-13 and B-14, the same very slight improvement in the capacitance is noted as a result of increasing NS.

In the fourth case considered, D/R = 3.0, the charge distribution is fairly constant over the entire wire. The capacitance curve rises more sharply and levels off again to a very slow convergence.

As shown by the results with NS = 8, the total charge under the entire curve is fairly well approximated, and with NS = 17, 18, 19, and 20 the approximate charge in the region from 1.57 to 4.71 meters is very close to the actual charge and outside this region there is fairly good agreement. Noting the values on p. B-15, the capacitance is accurate to two decimal places beginning with NS = 14 indicating that the approximation ha' picked up most of the charge with low values NS, and that increasing NS has an effect only in latter decimal places. From observing the charge distribution for NS = 17, 18, 19, and 20 it seems probable that some accuracy is gained in the slightly curved region of the charge density curve by increasing NS; yet, it must be remembered that the length of the polygonal boundary is increasing with NS, and thus, the charge gained by the extra length may be comparable to the amount of charge gained by a better approximation to the curve. If this is the case, then from this point on convergence will be slow since it will be limited by the convergence of the boundary.

The value of D/R = 10.0, pp. B-19 to B-21, represents very wide spacing; it also exemplifies this last consideration. With NS = 3, the approximate charge coincides closely with the exact, the differences in capacitance being clearly due to the differences in length. With NS = 20, the length of the polygonal boundary is close to the exact, and the two charge distributions are virtually coincident. The same trend as with D/R = 3.0 is now noted. Beginning with NS = 14, the capacitance is accurate to two decimal places and additional values of NS produce only very little change. From NS = 14 to NS = 20 the capacitance changes by 0.000054 picofarads and it is probable that the increase in length is responsible for most of this change. Thus, it is clear

that the computation of the capacitance by this method to any specific degree of accuracy is always going to be limited by the convergence of the boundary no matter how constant the charge is over the surfaces.

In summary, it was determined that two causes contribute to the slow convergence of this method. These were the slow convergence of the approximate boundary to the actual boundary and the poor ability of this method to fit regions of rapidly changing charge density. For close spacings, the error was due primarily to rapidly changing charge density and for moderately wide spacing (D/R = 3.0) the two errors were coupled such that it was difficult to determine which contributed the most. For wide spacing (D/R = 10.0) it is believed that the error is determined primarily by the convergence of the boundary. In all casesthe convergence is slow with respect to the number of strips per wire needed; however, for the wider spacings two decimal place accuracy is obtained with relatively low values of NS. Consequently, this method is useful primarily in cases of wide spacings where little accuracy is necessary. However, this is not the case of interest since there are already good approximations for multiconductor systems under the conditions of widely spaced wires [11]. Therefore, it is necessary to seek methods which will give very good accuracy with wide spacing and reasonably good accuracy with close spacing. This is attempted in following chapters.

# CHAPTER III

# CIRCULAR STRIPS APPROXIMATION

## 3.1 Introduction

In Chapter 2, two reasons were found for the slow convergence of the polygonal approximation. These were: (1) the inability of the assumed charge distribution to fit regions of rapidly varying charge density, and (2) the slow convergence of the approximate boundary to the actual boundary. The first condition was predominant for close spacings and the second was predominant for wide spacings. In this chapter, the error due to the boundary approximation is eliminated by assuming the charge distribution to be constant over circular subsections of the wire leaving the boundary unaltered. However, the $D_{ij}$ terms resulting from the circular strips do not seem to be integrable in closed form, and thus, numerical integration must be employed in order to obtain values for these terms. This, in turn, requires a closer look at the computational error. Overall, the general procedure and the specific problem solved are exactly the same as in Chapter 2 with the same type of data being reproduced.

## 3.2 The Development of the $D_{ij}$ Terms for the Circular Strips

Consider Figure 3-1 where a typical circular strip C' between the limits $\theta_1$ and $\theta_2$ on the surface S' is shown. A cylindrical coordinate system is employed since it is the most readily adaptable to this problem. The potential at the point $(r,\theta)$ is

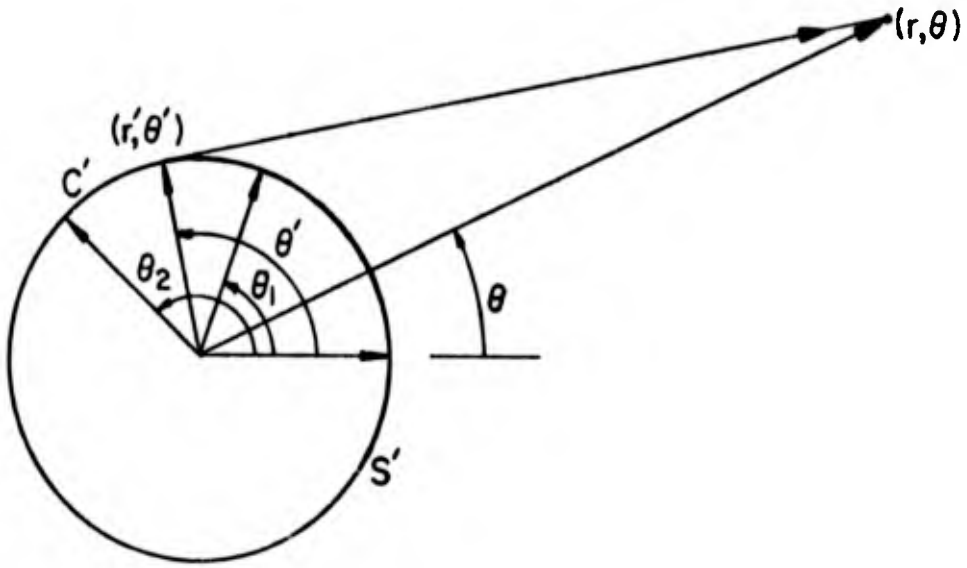


Fig. 3-1. -- The geometry for circular strips.

$$\phi(r,\theta) = \frac{-1}{4\pi\varepsilon_o} \int_{C'} \ln(r^2 + r'^2 - 2rr'\cos(\theta'-\theta))r'd\theta'. \qquad (3\text{-}1)$$

When the point $(r,\theta)$ represents the $i^{th}$ match point $(r_i,\theta_i)$ and C' represents the $j^{th}$ source $C'_j$, equation (3-1) becomes

$$D_{ij} = \frac{-1}{4\pi\varepsilon_o} \int_{C'_j} \ln(r_i^2 + r'^2 - 2r_i r' \cos(\theta'-\theta_i))r'd\theta'. \qquad (3\text{-}2)$$

where r' is the radius of the wire and is set equal to one meter. Each $D_{ij}$ term represents the potential at a point i due to a one coulomb per square meter charge density on the circular strip j.

For the flat strip the integrand of the $D_{ij}$ term was exactly integrable; however, this does not seem to be the case for equation (3-2). Thus, the evaluation of the $D_{ij}$'s is accomplished numerically by the use of gaussian quadrature formulas. These formulas are available in double precision arithmetic in the IBM Scientific

Subroutine Package and are listed according to the number of terms used to approximate the integral, i.e., DQG4, DQG8, DQG12, DQG16, DQG24, and DQG32. In this problem, DQG32 is used to obtain maximum accuracy when i=j since the integrand is singular in this case. Specifically, if i=j, the total integral is calculated as twice the value yielded by DQG32 when applied to the interval extending from the singularity to one half of the length of the strip. For the off-diagonal ($i \neq j$) terms of the $\underset{\sim}{D}$ matrix, a comparison of the capacitance obtained using the 4,8,12,16 and 24 term gaussian formulas was done for NS=2 and D/R=2.1. These results are listed in Table 3-1.

TABLE 3-1

GAUSSIAN QUADRATURE DATA

| Gaussian Formula | Approx. Capacitance |
|---|---|
| DQG4 | $0.3290492696331365 \times 10^{-10}$ |
| DQG8 | $0.3291890758864015 \times 10^{-10}$ |
| DQG12 | $0.3291886095295901 \times 10^{-10}$ |
| DQG16 | $0.3291886055518649 \times 10^{-10}$ |
| DQG24 | $0.3291886055468857 \times 10^{-10}$ |

The capacitance converges as the number of terms used in the gaussian formula to determine the off-diagonal elements of $\underset{\sim}{D}$ matrix increases. The 16-point and 24-point formulas agree to ten decimal places, and thus, DQG16 was chosen as sufficiently accurate. At this point, it is worthy to note that the above reasoning is not as rigorous as one might desire; however, the procedure employed proved to be sufficiently accurate to yield the expected results. For a more rigorous explanation of the gaussian quadrature technique see Conte and DeBoor [21].

## 3.3 Results and Discussion

The computer analysis with the circular strips parallels that of the flat strips. The data and plots obtained are arranged in Appendix C under the same format as Appendix B, and the values of D/R are 2.1, 2.2, 2.3, 3.0, and 10.0 with NS varying from 3 to 20 in each case. Some of the charge distribution plots analogous to those of the polygonal approximation are also included for the sake of comparison. As before, the D/R values of 2.1, 2.2, and 2.3 are considered as closely spaced; D/R = 3.0 is moderately spaced; and D/R = 10.0 is widely spaced.

A comparison of the data obtained by the two methods shows that for a particular value of D/R the convergence is much improved using the circular strips. The capacitance curve rises faster as NS increases, and the eventual accuracy achieved with NS = 20 is much closer to the exact value. For D/R = 2.1, the error is 9.87% for NS = 20 using the flat strips. Using the circular strips, the accuracy is better than 9.87% with NS = 11 and one digit accuracy is achieved with NS = 12. Note that it was previously estimated that it would require a value of NS = 32 to attain one digit accuracy if the polygonal approximation were used. The charge distribution plots for NS = 12,13,14, and 15 on pp.C-2 and C-3 show that the region from 1.57 to 4.71 meters is well approximated in all cases, and thus, increasing NS beyond twelve will give a better approximation only to the region of steep slope, i.e., from 0-1.47 and from 4.71 - 6.28 meters. This would indicate that increasing NS beyond this point will give very slow improvement in the capacitance since the circular strips are not expected to improve the accuracy in regions of rapidly varying charge density. The data on p.C-1 verifies this as two digit accuracy is not achieved by NS = 20.

For the remaining values of D/R the behavior is the same as for D/R = 2.1. The only difference is that as D/R increases the number of accurate digits attainable increases. For D/R = 2.2, two digit accuracy is obtained with NS = 15; for D/R = 2.3, two digit accuracy is obtained with NS = 14; and for D/R = 3.0, three digit accuracy is obtained by NS = 10; and finally, the capacitance with D/R = 10.0 is accurate to five digits with NS = 8. In all cases, the number of accurate digits is attained with relatively low values of NS, and then, does not seem to get much better as NS increase. Thus, one might wonder if the number of digits will ever become better by making NS very large. This point was investigated by setting NS = 32 and obtaining the capacitance for each D/R. These results are listed in Table 3-2, and show that the capacitance with D/R = 2.1, 2.2, and 10.0 show no improvement in the correct number of digits. The capacitance with D/R = 2.3 and 3.0 show an improvement of one and two digits respectively.

TABLE 3-2

CIRCULAR STRIPS DATA

| D/R | Approx. Capacitance* | |
|---|---|---|
| | NS=20 | NS=32 |
| 2.1 | 0.8677338 | 0.8799521 |
| 2.2 | 0.6239991 | 0.6258491 |
| 2.3 | 0.5126004 | 0.5132298 |
| 3.0 | 0.2885928 | 0.2886217 |
| 10.0 | 0.1211730 | 0.1211726 |

*Capacitance values are multiplied by $10^{-10}$.

This indicates rather strongly that trying to improve the accuracy of the capacitance beyond the value obtained for low values of NS is not advisable.

In light of the above discussion it seems reasonable to draw a few general conclusions for this problem. These are: (1) the method of circular strips along with numerical integration for determining the values in the $\underset{\sim}{D}$ matrix is always better than the polygonal approximation; (2) the method of circular strips is limited to a certain degree of accuracy depending upon the value of D/R; and (3) using values of NS beyond the neighborhood of fifteen regardless of D/R is not likely to improve the accuracy.

CHAPTER IV

# Fourier Series Approximation

## 4.1 Introduction

In the previous two chapters, the charge density was expanded into a piecewise constant function over the boundaries of the conductors and the capacitance was determined as the area under the resulting charge distribution. The results have shown that under close spacing conditions only rough estimates of the capacitance can be obtained, and that under wide spacing the degree of accuracy is limited. With the polygonal approximation the maintenance of the boundary was sacrificed for the ability to compute the integrals of the $\underset{\sim}{D}$ matrix in closed form. This procedure was inadequate as the accuracy of the capacitance turned out to be limited by the convergence of the boundary regardless of the spacing of the wires. With the circular strips approximation the boundaries were left intact but the integrals of the $\underset{\sim}{D}$ matrix had to be computed numerically. This procedure was much better than the polygonal approximation but was ultimately limited by the degree of accuracy of the terms in the $\underset{\sim}{D}$ matrix and by the inability of the piecewise constant distribution to match regions of rapidly varying charge density. Thus, the analysis comes to a point where the piecewise constant assumption must be refined for better accuracy or must be abandoned in search of a more suitable expansion. The latter procedure will be followed.

In light of the above discussion, a method is desired whereby: (1) the boundaries are not altered; (2) the charge density is in good

agreement with the exact charge density for all points on the boundary; and, (3) the integrals in the $\underline{D}$ matrix are obtainable in closed form. Automatically, a piecewise linear, piecewise quadratic, or any higher order expansion of this type is ruled out since the integrals of the $\underline{D}$ matrix for circular strips are not expected to exist in closed form. If numerical integration were used, the results would likely yield better accuracy than the piecewise constant function; however, Adams* and a small amount of literature [5,8] indicate that a Fourier Series expansion over the entire circumference of the wire would probably be the most adaptable. Thus, the problem is now analyzed assuming a Fourier Series charge distribution over each wire and the results are found to be far superior to those of Chapters 2 and 3.

## 4.2 The Development of the Potential Due to a Fourier Series Charge Distribution over a Cylindrical Conducting Surface.

In Figure 4-1, a cylindrical conductor is shown supporting n infinitesimal line charges. If the line charge $\lambda_n$ at $(r_i', \theta_i')$ has a weight of $\cos n\theta'$ coulombs per unit length, then the potential at $(r,\theta)$ is:

$$\phi(r,\theta) = -\frac{\lambda_n \cos n\theta_i'}{4\pi\varepsilon_o} \ln(r^2 + r_i'^2 - 2rr_i' \cos(\theta_i' - \theta)). \qquad (4\text{-}1)$$

Similarly, if every line charge is weighted by its angular position, then the total potential $\phi$ due to all n line charges will be:

---

*Private communications with Dr. A.T. Adams of Syracuse University.

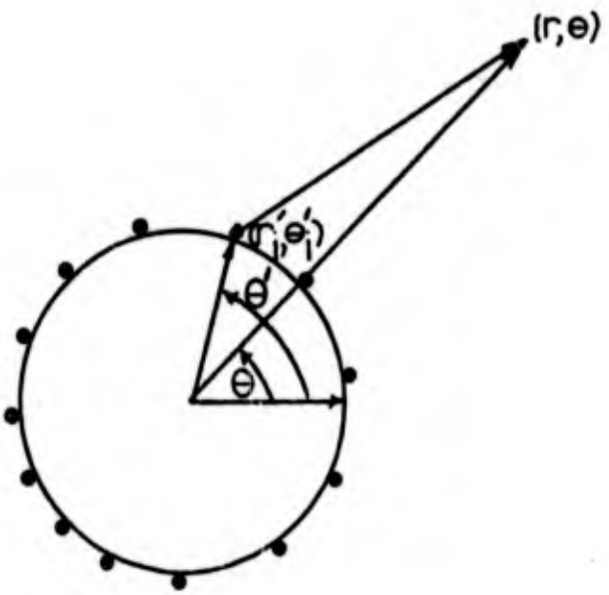


Figure 4-1. -- A cylindrical conductor supporting n infinitesimal line charges.

$$\phi(r,\theta) = \frac{-1}{4\pi\varepsilon_0} \sum_{i=1}^{n} \lambda_n \cos n\theta'_i \, \ell n(r^2 + r'^2_i - 2rr'_i\cos(\theta'_i - \theta)). \qquad (4\text{-}2)$$

As n becomes large each line charge can be considered to be uniformly distributed over the width $r'\Delta\theta'$, and $\lambda_n \cos n\theta'_i$ is replaced by $\sigma_n \cos n\theta'_i r'_i \Delta\theta'_i$ where $\sigma_n$ is a surface charge density per unit length as in Chapter 2. Equation (4-2) now becomes

$$\phi(r,\theta) \approx \frac{-1}{4\pi\varepsilon_0} \sum_{i=1}^{n} \sigma_n \cos n\theta'_i \ell n(r^2 + r'^2_i - 2rr'_i\cos(\theta'_i - \theta)) r'_i \Delta\theta'_i. \qquad (4\text{-}3)$$

Finally, as n approaches infinity the discrete variables $r'_i$ and $\theta'_i$ become the continuous variables r' and θ' while the incremental angle $\Delta\theta'$ becomes the differential angle $d\theta'$ and the summation becomes an integral. Thus, the potential at (r,θ) due to a charge distribution of the form $\sigma_n \cos n\theta'$ distributed over an infinitely long cylinder is:

$$\phi_c(r,\theta) = \frac{-1}{4\pi\varepsilon_0} \int_0^{2\pi} \sigma_n \cos n\theta' \ell n(r^2 + r'^2 - 2rr'\cos(\theta' - \theta)) r' d\theta', \qquad (4\text{-}4)$$

where the subscript "c" denotes that the distribution is cosinusoidal. For a sinusoidal distribution of charge a similar development as above yields

$$\phi_s(r,\theta) = \frac{-1}{4\pi\varepsilon_o}\int_o^{2\pi}\hat{\sigma}_n \sin n\theta' \ln(r^2+r'^2 - 2rr'\cos(\theta'-\theta))r'd\theta'. \quad (4\text{-}5)$$

If the total charge distribution over the cylinder is now assumed to be of the form

$$\sigma(\theta) = \sigma_o + \sum_{j=1}^{k}(\sigma_j \cos j\theta' + \hat{\sigma}'_j \sin j\theta'), \quad (4\text{-}6)$$

then the total potential at a point $(r,\theta)$ is:

$$\phi_T(r,\theta) = \phi_o - \frac{1}{4\pi\varepsilon_o}\sum_{j=1}^{k}\sigma_j\int_o^{2\pi}\cos j\theta' \ln(r^2+r'^2-2rr'\cos(\theta'-\theta))r'd\theta'$$

$$- \frac{1}{4\pi\varepsilon_o}\sum_{j=1}^{k}\sigma'_j\int_o^{2\pi}\sin j\theta' \ln(r^2+r'^2-2rr'\cos(\theta'-\theta))r'd\theta', \quad (4\text{-}7)$$

where

$$\phi_o = \frac{-\sigma_o}{4\pi\varepsilon_o}\int_o^{2\pi}\ln(r^2+r'^2-2rr'\cos(\theta'-\theta))r'd\theta'. \quad (4\text{-}8)$$

Equation (4-7) can now be expressed in the linear form

$$\phi_T(r,\theta) = \sigma_o D_o(r,\theta) + \sum_{j=1}^{k}\sigma_j D_j(r,\theta) + \sum_{j=1}^{k}\hat{\sigma}_j\hat{D}_j(r,\theta), \quad (4\text{-}9)$$

where

$$D_o(r,\theta) = \frac{-1}{4\pi\varepsilon_o}\int_o^{2\pi}\ln(r^2+r'^2-2rr'\cos(\theta'-\theta))r'd\theta', \quad (4\text{-}10)$$

and

$$D_j(r,\theta) = \frac{-1}{4\pi\varepsilon_o}\int_o^{2\pi}\cos j\theta' \ln(r^2+r'^2-2rr'\cos(\theta'-\theta))r'd\theta', \qquad (4\text{-}11)$$

and finally,

$$\hat{D}_j(r,\theta) = \frac{-1}{4\pi\varepsilon_o}\int_o^{2\pi}\sin j\theta' \ln(r^2+r'^2-2rr'\cos(\theta'-\theta))r'd\theta'. \qquad (4\text{-}12)$$

Equations (4-10), (4-11), and (4-12) are integrals which, at first sight, seem difficult to evaluate; however, these integrals can be handled in a straight-forward manner with the use of an integral table. Beginning with equation (4-10), let $\alpha' = \theta'-\theta$, then

$$D_o(r,\theta) = \frac{-r'}{4\pi\varepsilon_o}\int_o^{2\pi}\ln(r^2+r'^2-2rr'\cos\alpha')d\alpha', \qquad (4\text{-}13)$$

where the limits of integration are unchanged since the integrand is periodic with a period of $2\pi$. Now, using Dwight [2D], integral number 865.73, equation (4-13) becomes:

$$D_o(r,\theta) = \frac{-r'\ln r}{\varepsilon_o} \qquad r \geq r' \qquad (4\text{-}14)$$

Proceeding with equation (4-11), let $\alpha' = \theta' - \theta$ as before. Again the limits of integration can be left unchanged as the integrand is periodic with a period of $2\pi$. This gives

$$D_j(r,\theta) = \frac{-1}{4\pi\varepsilon_o}\int_o^{2\pi}\cos j(\alpha'+\theta)\ln(r^2+r'^2-2rr'\cos\alpha')r'd\alpha'. \qquad (4\text{-}15)$$

Expanding $\cos j(\alpha'+\theta)$, equation (4-15) now becomes:

$$D_j(r,\theta) = \frac{-r'}{4\pi\varepsilon_o}\int_o^{2\pi}\cos j\alpha'\cos j\theta\ \ell n(r^2+r'^2-2rr'\cos\alpha')d\alpha'$$

$$+\frac{r'}{4\pi\varepsilon_o}\int_o^{2\pi}\sin j\alpha'\sin j\theta\ \ell n(r^2+r'^2-2rr'\cos\alpha')d\alpha' \qquad (4\text{-}16)$$

The second integral in equation (4-16) contains the product of an odd function $\sin j\alpha'$ and an even function $\ell n(r^2+r'^2-2rr'\cos\alpha')$, and thus, this integral is identically equal to zero when integrated over one period. Equation (4-16) reduces to:

$$D_j(r,\theta) = \frac{-r'\cos j\theta}{4\pi\varepsilon_o}\int_o^{2\pi}\cos j\alpha'\ \ell n(r^2+r'^2-2rr'\cos\alpha')d\alpha' \qquad (4\text{-}17)$$

$$= \frac{-r'\cos j\theta}{4\pi\varepsilon_o}\int_o^{2\pi}\cos j\alpha'\ \ell n(r^2(1+(r'/r)^2-2(r'/r)\cos\alpha'))d\alpha' \qquad (4\text{-}18)$$

$$= \frac{-r'\cos j\theta}{4\pi\varepsilon_o}\ \ell n(r^2)\int_o^{2\pi}\cos j\alpha'd\alpha'$$

$$-\frac{r'\cos j\theta}{4\pi\varepsilon_o}\int_o^{2\pi}\cos j\alpha'\ \ell n(1+(r'/r)^2-2(r'/r)\cos\alpha')d\alpha' \qquad (4\text{-}19)$$

Finally, using Dwight [20] integral number 865.74, equation (4-19) becomes:

$$D_j(r,\theta) = \frac{(r')^{j+1}\cos j\theta}{2j\varepsilon_o r^j} \qquad r \geq r' \qquad (4\text{-}20)$$

and thus, $D_j(r,\theta)$ is obtained in closed form. $\hat{D}_j(r,\theta)$ can be obtained by replacing $\sin j\theta'$ by $\cos(j\theta'-90°)$ and following the same procedure as for $D_j(r,\theta)$. The results are:

$$\hat{D}_j(r,\theta) = \frac{(r')^{j+1}\sin j\theta}{2j\varepsilon_o r^j} \qquad r \geq r' \tag{4-21}$$

Returning to equation (4-9) and substituting the closed form values of $D_o, D_j$, and $\hat{D}_j$, the potential at a point $(r,\theta)$ due to Fourier Series charge distribution is:

$$\phi(r,\theta) = -\sigma_o \frac{r' \ell n\, r}{\varepsilon_o} + \frac{1}{2\varepsilon_o}\sum_{j=1}^{k} \sigma_j \frac{(r')^{j+1}\cos j\theta}{jr^j} + \frac{1}{2\varepsilon_o}\sum_{j=1}^{k} \hat{\sigma}_j \frac{(r')^{j+1}\sin j\theta}{jr^j} \tag{4-22}$$

where the subscript "T" has now been dropped.

## 4.3 The Application of the Fourier Series to the Two Bare Wire Problem

The results of Section 4.2 can now be applied to the two bare wire problem illustrated in Figure 4-2. With wire 1 and wire 2 adjusted to a potential of +1 and -1 volt respectively, the plane established by $x-\bar{x}$ is a plane of symmetry. The charge distribution on wire 2 is the image of the charge distribution on wire 1 with respect to this plane. Thus, the $\hat{\sigma}_j$ terms of equation (4-6) will be identically equal to zero and the Fourier distribution on the wires will be

$$\sigma^1(\theta_1') = \sigma_0^1 + \sum_{j=1}^{k} \sigma_j^1 \cos j\theta_1' \tag{4-23}$$

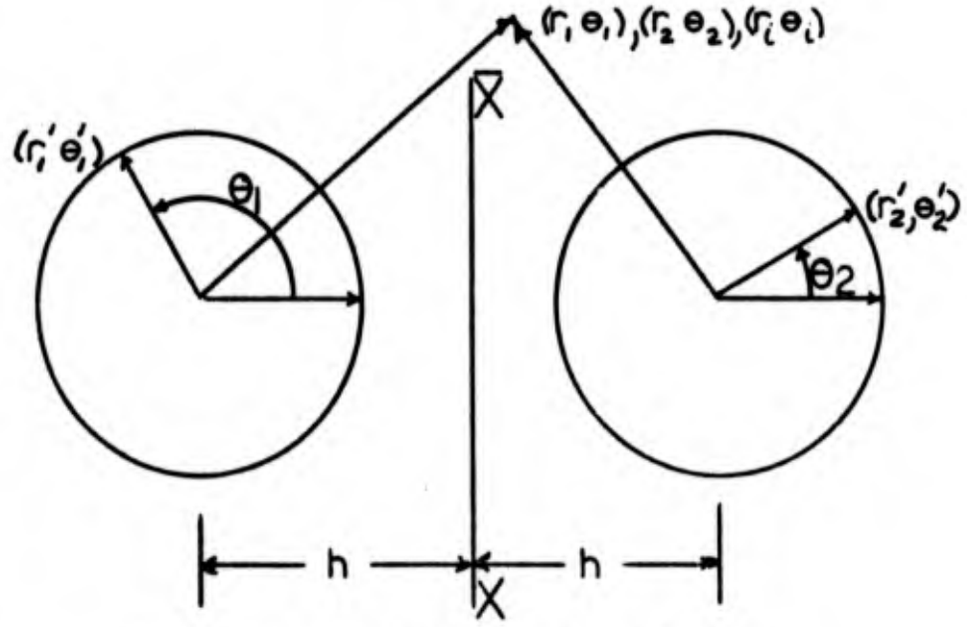


Fig. 4-2. -- Two bare wires with Fourier Series Charge distributions.

for wire 1, and

$$\sigma^2(\theta_2') = \sigma_0^2 + \sum_{j=1}^{k} \sigma_j^2 \cos j\theta_2' \tag{4-24}$$

for wire 2. The potential at the point $(r_i,\theta_i)$ will be the superposition of the potential due to each wire. Thus,

$$\phi(r_i,\theta_i) = \phi^1(r_1,\theta_1) + \phi^2(r_2,\theta_2), \tag{4-25}$$

where

$$\phi^1(r_1,\theta_1) = -\sigma_0^1 r_1' \frac{\ln r_1}{\varepsilon_0} + \frac{1}{2\varepsilon_0} \sum_{j=1}^{k} \sigma_j^1 \frac{(r')^{j+1}\cos j\theta_1'}{j r_1^{\,j}}, \tag{4-26}$$

and

$$\phi^2(r_2,\theta_2) = -\sigma_0^2 r_2' \frac{\ln r_2}{\varepsilon_0} + \frac{1}{2\varepsilon_0} \sum_{j=1}^{k} \sigma_j^2 \frac{(r_2')^{j+1}\cos j\theta_2'}{j r_2^{\,j}}. \tag{4-27}$$

Let

$$D^1_{i(j+1)} = \frac{1}{2\varepsilon_0} \frac{(r'_1)^{j+1}\cos j\theta'_1}{j r_1^{\,j}} ; \tag{4-28}$$

$$D^2_{i(j+1)} = \frac{1}{2\varepsilon_0} \frac{(r'_2)^{j+1}\cos j\theta'_2}{j r_2^{\,j}} ; \tag{4-29}$$

$$D^1_{11} = \frac{-r_1' \ \ln r_1}{\varepsilon_0} ; \tag{4-30}$$

and finally,

$$D^2_{11} = \frac{-r_2' \ \ln r_2}{\varepsilon_0} . \tag{4-31}$$

Equation (4-25) now becomes the linear form

$$\phi(r_i,\theta_i) = \sigma^1_0 D^1_{11} + \sum_{j=1}^{k} \sigma^1_j D^1_{i(j+1)} + \sigma^2_0 D^2_{11} + \sum_{j=1}^{k} \sigma^2_j D^2_{i(j+1)} \tag{4.32}$$

Equation (4.32) is one equation in (2k+2) unknowns, and if k+1 match points are chosen on each wire, then a set of matrix equations is obtained which can be solved for the unknown Fourier coefficients. These equations appear IN the partitioned form

(4-34)

$$\left[\begin{array}{ccc:ccc}
D^{11}_{11} & D^{11}_{12} \cdots & D^{11}_{1(k+1)} & D^{12}_{11} & D^{12}_{12} \cdots & D^{12}_{1(k+1)} \\
D^{1}_{21} & & & D^{12}_{21} & & \\
\vdots & & & \vdots & & \\
D^{11}_{(k+1)1} & & D^{11}_{(k+1)(k+1)} & D^{12}_{(k+1)1} & \cdots & D^{12}_{1(k+1)} \\
\hdashline
D^{21}_{11} & \cdots & D^{21}_{1(k+1)} & D^{22}_{11} & \cdots & D^{22}_{1(k+1)} \\
\vdots & & & \vdots & & \\
D^{21}_{(k+1)1} & \cdots & D^{21}_{(k+1)(k+1)} & D^{22}_{(k+1)} & \cdots & D^{22}_{(k+1)(k+1)}
\end{array}\right]
\left[\begin{array}{c} \sigma^1_0 \\ \vdots \\ \sigma^1_k \\ \hdashline \sigma^2_0 \\ \vdots \\ \sigma^2_k \end{array}\right]
=
\left[\begin{array}{c} +1 \\ \vdots \\ +1 \\ \hdashline -1 \\ \vdots \\ -1 \end{array}\right]$$

Or, more simply

$$\begin{bmatrix} \underline{D}_{11} & \underline{D}_{12} \\ \underline{D}_{21} & \underline{D}_{22} \end{bmatrix} \begin{bmatrix} \underline{\sigma}_1 \\ \underline{\sigma}_2 \end{bmatrix} = \begin{bmatrix} +\underline{1} \\ -\underline{1} \end{bmatrix} . \qquad (4\text{-}35)$$

Each $\underline{D}_{mn}$ can be interpreted as the submatrix of potentials on wire m at the k+1 distinct match points due to the k+1 sources on wire n. Each $D_{ij}^{mn}$ can be interpreted as the potential at match point i on wire m due to "source" j on wire n. Once equation (4-34) is solved, the capacitance is

$$C = \frac{2\pi R_1 \sigma_0^1}{V_1 - V_2} \qquad (4\text{-}36)$$

where $\sigma_0^1$ is the average value of the charge density on wire 1, $R_1$ is the radius of wire 1, and $V_1-V_2$ is the difference in the potential of the two conductors. In this case $V_1-V_2 = 2$ volts.

## 4.4 Results and Discussion of the Fourier Series Approximation

Listed in Appendix D is the data for the Fourier Series approximation. The same D/R values as in Chapters 2 and 3 are analyzed. NF stands for the number of Fourier coefficients used for each wire. The capacitance plots are marked by two symbols. The "*" indicates the capacitance value obtained using an even number of Fourier coefficients, while the "Δ" indicates an odd number. A detailed discussion of this data for each D/R value is not considered. A quick analysis of the data will show the Fourier Series approximation to be far better than the methods of Chapters 2 and 3. Instead some specific points of interest are discussed.

It was stated earlier that one of the main goals of this method was to achieve an approximate charge distribution which was in good agreement with the exact charge distribution for all points on the boundaries of the wires. Choosing the data with D/R = 2.1, the plots on pp. D-2 through D-11 illustrate the nice convergence of the Fourier Series approximation even in the region of rapidly varying charge density i.e. from 0 to 90° & 270° to 360°. A value of NF = 20 indicates no visual difference between the actual and the approximate charge distribution, while the values listed in Table 4-1 demonstrate the precision with which each plotted point in the region from 227° to 360° has been approximated. Emphasizing that these results are for D/R=2.1, it will certainly be true that agreement will be even better for larger D/R values.

A second point of interest has to do with match point selection. Consider Figure (4-2) where unit magnitude cosinusoidal charge distributionsare shown distributed on cylinders with radii equal to one meter.

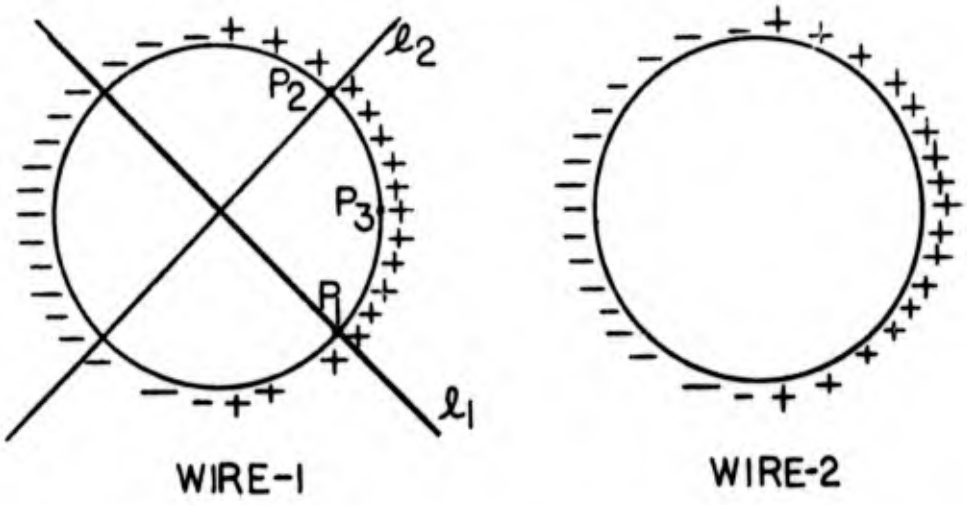


Fig. 4-3. -- Cosinusoidal charge distributions

TABLE 4-1

FOURIER SERIES APPROXIMATION VERSUS THE EXACT CHARGE DISTRIBUTION. D/R=2.1. NF=20.

| Degrees | Approx. Crg. Den. | Exact Crg. Den. |
|---|---|---|
| 0.22679997E 03 | 0.52011980E-11 | 0.51822296E-11 |
| 0.23039998E 03 | 0.53218020E-11 | 0.53269490E-11 |
| 0.23399998E 03 | 0.54667902E-11 | 0.54884005E-11 |
| 0.23759998E 03 | 0.56616248E-11 | 0.56682237E-11 |
| 0.24119998E 03 | 0.58889933E-11 | 0.58683197E-11 |
| 0.24479997E 03 | 0.61131907E-11 | 0.60908978E-11 |
| 0.24839998E 03 | 0.63325560E-11 | 0.63385269E-11 |
| 0.25199998E 03 | 0.65881137E-11 | 0.66142083E-11 |
| 0.25559998E 03 | 0.69129910E-11 | 0.69214530E-11 |
| 0.25919995E 03 | 0.72895353E-11 | 0.72643905E-11 |
| 0.26279980E 03 | 0.76757897E-11 | 0.76478919E-11 |
| 0.26639990E 03 | 0.80702927E-11 | 0.80777295E-11 |
| 0.26999976E 03 | 0.85268927E-11 | 0.85607823E-11 |
| 0.27359985E 03 | 0.90934248E-11 | 0.91052825E-11 |
| 0.27719995E 03 | 0.97538887E-11 | 0.97211466E-11 |
| 0.28079980E 03 | 0.10458029E-10 | 0.10420388E-10 |
| 0.28439990E 03 | 0.11207482E-10 | 0.11217656E-10 |
| 0.28799976E 03 | 0.12082622E-10 | 0.12130941E-10 |
| 0.29159985E 03 | 0.13163772E-10 | 0.13182498E-10 |
| 0.29519995E 03 | 0.14446341E-10 | 0.14400069E-10 |
| 0.29879980E 03 | 0.15874288E-10 | 0.15818527E-10 |
| 0.30239990E 03 | 0.17466056E-10 | 0.17482085E-10 |
| 0.30599976E 03 | 0.19368868E-10 | 0.19447277E-10 |
| 0.30959985E 03 | 0.21751892E-10 | 0.21787058E-10 |
| 0.31319995E 03 | 0.24668309E-10 | 0.24596380E-10 |
| 0.31679980E 03 | 0.28092279E-10 | 0.27999811E-10 |
| 0.32039990E 03 | 0.32129480E-10 | 0.32161884E-10 |
| 0.32399976E 03 | 0.37146175E-10 | 0.37300635E-10 |
| 0.32759985E 03 | 0.43618734E-10 | 0.43704623E-10 |
| 0.33119995E 03 | 0.51870230E-10 | 0.51751103E-10 |
| 0.33479980E 03 | 0.62081423E-10 | 0.61918012E-10 |
| 0.33839990E 03 | 0.74657489E-10 | 0.74767581E-10 |
| 0.34199976E 03 | 0.90442459E-10 | 0.90848037E-10 |
| 0.34559985E 03 | 0.11013050E-09 | 0.11040494E-09 |
| 0.34919995E 03 | 0.13292510E-09 | 0.13274931E-09 |
| 0.35279980E 03 | 0.15549681E-09 | 0.15528677E-09 |
| 0.35639990E 03 | 0.17250240E-09 | 0.17295085E-09 |
| 0.35999976E 03 | 0.17886860E-09 | 0.17977643E-09 |

Suppose one match point, $P_1$, is chosen along the line $\ell_1$ and another, $P_2$, along $\ell_2$ both in the region of positive charge. Using symmetry the potential at $P_1$ due to the cosine distribution on wire 1 is the same as the potential at $P_2$. Also, since $P_1$ and $P_2$ are symmetrically disposed with respect to the distribution on wire 2, the potentials at these points due to the distribution on wire 2 will again be equal. Similarly, the potentials at $P_1$ and $P_2$ due to all terms originally assumed in the Fourier Series will be the same. Hence, simultaneously choosing $P_1$ and $P_2$ as match points yields two identical rows in the $\underset{\sim}{D}$ matrix, and thus, $\underset{\sim}{D}$ will be singular. In this case, the system of equations

$$\underset{\sim}{D}\underline{\sigma} = \underline{V}$$

will not possess a unique solution. Consequently, one cannot choose match points which possess the relationship exhibited by $P_1$ and $P_2$.

With the above in mind, a procedure was devised whereby the match points selected would always yield a non-singular $\underset{\sim}{D}$. Initially each wire was divided into NF equal sectors with the match points being chosen where the sector cut the boundary of the wire. Then, all the match points were rotated counter-clockwise by 180/(NF+1) degrees. This procedure is illustrated in Figure 4-3 for NF=3. An advantage of this technique is that the structure of $\underset{\sim}{D}$ will be

$$\begin{bmatrix} \underset{\sim}{A} & \underset{\sim}{B} \\ \underset{\sim}{C} & \underset{\sim}{A} \end{bmatrix},$$

and thus, only $3X(NF)^2$ terms need to be generated thus saving computer time. For a system of n identical bare wires arbitrarily spaced,

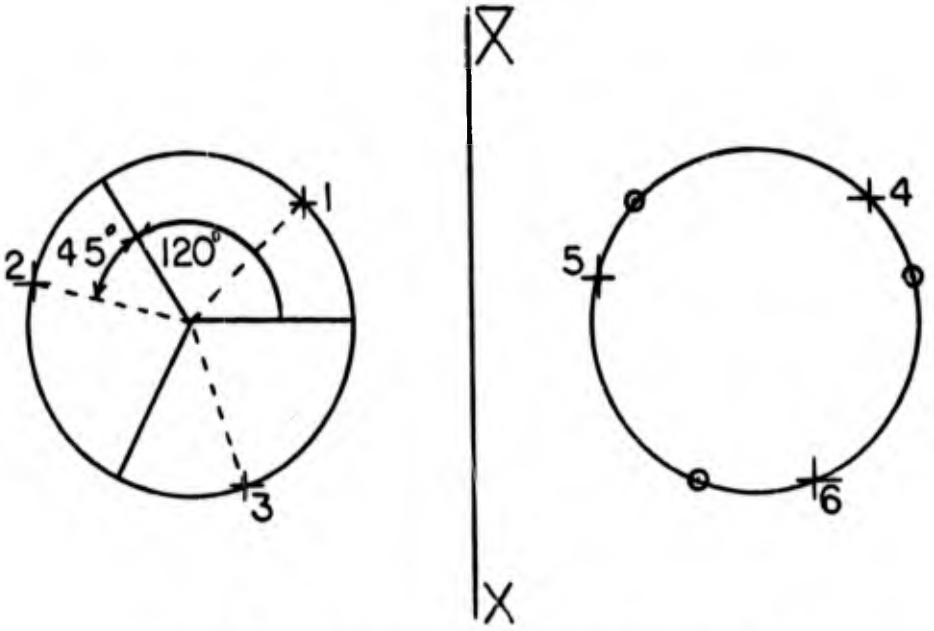


Fig. 4-4. -- Match point selection for NF=3.

selection of the match points by this method will yield $\underline{D}$ in the partitioned form

$$\begin{bmatrix} \underline{A} & & \\ & \underline{A} & \\ & & \ddots \\ & & & \underline{A} \end{bmatrix}$$

reducing the number of terms to be generated by $(n-1)x(NF)^2$.

Some peculiar behavior has been observed, however, when match points are chosen in this manner. The results in Appendix D show that with odd numbers of Fourier Coefficients the capacitance converges much faster. For example: with D/R=2.1, and NF=13, the capacitance is accurate to four decimal places. But, an examination of the first Fourier coefficient in Table 4-2 shows that the total charge on wire 2 is not equal in magnitude and opposite in sign to that on wire 1. Furthermore as the other Fourier coefficients are not equal in magnitude

the charge distribution, shown on p. D-21, will not be symmetrical with respect to the plane $x-\bar{x}$ of Figure 4-3. In this respect, values of capacitance obtained with small, odd values of NF are deceiving. As NF increases and remains odd, the total charge and the

TABLE 4-2

FOURIER COEFFICIENTS FOR
NF=3 AND D/R=2.1

| Wire 1 | Fourier Coeff. | Wire 2 | Fourier Coeff. |
|---|---|---|---|
| 1 | $.230140558X10^{-10}$ | 1 | $-.212405613X10^{-10}$ |
| 2 | $.259771906X10^{-10}$ | 2 | $.308622284X10^{-10}$ |
| 3 | $.136121991X10^{-10}$ | 3 | $-.166685021X10^{-10}$ |

TABLE 4-3

FOURIER COEFFICIENTS FOR
NF=4 AND D/R=2.1

| Wire 1 | | Wire 2 | |
|---|---|---|---|
| 1 | $.208034458X10^{-10}$ | 1 | $-.208034458X10^{-10}$ |
| 2 | $.263266360X10^{-10}$ | 2 | $.263266360X10^{-10}$ |
| 3 | $.161488055X10^{-10}$ | 3 | $-.161488055X10^{-10}$ |
| 4 | $.828778084X10^{-11}$ | 4 | $.828778084X10^{-11}$ |

charge distribution balance. In contrast, Table 4-3 shows that for small, even values of NF the total charge on the two wires is equal in magnitude and opposite in sign. The plot on p. D-24 shows that the charge distribution is exactly symmetrical about the plane $x-\bar{x}$ of Figure 4-3. This behavior is the same for all even values of NF.

Another method which may have been used for match point selection is the "image match point method." In this case, match points on wire 2 are selected as the images of those on wire 1 as determined by the plane of symmetry $x-\bar{x}$ in Figure 4-3. The circles on wire 2 are the images match points of the "+" on wire 1. An example of this method was done with D/R=2.1 while NF was varied from 1 to 25. These results are listed in Table 4-4 and show good convergence and overall smoothness.

TABLE 4-4

IMAGE MATCH POINT METHOD

| NF | APPROX. CAPACITANCE |
|---|---|
| 1 | .3290720 |
| 2 | .4581047 |
| 3 | .5675086 |
| 4 | .6535595 |
| 5 | .7187460 |
| 6 | .7667450 |
| 7 | .8013263 |
| 8 | .8258450 |
| 9 | .8430377 |
| 10 | .8550077 |
| 11 | .8633072 |
| 12 | .8690505 |
| 13 | .8730231 |
| 14 | .8757722 |
| 15 | .8776768 |
| 16 | .8789983 |
| 17 | .8799167 |
| 18 | .8805559 |
| 19 | .8810017 |
| 20 | .8813130 |
| 21 | .8820621 |
| 22 | .8816833 |
| 23 | .8820538 |
| 24 | .8818654 |
| 25 | .8820494 |

This particular method, however, destroys the previous structure of the $\underset{\sim}{D}$ matrix, and furthermore, is limited to systems possessing a plane of symmetry. Systems involving symmetry are treated in Adams [22,23] by taking advantage of the symmetry in order reduce the size of the $\underset{\sim}{D}$ matrix. Thus, the example given here merely serves as an illustration.

In conclusion, it has been determined that the Fourier Series gives much better results than the technique used in Chapters 2 and 3. The Fourier Series is also sensitive to match point selection and certain selections of match points will reduce the amount of work necessary in solving systems not possessing planes of symmetry. Finally, since the Fourier Series yields such good results, an extension to arbitrarily excited multiconductor bare wire systems is now made.

## 4.5 Multiconductor Bare Wire Systems and the Capacitance Matrix

Shown in Figure 4-4 is a system consisting of n bare wires. From Chapter 1 the relationship among the voltages and charges of the

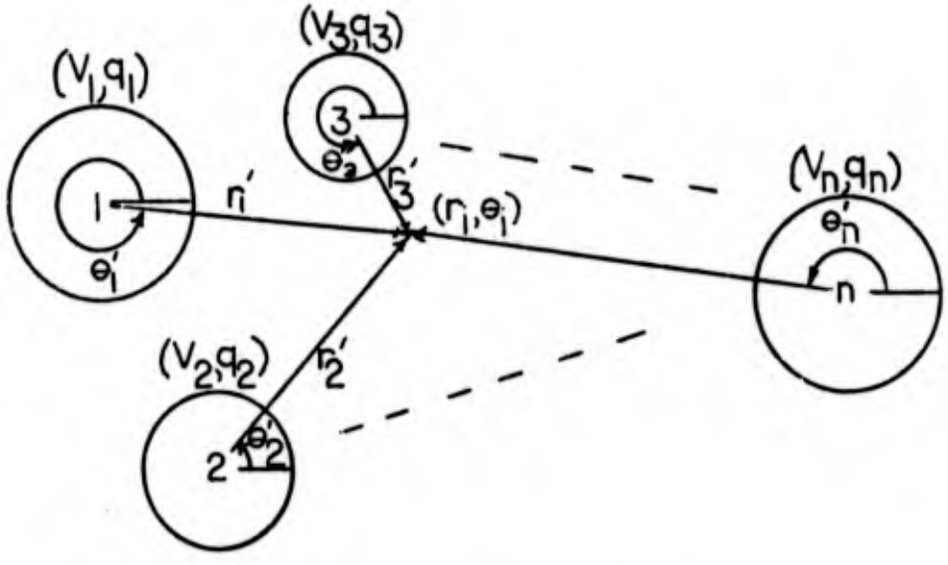


Fig. 4-5. -- A system of n arbitrarily excited bare wires.

conductors is written in the matrix form

$$\begin{bmatrix} q_1 \\ \cdot \\ \cdot \\ \cdot \\ q_n \end{bmatrix} = \begin{bmatrix} C_{11} & C_{12} & \cdots & C_{1n} \\ C_{12} & & & \cdot \\ \cdot & & & \cdot \\ C_{1n} & & \cdots & C_{nn} \end{bmatrix} \begin{bmatrix} V_1 \\ V_2 \\ \cdot \\ \cdot \\ V_n \end{bmatrix} \qquad (4\text{-}37)$$

or

$$q = \underset{\sim}{C}\, \underline{V} \qquad (4\text{-}38)$$

where $\underset{\sim}{C}$ is defined to be the capacitance matrix. Thus, a relationship of the form of equation (4-37) is sought and can be obtained using the methods of Section 4.3.

Referring again to Figure 4-4, let the charge distribution over each conductor be expressed as a 2k+1 term Fourier Series. Then, denote

$$\sigma^N(r'_N,\theta'_N) = \sigma_o^N + \sum_{j=1}^{k} (\sigma_j^N \cos \theta'_N + \hat{\sigma}_j^N \sin \theta'_N) \qquad (4\text{-}39)$$

as the charge distribution on wire N with respect to a cylindrical coordinate system at the center of wire N. Using the superposition of potentials from all charge distributions, the potential at a field point $(r_i,\theta_i)$ is:

$$\phi(r_i,\theta_i) = \sum_{N=1}^{n} \phi^N(r_N,\theta_N), \qquad (4\text{-}40)$$

where

$$\phi^N(r_N,\theta_N) = D_{11}^N \sigma_0^N + \sum_{j=1}^{k} (D_{i(j+1)}^N \sigma_j^N + \hat{D}_{i(j+1)}^N \hat{\sigma}_j^N \qquad (4\text{-}41)$$

$$D_{11}^{N} = -r_N' \frac{\log r_N}{\varepsilon_0}, \tag{4-42}$$

$$D_{i(j+1)}^{N} = \frac{1}{2\varepsilon_0} \frac{(r_N')^{j+1} \cos j\theta_N'}{j r_N^j}, \tag{4-43}$$

and

$$\hat{D}_{i(j+1)}^{N} = \frac{1}{2\varepsilon_0} \frac{(r_N')^{j+1} \sin j\theta_N'}{j r_N^j}. \tag{4-44}$$

Combining equation (4-40) and (4-41),

$$\phi(r_i,\theta_i) = \sum_{N=1}^{n} (D_{11}^{N} \sigma_0^{N} + \sum_{j=1}^{k} (D_{i(j+1)}^{N} \sigma_j^{N} + \hat{D}_{i(j+1)} \hat{\sigma}_j^{N}) \tag{4-45}$$

Equation (4-44) is now one equation in terms of n×(2k+1) unknowns, and thus, by selecting 2k+1 distinct match points on each conductor and writing equation (4-44) for each point, a set of equations in matrix form results. These are:

$$\begin{bmatrix} \underset{\sim}{D}_{11} & \underset{\sim}{D}_{12} & \cdots & \underset{\sim}{D}_{1n} \\ \underset{\sim}{D}_{21} & & & \underset{\sim}{D}_{2n} \\ \vdots & & & \vdots \\ \underset{\sim}{D}_{n1} & \underset{\sim}{D}_{n2} & \cdots & \underset{\sim}{D}_{nn} \end{bmatrix} \begin{bmatrix} \underline{\sigma}_1 \\ \underline{\sigma}_2 \\ \vdots \\ \underline{\sigma}_n \end{bmatrix} = \begin{bmatrix} \underline{V}_1 \\ \underline{V}_2 \\ \vdots \\ V_n \end{bmatrix} \tag{4-46}$$

where each (2k+1)x(2k+1) submatrix $\underset{\sim}{D}_{MN}$ relates the sources on wire N to the match points on wire M. A typical submatrix is

$$\underline{\underline{D}}_{MN} = \begin{bmatrix} D_{11}^{MN} & D_{12}^{MN} & \cdots & D_{1(k+1)}^{MN} & \hat{D}_{12}^{MN} & \cdots & \hat{D}_{1(k+1)}^{MN} \\ D_{21}^{MN} & D_{22}^{MN} & & D_{2(k+1)}^{MN} & \hat{D}_{22}^{MN} & & \hat{D}_{2(k+1)}^{MN} \\ \vdots & & & & & & \vdots \\ D_{(2k+1)1}^{MN} & \cdots & & D_{(2k+1)(k+1)}^{MN} & \hat{D}_{(2k+1)2}^{MN} & \cdots & \hat{D}_{(2k+1)(k+1)}^{MN} \end{bmatrix} . \tag{4-47}$$

The vectors $\underline{\sigma}_N$ and $\underline{V}_M$ are:

$$\underline{\sigma}_N = \begin{bmatrix} \sigma_0^N \\ \vdots \\ \sigma_k^N \\ \hat{\sigma}_1^N \\ \vdots \\ \hat{\sigma}_k^N \end{bmatrix}, \text{ and } \underline{V}_M = \begin{bmatrix} V_M \\ V_M \\ V_M \\ \\ \vdots \\ V_M \end{bmatrix} . \tag{4-48}$$

Thus, a set of matrix equations of the form

$$\underline{\underline{D}}\underline{\sigma} = \underline{V} \tag{4-49}$$

is obtained. Solving equation (4-49) by matrix inversion now yields, in partitioned submatrix form,

$$\begin{bmatrix} \underline{\sigma}_1 \\ \underline{\sigma}_2 \\ \vdots \\ \underline{\sigma}_n \end{bmatrix} \quad \begin{bmatrix} \underline{T}_{11} & \underline{T}_{12} & \cdots & \underline{T}_{1n} \\ \vdots & & & \\ \underline{T}_{n1} & \cdots & & \underline{T}_{nn} \end{bmatrix} \begin{bmatrix} \underline{V}_1 \\ \underline{V}_2 \\ \vdots \\ \underline{V}_n \end{bmatrix} , \qquad (4\text{-}50)$$

where $\underline{T} = \underline{D}^{-1}$. Recall from equation (4-38) that a relationship between the voltages and the total charges on all the conductors is necessary in order to determine the capacitance matrix. This relationship can be obtained from equation (4-50) by first recognizing that the total charge per unit length on each conductor will be simply the average value of the Fourier Series charge distribution times the circumference of that conductor i.e.,

$$\begin{aligned} q_1 &= 2\pi R_1 \, \sigma_0^1 \\ q_2 &= 2\pi R_2 \, \sigma_0^2 \\ &\vdots \\ q_n &= 2\pi R_n \, \sigma_0^n \end{aligned} \qquad (4\text{-}51)$$

, or in terms of the values in $\underline{T}$,

$$\begin{aligned} q_1 &= 2\pi R_1 \left( \sum_{j=1}^{2k+1} T_{1j}^{11} V_1 + \sum_{j=1}^{2k+1} T_{1j}^{12} V_2 + \ldots + \sum_{j=1}^{2k+1} T_{1j}^{1n} V_n \right) \\ q_2 &= 2\pi R_2 \left( \sum_{j=1}^{2k+1} T_{1j}^{21} V_1 + \sum_{j=1}^{2k+1} T_{1j}^{22} V_2 + \ldots + \sum_{j=1}^{2k+1} T_{1j}^{2n} V_n \right) \\ &\vdots \\ q_n &= 2\pi R_n \left( \sum_{j=1}^{2k+1} T_{1j}^{n1} V_1 + \sum_{j=1}^{2k+1} T_{1j}^{n2} V_2 + \ldots + \sum_{j=1}^{2k+1} T_{1j}^{nn} V_n \right) \end{aligned} \qquad (4\text{-}52)$$

and thus each term in the capacitance matrix is

$$c_{ij} = 2\pi R_i \sum_{m=1}^{2k+1} T_{1m}^{ij} . \qquad (4\text{-}53)$$

In words, equation (4-53) says that in order to determine the $(ij)^{th}$ value of capacitance go to the $(ij)^{th}$ submatrix of $\underset{\sim}{T} = \underset{\sim}{D}^{-1}$ and add up all the terms in the first row. Thus, equation (4-52) is the desired form indicated by equation (4-38).

# CHAPTER V

# The Application of the Fourier Series to Problems Involving Dielectrics

## 5.1 Introduction

The ultimate goal of this text is to present a procedure for the computation of the capacitance matrix for systems of dielectric-coated wires. The methods of Chapters 2 and 3 have proven inadequate for generalization to multi-wire systems due to relatively poor results obtained when these methods were applied to the simple two bare wire case. Thus, generalization of the polygonal and the circular strips approximation would be merely academic. In contrast, the Fourier Series approximation yielded very good results for two bare wires and in Section 4.5 was extended to multiconductor bare wire systems. Now with a few additional equations and another boundary condition the results of Chapter 4 can be expanded to take into account dielectric coating.

Since the introduction of dielectrics around the wires increases the number of parameters affecting the solution, this chapter begins with a general analysis of two dielectric-coated wires. Then, some results for this case are presented. Finally, the procedure is generalized to the computation of the capacitance matrix for a system of arbitrarily excited dielectric-coated wires.

## 5.2 Two Dielectric Coated Wires

Consider Figure 5-1 where two wires coated by linear, homogeneous, and isotropic dielectrics are shown. The relative dielectric constants $\epsilon_{R1}$ and $\epsilon_{R2}$

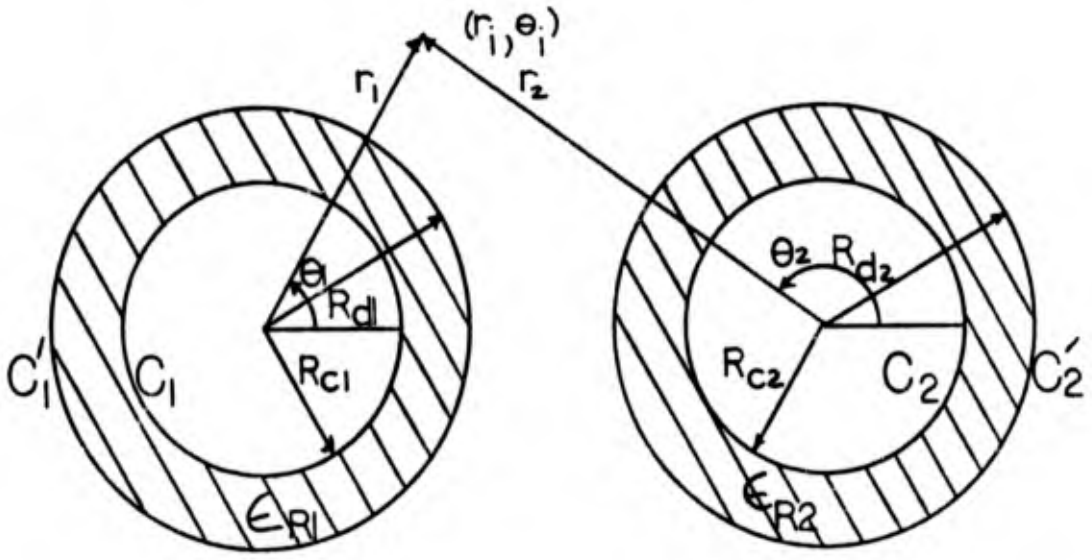


Fig. 5-1. -- Two dielectric-coated wires.
Unprimed quantities identify the conductor boundaries
and primed quantities identify the dielectric boundaries.

completely specify the dielectric properties and $R_{d1}$, $R_{d2}$, $R_{c1}$, and $R_{c2}$ specify the geometry of the wires. It is well-known that the addition of a dielectric material into an electric field produces in effect a net drift of charge to the surfaces of the dielectric. This effect is characterized by a surface distribution of bound charge, where bound charge is distinguished from free charge which may arise on conductor surfaces in free space. The potential and electric fields produced are functions of the total (bound plus free) charge. Thus, a matrix equation can be formulated as follows: (1) replace the dielectric boundaries with 2k+1 term Fourier Series distributions of bound charge; replace the conductor-dielectric boundary with 2k+1 term Fourier Series distributions of total charge; (2) choose 2k+1 match points along each of the surfaces in (1); and, (3) force

the potential to be constant at match points on the conductor boundaries, and force the normal component of the displacement vector D = εE to be continuous across the dielectric boundaries.

The matrix equation which results will appear in the partitioned form

$$\begin{bmatrix} \underset{\sim}{D}_{11} & \underset{\sim}{D}_{12} & \underset{\sim}{D}_{11'} & \underset{\sim}{D}_{12'} \\ \underset{\sim}{D}_{21} & \underset{\sim}{D}_{22} & \underset{\sim}{D}_{21'} & \underset{\sim}{D}_{22'} \\ \underset{\sim}{D}_{1'1} & \underset{\sim}{D}_{1'2} & \underset{\sim}{D}_{1'1'} & \underset{\sim}{D}_{1'2'} \\ \underset{\sim}{D}_{2'1} & \underset{\sim}{D}_{2'2} & \underset{\sim}{D}_{2'1'} & \underset{\sim}{D}_{2'2'} \end{bmatrix} \begin{bmatrix} \underline{\sigma}_1 \\ \underline{\sigma}_2 \\ \underline{\sigma}'_1 \\ \underline{\sigma}'_2 \end{bmatrix} = \begin{bmatrix} \underline{V}_1 \\ \underline{V}_2 \\ \underline{0} \\ \underline{0} \end{bmatrix} , \qquad (5\text{-}1)$$

where $\underline{\sigma}_1$ and $\underline{\sigma}_2$ are vectors of length 2k+1 containing the Fourier coefficients of combined free and bound charge densities on the conductor-dielectric boundaries, and $\underline{\sigma}'_1$ and $\underline{\sigma}'_2$ are vectors of length 2k+1 containing the Fourier coefficients of bound charge densities on the dielectric boundaries. $\underline{V}_1$ and $\underline{V}_2$ are also vectors of length 2k+1 which establish the potential boundary conditions on the conductors. Each (2k+1)x(2k+1) submatrix $\underset{\sim}{D}_{MN}$ above the dashed line contains the potentials on conductor M due to unit magnitude sources along boundary N, where M=1,2, and N=1,2,1',2' consistent with Figure 5-1. Each (2k+1)x(2k+1) submatrix $\underset{\sim}{D}_{MN}$ below the dashed line contains the difference between the displacement vector D=εE just inside and just outside the match points on boundary M due to the sources on the boundaries N, where M=1'2', and N=1,2,1',2'. The distinction of "just inside" or "just outside" has special significance when the match points fall on the same surface as the sources because the electric field changes by $\rho_s/\varepsilon_0$ as a field point passes through a charged surface of $\rho_s$ coulombs per square meter in free space.

As in Chapter 4, a matrix equation

$$\begin{bmatrix} q_{1f} \\ q_{2f} \end{bmatrix} = \begin{bmatrix} c_{11} & c_{12} \\ c_{21} & c_{22} \end{bmatrix} \begin{bmatrix} V_1 \\ V_2 \end{bmatrix} \tag{5-2}$$

relating the free charge (denoted by the subscript "f") arising on the conductors to the potentials of the conductors is desired since this defines the capacitance matrix $\underset{\sim}{c}$. This relationship can be extracted from the matrix equation

$$\begin{bmatrix} \underline{\sigma}_1 \\ \underline{\sigma}_2 \\ \underline{\sigma}_1' \\ \underline{\sigma}_2' \end{bmatrix} = \begin{bmatrix} \underset{\sim}{T}_{11} & \underset{\sim}{T}_{12} & \underset{\sim}{T}_{11'} & \underset{\sim}{T}_{12'} \\ \underset{\sim}{T}_{21} & \underset{\sim}{T}_{22} & \underset{\sim}{T}_{21'} & \underset{\sim}{T}_{22'} \\ \underset{\sim}{T}_{1'1} & \underset{\sim}{T}_{1'2} & \underset{\sim}{T}_{1'1'} & \underset{\sim}{T}_{1'2'} \\ \underset{\sim}{T}_{2'1} & \underset{\sim}{T}_{2'2} & \underset{\sim}{T}_{2'1'} & \underset{\sim}{T}_{2'2'} \end{bmatrix} \begin{bmatrix} \underline{V}_1 \\ \underline{V}_2 \\ \underline{0} \\ \underline{0} \end{bmatrix} \tag{5-3}$$

which is the solution of equation (5-1) by matrix inversion with $\underset{\sim}{T}=\underset{\sim}{D}^{-1}$. The total (bound + free) charge on the conductors is

$$q_1 = 2\pi R_{c1}\, \sigma_0^1 \tag{5-4}$$

$$q_2 = 2\pi R_{c2}\, \sigma_0^2 \tag{5-5}$$

where $\sigma_0^1$ and $\sigma_0^2$ are the average values of total charge density on conductors 1 and 2 respectively. The bound charge arising on the dielectric boundaries is

$$q_1' = 2\pi R_{d1}\, \sigma_0^{1'} \tag{5-6}$$

$$q_2' = 2\pi R_{d2}\, \sigma_0^{2'} \; . \tag{5-7}$$

The total charge $q_1$ is the free charge on the conductor-dielectric of wire 1 plus an amount of bound charge equal in magnitude but opposite in sign to $q_1'$. The same is true for $q_2$ and $q_2'$. Therefore,

$$q_{1f} = q_1 + q_1' \tag{5-8}$$

and

$$q_{2f} = q_2 + q_2' \ . \tag{5-9}$$

Now, combining equations (5-4), (5-5), (5-6), (5-7), and (5-3), the relationship of equation (5-2) is obtained with

$$c_{11} = 2\pi(R_{c1} \sum_{m=1}^{2k+1} T_{1m}^{11} + R_{d1} \sum_{m=1}^{2k+1} T_{1m}^{1'1}) \tag{5-10}$$

$$c_{12} = 2\pi(R_{c1} \sum_{m=1}^{2k+1} T_{1m}^{12} + R_{d1} \sum_{m=1}^{2k+1} T_{1m}^{1'2}) \tag{5-11}$$

$$c_{21} = 2\pi(R_{c2} \sum_{m=1}^{2k+1} T_{1m}^{21} + R_{d2} \sum_{m=1}^{2k+1} T_{1m}^{2'1}) \tag{5-12}$$

$$c_{22} = 2\pi(R_{c2} \sum_{m=1}^{2k+1} T_{1m}^{22} + R_{d2} \sum_{m=1}^{2k+1} T_{1m}^{2'2}) \ . \tag{5-13}$$

## 5.3 The Potential and Electric Field of a Fourier Series Charge Distribution

In order to compute the fields necessary for the generation of the $\underline{D}$ matrix of Section 5.2, consider Figure 5-2, where

$$\sigma(\theta) = \sigma_0 + \sum_{j=1}^{k} (\sigma_j \cos j\theta' + \hat{\sigma}_j \sin j\theta'). \qquad (5\text{-}14)$$

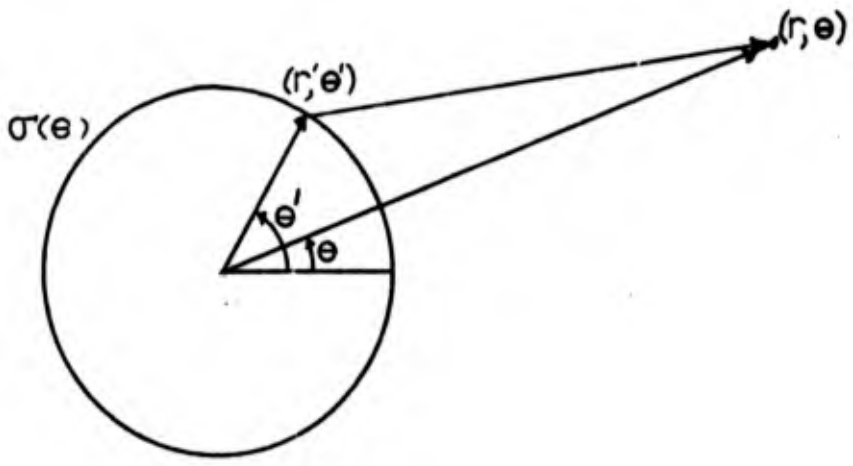


Fig. 5-2. -- A Fourier Series charge distribution.
r'=R.

The potential at a point $(r,\theta)$ with $r>r'$ due to $\sigma(\theta)$ was developed in Chapter 4. For convenience, this expression was

$$\phi(r,\theta) = -\sigma_o \frac{r'\ell n(r)}{\epsilon_0} + \frac{1}{2\epsilon_0} \sum_{j=1}^{k} \sigma_j \frac{(r')^{j+1}\cos j\theta}{jr^j} + \frac{1}{2\epsilon_0} \sum_{j=1}^{k} \hat{\sigma}_j \frac{(r')^{j+1}\sin j\theta}{jr^j} \qquad (5\text{-}15)$$

The electric field for $r>r'$ can be obtained from equation (5-15) using

$$\bar{E}(r,\theta) = -\nabla\phi(r,\theta) \qquad (5\text{-}16)$$

where
$$\nabla = -\frac{\partial}{\partial r}\,\bar{r} - \frac{1}{r}\frac{\partial}{\partial \theta}\,\bar{\theta}. \qquad (5\text{-}17)$$

This gives

$$\bar{E}(r,\theta) = \frac{(r'/r)}{\varepsilon_0}\bar{r} + \frac{1}{2\varepsilon_0}\sum_{j=1}^{k}\sigma_j(r'/r)^{j+1}(\cos j\theta\,\bar{r} + \sin j\theta\,\bar{\theta})$$

$$+ \frac{1}{2\varepsilon_0}\sum_{j=1}^{k}\hat{\sigma}_j(r'/r)^{j+1}(\sin j\theta\,\bar{r} - \cos j\theta\,\bar{\theta}) \qquad (5\text{-}18)$$

Similarly, for $r<r'$,

$$\phi(r,\theta) = \frac{-r'\log(r')}{\varepsilon_0} + \frac{1}{2\varepsilon_0}\sum_{j=1}^{k}\sigma_j\frac{r^j\cos j\theta}{j(r')^{j-1}}$$

$$+ \frac{1}{2\varepsilon_0}\sum_{j=1}^{k}\hat{\sigma}_j\frac{r^j\sin j\theta}{j(r')^{j-1}} \; . \qquad (5\text{-}19)$$

$$\bar{E}(r,\theta) = \bar{0}\;\frac{-1}{2\varepsilon_0}\sum_{j=1}^{k}\sigma_j(r/r')^{j-1}(\cos j\theta\,\bar{r} - \sin j\theta\,\bar{\theta})$$

$$\frac{-1}{2\varepsilon_0}\sum_{j=1}^{k}\hat{\sigma}_j(r/r')^{j-1}(\sin j\theta\,\bar{r} + \cos j\theta\,\bar{\theta}). \qquad (5\text{-}20)$$

All of the terms occurring in the $\underset{\sim}{D}$ matrix will now be identifiable as terms or combinations of the terms in equations (5-15), (5-18), (5-19), and (5-20). Equation (5-20) includes only 2k non-zero terms since the leading term which represents the electric field due to $\sigma_0$ with $r<r'$ will always be zero; however, this zero term must be taken into account when generating the $\underset{\sim}{D}$ matrix, and thus, the zero appears explicitly in equation (5-20).

## 5.4 Two Identical Dielectric-Coated Wires

The method of Section 5.2 is now applied to some problems which have been drawn to scale in Figure 5-3. RW is the wire radius; RD is the dielectric radius; D is the distance between centers; and $\varepsilon_R$ is the relative dielectric constant. The potentials of the wires are set to $V_1 = +1$ and $V_2 = -1$ volt. The match points were selected by the image method given in Chapter 4. The results are given in Appendix E as follows:

(1) each plot of the capacitance versus the number of Fourier components includes the values obtained if the dielectric were not present (with the points are marked by a "+");

(2) each charge distribution plot contains the total charge distribution (with the points marked by an "*") along the conductor-dielectric boundary and the bound charge distribution (with the points marked by a "+") along the free space-dielectric boundary;

(3) the charge distribution with the dielectric removed (at the top of the page).

Overall, the capacitance shows stable and accurate behavior. With NF being limited to 20, the capacitance indicates convergence to 2 digits for the problems of Figure 5-3(a), (b), and (c), while for (d) and (e) the accuracy obtained is 6 and 12 digits respectively. However, the more important observation is that good accuracy is achieved with low values of NF. For example, it is reasonable to assume that the problem in Figure 5-3(a) has 42 picofarads as an upper bound on the

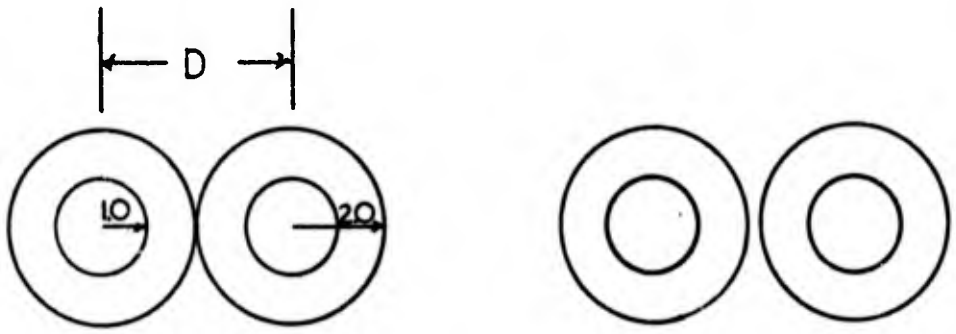


(a) D=4.0, ER=3.0
Rw=1.0, RD=2.0

(b) D=4.1

(c) D=4.2

(d) D=5.0

(e) D=10.0

Fig. 5-3. -- The Geometry of the Problems Solved.

capacitance. Hence, the capacitance obtained with NF=10 is in error by at most 4.4%. Now, if the capacitance matrix for an n-wire bundle (all the wires being identical to the one used here) is desired, then using the Fourier series method with NF=10 should yield approximately 5% accuracy for the entries in the matrix. In many applications this accuracy is sufficient.

The total charge distribution curve along the conductor-dielectric boundary has about the same shape as the distribution that would occur if the dielectric were not present. The only difference is that the total charge now couples positive free charge and negative bound charge and has decreased with the addition of the dielectric. The accuracy of the free charge distribution is about 12 decimal places (D=4.0) as indicated by the capacitance and the results given in Chapter 4; therefore, the total charge distribution should have close to the same accuracy. On the other hand, the bound charge distribution along the free space-dielectric boundary is probably accurate only to 2 decimal places. The steepness of curve and the analysis of Chapter 4 indicate this to be the case. Thus, in order to improve the capacitance, it would be necessary to get a more accurate distribution on this surface. This says that the Fourier series need more terms, but only for the distribution along the free space-dielectric boundary. This presents no problem, however, since the problem could have been formulated this way to begin with.

In summary, it has been found that the Fourier series method shows much promise for generalization to multiple dielectric-coated wire problems. This generalization is now given.

## 5.5 The Dielectric-Coated, Multiwire Case

The methods of Section 5.2 can now be combined with the equations of Section 5.3 to extend this analysis to the dielectric-coated multi-wire case. Consider Figure 5-4 where n arbitrarily excited

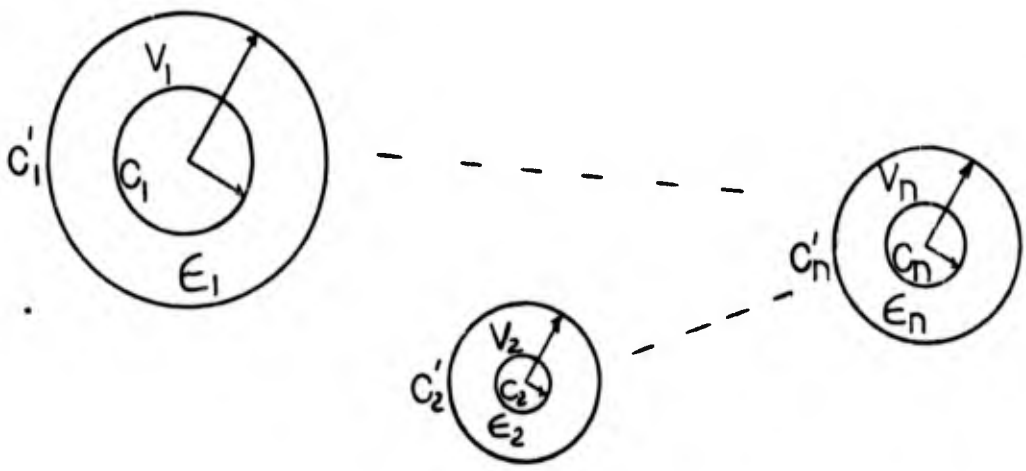


Fig. 5-4. -- n dielectric-coated wires.

dielectric-coated wires are shown. Each dielectric is linear, homogeneous, and isotropic. As in Section 5.2, the procedure begins as follows.

(1) Assume a 2k+1 term Fourier Series distribution to total charge over each boundary $C_j$ with j=1,2,...n.

(2) Assume a 2k+1 term Fourier Series distribution of bound charge over each boundary $C_j'$ with j'=1',2',...n'.

(3) Choose 2k+1 match points on each $C_j$.

(4) Choose 2k+1 match points on each $C_j'$.

(5) Using the equations of Section 5.3, enforce

$$V = V_1 \tag{5-21}$$

at all match points on the conductor boundaries, and

$$\varepsilon_1 E_n^1 - \varepsilon_0 E_n^0 = 0 \qquad (5\text{-}22)$$

at all match points on the dielectric boundaries. $E_n^1$ and $E_n^0$ are the normal components of the electric field just inside and just outside the dielectric respectively. $\varepsilon_0$ is the dielectric constant of free space.

Steps (1) through (5) will produce the matrix equation

$$\begin{bmatrix} \underset{\sim}{D}_{11} & \underset{\sim}{D}_{12} & \cdots & \underset{\sim}{D}_{1n} & \underset{\sim}{D}_{11'} & \cdots & \underset{\sim}{D}_{1n'} \\ \underset{\sim}{D}_{21} & & & \vdots & \vdots & & \vdots \\ \vdots & & & & & & \\ \underset{\sim}{D}_{n1} & \cdots & & \underset{\sim}{D}_{nn} & \underset{\sim}{D}_{n1} & \cdots & \underset{\sim}{D}_{nn'} \\ \hline \underset{\sim}{D}_{1'1} & \cdots & & \underset{\sim}{D}_{1'n} & \underset{\sim}{D}_{1'1'} & \cdots & \underset{\sim}{D}_{1'n'} \\ \vdots & & & \vdots & \vdots & & \vdots \\ \underset{\sim}{D}_{n'1} & \cdots & & \underset{\sim}{D}_{n'n} & \underset{\sim}{D}_{n'1} & \cdots & \underset{\sim}{D}_{n'n'} \end{bmatrix} \begin{bmatrix} \underline{\sigma}_1 \\ \underline{\sigma}_2 \\ \vdots \\ \underline{\sigma}_n \\ \underline{\sigma}'_1 \\ \underline{\sigma}'_2 \\ \vdots \\ \underline{\sigma}'_n \end{bmatrix} = \begin{bmatrix} \underline{V}_1 \\ \underline{V}_2 \\ \vdots \\ \underline{V}_n \\ \underline{0} \\ \underline{0} \\ \vdots \\ \underline{0} \end{bmatrix} \qquad (5\text{-}23)$$

where each (2k+1)x(2k+1) submatrix $\underset{\sim}{D}_{MN}$ above the dashed line represents the potentials on conductor M due to the unit magnitude sources along boundary N. Each (2k+1)x(2k+1) submatrix $\underset{\sim}{D}_{MN}$ below the dashed line represents the difference between the displacement vector D just inside and just outside the dielectric boundary at the match points on M due to unit magnitude sources along boundary N.

From this point, the next step is:

(6) solve equation (5-23) by matrix inversion to obtain the matrix equation

$$\begin{bmatrix} \underline{\sigma}_1 \\ \underline{\sigma}_2 \\ \vdots \\ \underline{\sigma}_n \\ \underline{\sigma}'_1 \\ \underline{\sigma}'_2 \\ \vdots \\ \sigma'_n \end{bmatrix} = \begin{bmatrix} \underline{T}_{11} & \underline{T}_{12} \cdots \underline{T}_{1n} & \underline{T}_{11'} & \underline{T}_{1n'} \\ \vdots & & & \\ \underline{T}_{n1} \cdots \underline{T}_{nn} & \underline{T}_{n1'} \cdots \underline{T}_{nn'} \\ \underline{T}_{1'1} \cdots \underline{T}_{1'n} & \underline{T}_{1'1'} & \underline{T}_{1'n'} \\ \vdots & & & \\ \underline{T}_{n'1} \quad \underline{T}_{n'n} & \underline{T}_{n'1'} & \underline{T}_{n'n'} \end{bmatrix} \begin{bmatrix} \underline{V}_1 \\ \\ \\ \underline{V}_n \\ \underline{0} \\ \underline{0} \\ \underline{0} \\ \underline{0} \end{bmatrix} \qquad (5\text{-}24)$$

from which the capacitance matrix can now be extracted. As in Section 5.2

$$\begin{bmatrix} q_{1f} \\ q_{2f} \\ \vdots \\ q_{nf} \end{bmatrix} = \begin{bmatrix} q_1+q'_1 \\ q_2+q'_2 \\ \vdots \\ q_n+q'_n \end{bmatrix} = 2\pi \begin{bmatrix} R_{c1}\sigma_0^1 + R_{d1}\sigma_0^{1'} \\ R_{c2}\sigma_0^2 + R_{d2}\sigma_0^{2'} \\ \vdots \\ R_{cn}\sigma_0^n + R_{d2}\sigma_0^{n'} \end{bmatrix} . \qquad (5\text{-}25)$$

From equation (5-24)

$$\begin{aligned} \sigma_0^1 &= \sum_{m=1}^{2k+1} (T_{1m}^{11}V_1 + T_{1m}^{12}V_2 + \ldots + T_{1m}^{1n}V_n) \\ \sigma_0^2 &= \sum_{m=1}^{2k+1} (T_{1m}^{21}V_1 + T_{1m}^{22}V_2 + \ldots + T_{1m}^{2n}V_n) \\ &\vdots \\ \sigma_0^n &= \sum_{m=1}^{2k+1} (T_{1m}^{n1}V_1 + T_{1m}^{n2}V_2 + \ldots + T_{1m}^{nn}V_n) \end{aligned} \qquad (5\text{-}26)$$

Also, from equation (5-24)

$$\begin{aligned}
\sigma_0^{1'} &= \sum_{m=1}^{2k+1} (T_{1m}^{1'1} V_1 + T_{1m}^{1'2} V_2 + \ldots + T_{1m}^{1'n} V_n) \\
\sigma_0^{2'} &= \sum_{m=1}^{2k+1} (T_{1m}^{2'1} V_1 + T_{1m}^{2'2} V_2 + \ldots + T_{1m}^{2'n} V_n) \\
&\vdots \\
\sigma_0^{n'} &= \sum_{m=1}^{2k+1} (T_{1m}^{n'1} V_1 + T_{1m}^{n'2} V_2 + \ldots + T_{1m}^{n'n} V_n).
\end{aligned} \tag{5-27}$$

Now, equation (5-26) and (5-27) can be added according to equation (5-25) to yield the desired relationship

$$\begin{bmatrix} q_{1f} \\ q_{2f} \\ \vdots \\ q_{nf} \end{bmatrix} = \begin{bmatrix} c_{11} & c_{12} & \cdots & c_{1n} \\ \vdots & & & \\ & & & \\ c_{n1} & \cdots & & c_{nn} \end{bmatrix} \begin{bmatrix} V_1 \\ V_2 \\ \vdots \\ V_n \end{bmatrix}, \tag{5-28}$$

where

$$c_{ij} = 2\pi \sum_{m=1}^{2k+1} (R_{ci} T_{1m}^{ij} + R_{di} T_{1m}^{i'j}). \tag{5-29}$$

# CHAPTER VI

# CONCLUSIONS

A method which may be used to compute the capacitance matrix of a system of bare or dielectric-coated wires has been presented. The method was obtained as follows:

(1) formulate an approximate method for two bare wires;

(2) compare the results obtained by the approximate method to the exact results which are known for two bare wires;

(3) if the approximate method compares favorably with the exact results for two bare wires, then extend the method to multiwire systems.

In Chapter 2, a two circular conductor system was replaced by a system of two polygonal conductors. This method had the advantage that the entries in the coefficient matrix (the Q matrix) of the matrix equation which approximated the defining integral equation were obtained in closed form. However, the slow convergence of the approximate boundary to the actual boundary limited the accuracy of this method. This limitation led to the second approach taken in Chapter 3 in which the two wires were broken into circular strips instead of polygonal strips. One disadvantage of using circular strips was that the entries in the Q matrix could not be computed in closed form, and as a result,

numerical integration had to be used. The numerical integration caused increased computation time and limited the accuracy to which each term in the D matrix could be computed. Overall, the circular strips method was better than the polygonal strips method, but neither was sufficiently accurate to allow generalization to multiwire systems.

The third method involved the assumption of a Fourier Series charge distribution over the entire circumference of the two wires. This method incorporated the advantages of the polygonal and the circular strips approximation in that the entries in the D matrix were obtained in closed form without altering the boundaries. In addition, the charge distribution at all points on the wire boundaries was accurately obtained using a small number of Fourier Coefficients, a result which was true even when the wires were closely spaced. The polygonal and the circular strips approximations did not yield a good charge distribution over the surfaces of closely spaced wires. Thus, since the results of the Fourier Series method were so good for two wires, the analysis was extended to multi-bare-wire systems. Finally, in Chapter 5, the Fourier Series methods of Chapter 4 were coupled with the concepts of total, free, and bound charge distributions and a method for obtaining the capacitance matrix of multi-dielectric-coated-wire systems was derived. The case of two identical dielectric-coated wires was

solved explicitly thus completing the analysis.

Some of the topics of future interest involve first of all the application of the methods outlined herein to systems of more than two conductors. Other topics might be:

(1) the possible improvement of the capacitance by use of the "Method of Least Squares" [24] or by extrapolation techniques [5];

(2) the optimization of match point selection;

(3) the optimization of computer techniques for the $\underset{\sim}{D}$ matrix generation;

BIBLIOGRAPHY


[1] William H. Hayt, Engineering Electromagnetics. New York: McGraw Hill, 1967

[2] Edward C. Jordan and Keith G. Balmain, Electromagnetic Waves and Radiating Systems. Englewood Cliffs, N.J.: Prentice-Hall, 1967

[3] William R. Smythe, Static and Dynamic Electricity. New York: McGraw Hill, 1950

[4] William T. Weeks, "Calculation of Coefficients of Capacitance of Multiconductor Transmission Lines in the Presence of a Dielectric Interface," IEEE Transactions on Microwave Theory and Techniques, Vol. MTT-16, pp. 925-937, November 1968.

[5] David W. Kammler, "Calculation of Characteristic Admittances and Coupling Coefficients for Strip Transmission Lines," IEEE Transactions on Microwave Theory and Techniques, Vol. MTT-16, pp. 925-937, November 1968

[6] Fung-Yuel Chang, "Transient Analysis of Lossless Coupled Transmission Lines in a Nonhomogeneous Dielectric Medium," IEEE Transactions on Microwave Theory and Techniques, Vol. MTT-18, pp. 616-626, September 1970.

[7] Paul C. Chestnut, "On Determining the Capacitances of Shielded Multicondcutor Transmission Lines," IEEE Transactions on Microwave Theory and Techniques, Vol. MTT-17, pp. 734-745, October 1969

[8] Maruvada P. Sarma and Wasyl Janischewskyj, "Electrostatic Field of a System of Parallel Cylindrical Conductors," IEEE Transactions on Power Apparatus and Systems, Vol. PAS-88, pp. 1069-1079, July 1969

[9] Maruvada P. Sarma, "Application of Moment Methods to the Computation of Electrostatic Fields: Part I - Parallel Cylindrical Conductor Systems," IEEE PES Summer Meeting, San Francisco, Cal., July 1972

[10] Mohamed S. Abou-Seada and Essam Nasser, "Digital Computer Calculation of the Potential and its Gradient of a Twin Cylindrical Conductor," IEEE Transactions on Power Apparatus and Systems, Vol. PAS-88, pp. 1802-1814, December 1969

[11] Warren B. Boast, Vector Fields. New York: Harper and Row, 1964.

[12] Electromagnetic Pulse Handbook for Missles and Aircraft in Flight, Sandia Laboratories, SC-M-710346, Albuquerque, New Mexico, September 1972.

[13] C.R. Paul and J.C. Clements, "Coupled Transmission Lines," IEEE SOUTHEAST-CON, Louisville, Ky., April 1973.

[14] C.R. Paul, "On Uniform Multimode Transmission Lines," IEEE Transactions on Microwave Theory and Techniques, Vol. MTT-21, pp. 556-558, August 1973

[15] C.R. Paul, "Efficient Numerical Computation of the Frequency Response of Cables Illuminated by an Electromagnetic Field," accepted for publication, IEEE Transactions on Microwave Theory and Techniques.

[16] "Focus on Flexible Flat Cables and PC's," Electronic Design, December 1972.

[17] Robert Plonsey and Robert E. Collin, Principles and Applications of Electromagnetic Fields. New York: McGraw Hill, 1961

[18] Thomas J. Higgins and Kenneth G. Black, "Rigorous Determination of the Parameters of Microstrip Transmission Lines," IRE Transactions on Microwave Theory and Techniques, Vol. MTT-3, pp. 93-113, March 1955.

[19] Roger F. Harrington, Field Computation by Moment Methods. New York: Macmillan, 1968.

[20] Herbert B. Dwight, Tables of Integrals and Other Mathematical Data. New York: Macmillan, 1961.

[21] S.D. Conte and Carl de Boor, Elementary Numerical Analysis: An Algorithmic Approach. New York: McGraw Hill, 1965.

[22] Arlon T. Adams and J.R. Mautz, "Computer Solutions of Electrostatic Problems by Matrix Inversion," Proceedings 1969 National Electronics Conference, pp. 198-201.

[23] Arlon T. Adams, Electromagnetics for Engineers. New York: Ronald Press, 1971

[24] Paul M. DeRusso, Rob J. Roy, and Charles M. Close, State Variables for Engineers. New York: John Wiley, 1966

## Appendix A

For two-dimensional problems the charge distribution can be considered to be composed of an infinite number of infinitely long but infinitesimally small filaments of charge. If the total charge is equal to zero, then for every positively charged filament, there will be another filament equal in magnitude and opposite in sign. Consider Figure A-1. The reference point is denoted by $r_0$. The potential at the point r with respect to the reference point is

$$\phi(r) = \frac{-\lambda}{2\pi\epsilon_0} (\ell n(r_1/r_{01}) - \ell n(r_2/r_{02})) \qquad \text{(A-1)}$$

$$= \frac{-\lambda}{2\pi\epsilon_0} (\ell n(r_1/r_2) + \ell n(r_{02}/r_{01})). \qquad \text{(A-2)}$$

As $r_0$ approaches infinity, the ratio $(r_{02}/r_{01})$ becomes unity and thus the last term in equation (A-2) becomes zero. Hence, the reference potential term is dropped from the integral equation.

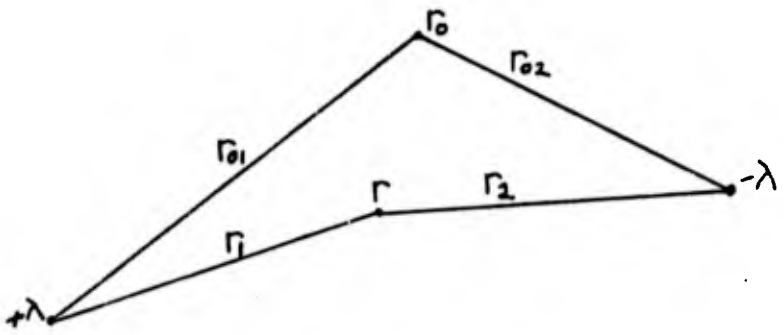


Fig. A-1. -- Two line charges of equal magnitude and opposite sign.

APPENDIX B

POLYGONAL STRIPS DATA

D/R=2.1. The exact capacitance = $0.8820449 \times 10^{-10}$

| NS | Approx. Capac.* | NS | Approx. Capac. |
|---|---|---|---|
| 3 | 0.2615826 | 12 | 0.6814623 |
| 4 | 0.3316383 | 13 | 0.7087031 |
| 5 | 0.4074227 | 14 | 0.7229073 |
| 6 | 0.4552477 | 15 | 0.7423409 |
| 7 | 0.5199159 | 16 | 0.7538670 |
| 8 | 0.5519137 | 17 | 0.7678073 |
| 9 | 0.6028258 | 18 | 0.7771930 |
| 10 | 0.6258819 | 19 | 0.7873501 |
| 11 | 0.6637001 | 20 | 0.7949929 |

*Capacitance values are multiplied by $10^{-10}$.

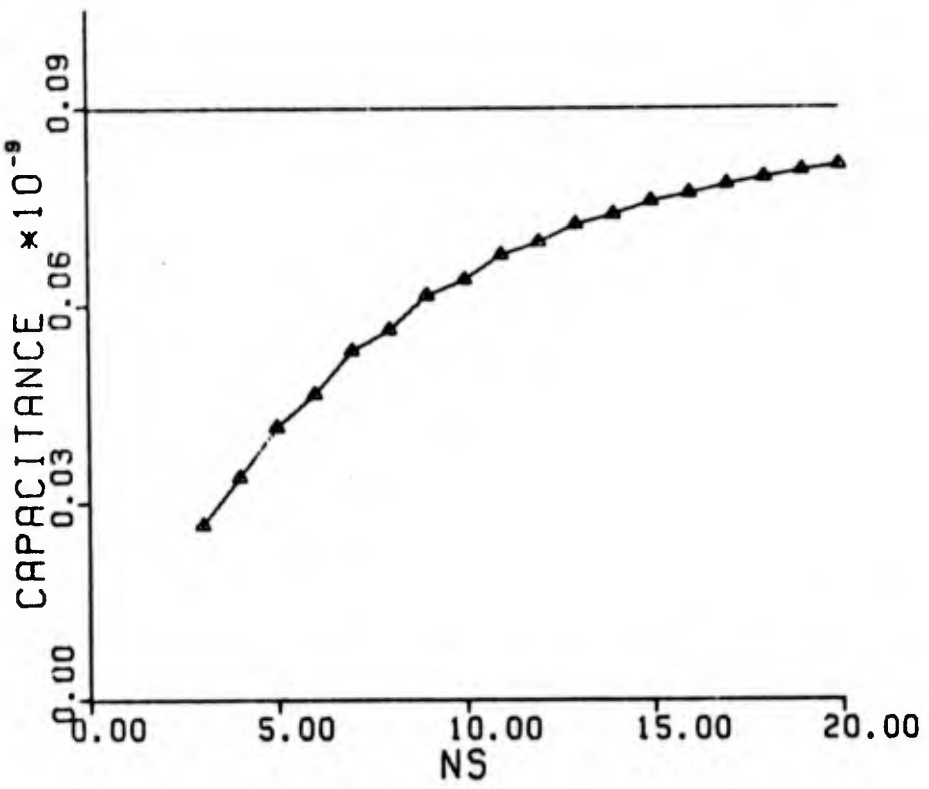

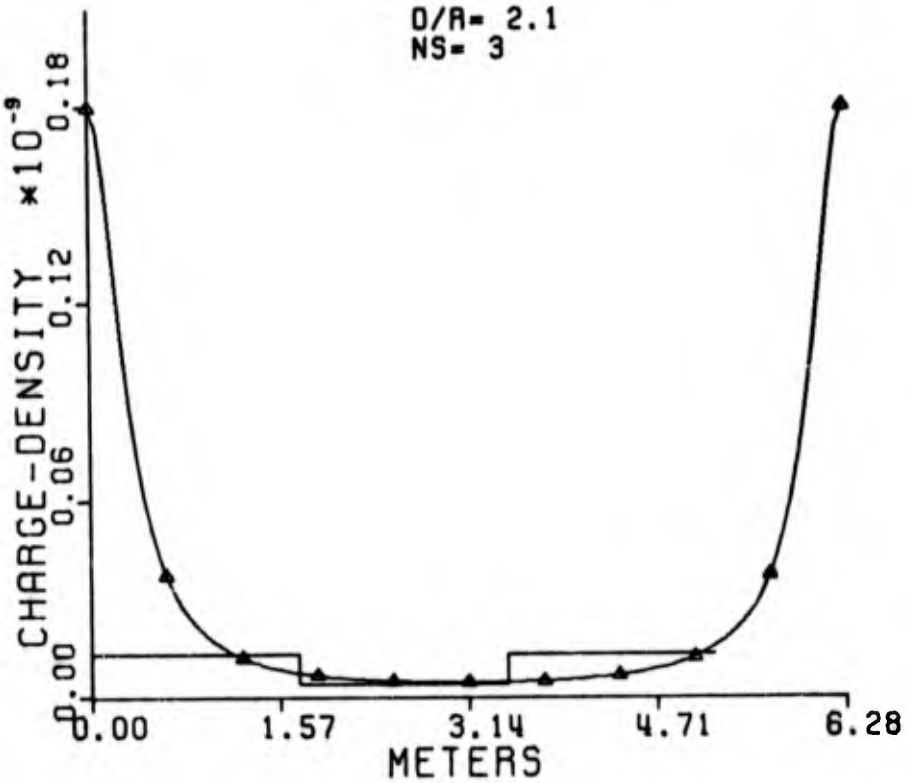
O/R= 2.1
NS= 3
CHARGE-DENSITY *10⁻⁹
0.18
0.12
0.06
0.00
0.00
1.57
3.14
4.71
6.28
METERS

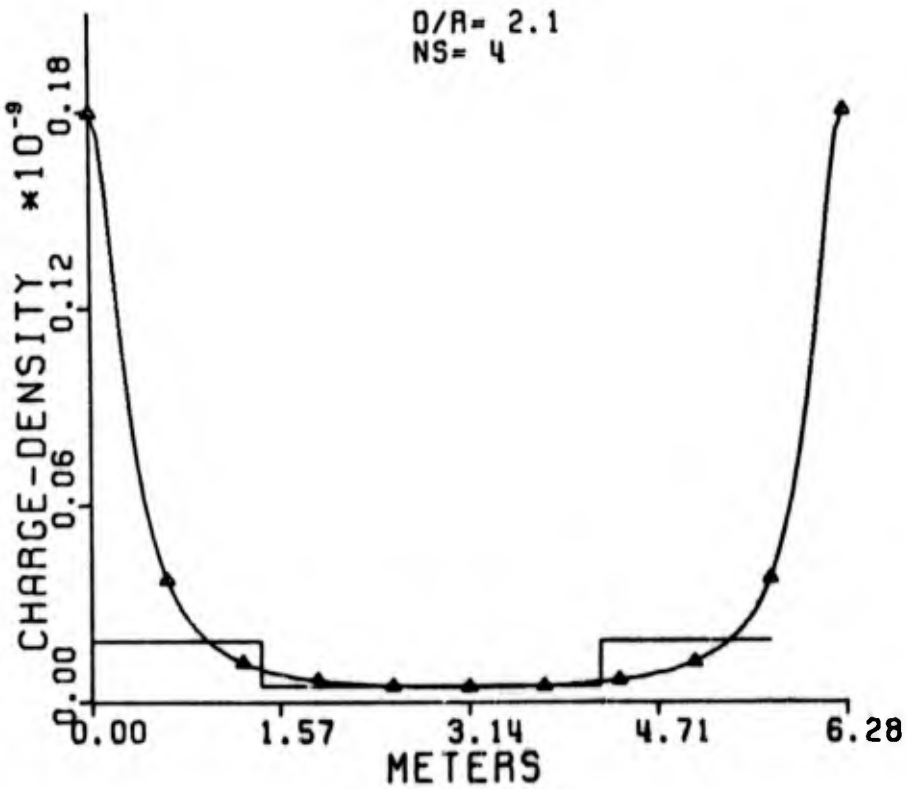
O/R= 2.1
NS= 4
CHARGE-DENSITY *10⁻⁹
0.18
0.12
0.06
0.00
0.00
1.57
3.14
4.71
6.28
METERS

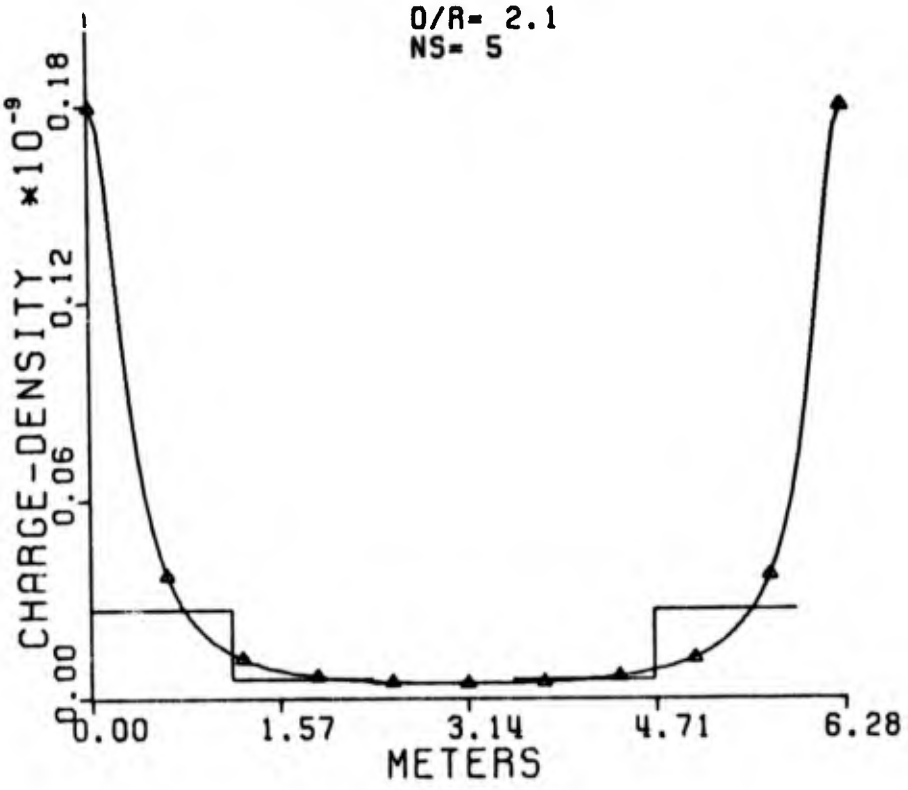
O/R= 2.1
NS= 5
CHARGE-DENSITY *10⁻⁹
0.18
0.12
0.06
0.00
0.00
1.57
3.14
4.71
6.28
METERS

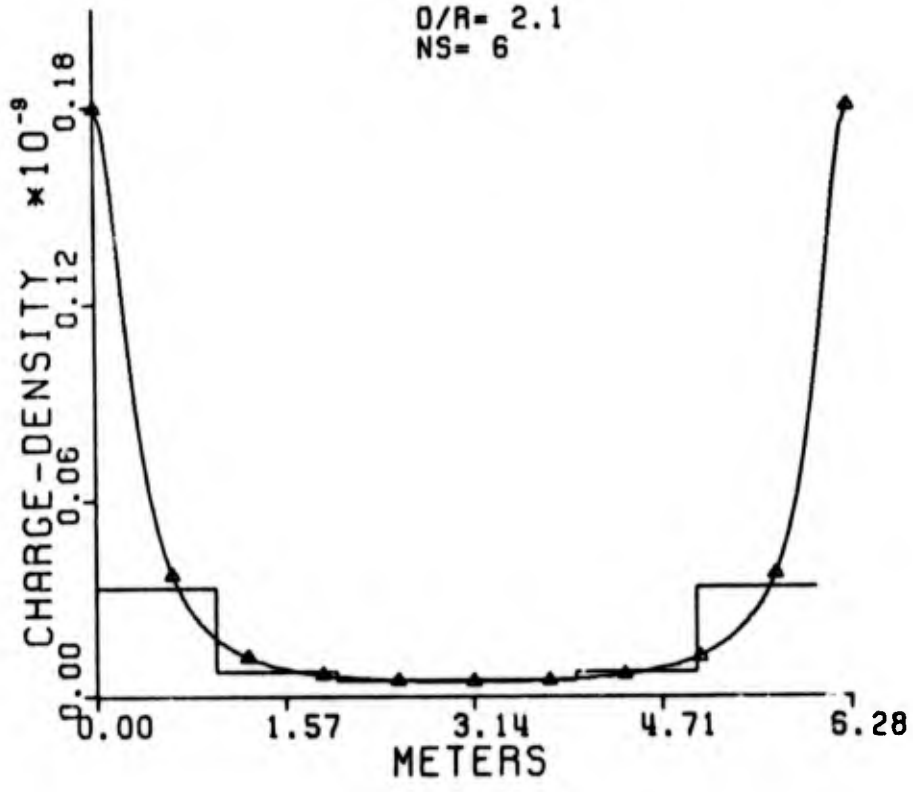
O/R= 2.1
NS= 6
CHARGE-DENSITY *10⁻⁹
0.18
0.12
0.06
0.00
0.00
1.57
3.14
4.71
6.28
METERS

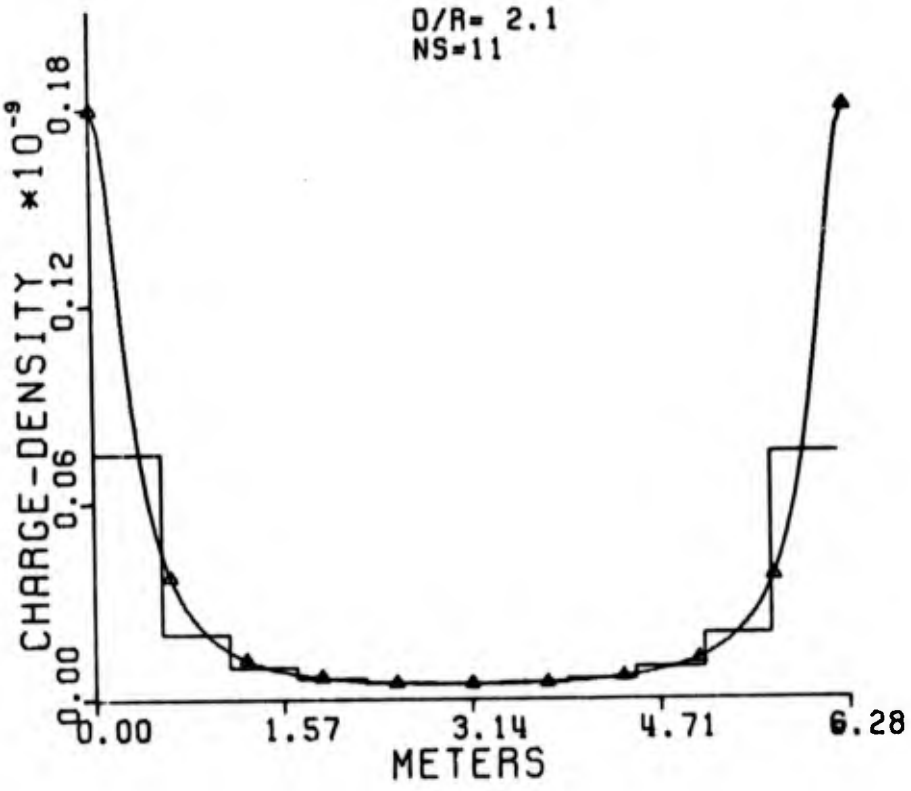
O/R= 2.1
NS=11
CHARGE-DENSITY *10⁻⁹
0.00
0.06
0.12
0.18
0.00
1.57
3.14
4.71
6.28
METERS

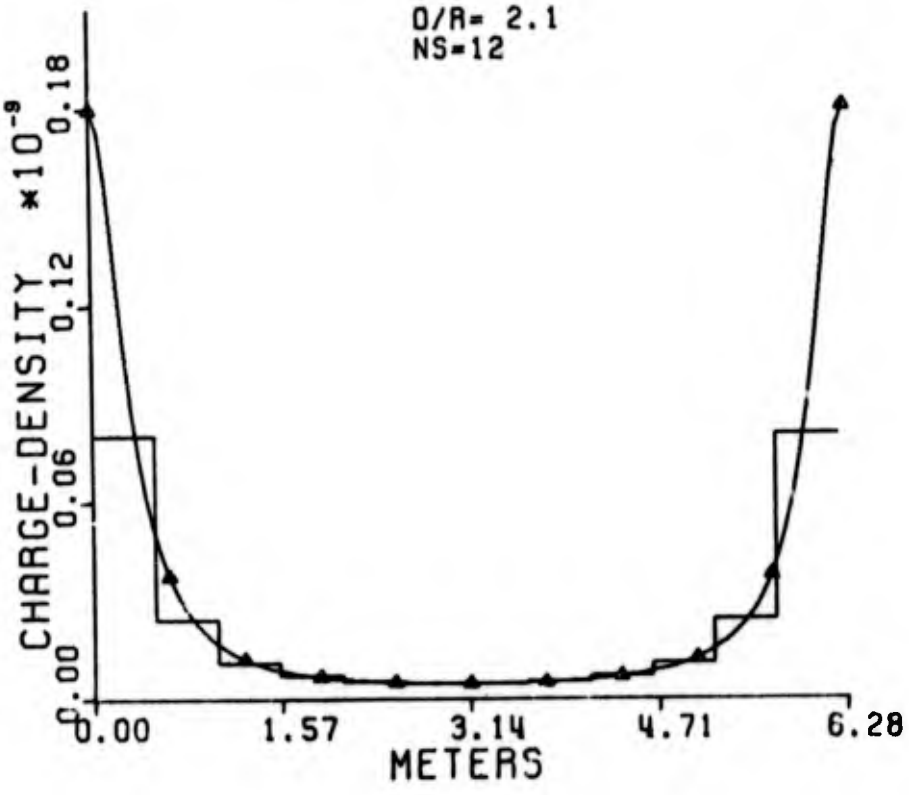
O/R= 2.1
NS=12
CHARGE-DENSITY *10⁻⁹
0.00
0.06
0.12
0.18
0.00
1.57
3.14
4.71
6.28
METERS

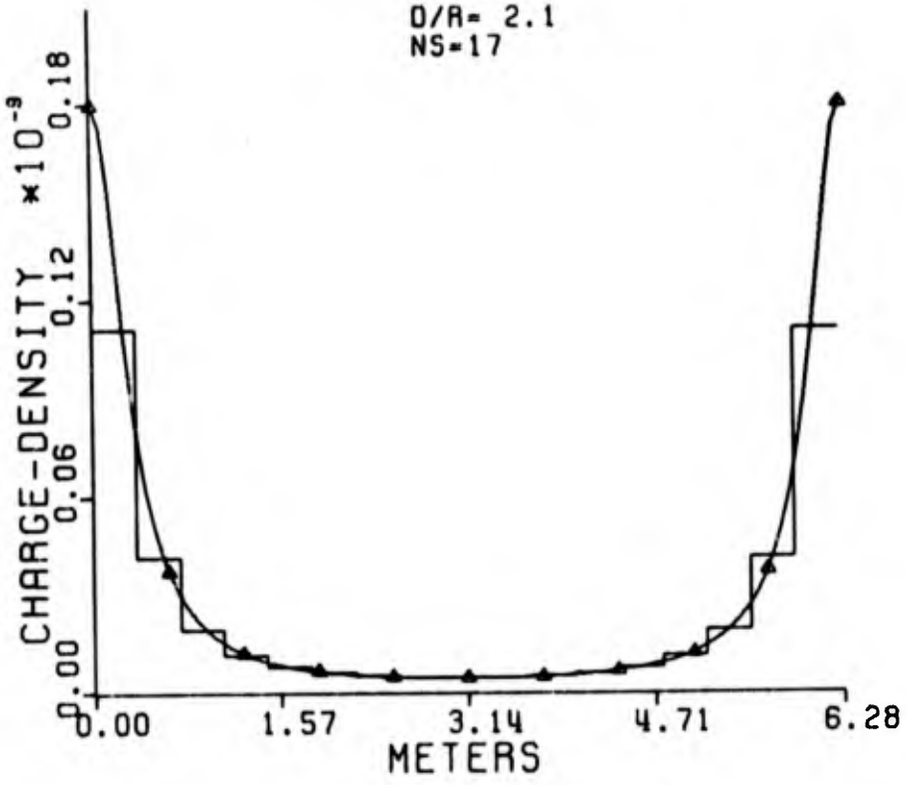
D/R= 2.1
NS=17
CHARGE-DENSITY *10⁻⁹
0.18
0.12
0.06
0.00
0.00
1.57
3.14
4.71
6.28
METERS

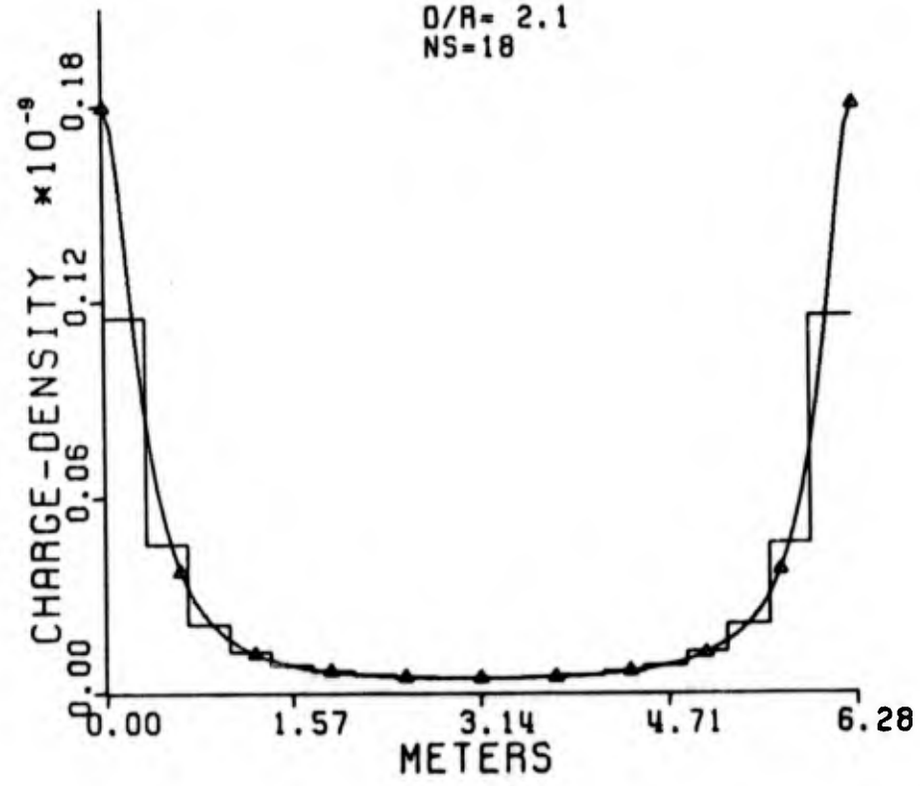
D/R= 2.1
NS=18
CHARGE-DENSITY *10⁻⁹
0.18
0.12
0.06
0.00
0.00
1.57
3.14
4.71
6.28
METERS

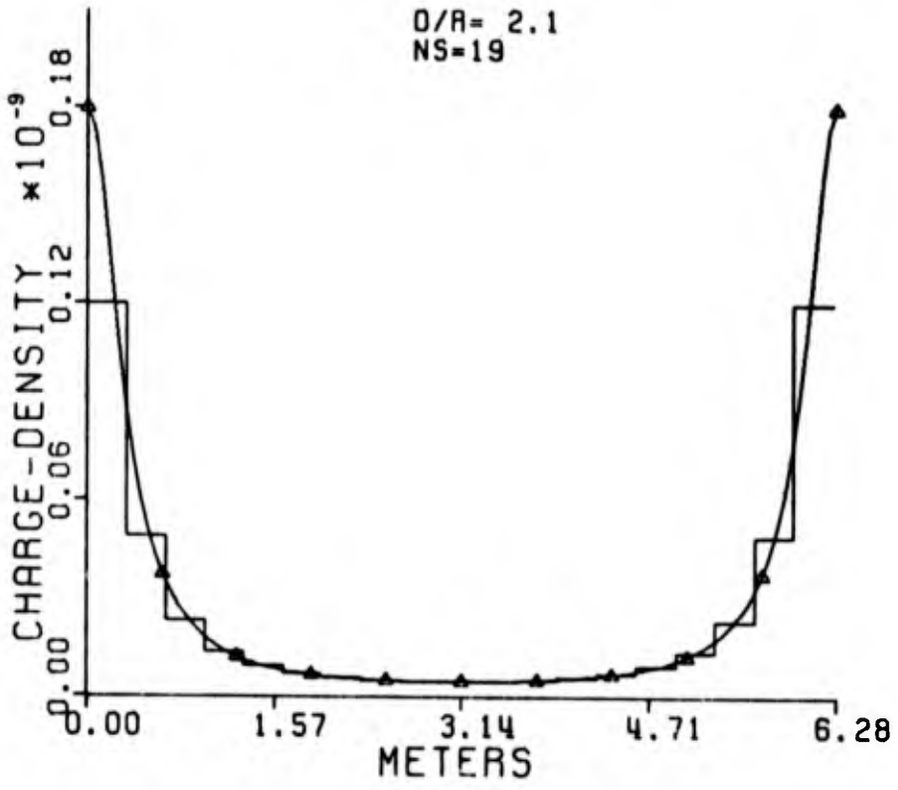
O/A= 2.1
NS=19
CHARGE-DENSITY *10^-9
0.00
0.06
0.12
0.18
0.00
1.57
3.14
4.71
6.28
METERS

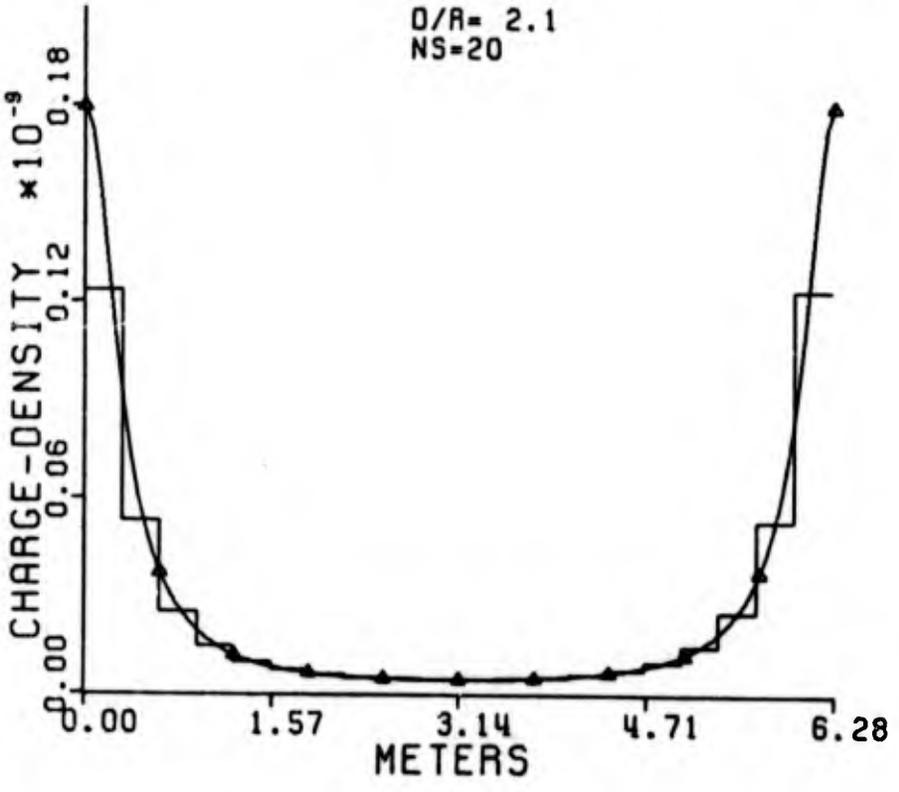
O/A= 2.1
NS=20
CHARGE-DENSITY *10^-9
0.00
0.06
0.12
0.18
0.00
1.57
3.14
4.71
6.28
METERS

POLYGONAL STRIPS

D/R=2.2. The exact capacitance = $.6262345 \times 10^{-10}$

| NS | Approx. Capac.* | NS | Approx. Capac. |
|---|---|---|---|
| 3 | .2483420 | 12 | .5434691 |
| 4 | .3098425 | 13 | .5550066 |
| 5 | .36867960 | 14 | .5628501 |
| 6 | .4067744 | 15 | .5706074 |
| 7 | .4481745 | 16 | .5763606 |
| 8 | .4718354 | 17 | .5817709 |
| 9 | .4991967 | 18 | .5860651 |
| 10 | .5148758 | 19 | .5899776 |
| 11 | .5325495 | 20 | .5932365 |

*Capacitance values are multiplied by $10^{-10}$.

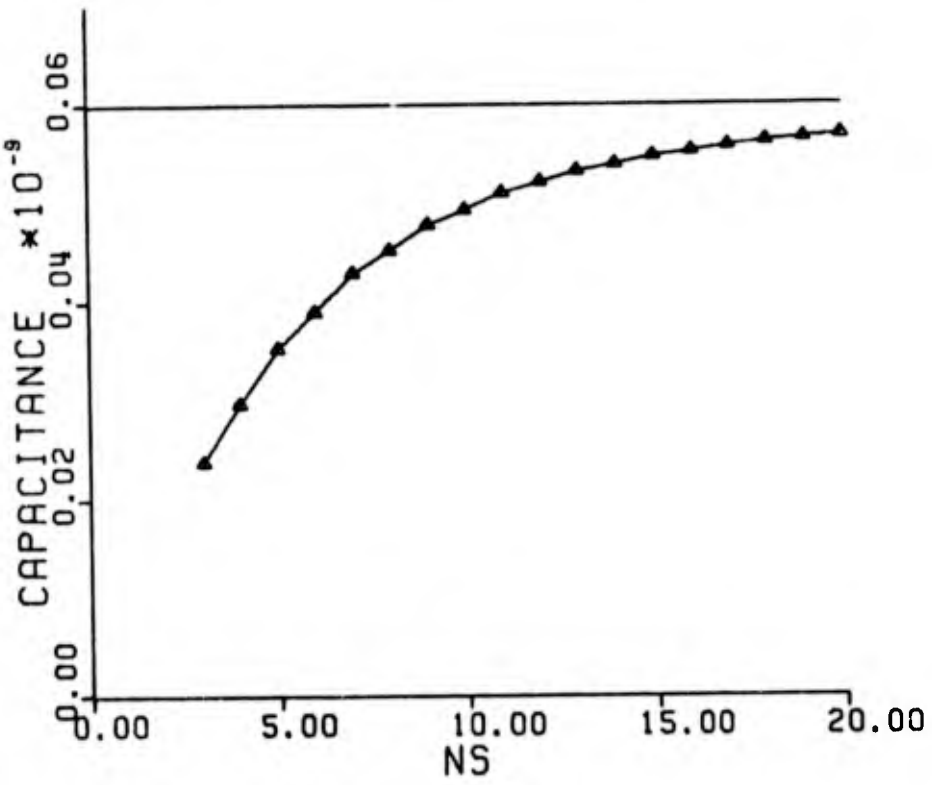

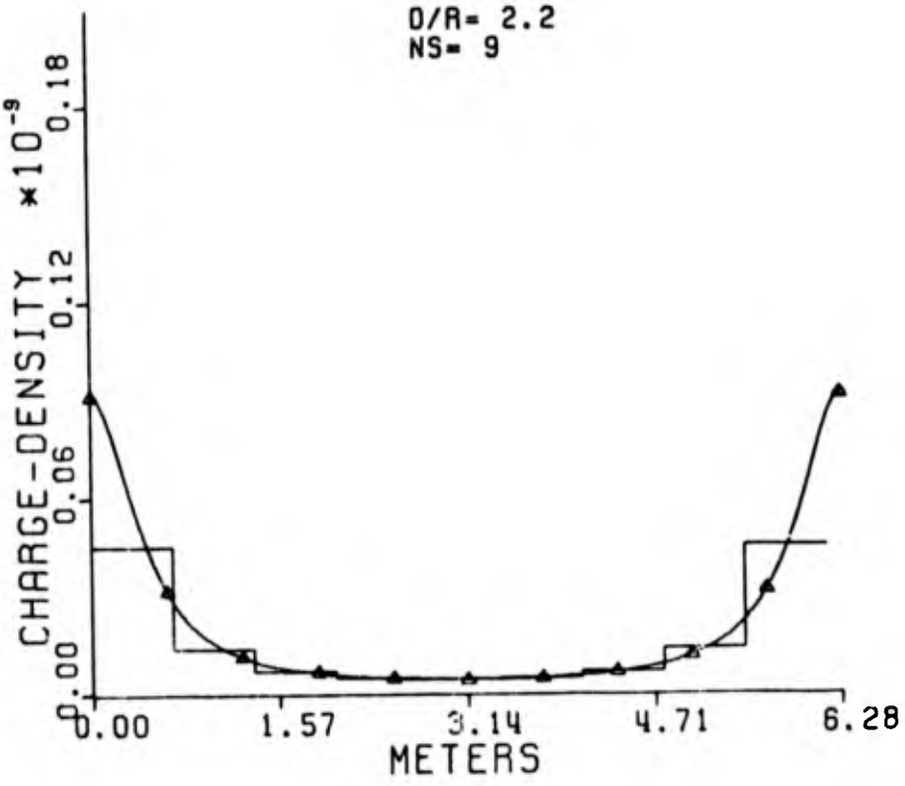
D/R= 2.2
NS= 9
CHARGE-DENSITY *10^-9
0.18
0.12
0.06
0.00
0.00
1.57
3.14
4.71
6.28
METERS

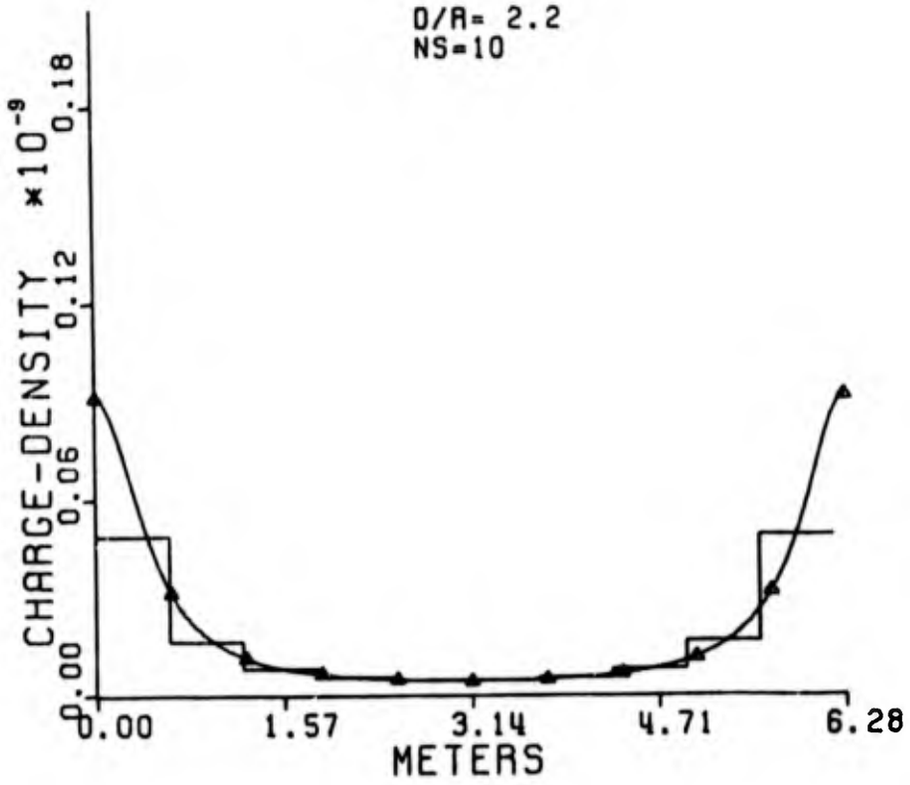
D/R= 2.2
NS=10
CHARGE-DENSITY *10^-9
0.18
0.12
0.06
0.00
0.00
1.57
3.14
4.71
6.28
METERS

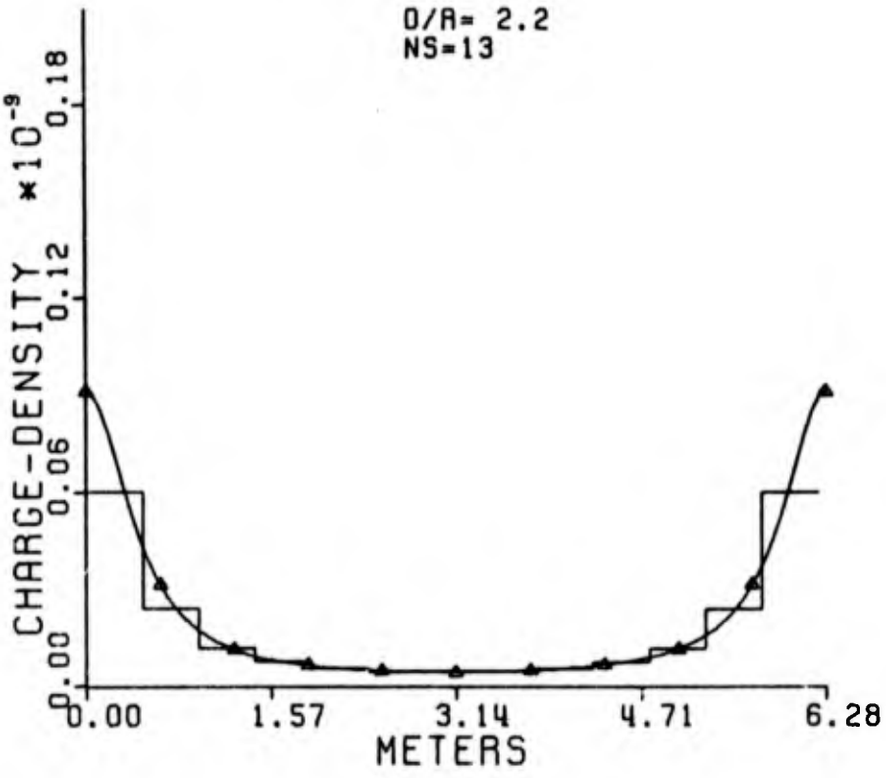
D/A= 2.2
NS=13
CHARGE-DENSITY *10⁻⁹
0.00
0.06
0.12
0.18
0.00
1.57
3.14
4.71
6.28
METERS

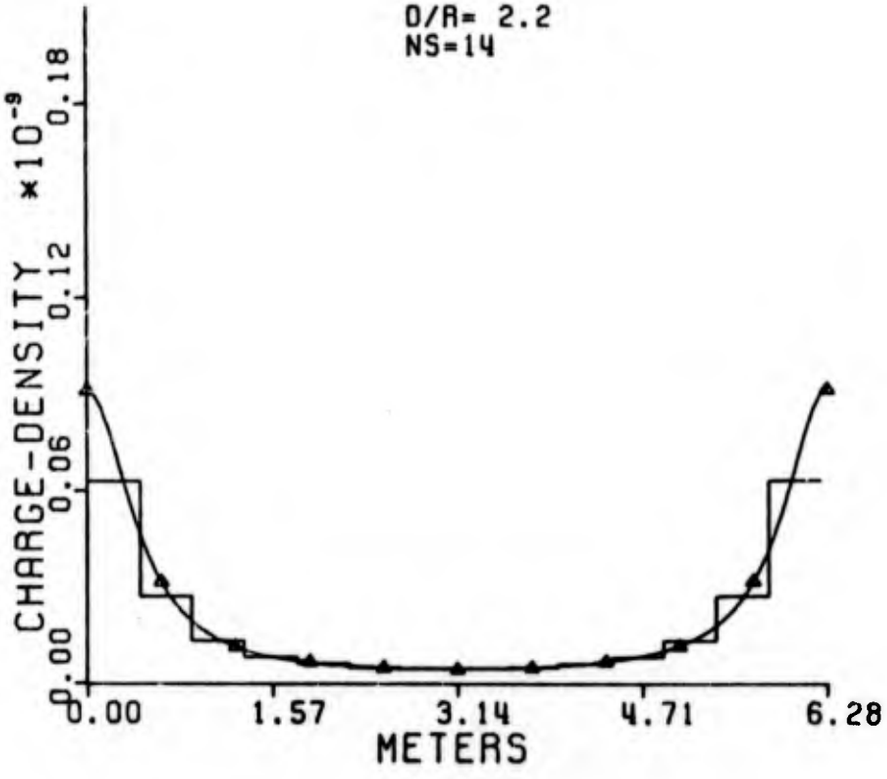
D/A= 2.2
NS=14
CHARGE-DENSITY *10⁻⁹
0.00
0.06
0.12
0.18
0.00
1.57
3.14
4.71
6.28
METERS

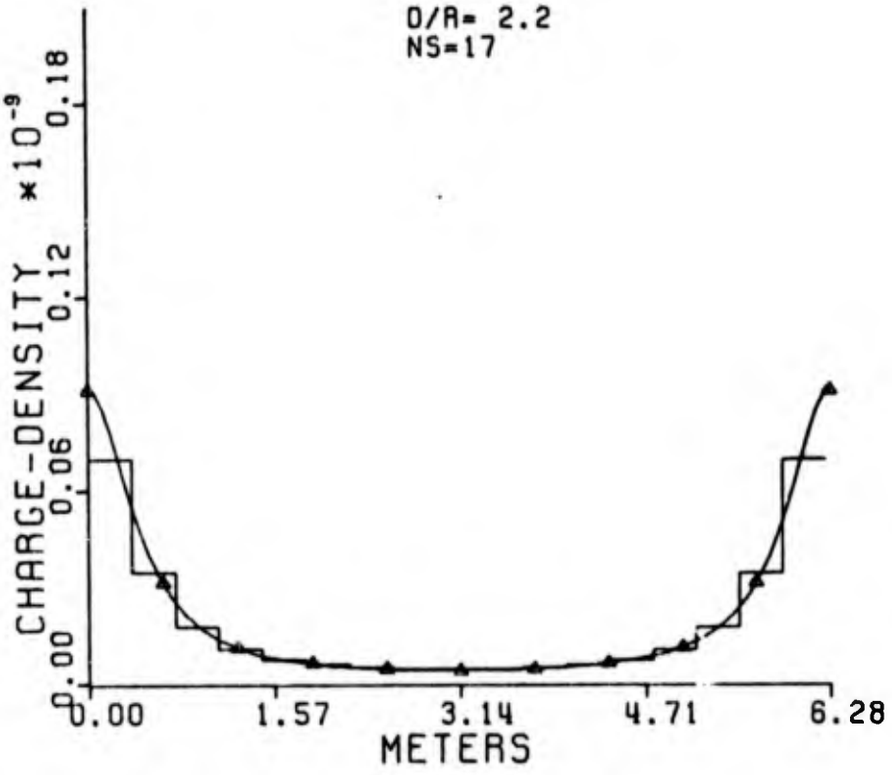
D/R= 2.2
NS=17
CHARGE-DENSITY *10⁻⁹
0.18
0.12
0.06
0.00
0.00
1.57
3.14
4.71
6.28
METERS

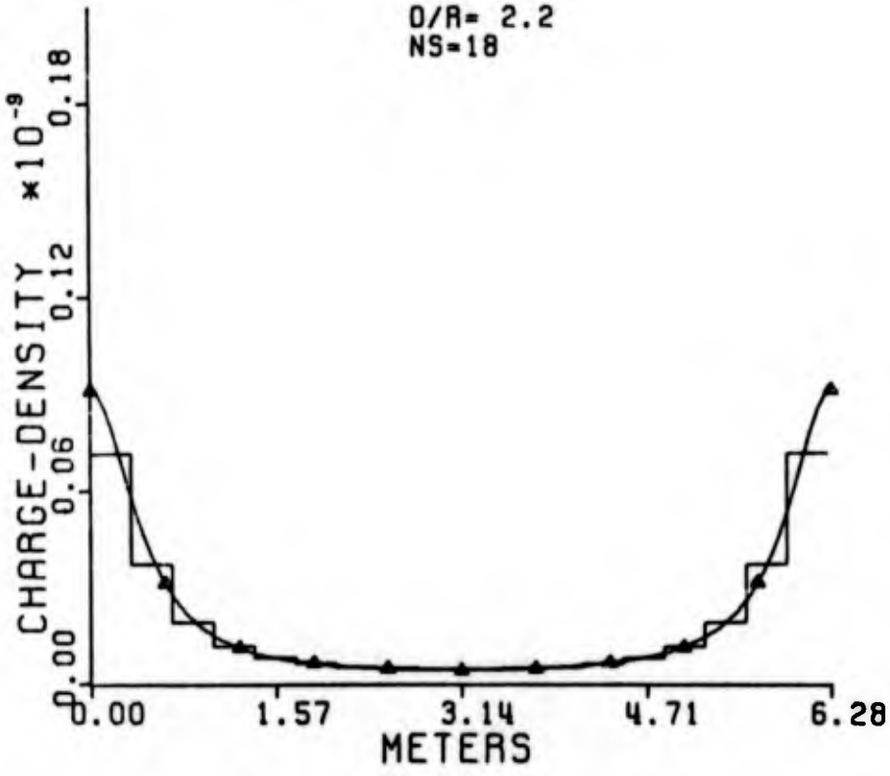
D/R= 2.2
NS=18
CHARGE-DENSITY *10⁻⁹
0.18
0.12
0.06
0.00
0.00
1.57
3.14
4.71
6.28
METERS

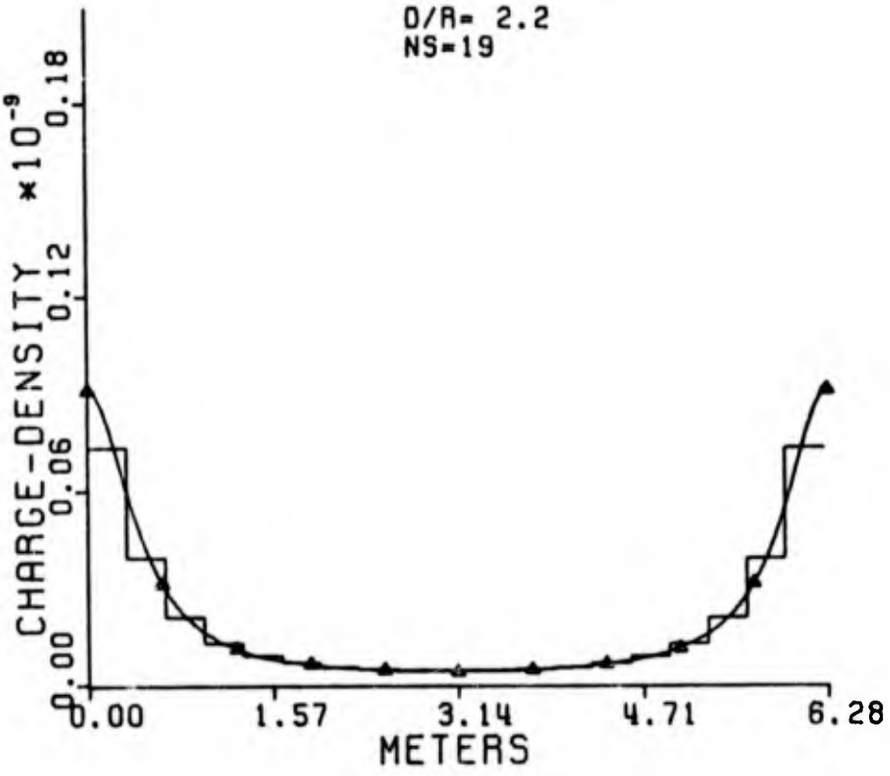
O/R= 2.2
NS=19
CHARGE-DENSITY *10⁻⁹
0.00
0.06
0.12
0.18
0.00
1.57
3.14
4.71
6.28
METERS

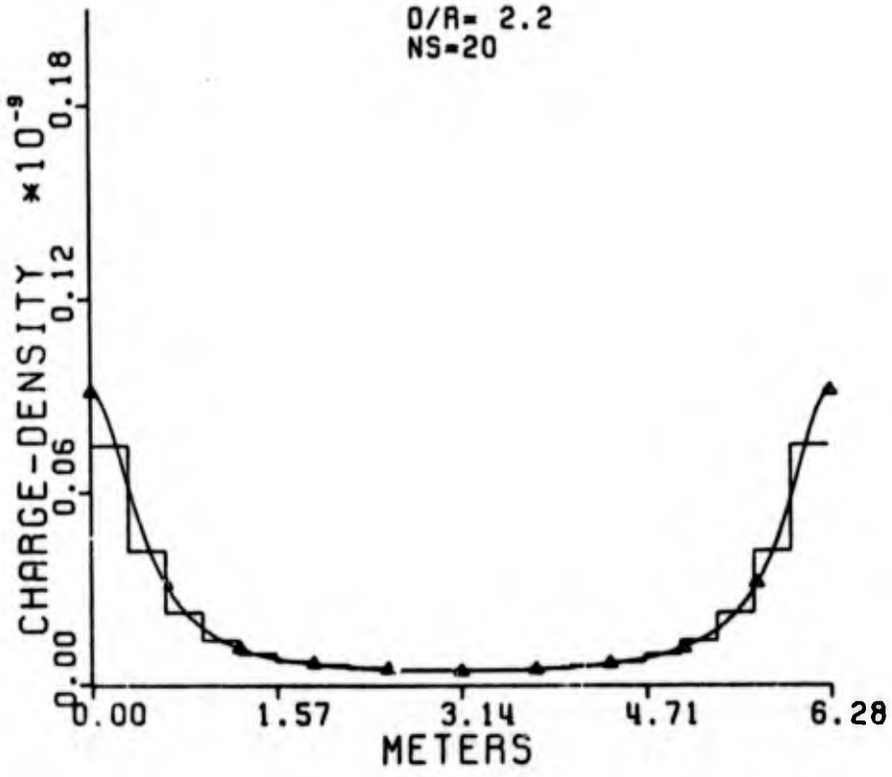
O/R= 2.2
NS=20
CHARGE-DENSITY *10⁻⁹
0.00
0.06
0.12
0.18
0.00
1.57
3.14
4.71
6.28
METERS

POLYGONAL STRIPS

D/R=2.3. The exact capacitance = $0.5133601 \times 10^{-10}$

| NS | Approx. Capac.* | NS | Approx. Capac. |
|---|---|---|---|
| 3 | .2371186 | 12 | .4648702 |
| 4 | .2918135 | 13 | .4715825 |
| 5 | .3394953 | 14 | .4766307 |
| 6 | .3706278 | 15 | .4810929 |
| 7 | .3999691 | 16 | .4846521 |
| 8 | .4180800 | 17 | .4877591 |
| 9 | .4355928 | 18 | .4903404 |
| 10 | .4468612 | 19 | .4925899 |
| 11 | .4574755 | 20 | .4945105 |

*Capacitance values are multiplied by $10^{-10}$.

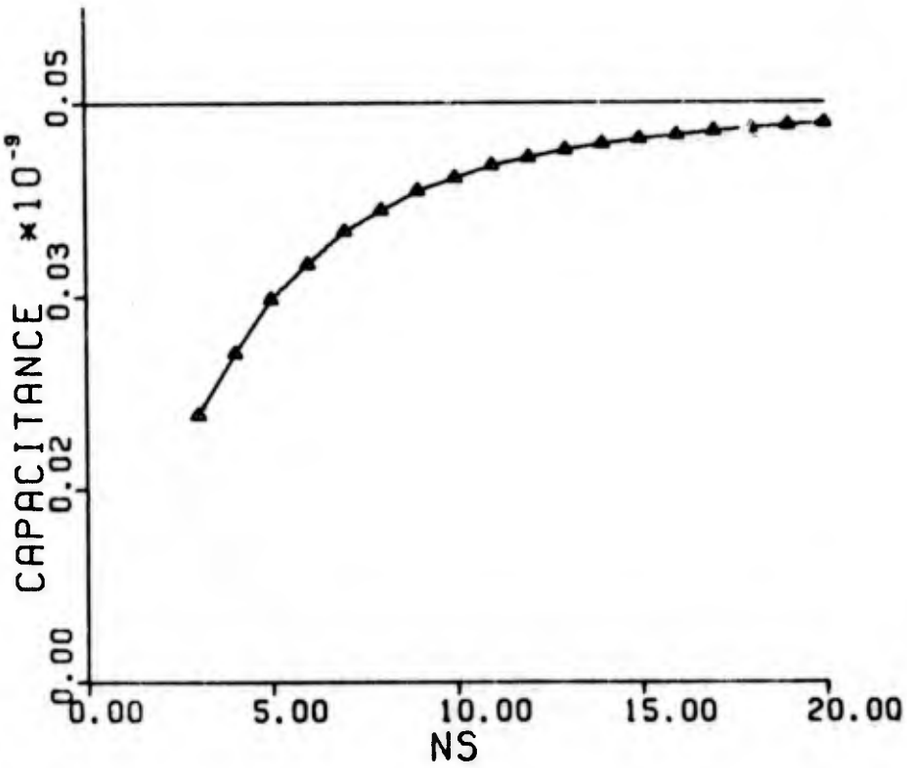

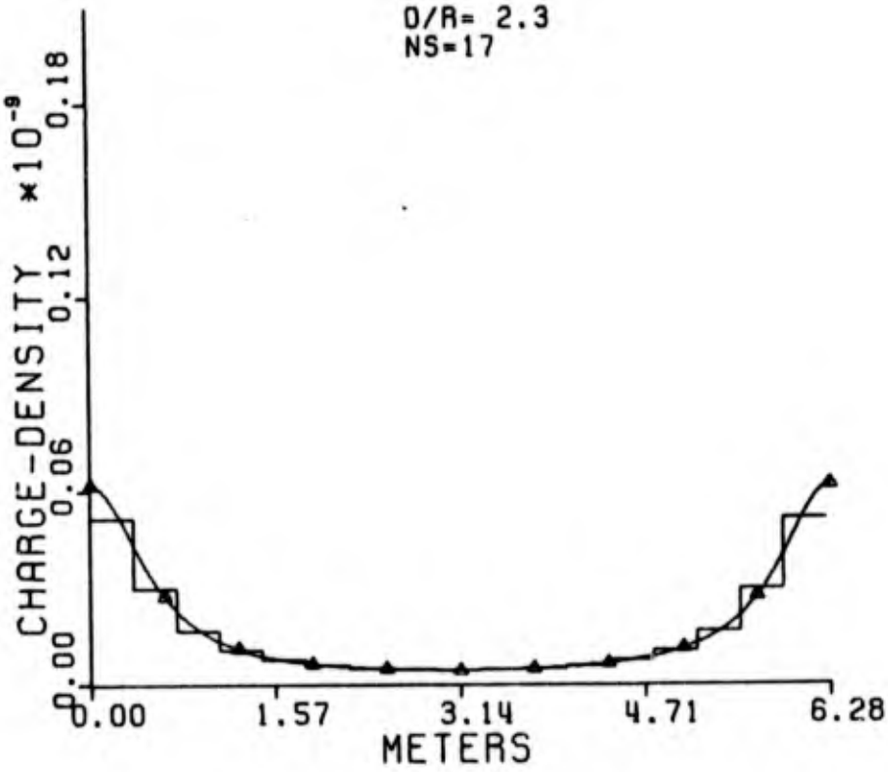
O/R= 2.3
NS=17
CHARGE-DENSITY *10⁻⁹
0.00
0.06
0.12
0.18
0.00
1.57
3.14
4.71
6.28
METERS

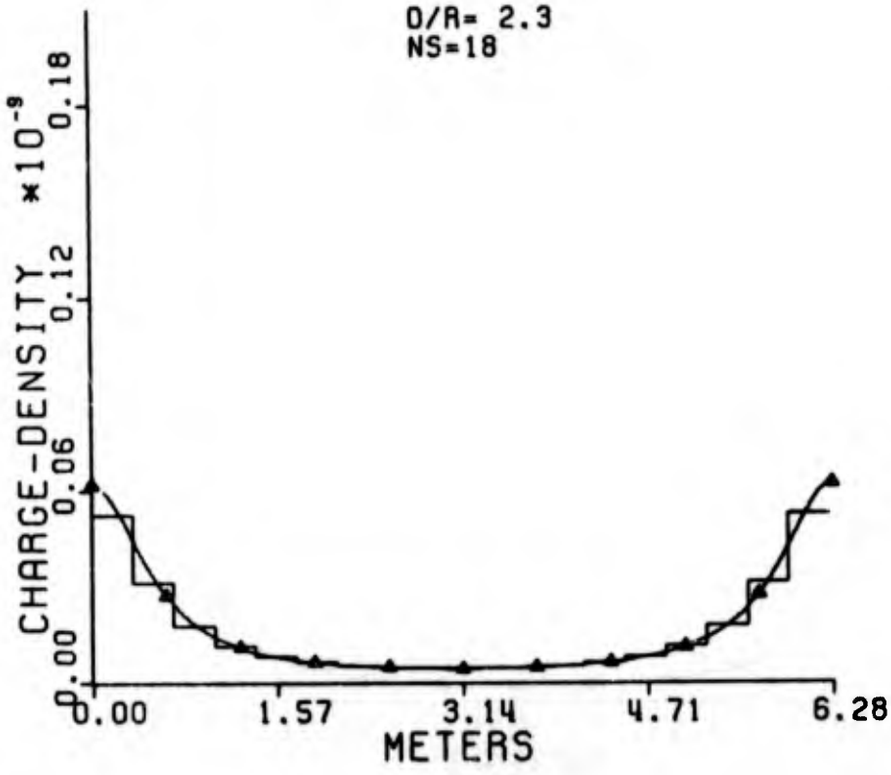
O/R= 2.3
NS=18
CHARGE-DENSITY *10⁻⁹
0.00
0.06
0.12
0.18
0.00
1.57
3.14
4.71
6.28
METERS

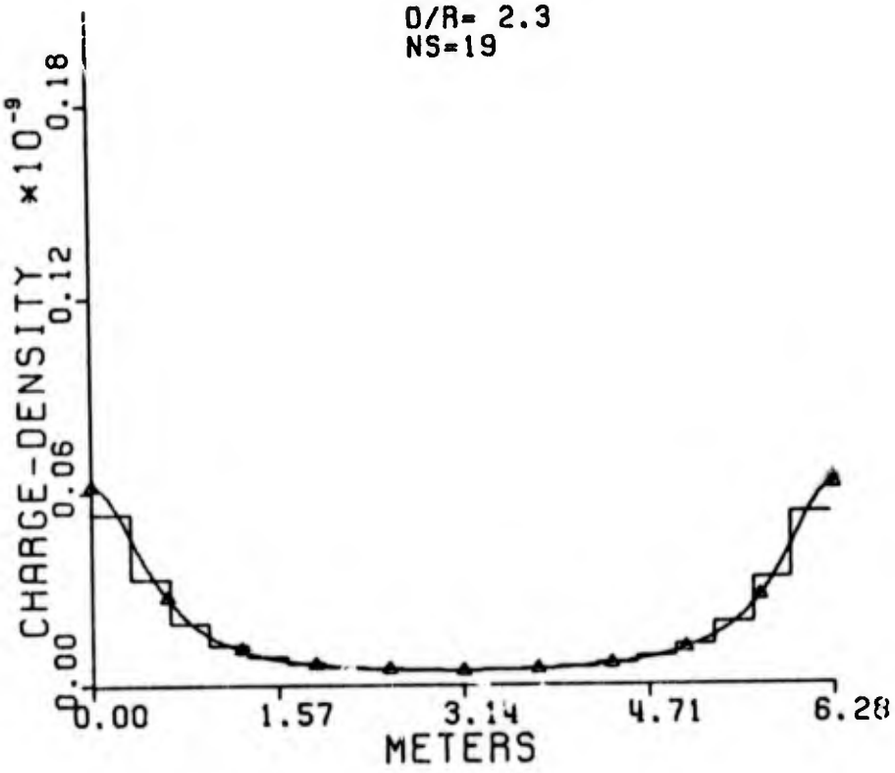
D/R= 2.3
NS=19
CHARGE-DENSITY *10^-9
0.00
0.06
0.12
0.18
0.00
1.57
3.14
4.71
6.28
METERS

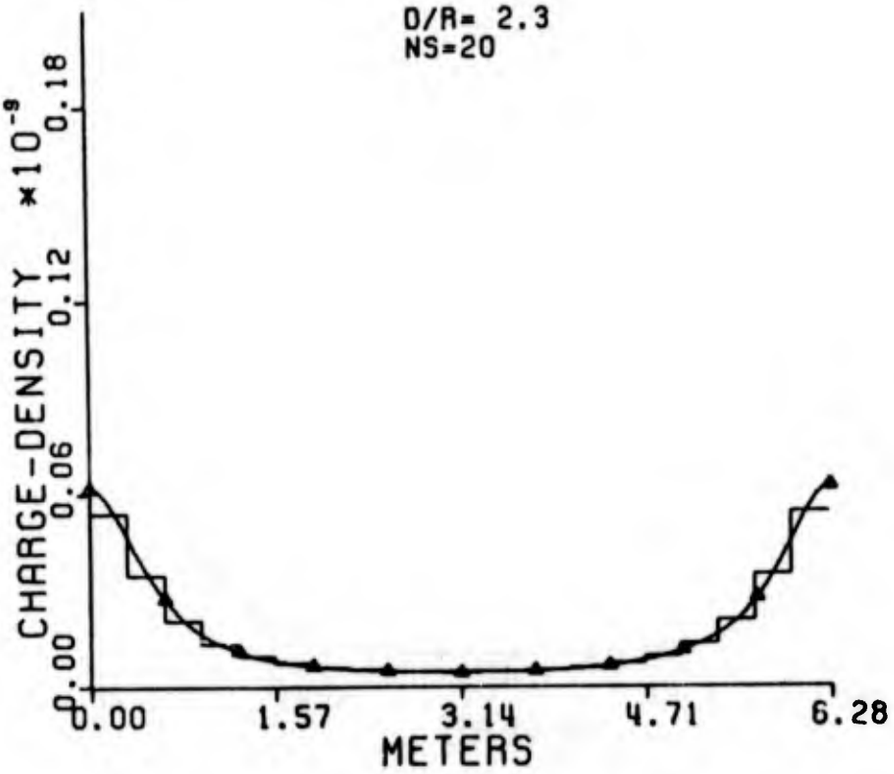
D/R= 2.3
NS=20
CHARGE-DENSITY *10^-9
0.00
0.06
0.12
0.18
0.00
1.57
3.14
4.71
6.28
METERS

## POLYGONAL STRIPS

D/R=3.0. The exact capacitance = $0.2886231 \times 10^{-10}$

| NS | Approx. Capac.* | NS | Approx. Capac. |
|---|---|---|---|
| 3 | .1887302 | 12 | .2779840 |
| 4 | .2193580 | 13 | .2794801 |
| 5 | .2391574 | 14 | .2806833 |
| 6 | .2516404 | 15 | .281666 |
| 7 | .2602671 | 16 | .2824781 |
| 8 | .2661709 | 17 | .2831569 |
| 9 | .2704883 | 18 | .2837297 |
| 10 | .2736667 | 19 | .2842172 |
| 11 | .2760984 | 20 | .2846361 |

*Capacitance values are multiplied by $10^{-10}$.

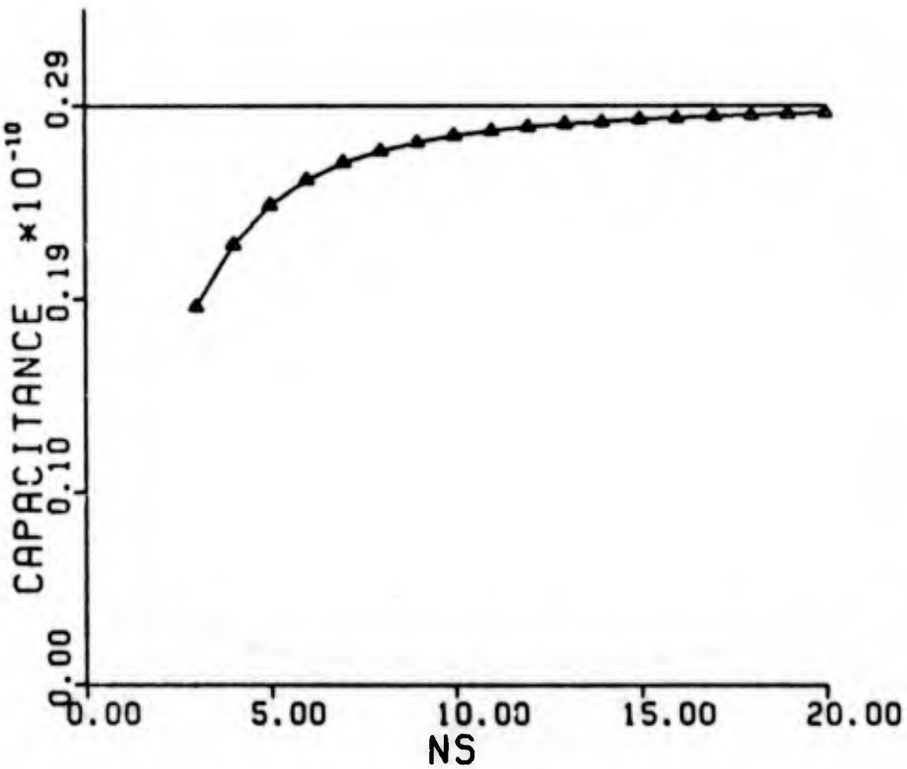

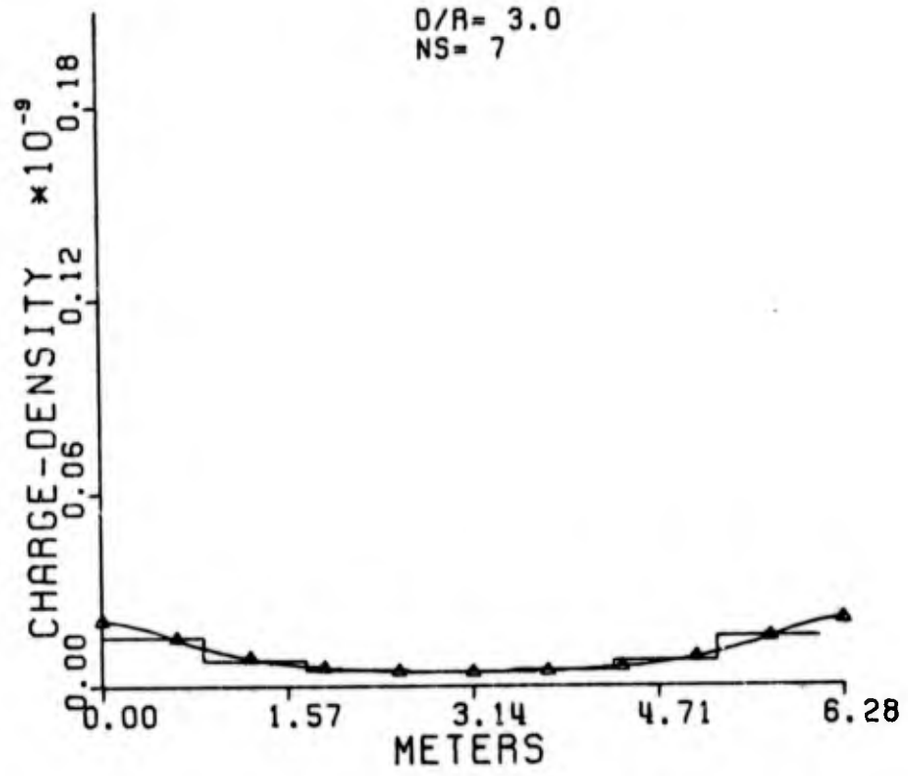
O/R= 3.0
NS= 7
CHARGE-DENSITY *10^-9
0.00
0.06
0.12
0.18
0.00
1.57
3.14
4.71
6.28
METERS

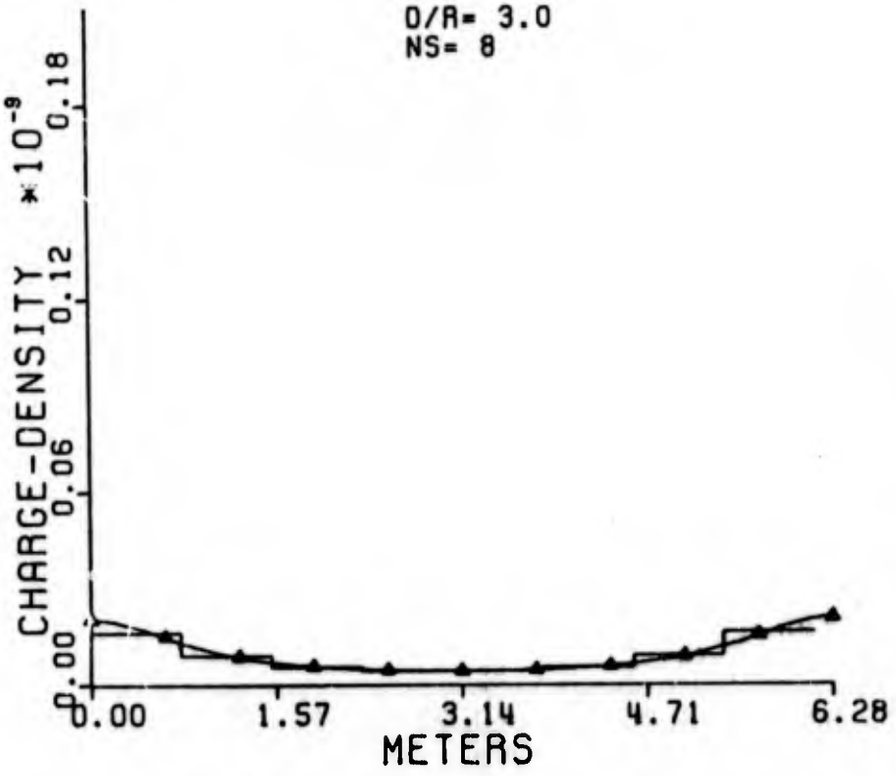
O/R= 3.0
NS= 8
CHARGE-DENSITY *10^-9
0.00
0.06
0.12
0.18
0.00
1.57
3.14
4.71
6.28
METERS

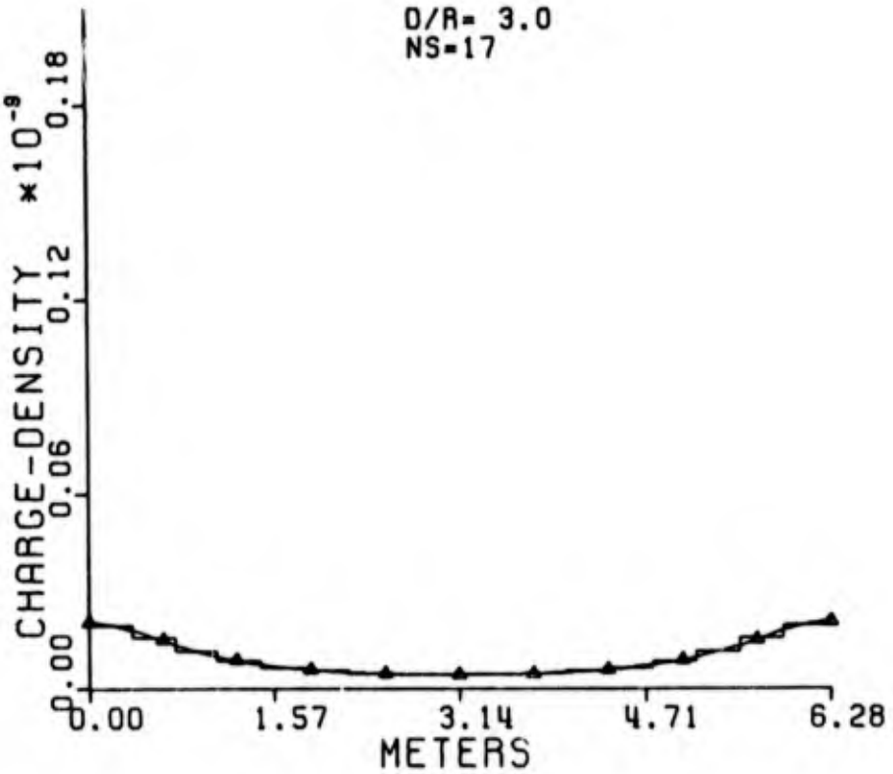
D/R= 3.0
NS=17
CHARGE-DENSITY *10⁻⁹
0.18
0.12
0.06
0.00
0.00
1.57
3.14
4.71
6.28
METERS

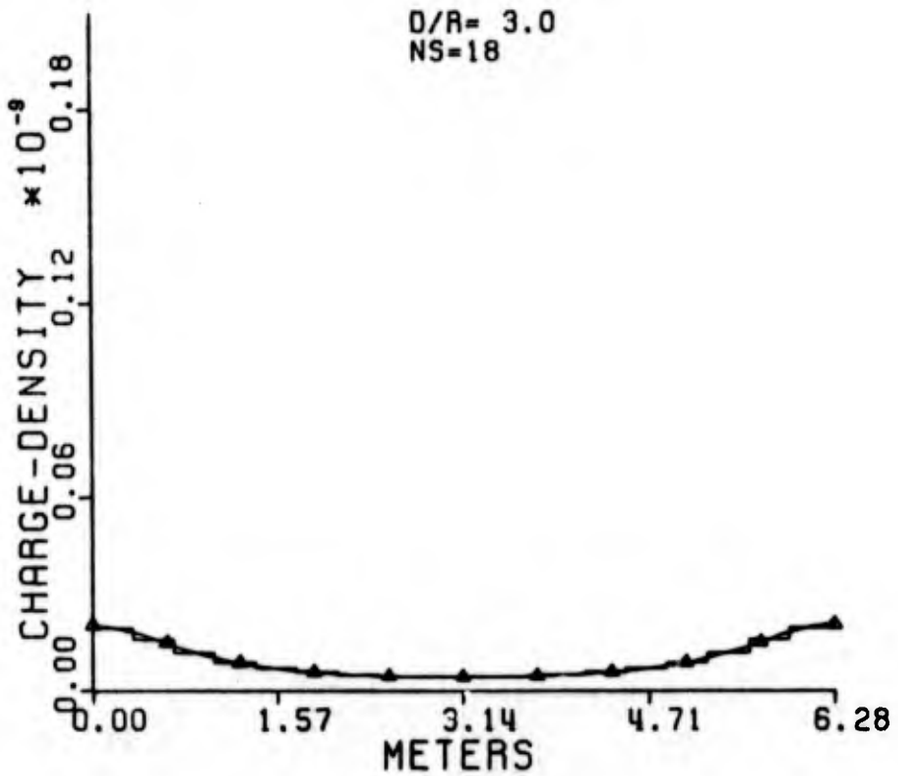
D/R= 3.0
NS=18
CHARGE-DENSITY *10⁻⁹
0.18
0.12
0.06
0.00
0.00
1.57
3.14
4.71
6.28
METERS

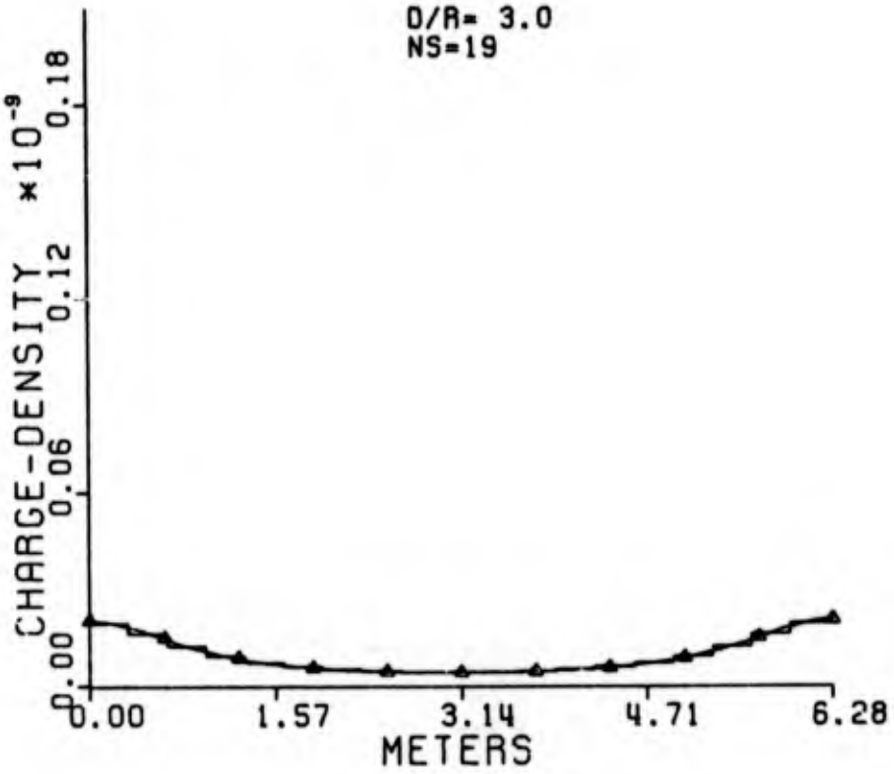
D/R= 3.0
NS=19
CHARGE-DENSITY *10⁻⁹
0.00
0.06
0.12
0.18
0.00
1.57
3.14
4.71
6.28
METERS

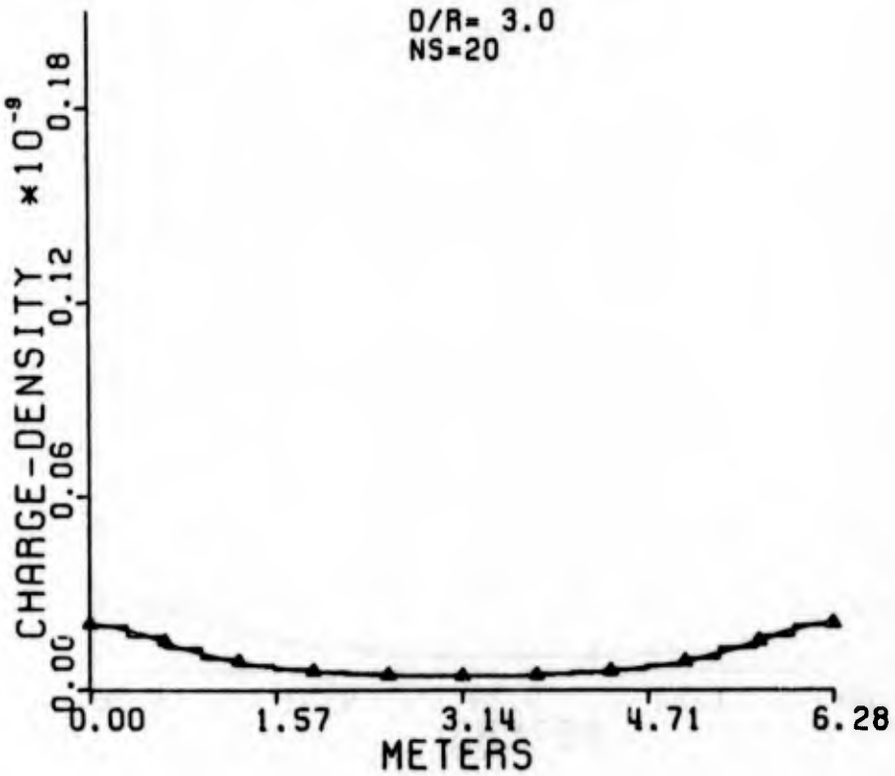
D/R= 3.0
NS=20
CHARGE-DENSITY *10⁻⁹
0.00
0.06
0.12
0.18
0.00
1.57
3.14
4.71
6.28
METERS

## POLYGONAL STRIPS

D/R=10.0. The exact capacitance = $0.1211716 \times 10^{-10}$

| NS | Approx. Capac.* | NS | Approx. Capac. |
|---|---|---|---|
| 3 | .102319 | 12 | .1197147 |
| 4 | .1097410 | 13 | .1199244 |
| 5 | .1135291 | 14 | .1200920 |
| 6 | .1157126 | 15 | .1202279 |
| 7 | .1170820 | 16 | .1203398 |
| 8 | .1179957 | 17 | .1204329 |
| 9 | .118635 | 18 | .1205112 |
| 10 | .1190995 | 19 | .1205777 |
| 11 | .1194474 | 20 | .1206346 |

*Capacitance values are multiplied by $10^{-10}$.

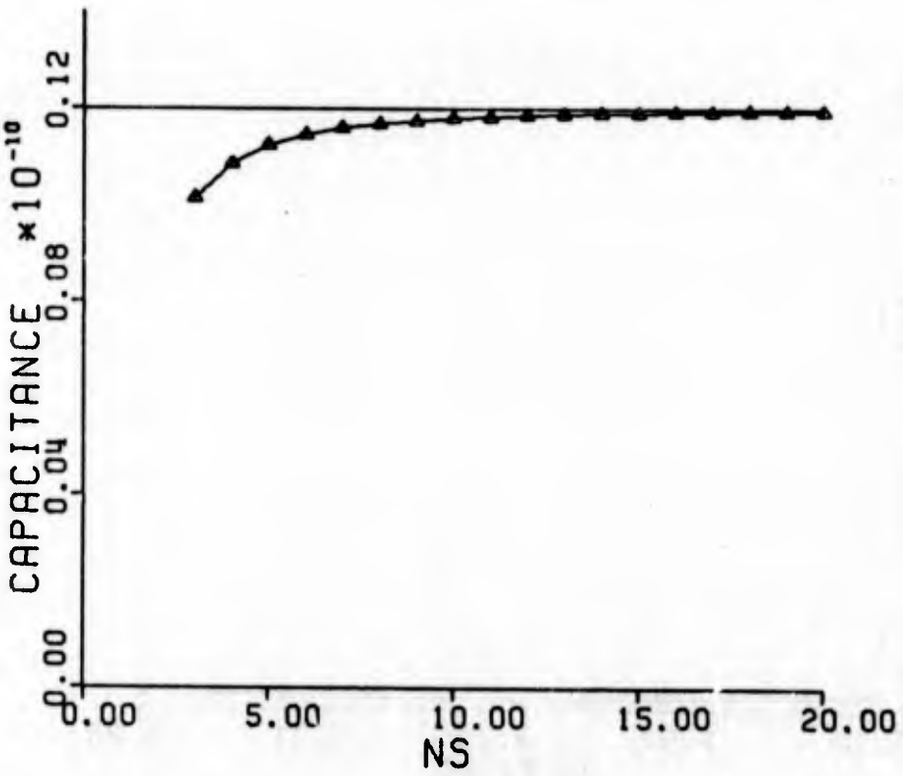

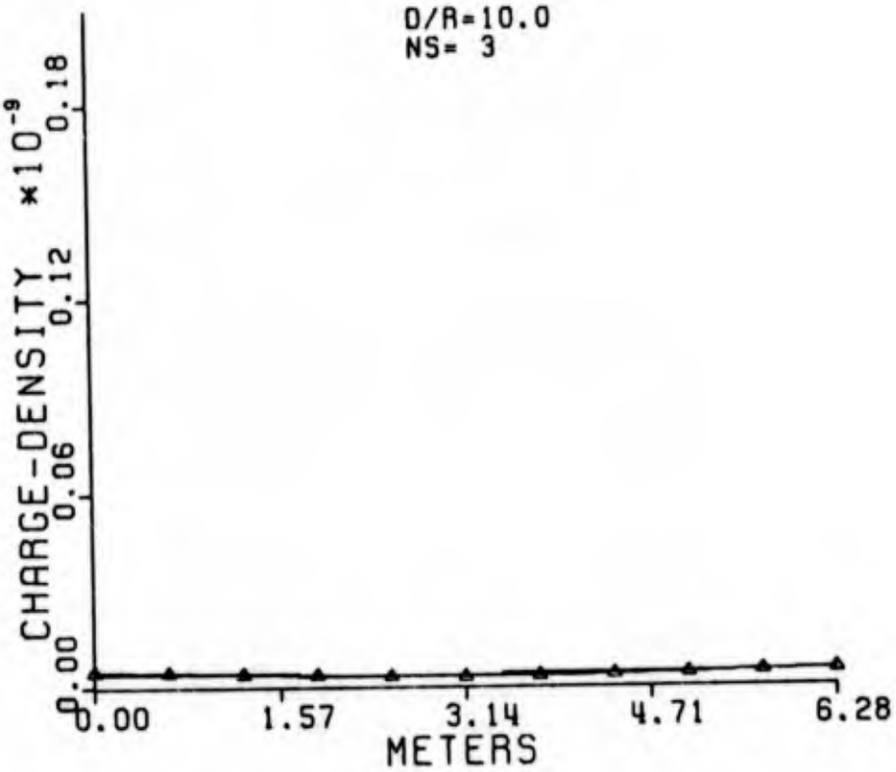
D/R=10.0
NS= 3
CHARGE-DENSITY *10^-9
0.00
0.06
0.12
0.18
0.00
1.57
3.14
4.71
6.28
METERS

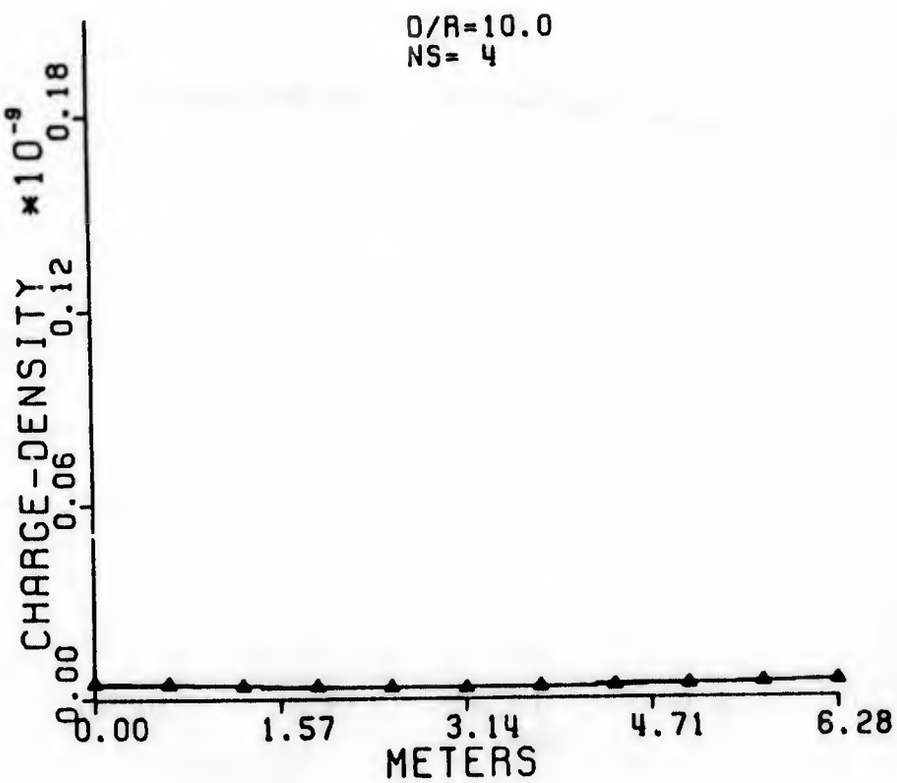
D/R=10.0
NS= 4
CHARGE-DENSITY *10^-9
0.00
0.06
0.12
0.18
0.00
1.57
3.14
4.71
6.28
METERS

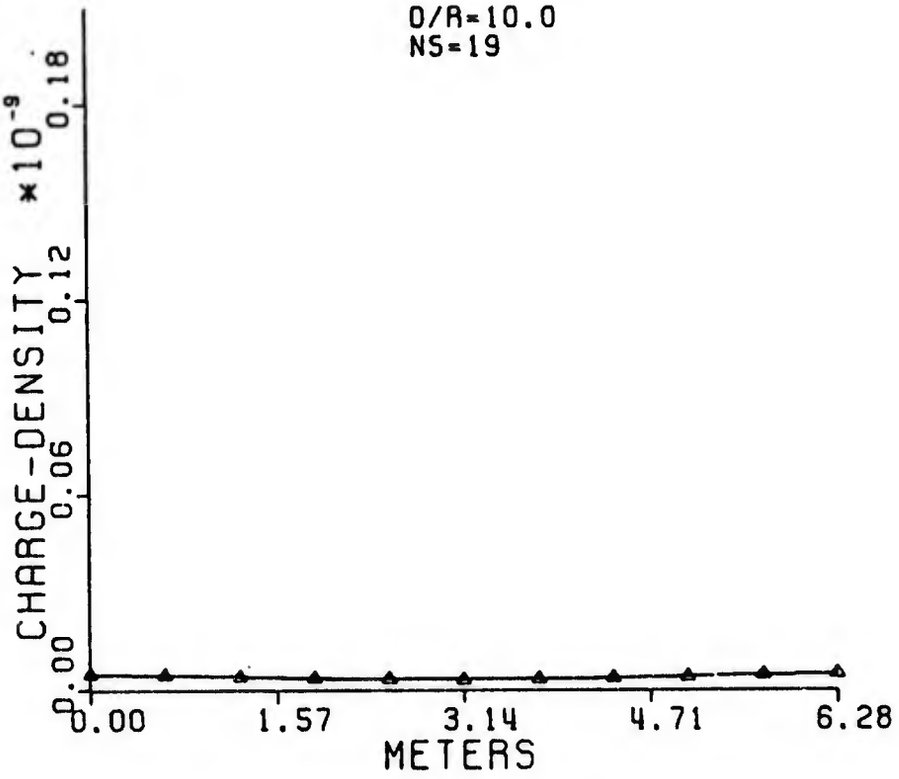
O/R=10.0
NS=19
CHARGE-DENSITY *10^-9
0.00
0.06
0.12
0.18
0.00
1.57
3.14
4.71
6.28
METERS

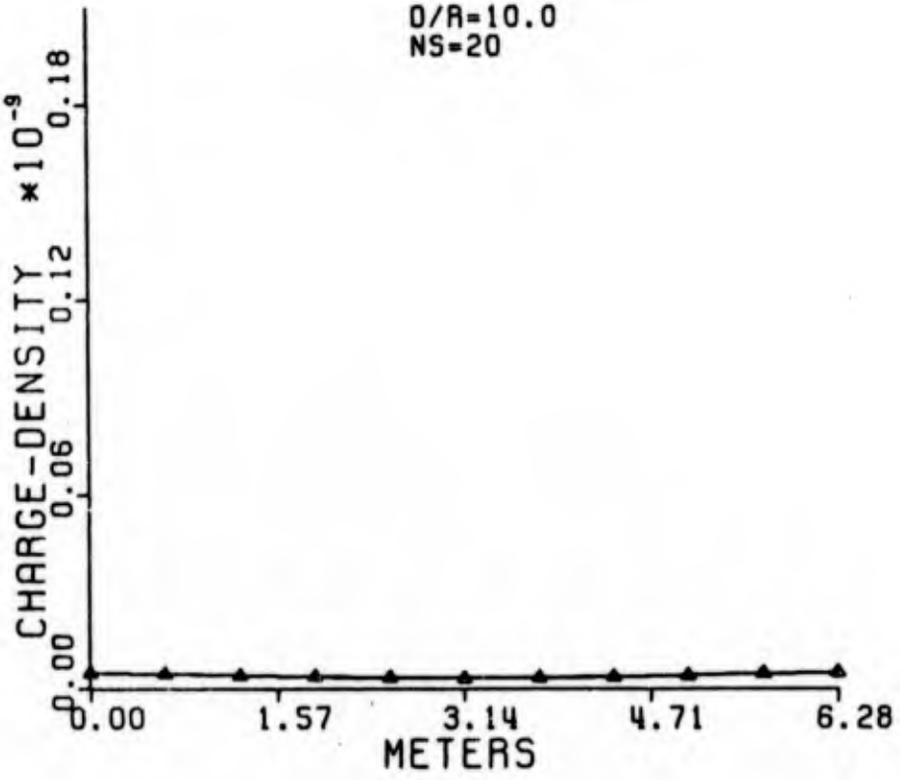
O/R=10.0
NS=20
CHARGE-DENSITY *10^-9
0.00
0.06
0.12
0.18
0.00
1.57
3.14
4.71
6.28
METERS

APPENDIX C

CIRCULAR STRIPS DATA

D/R=2.1. The exact capacitance = $0.8820449 \times 10^{-10}$

| NS | Approx. Capac.* | NS | Approx. Capac. |
|---|---|---|---|
| 3 | 0.3291886 | 12 | 0.8218238 |
| 4 | 0.5237110 | 13 | 0.8311374 |
| 5 | 0.5169441 | 14 | 0.8413939 |
| 6 | 0.6557058 | 15 | 0.8504604 |
| 7 | 0.6528785 | 16 | 0.8539576 |
| 8 | 0.7397262 | 17 | 0.8618065 |
| 9 | 0.7427161 | 18 | 0.8622050 |
| 10 | 0.7906166 | 19 | 0.8685625 |
| 11 | 0.7981673 | 20 | 0.8677338 |

*Capacitance values are multiplied by $10^{-10}$.

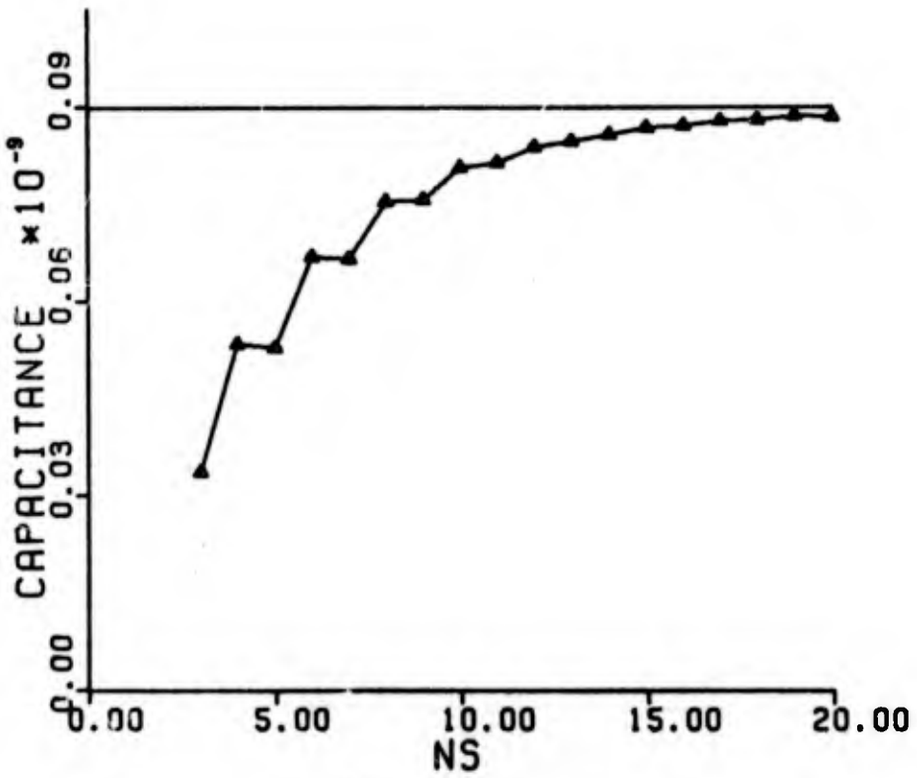

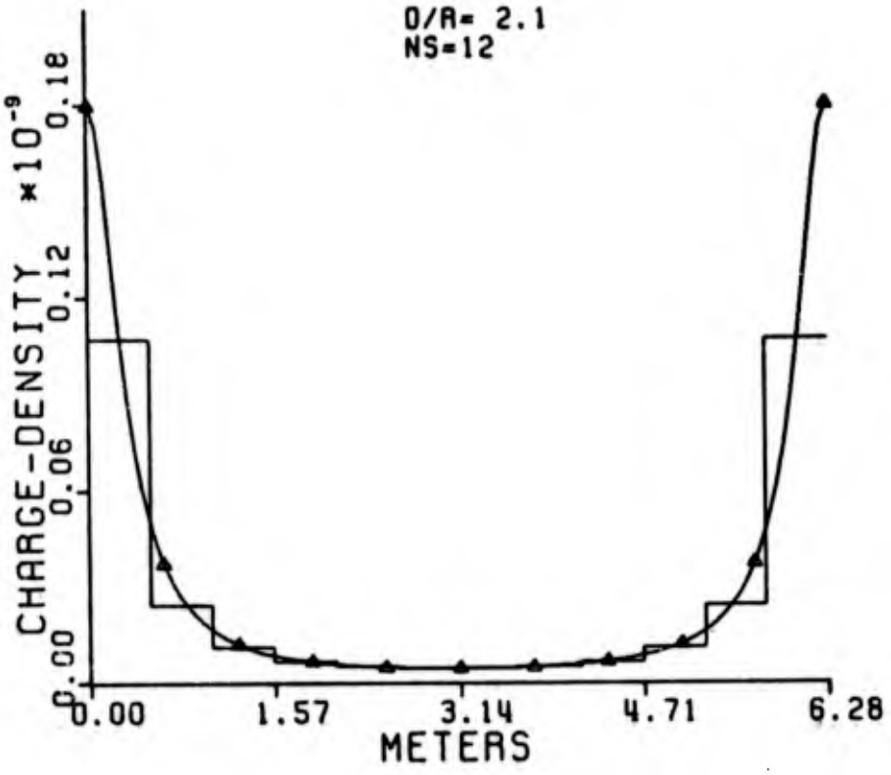
O/R= 2.1
NS=12
CHARGE-DENSITY *10^-9
0.18
0.12
0.06
0.00
0.00
1.57
3.14
4.71
6.28
METERS

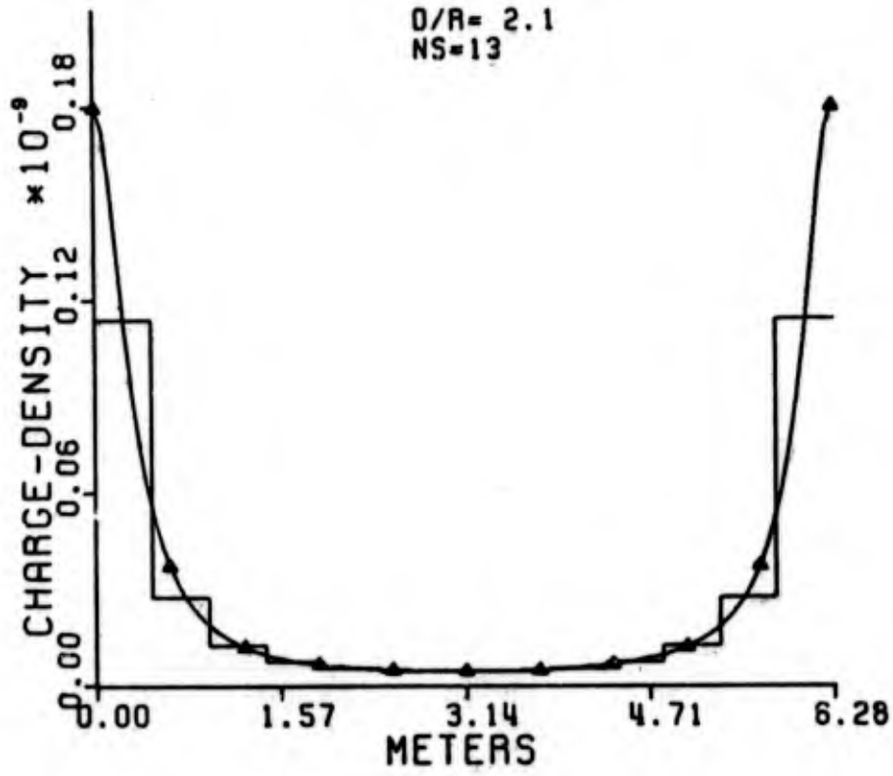
O/R= 2.1
NS=13
CHARGE-DENSITY *10^-9
0.18
0.12
0.06
0.00
0.00
1.57
3.14
4.71
6.28
METERS

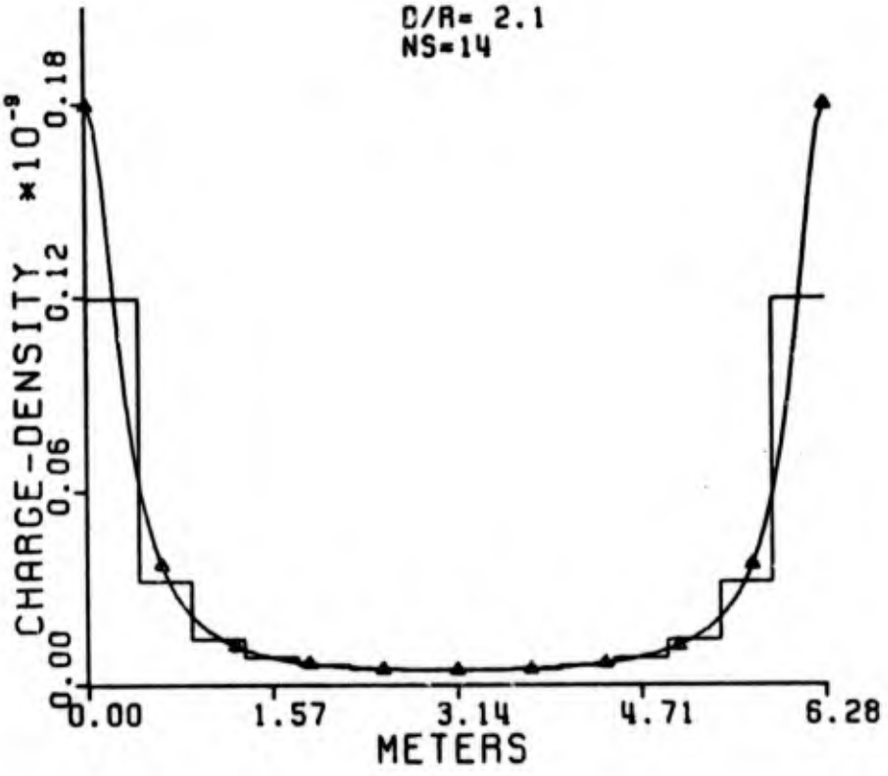
D/R= 2.1
NS=14
CHARGE-DENSITY *10^-9
0.18
0.12
0.06
0.00
0.00
1.57
3.14
4.71
6.28
METERS

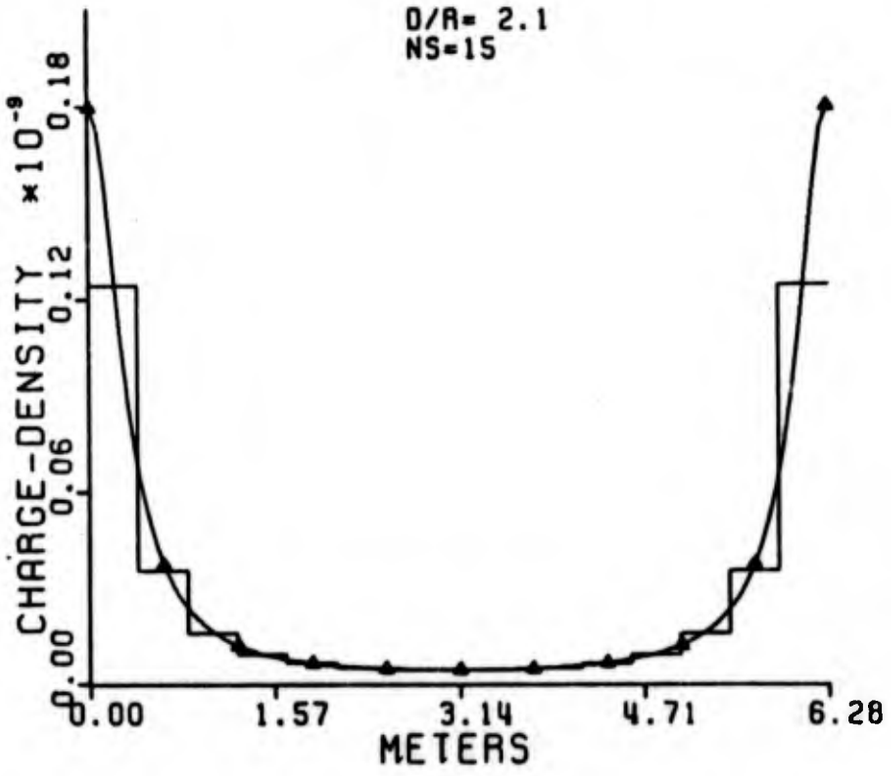
D/R= 2.1
NS=15
CHARGE-DENSITY *10^-9
0.18
0.12
0.06
0.00
0.00
1.57
3.14
4.71
6.28
METERS

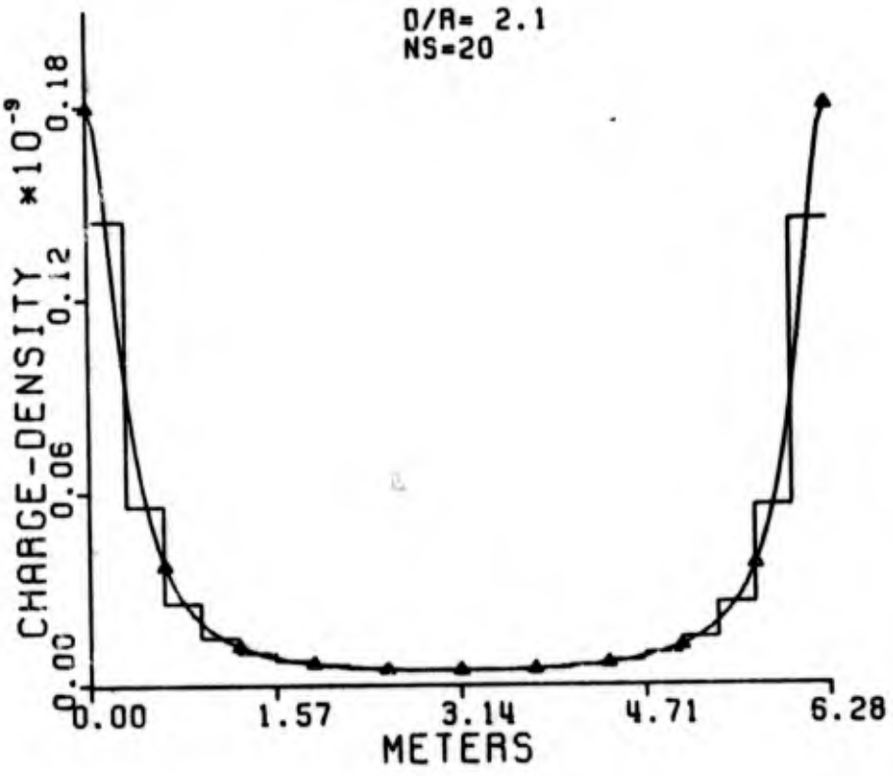
D/R= 2.1
NS=20
CHARGE-DENSITY *10^-9
0.00
0.06
0.12
0.18
0.00
1.57
3.14
4.71
6.28
METERS

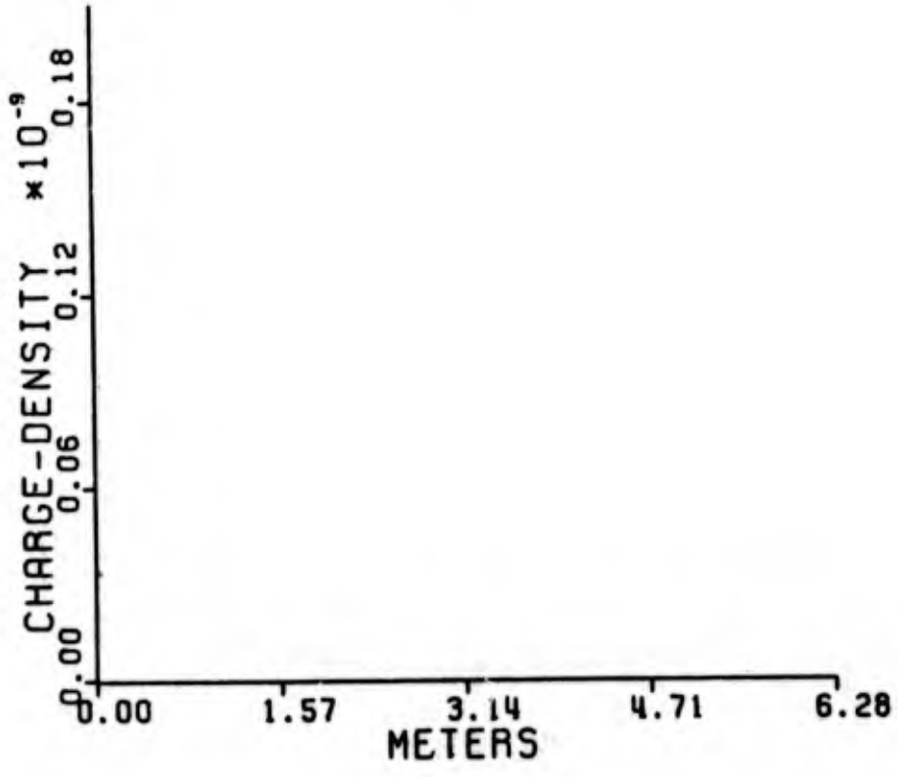
CHARGE-DENSITY *10^-9
0.00
0.06
0.12
0.18
0.00
1.57
3.14
4.71
6.28
METERS

CIRCULAR STRIPS

D/R=2.2, The exact capacitance = $0.6262345 \times 10^{-10}$

| NS | Approx. Capac.* | NS | Approx. Capac. |
|---|---|---|---|
| 3 | 0.3149170 | 12 | 0.6137877 |
| 4 | 0.4642286 | 13 | 0.6156086 |
| 5 | 0.4629508 | 14 | 0.6186966 |
| 6 | 0.5453769 | 15 | 0.6201285 |
| 7 | 0.5455589 | 16 | 0.6214225 |
| 8 | 0.5854490 | 17 | 0.6224494 |
| 9 | 0.5867809 | 18 | 0.6230188 |
| 10 | 0.6044171 | 19 | 0.6237217 |
| 11 | 0.6063429 | 20 | 0.6239991 |

*All capacitance values are multiplied by $10^{-10}$.

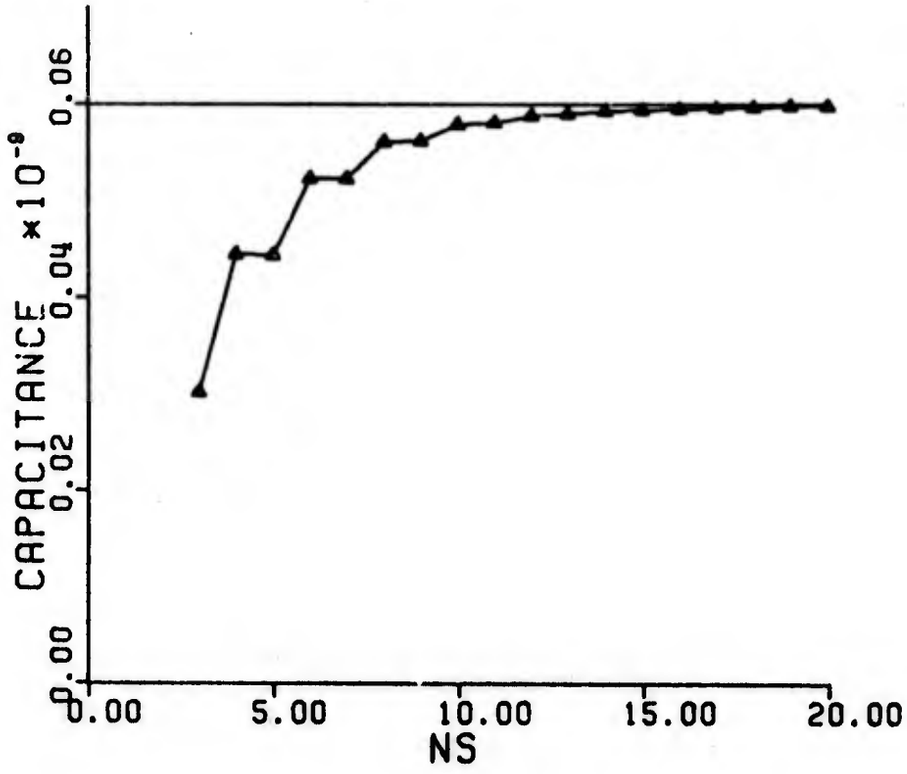

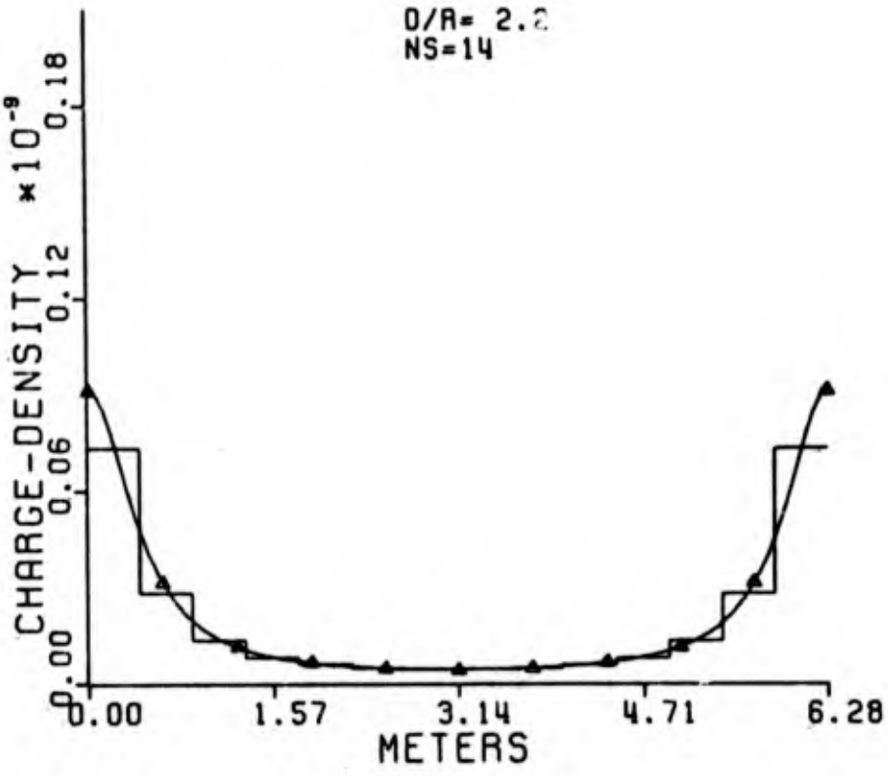
D/R= 2.2
NS=14
CHARGE-DENSITY *10^-9
0.00
0.06
0.12
0.18
0.00
1.57
3.14
4.71
6.28
METERS

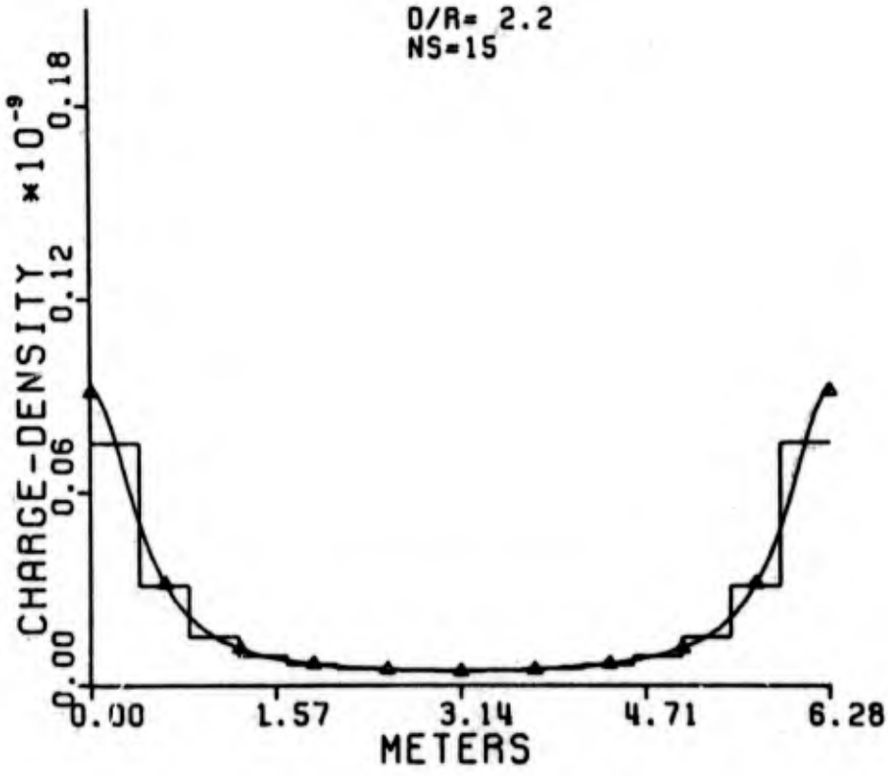
D/R= 2.2
NS=15
CHARGE-DENSITY *10^-9
0.00
0.06
0.12
0.18
0.00
1.57
3.14
4.71
6.28
METERS

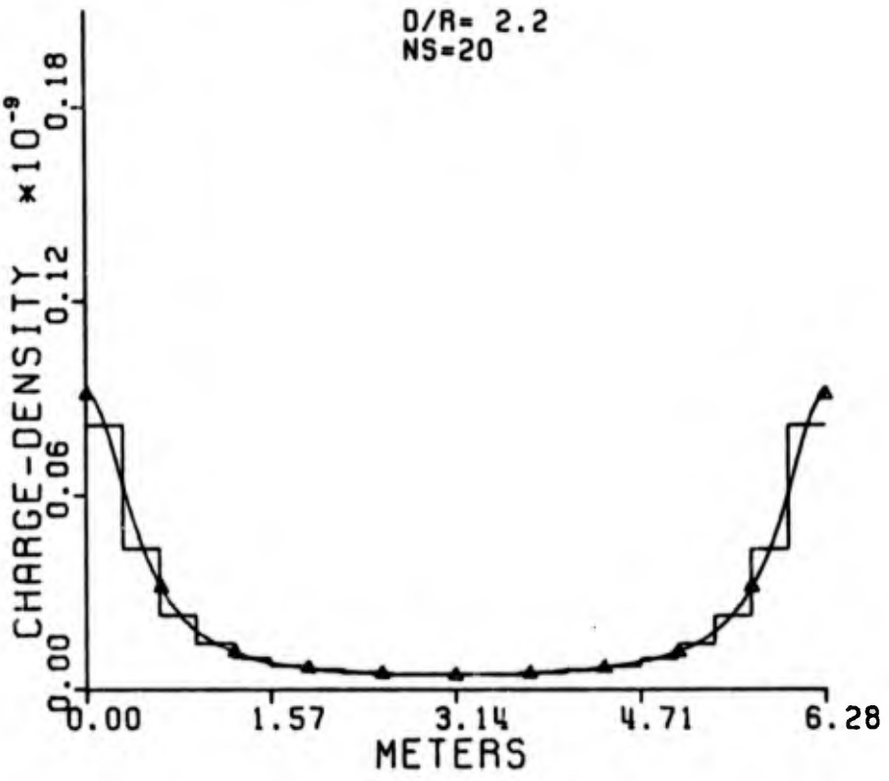
D/R= 2.2
NS=20
CHARGE-DENSITY ×10⁻⁹
0.00
0.06
0.12
0.18
0.00
1.57
3.14
4.71
6.28
METERS

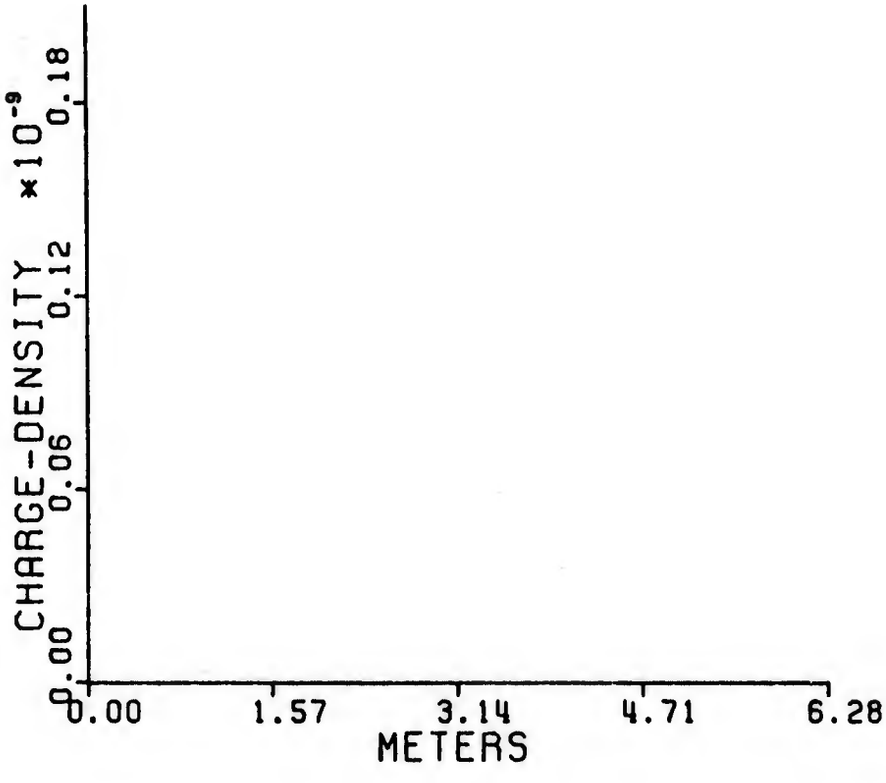
CHARGE-DENSITY ×10⁻⁹
0.00
0.06
0.12
0.18
0.00
1.57
3.14
4.71
6.28
METERS

CIRCULAR STRIPS

D/R=2.3. The exact capacitance = $0.5133601 \times 10^{-10}$

| NS | Approx. Capac.* | NS | Approx. Capac. |
|---|---|---|---|
| 3 | 0.3022011 | 12 | 0.5089151 |
| 4 | 0.4201860 | 13 | 0.5095768 |
| 5 | 0.4214839 | 14 | 0.5107542 |
| 6 | 0.4741287 | 15 | 0.5112088 |
| 7 | 0.4753186 | 16 | 0.5117196 |
| 8 | 0.4962211 | 17 | 0.5120168 |
| 9 | 0.4972017 | 18 | 0.5122680 |
| 10 | 0.5050733 | 19 | 0.5124596 |
| 11 | 0.5059423 | 20 | 0.5126004 |

*All capacitance values are multiplied by $10^{-10}$.

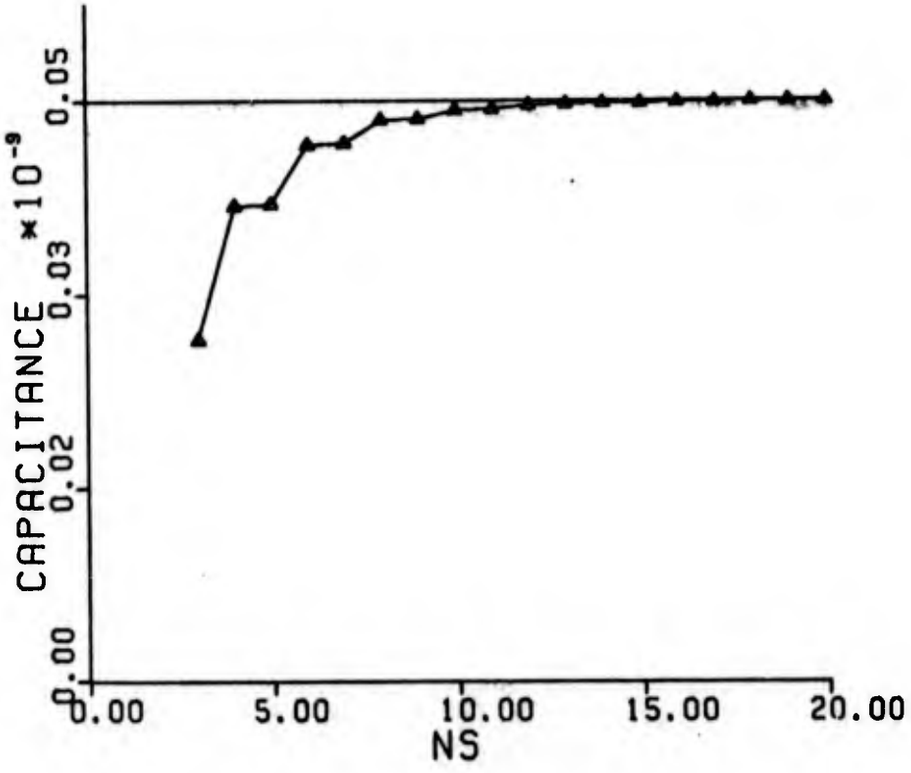

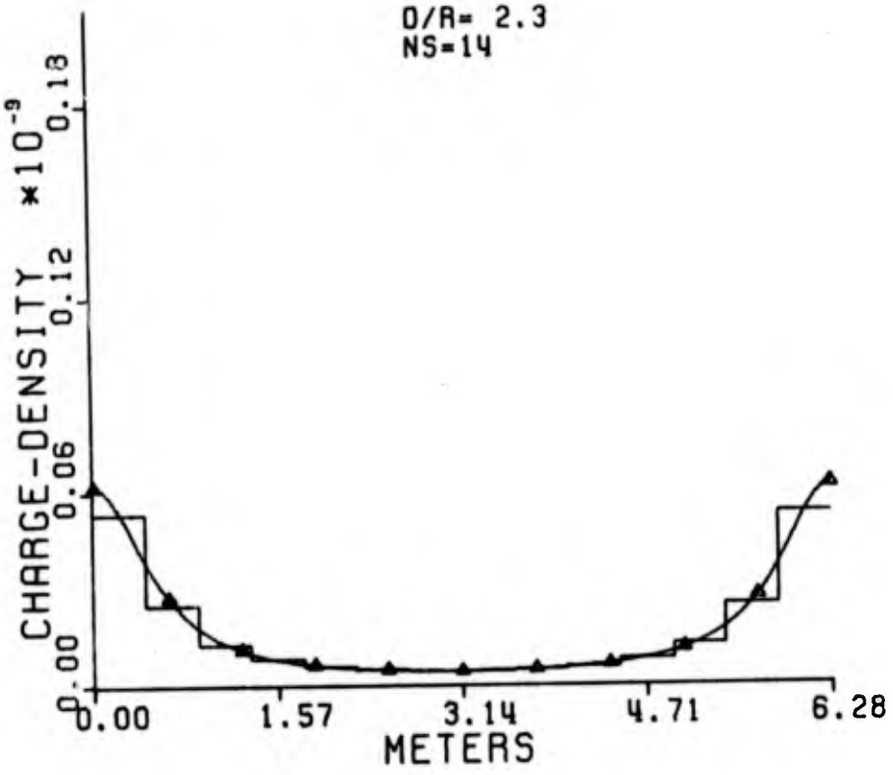
O/R= 2.3
NS=14
CHARGE-DENSITY *10^-9
0.18
0.12
0.06
0.00
0.00
1.57
3.14
4.71
6.28
METERS

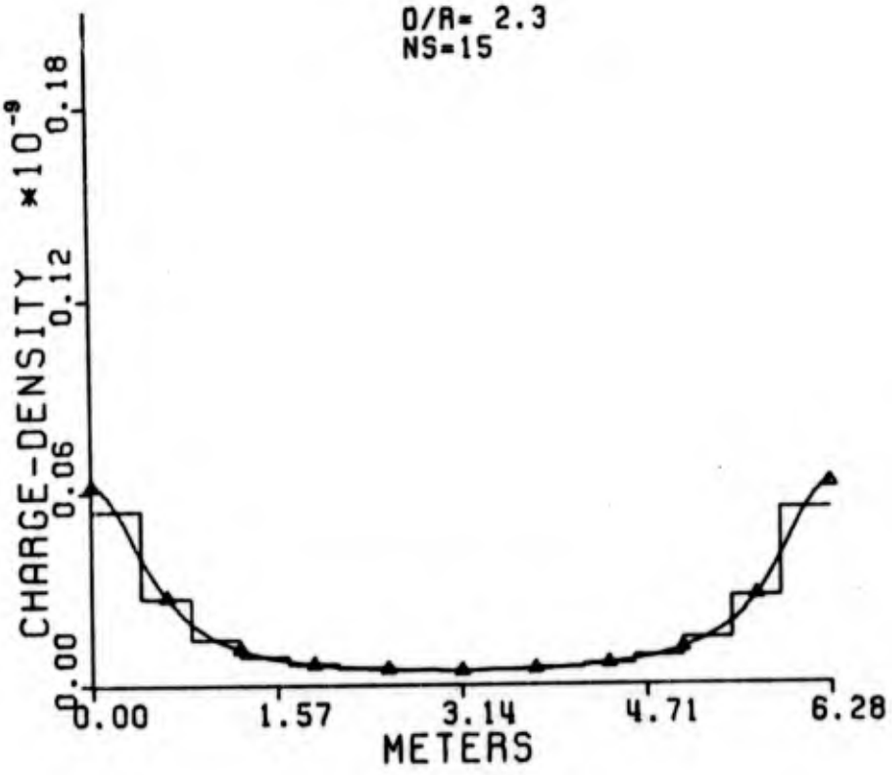
O/R= 2.3
NS=15
CHARGE-DENSITY *10^-9
0.18
0.12
0.06
0.00
0.00
1.57
3.14
4.71
6.28
METERS

CIRCULAR STRIPS

D/R=3.0. The exact capacitance = $0.2886231 \times 10^{-10}$

| NS | Approx. Capac.* | NS | Approx. Capac. |
|---|---|---|---|
| 3 | 0.2413373 | 12 | 0.2884186 |
| 4 | 0.2770143 | 13 | 0.2884678 |
| 5 | 0.2795018 | 14 | 0.2885058 |
| 6 | 0.2857513 | 15 | 0.2885316 |
| 7 | 0.2865276 | 16 | 0.2885513 |
| 8 | 0.2876984 | 17 | 0.2885659 |
| 9 | 0.2879519 | 18 | 0.2885771 |
| 10 | 0.2882262 | 19 | 0.2885859 |
| 11 | 0.2883301 | 20 | 0.2885928 |

*All capacitance values are multiplied by $10^{-10}$.

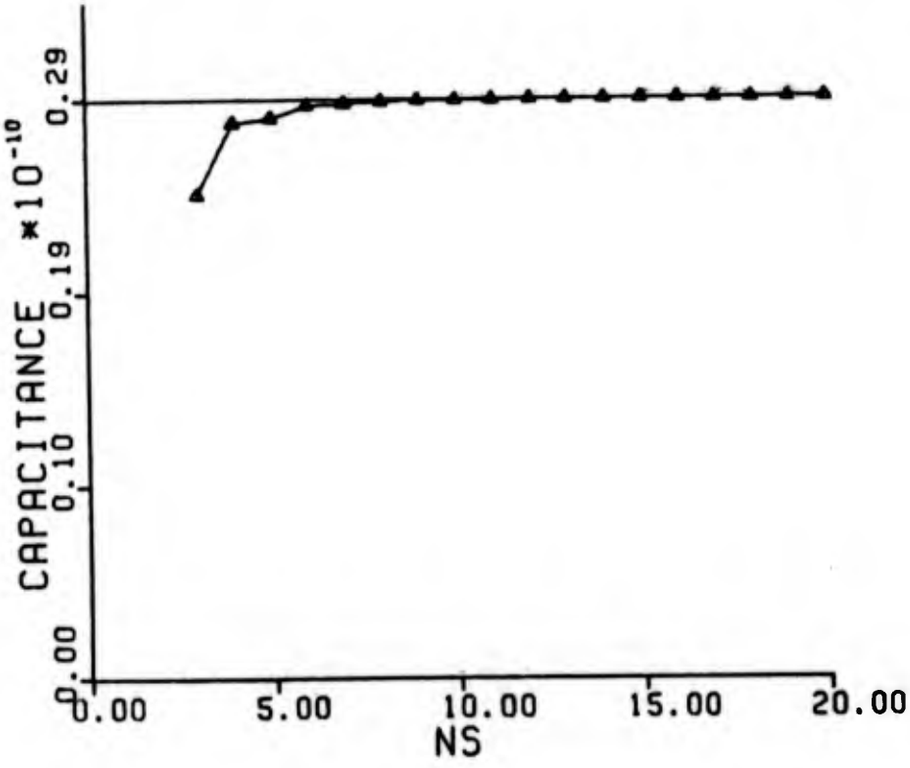

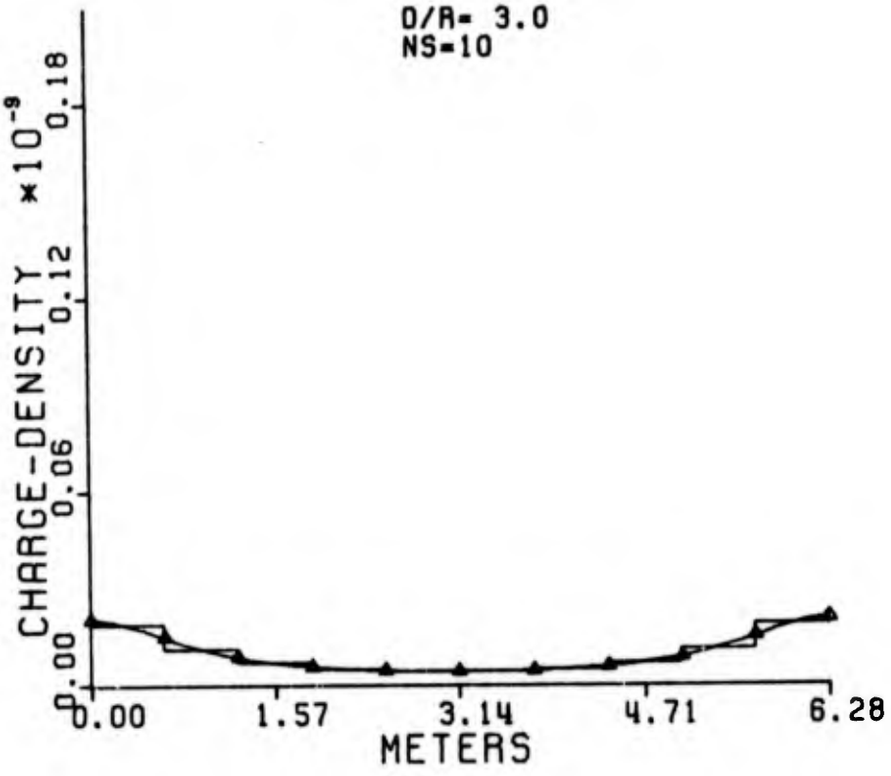
D/R= 3.0
NS=10
CHARGE-DENSITY *10^-9
0.00
0.06
0.12
0.18
0.00
1.57
3.14
4.71
6.28
METERS

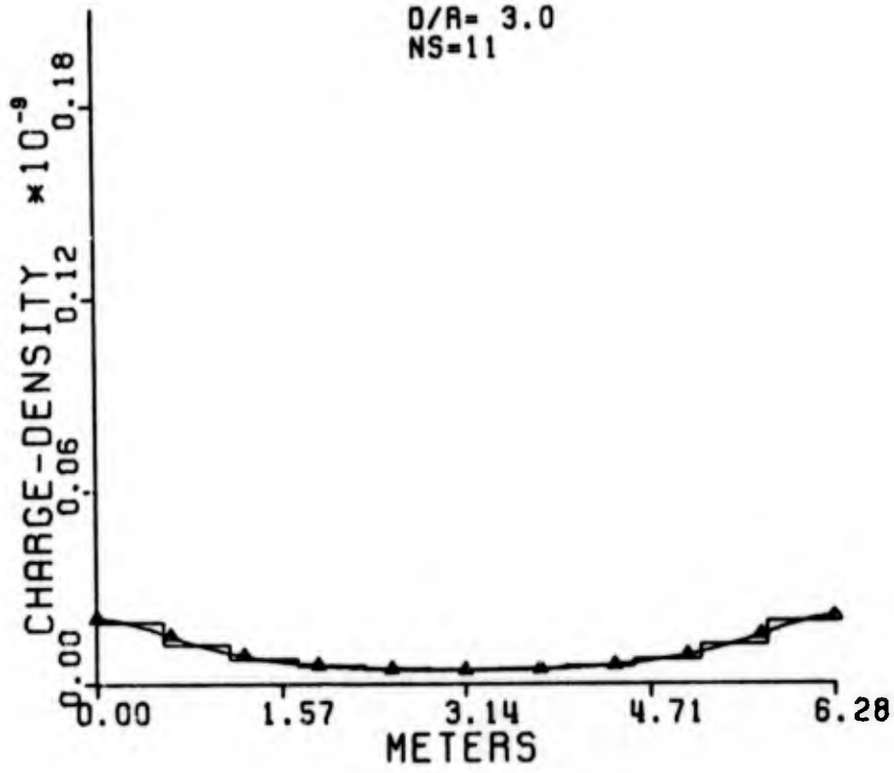
D/R= 3.0
NS=11
CHARGE-DENSITY *10^-9
0.00
0.06
0.12
0.18
0.00
1.57
3.14
4.71
6.28
METERS

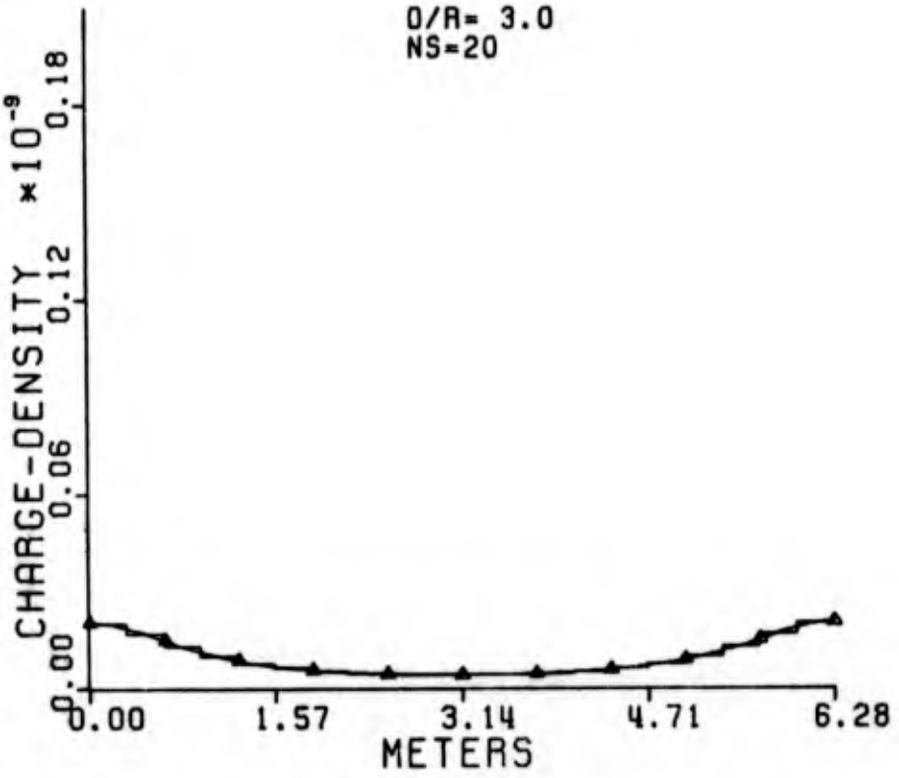
O/R= 3.0
NS=20
CHARGE-DENSITY ×10⁻⁹
0.00
0.06
0.12
0.18
0.00
1.57
3.14
4.71
6.28
METERS

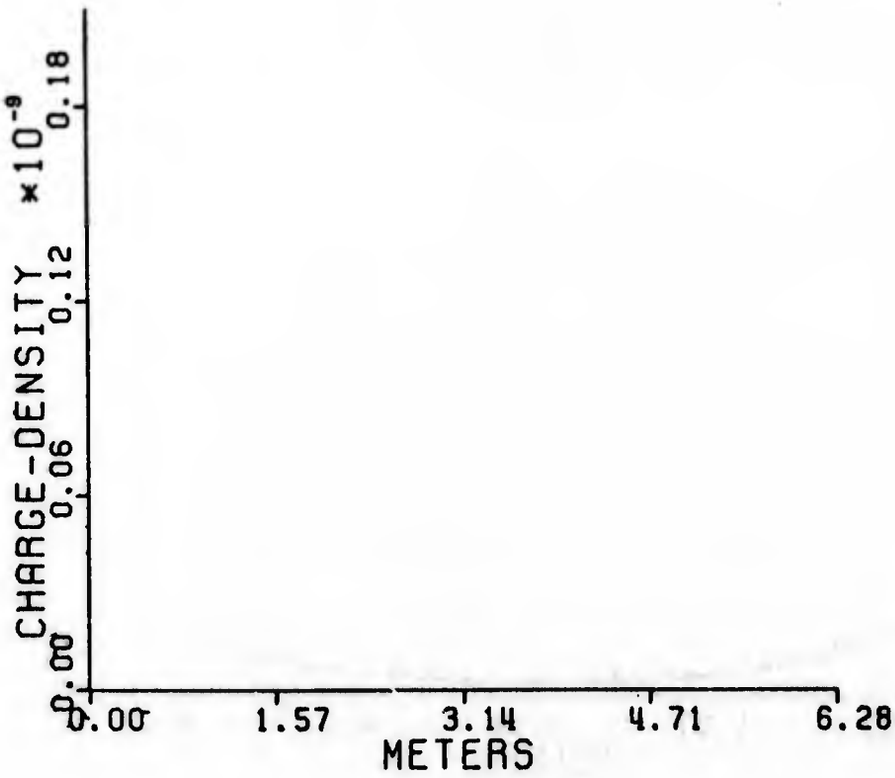
CHARGE-DENSITY ×10⁻⁹
0.00
0.06
0.12
0.18
0.00
1.57
3.14
4.71
6.28
METERS

CIRCULAR STRIPS

D/R=10.0. The exact capacitance = $0.1211716 \times 10^{-10}$

| NS | Approx. Capac.* | NS | Approx. Capac. |
|---|---|---|---|
| 3 | 0.1203928 | 12 | 0.1211730 |
| 4 | 0.1210853 | 13 | 0.1211732 |
| 5 | 0.1211405 | 14 | 0.1211732 |
| 6 | 0.1211606 | 15 | 0.1211732 |
| 7 | 0.1211671 | 16 | 0.1211732 |
| 8 | 0.1211701 | 17 | 0.1211731 |
| 9 | 0.1211716 | 18 | 0.1211731 |
| 10 | 0.1211724 | 19 | 0.1211731 |
| 11 | 0.1211728 | 20 | 0.1211730 |

*All capacitance values are multiplied by $10^{-10}$.

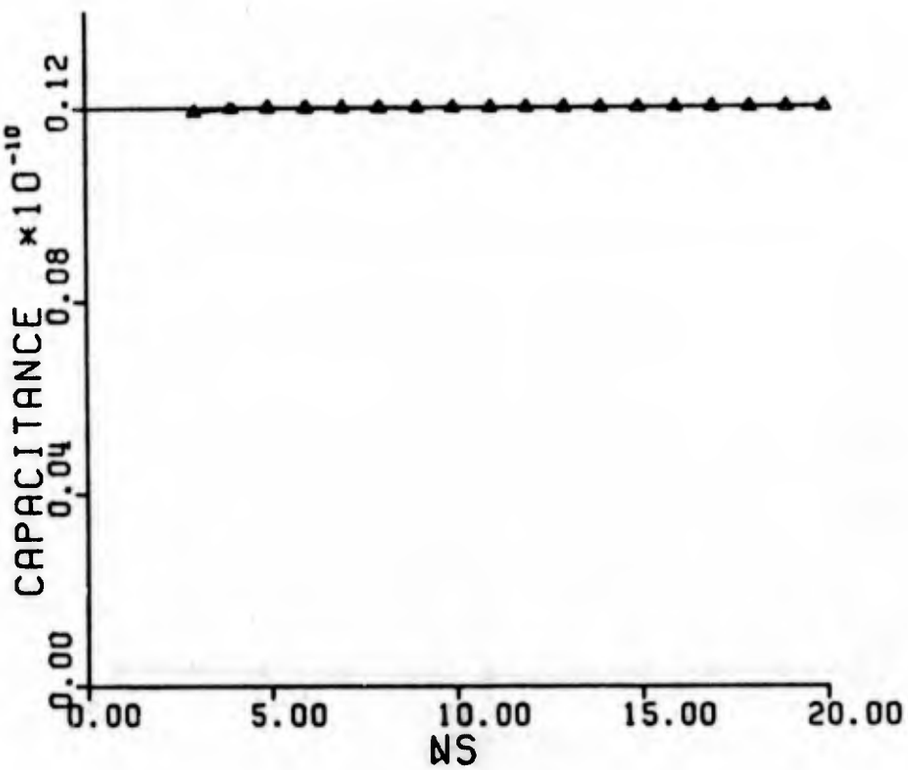

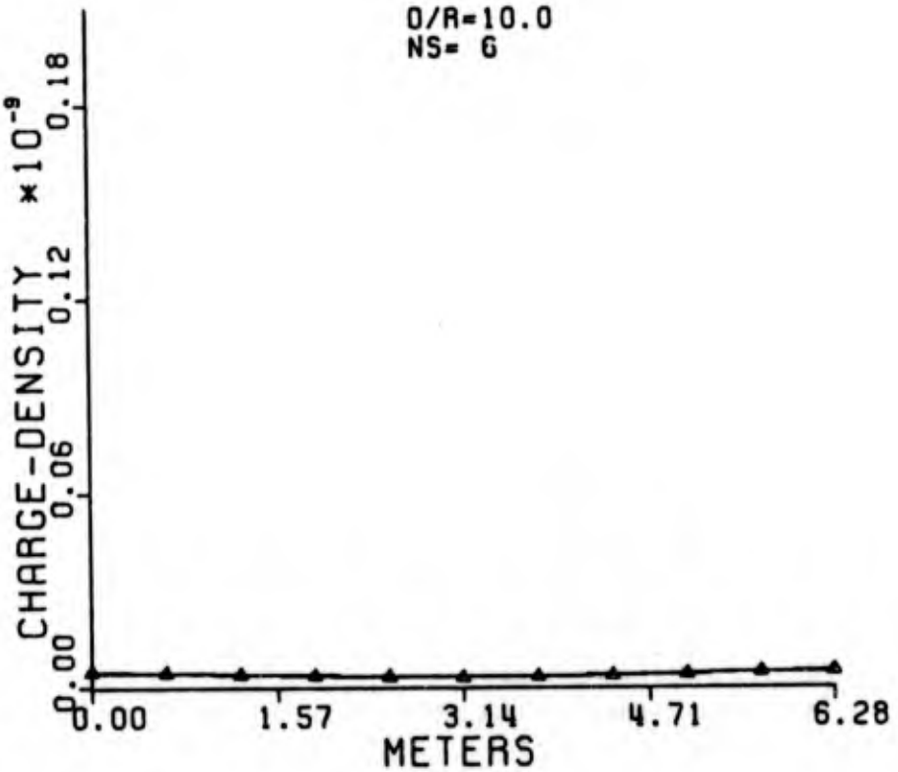
O/R=10.0
NS= 6
CHARGE-DENSITY *10^-9
0.00
0.06
0.12
0.18
0.00
1.57
3.14
4.71
6.28
METERS

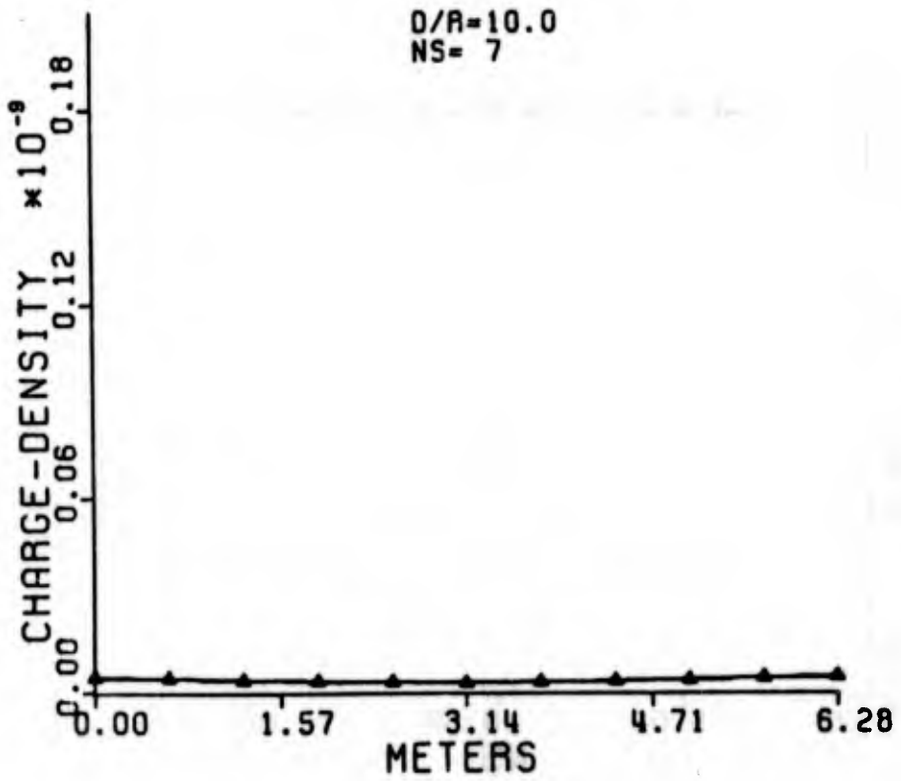
O/R=10.0
NS= 7
CHARGE-DENSITY *10^-9
0.00
0.06
0.12
0.18
0.00
1.57
3.14
4.71
6.28
METERS

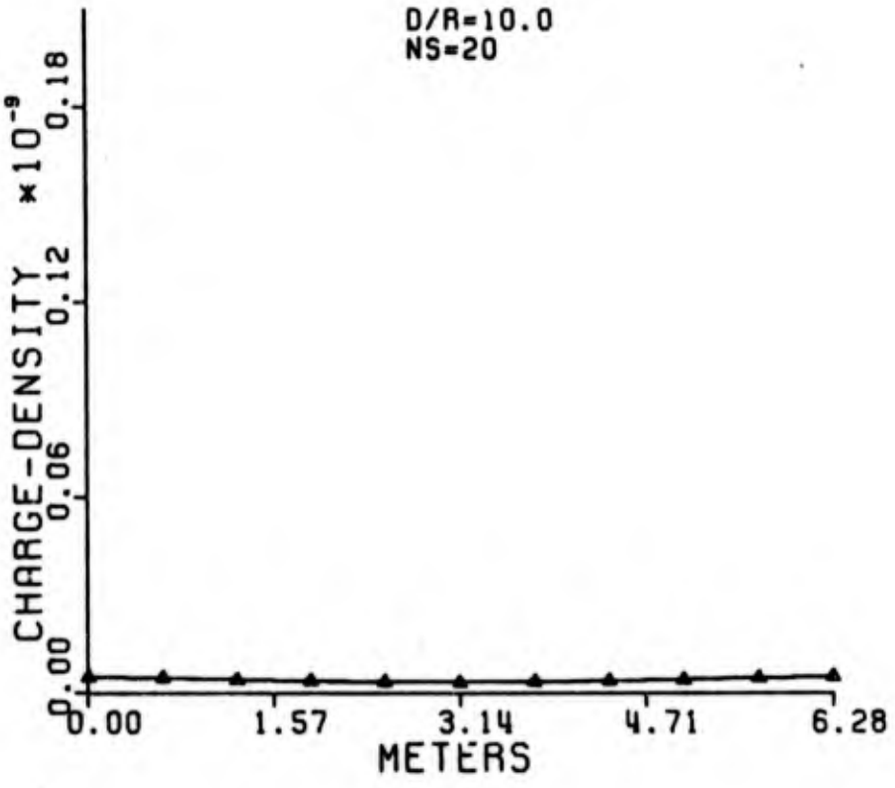
D/R=10.0
NS=20
CHARGE-DENSITY *10^-9
0.00
0.06
0.12
0.18
0.00
1.57
3.14
4.71
6.28
METERS

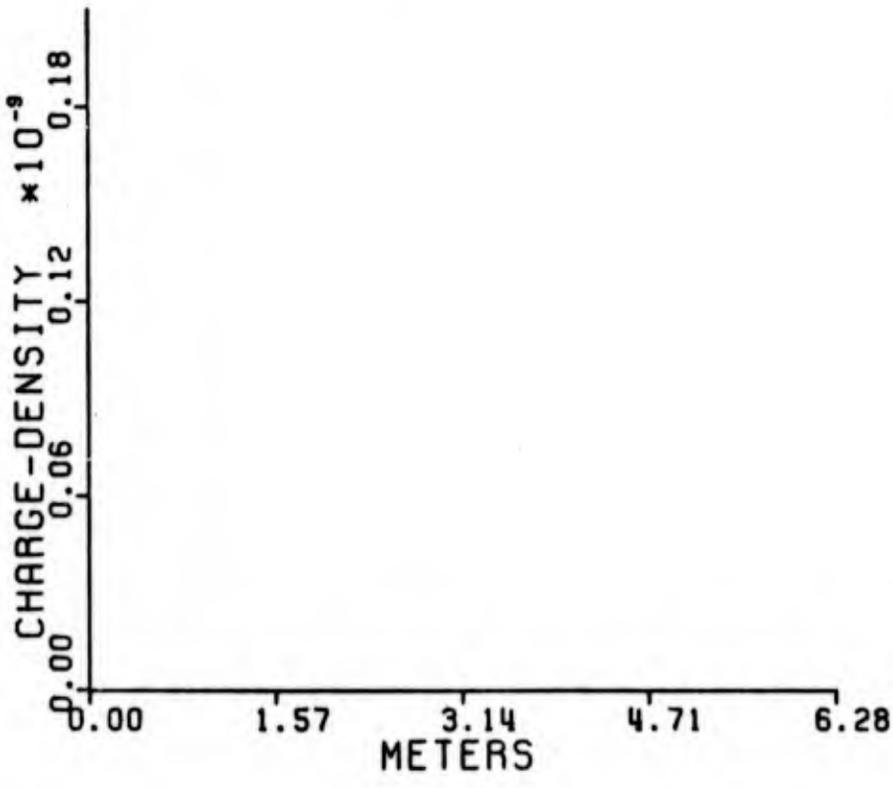
CHARGE-DENSITY *10^-9
0.00
0.06
0.12
0.18
0.00
1.57
3.14
4.71
6.28
METERS

APPENDIX D

FOURIER SERIES DATA

D/R=2.1. The exact capacitance = $0.8820449 \times 10^{-10}$
Δ-Odd values of NF. *-Even values of NF.

| NF | Approx.* Capac. | NF | Approx. Capac |
|---|---|---|---|
| 1 | 0.3290720 | 11 | 0.8814642 |
| 2 | 0.4581047 | 12 | 0.8690505 |
| 3 | 0.7230078 | 13 | 0.8820250 |
| 4 | 0.6535595 | 14 | 0.8757722 |
| 5 | 0.8355288 | 15 | 0.8821101 |
| 6 | 0.7667449 | 16 | 0.8789983 |
| 7 | 0.8694290 | 17 | 0.8820979 |
| 8 | 0.8258450 | 18 | 0.8805559 |
| 9 | 0.8789833 | 19 | 0.8820767 |
| 10 | 0.8550077 | 20 | 0.8813130 |

*Capacitance values are multiplied by $10^{-10}$.

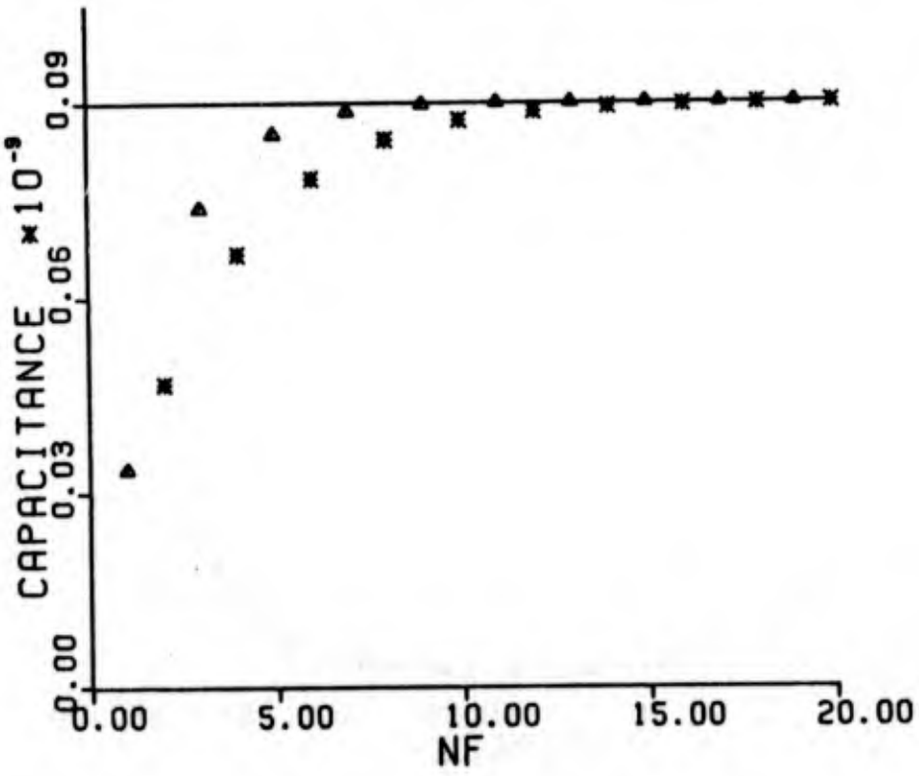

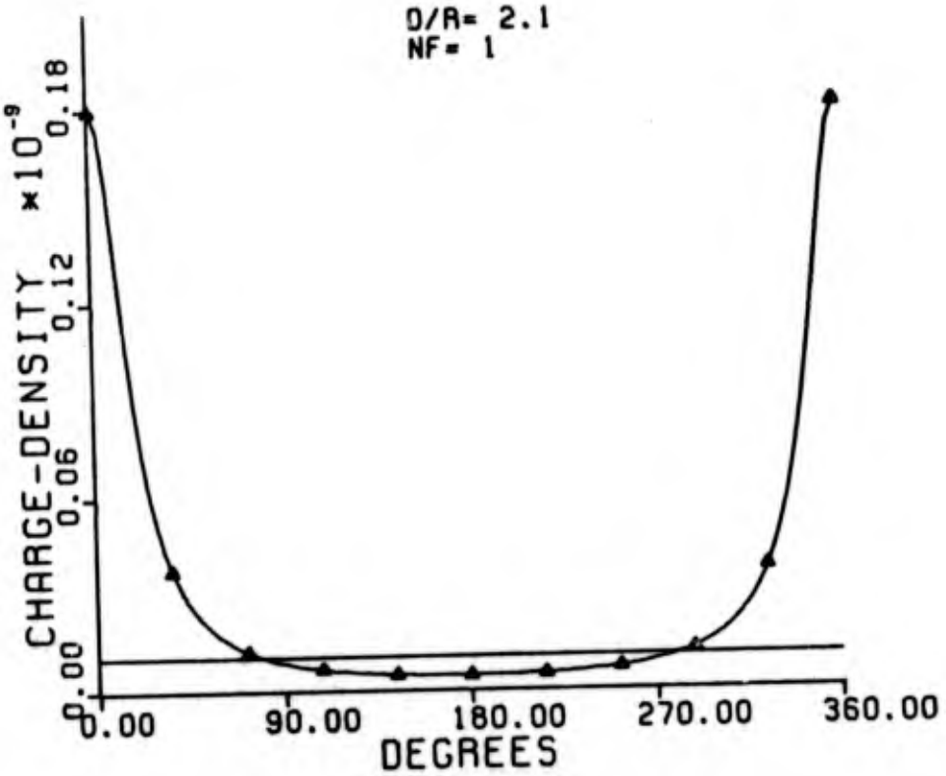
D/R= 2.1
NF= 1
CHARGE-DENSITY ×10⁻⁹
0.18
0.12
0.06
0.00
0.00
90.00
180.00
270.00
360.00
DEGREES

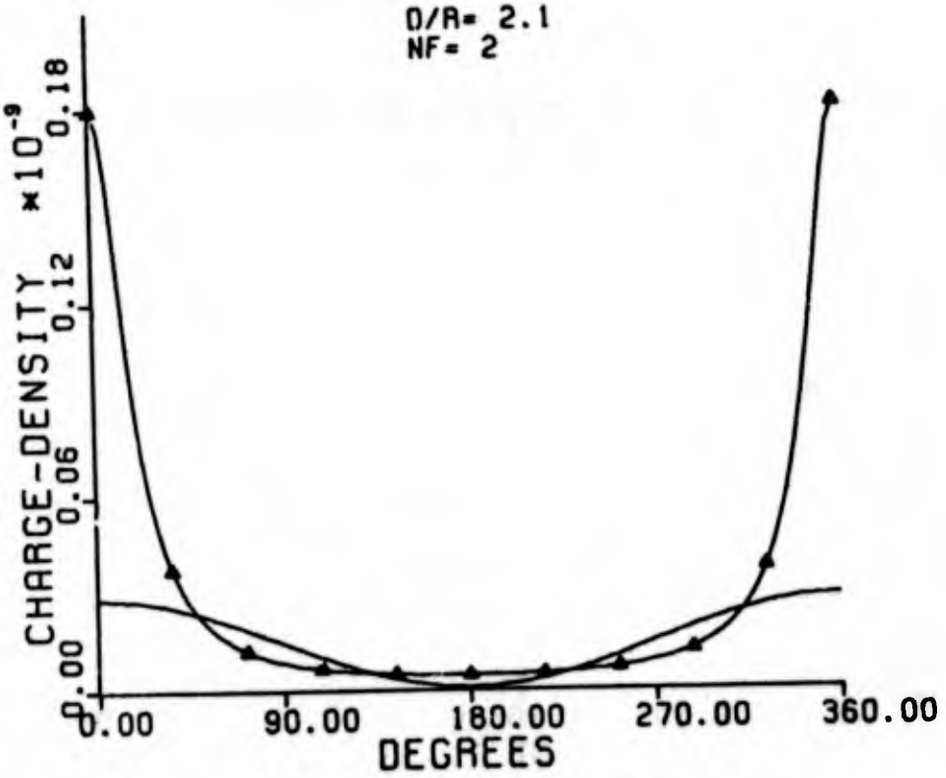
D/R= 2.1
NF= 2
CHARGE-DENSITY ×10⁻⁹
0.18
0.12
0.06
0.00
0.00
90.00
180.00
270.00
360.00
DEGREES

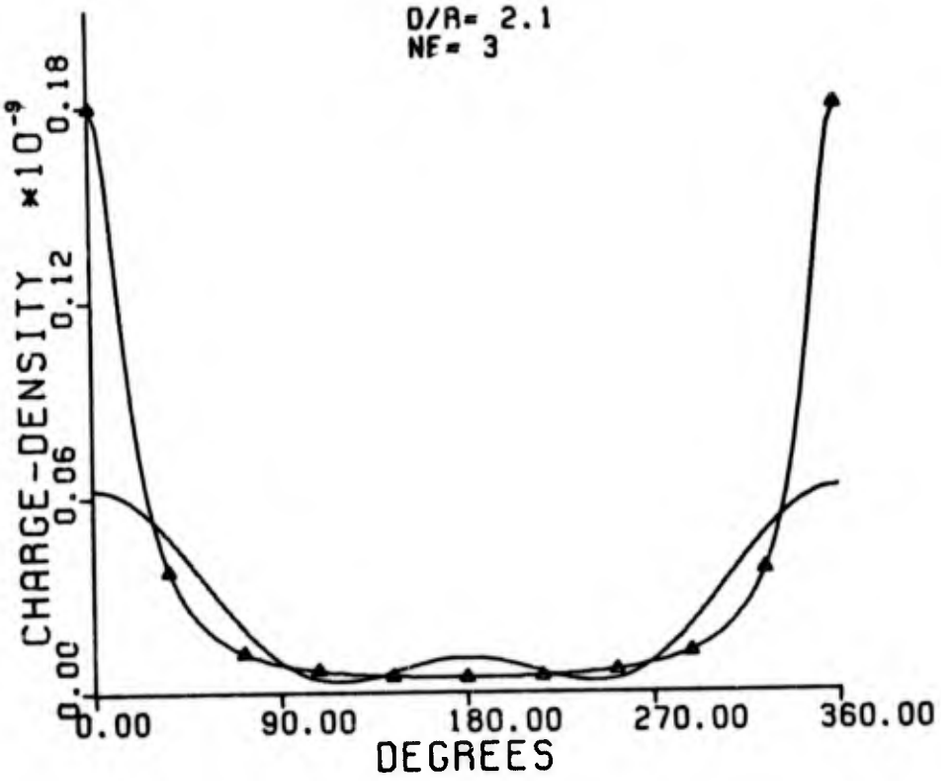
D/R= 2.1
NF= 3
CHARGE-DENSITY *10^-9
0.18
0.12
0.06
0.00
0.00
90.00
180.00
270.00
360.00
DEGREES

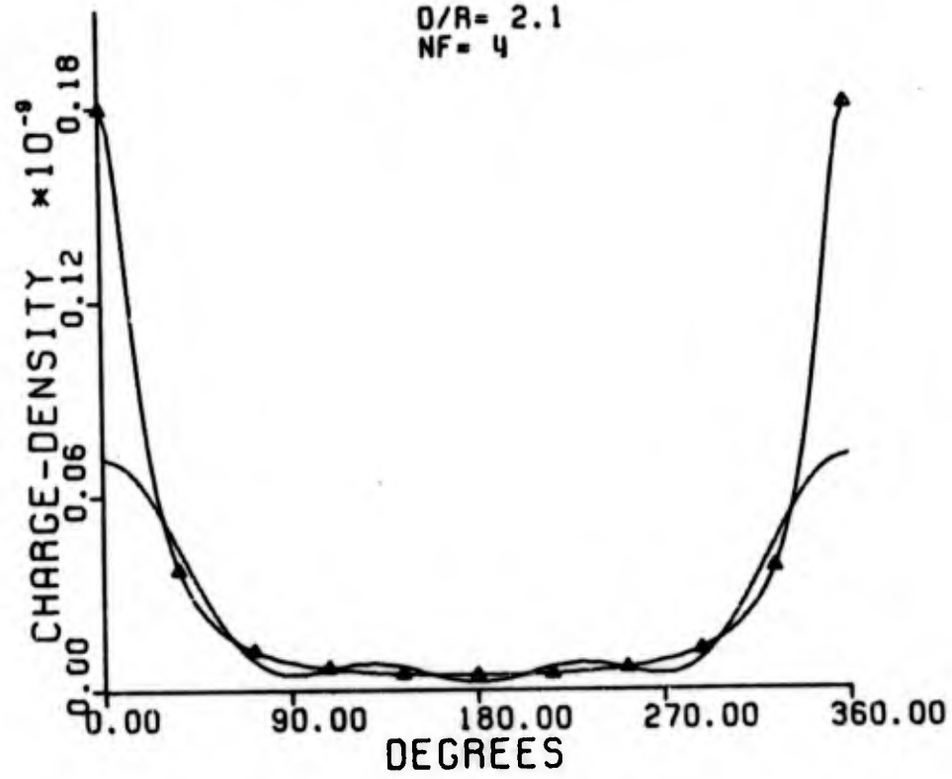
D/R= 2.1
NF= 4
CHARGE-DENSITY *10^-9
0.18
0.12
0.06
0.00
0.00
90.00
180.00
270.00
360.00
DEGREES

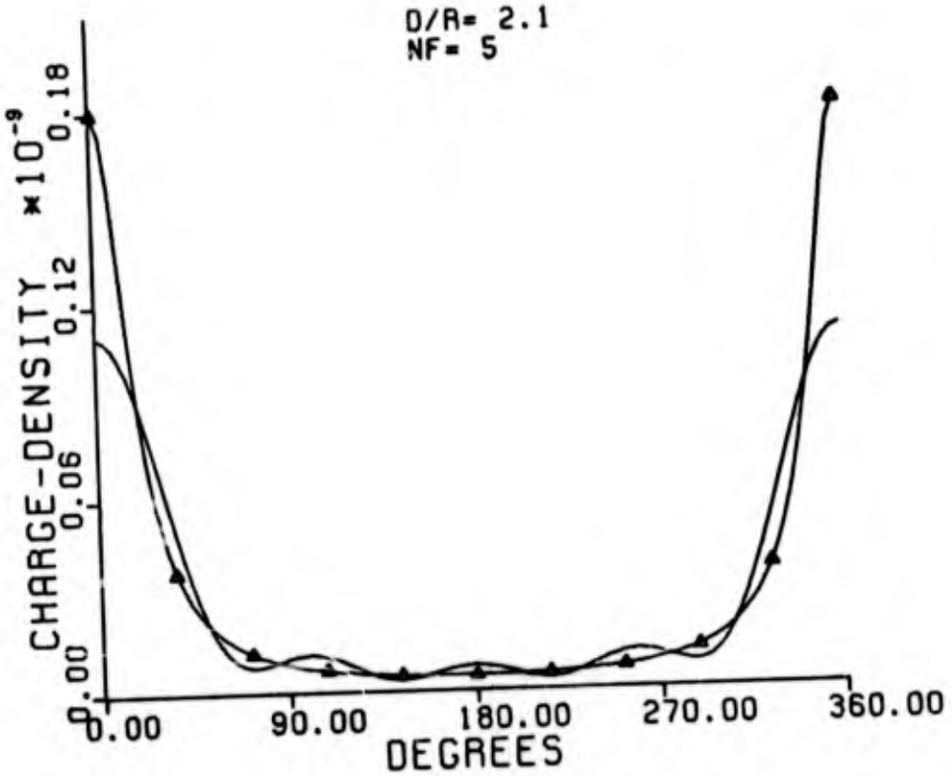
D/R= 2.1
NF= 5
CHARGE-DENSITY ×10⁻⁹
0.00
0.06
0.12
0.18
0.00
90.00
180.00
270.00
360.00
DEGREES

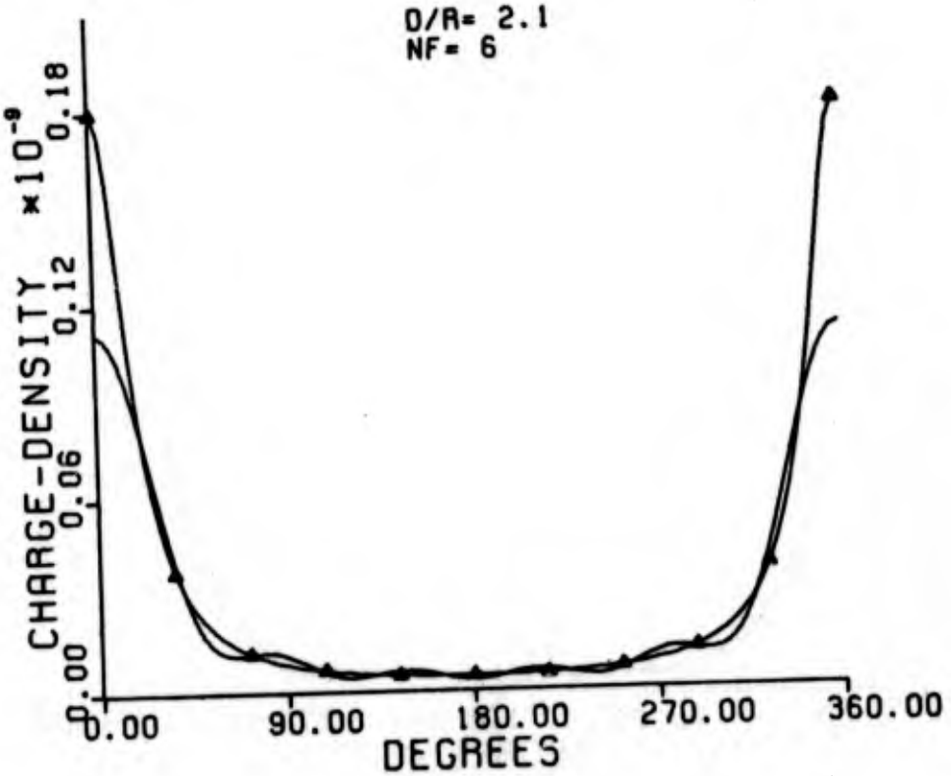
D/R= 2.1
NF= 6
CHARGE-DENSITY ×10⁻⁹
0.00
0.06
0.12
0.18
0.00
90.00
180.00
270.00
360.00
DEGREES

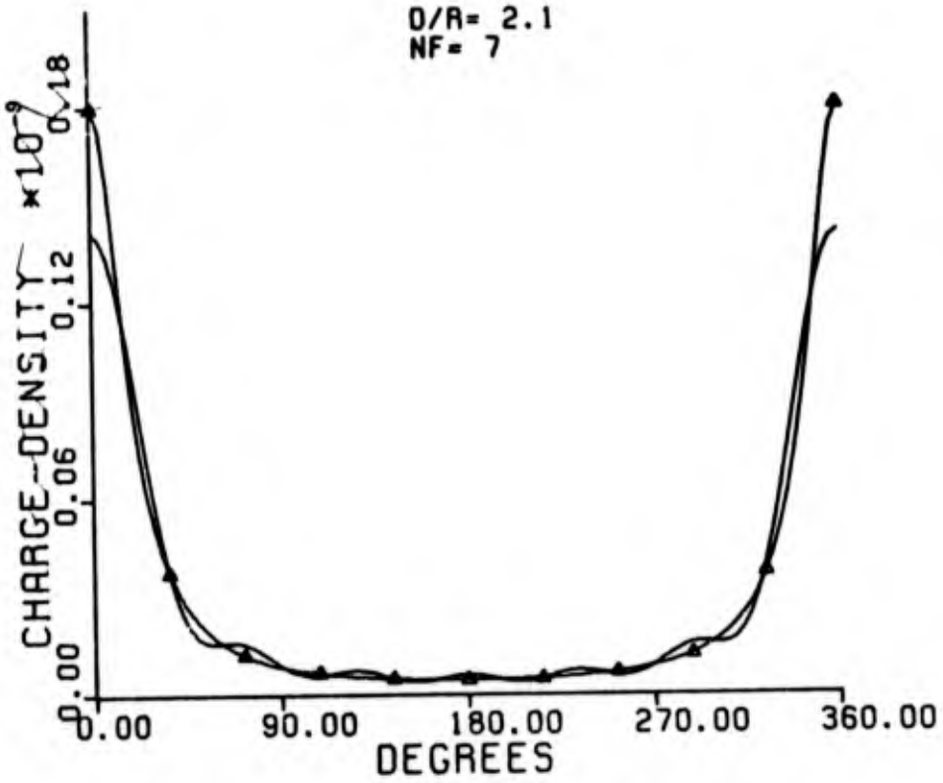
D/R= 2.1
NF= 7
CHARGE-DENSITY ×10⁻⁹
0.18
0.12
0.06
0.00
0.00
90.00
180.00
270.00
360.00
DEGREES

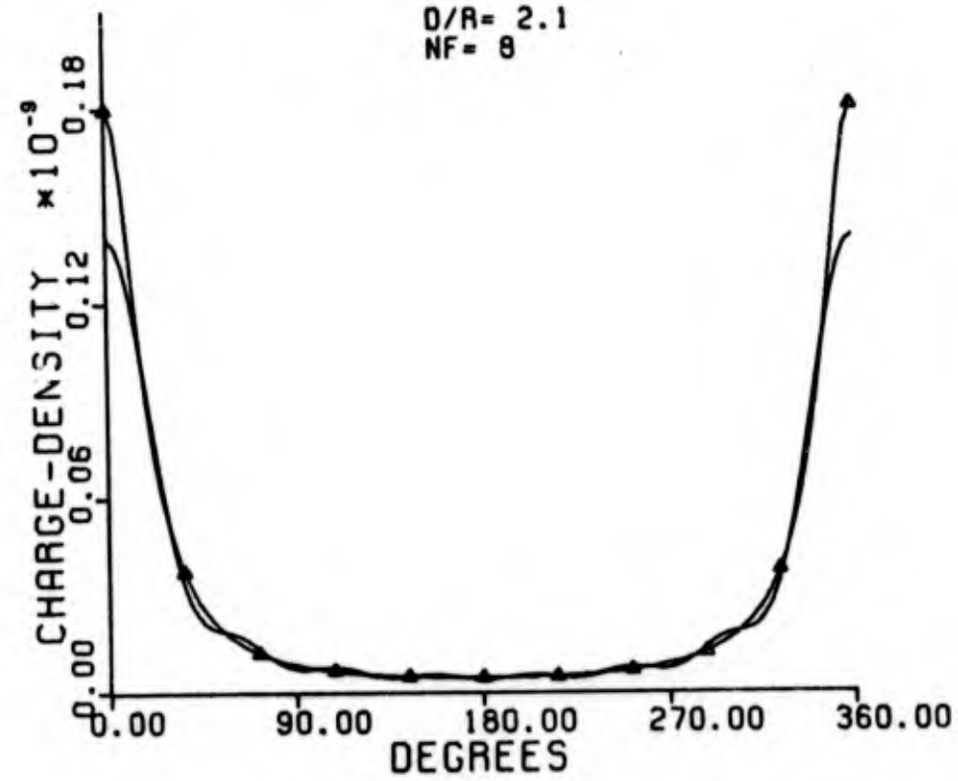
D/R= 2.1
NF= 8
CHARGE-DENSITY ×10⁻⁹
0.18
0.12
0.06
0.00
0.00
90.00
180.00
270.00
360.00
DEGREES

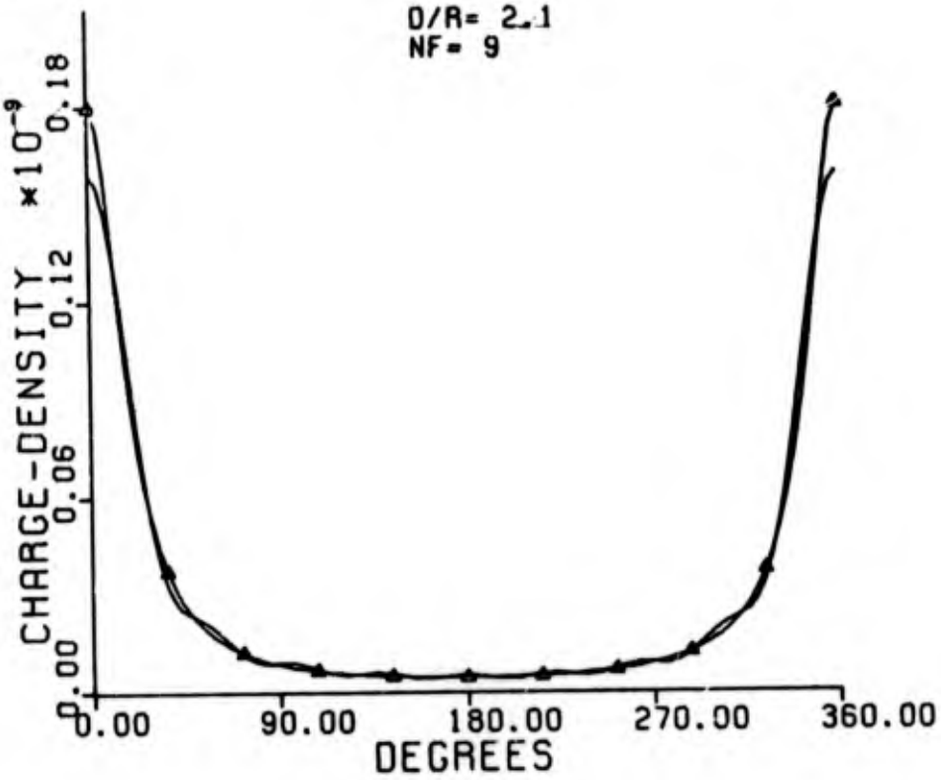
D/R= 2.1
NF= 9
CHARGE-DENSITY *10^-9
0.00
0.06
0.12
0.18
0.00
90.00
180.00
270.00
360.00
DEGREES

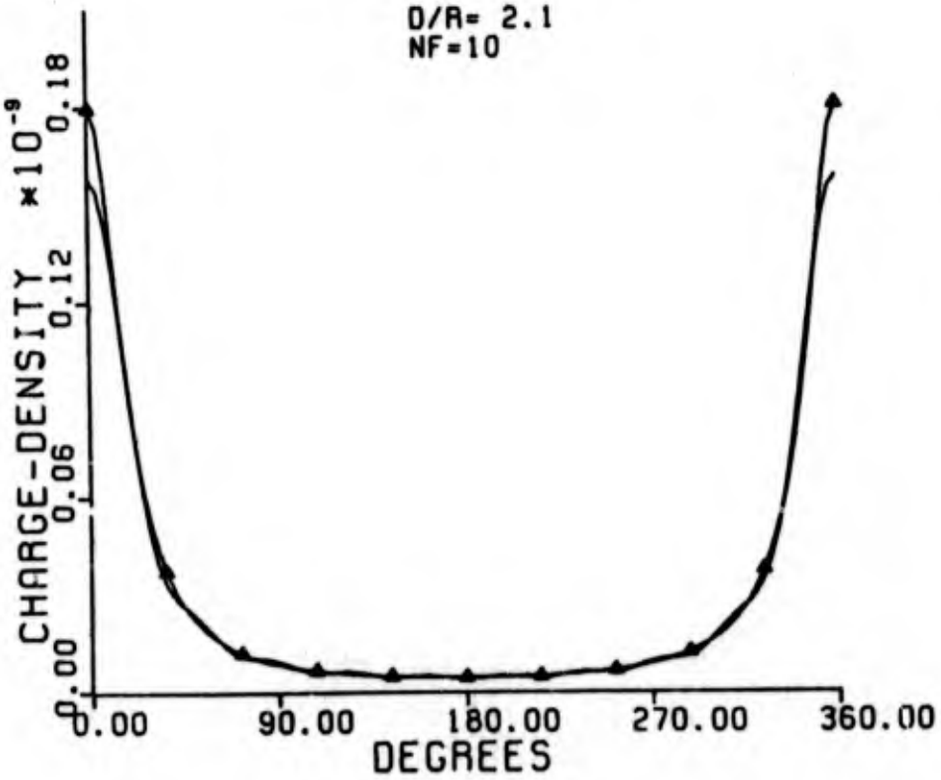
D/R= 2.1
NF=10
CHARGE-DENSITY *10^-9
0.00
0.06
0.12
0.18
0.00
90.00
180.00
270.00
360.00
DEGREES

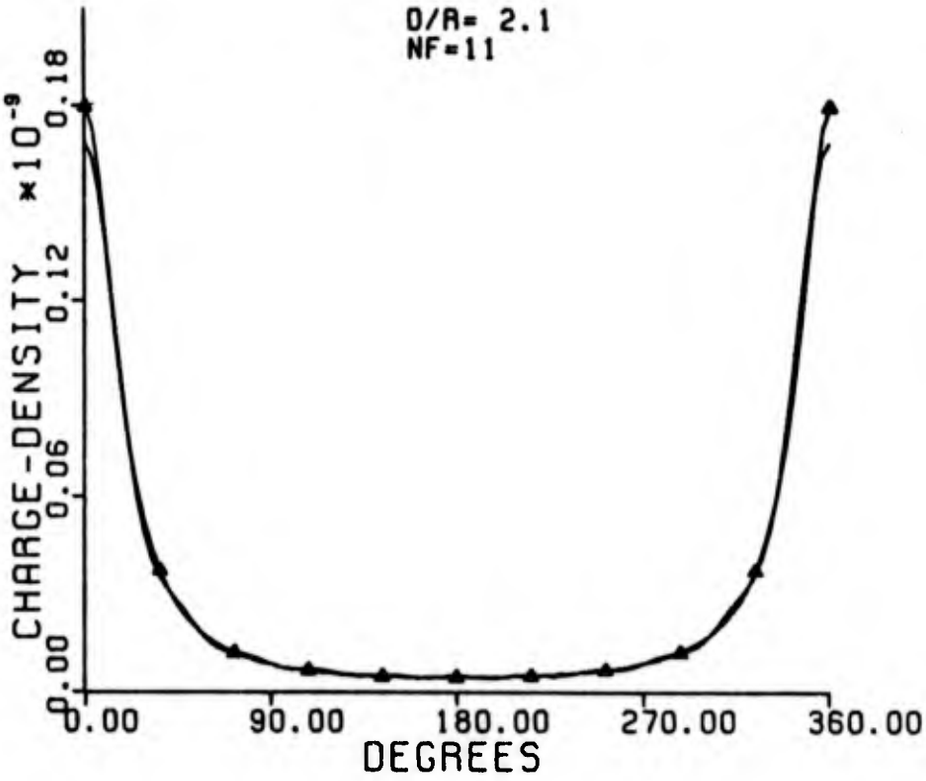
D/R= 2.1
NF=11
CHARGE-DENSITY ×10⁻⁹
0.18
0.12
0.06
0.00
0.00
90.00
180.00
270.00
360.00
DEGREES

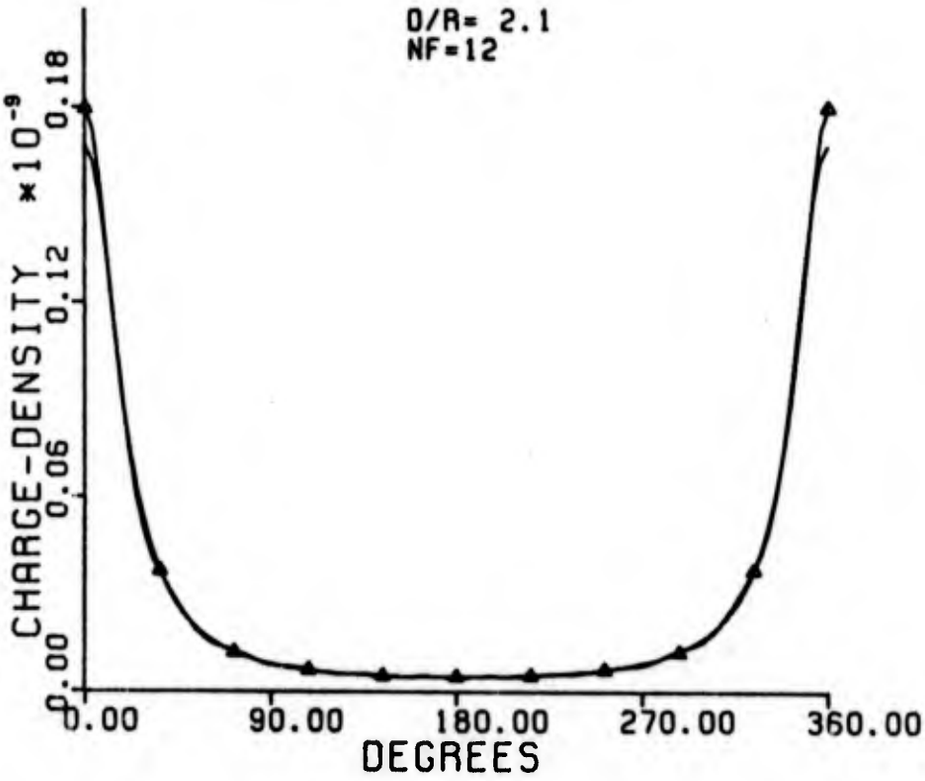
D/R= 2.1
NF=12
CHARGE-DENSITY ×10⁻⁹
0.18
0.12
0.06
0.00
0.00
90.00
180.00
270.00
360.00
DEGREES

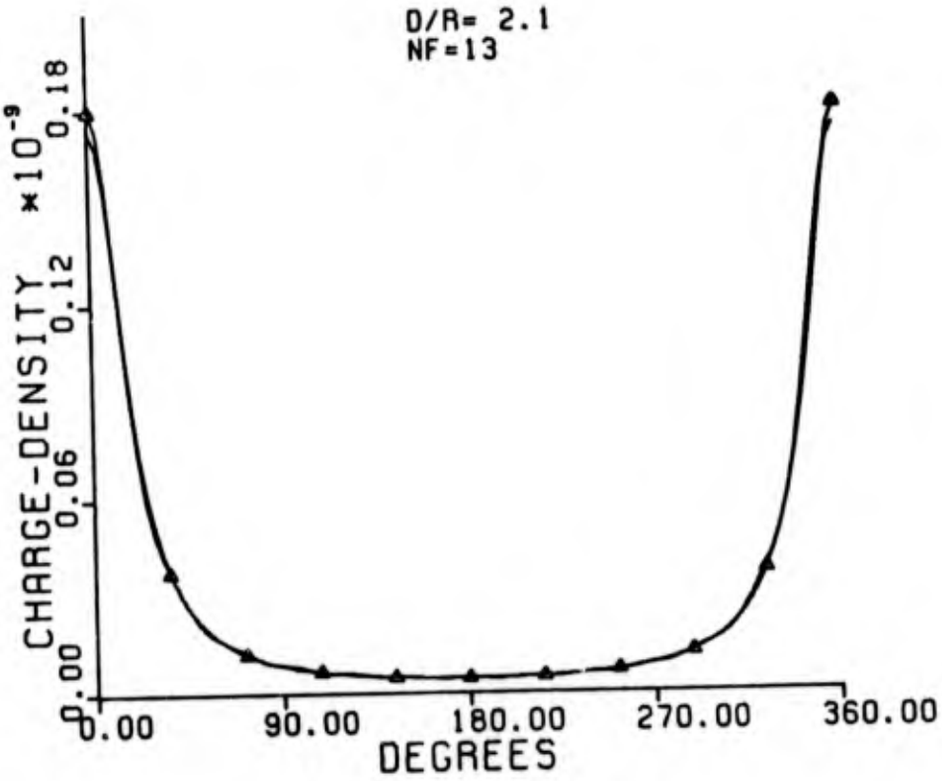
D/R= 2.1
NF=13
CHARGE-DENSITY ×10⁻⁹
0.00
0.06
0.12
0.18
0.00
90.00
180.00
270.00
360.00
DEGREES

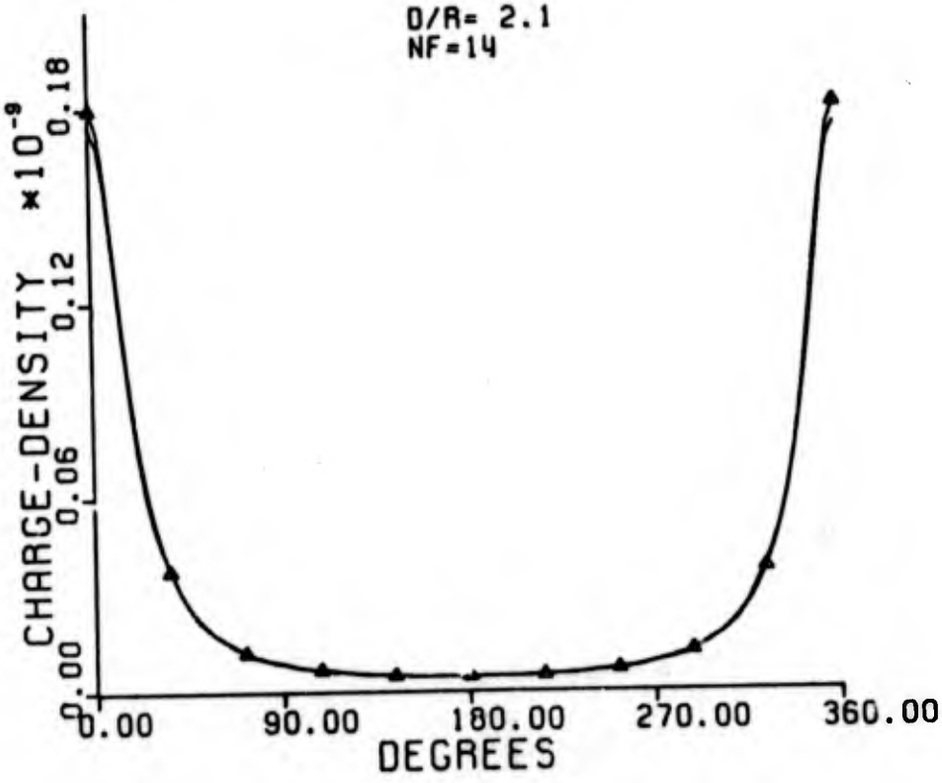
D/R= 2.1
NF=14
CHARGE-DENSITY ×10⁻⁹
0.00
0.06
0.12
0.18
0.00
90.00
180.00
270.00
360.00
DEGREES

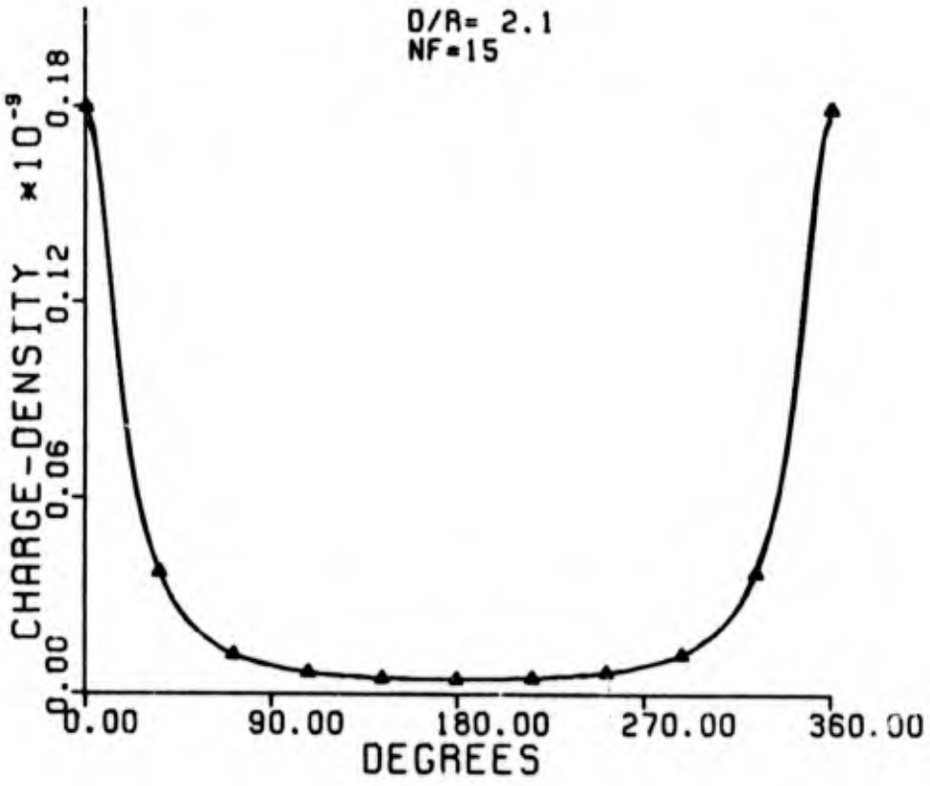
D/R= 2.1
NF=15
CHARGE-DENSITY *10^-9
0.00
0.06
0.12
0.18
0.00
90.00
180.00
270.00
360.00
DEGREES

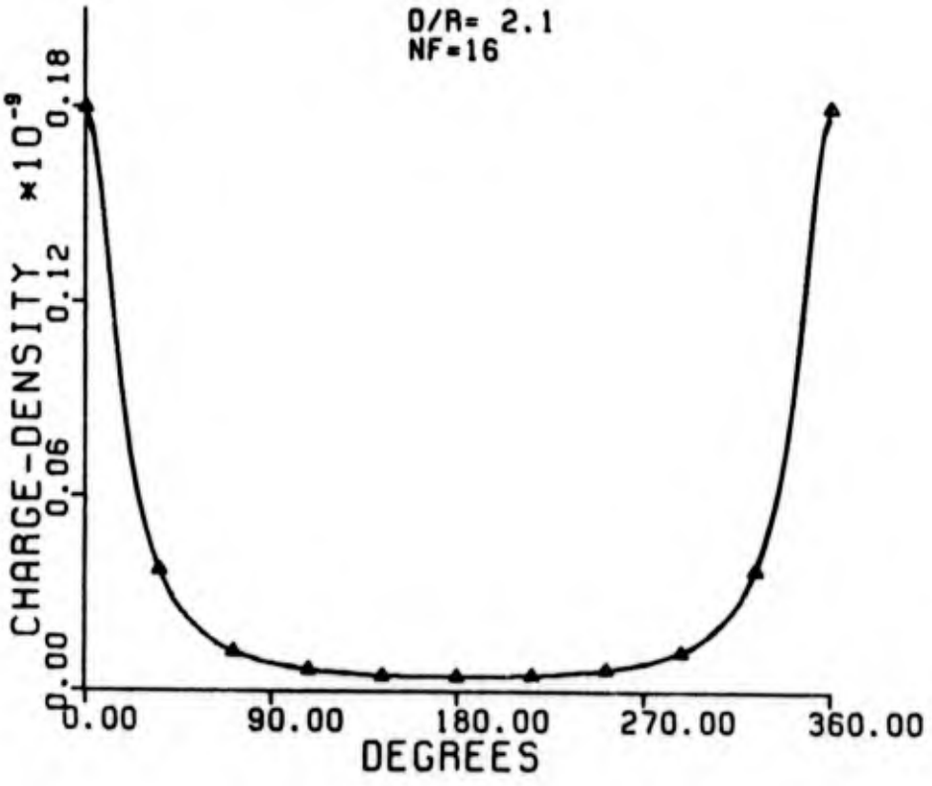
D/R= 2.1
NF=16
CHARGE-DENSITY *10^-9
0.00
0.06
0.12
0.18
0.00
90.00
180.00
270.00
360.00
DEGREES

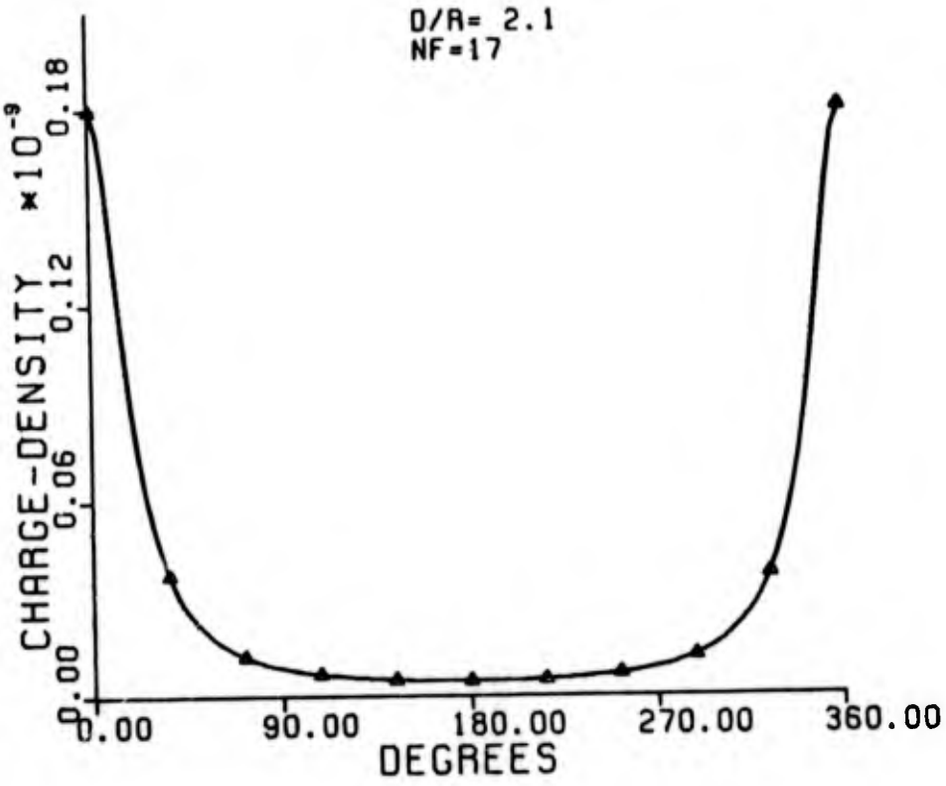
D/R= 2.1
NF=17
CHARGE-DENSITY ×10⁻⁹
0.18
0.12
0.06
0.00
0.00
90.00
180.00
270.00
360.00
DEGREES

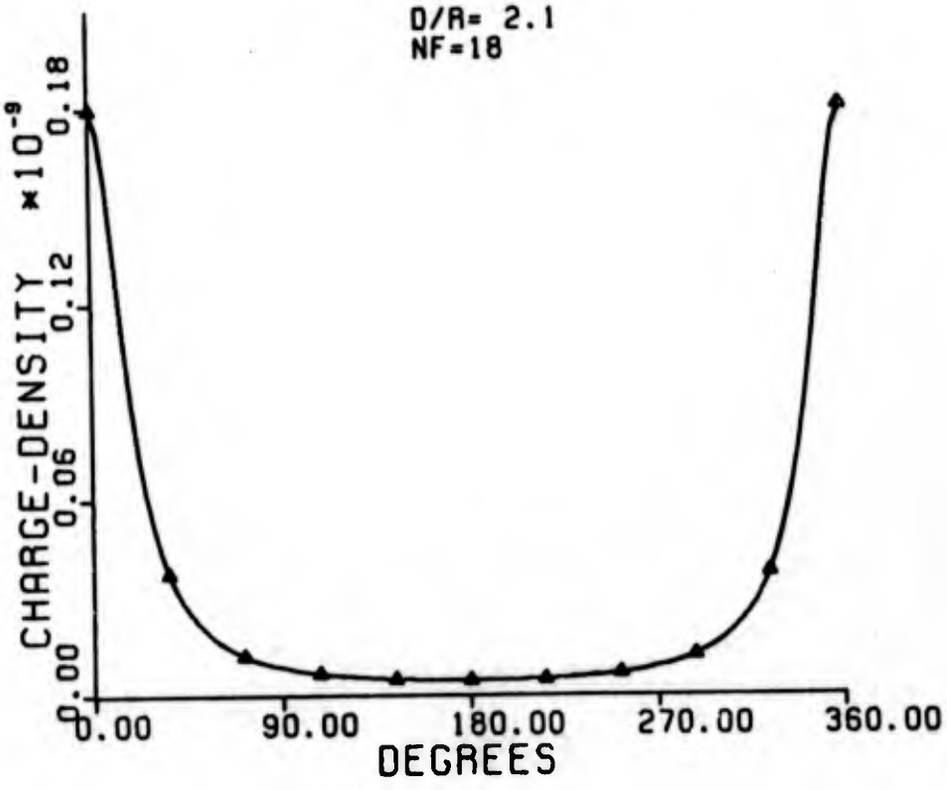
D/R= 2.1
NF=18
CHARGE-DENSITY ×10⁻⁹
0.18
0.12
0.06
0.00
0.00
90.00
180.00
270.00
360.00
DEGREES

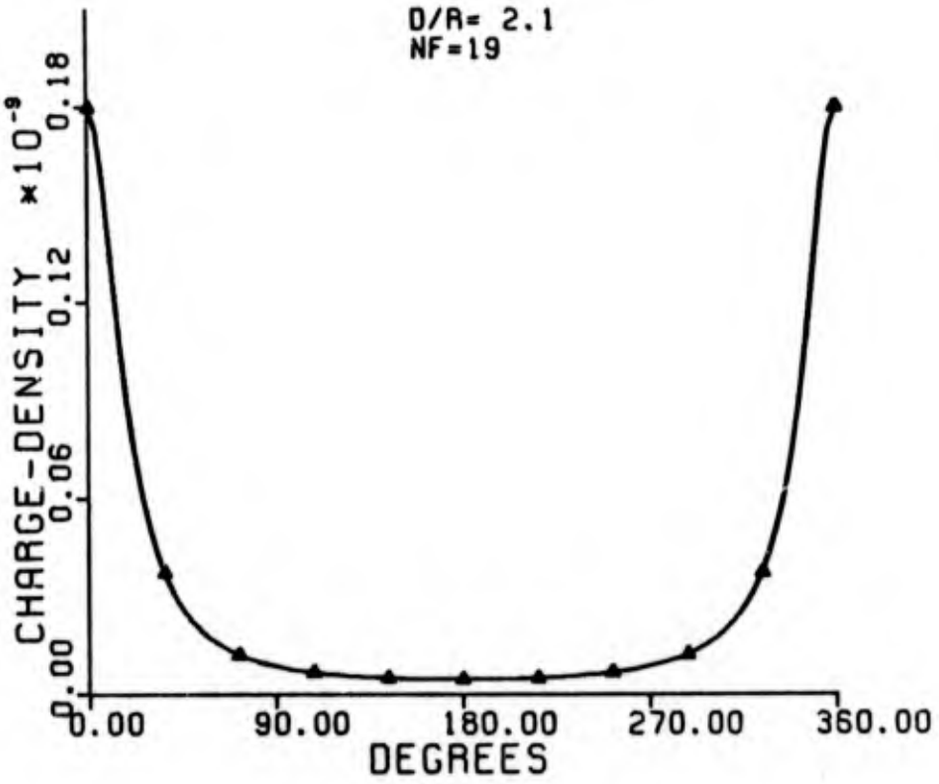
D/R= 2.1
NF=19
CHARGE-DENSITY ×10⁻⁹
0.00
0.06
0.12
0.18
0.00
90.00
180.00
270.00
360.00
DEGREES

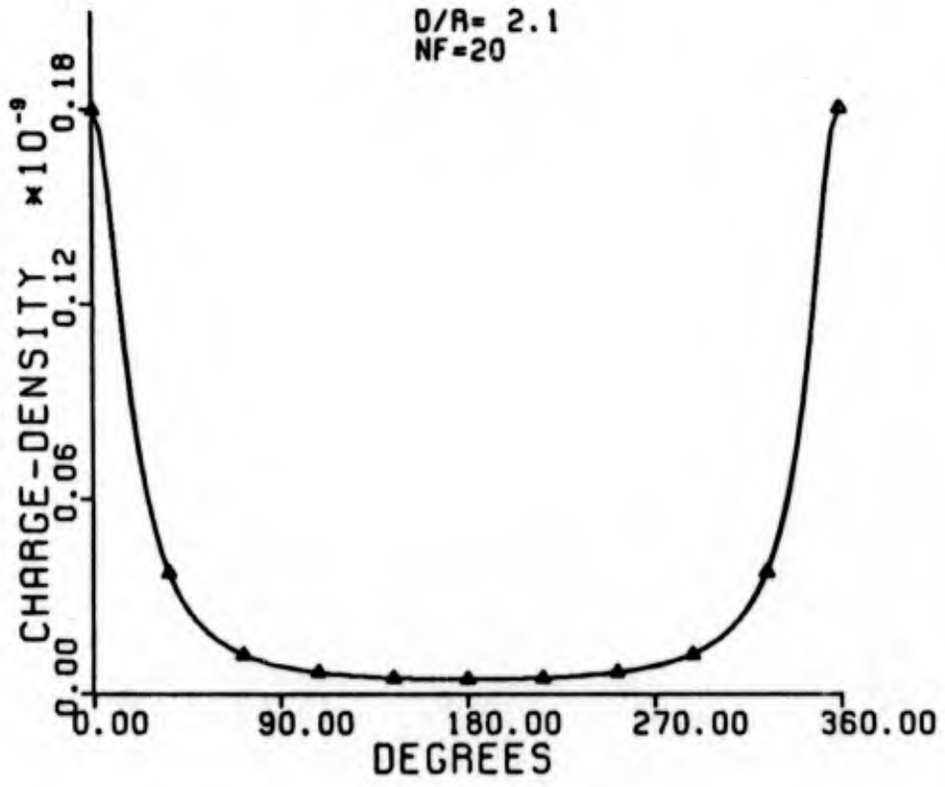
D/R= 2.1
NF=20
CHARGE-DENSITY ×10⁻⁹
0.00
0.06
0.12
0.18
0.00
90.00
180.00
270.00
360.00
DEGREES

FOURIER SERIES

D/R=2.2. The exact capacitance = $.6262345 \times 10^{-10}$
Δ-Odd values of NF. *-Even values of NF.

| NF | Approx.* Capac. | NF | Approx. Capac. |
|---|---|---|---|
| 1 | 0.3148103 | 11 | 0.6263823 |
| 2 | 0.4202215 | 12 | 0.6250297 |
| 3 | 0.5866351 | 13 | 0.6262954 |
| 4 | 0.5478852 | 14 | 0.6257977 |
| 5 | 0.6217818 | 15 | 0.6262579 |
| 6 | 0.5985988 | 16 | 0.6260741 |
| 7 | 0.6262644 | 17 | 0.6262433 |
| 8 | 0.6166271 | 18 | 0.6261750 |
| 9 | 0.6265190 | 19 | 0.6262378 |
| 10 | 0.6228599 | 20 | 0.6262122 |

*Capacitance value are multiplied by $10^{-10}$.

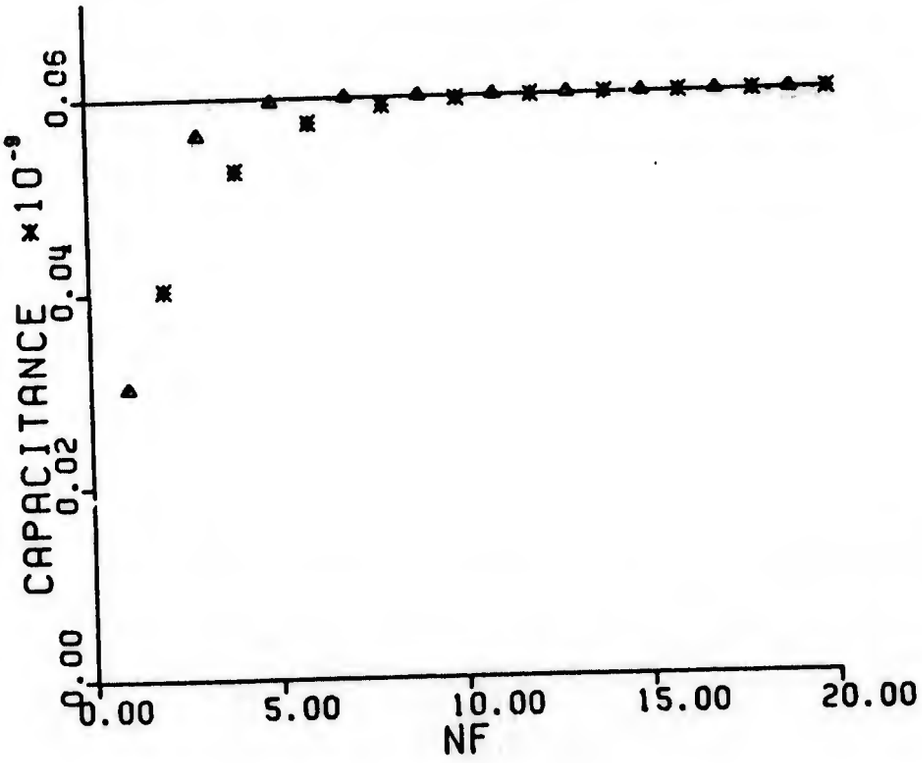

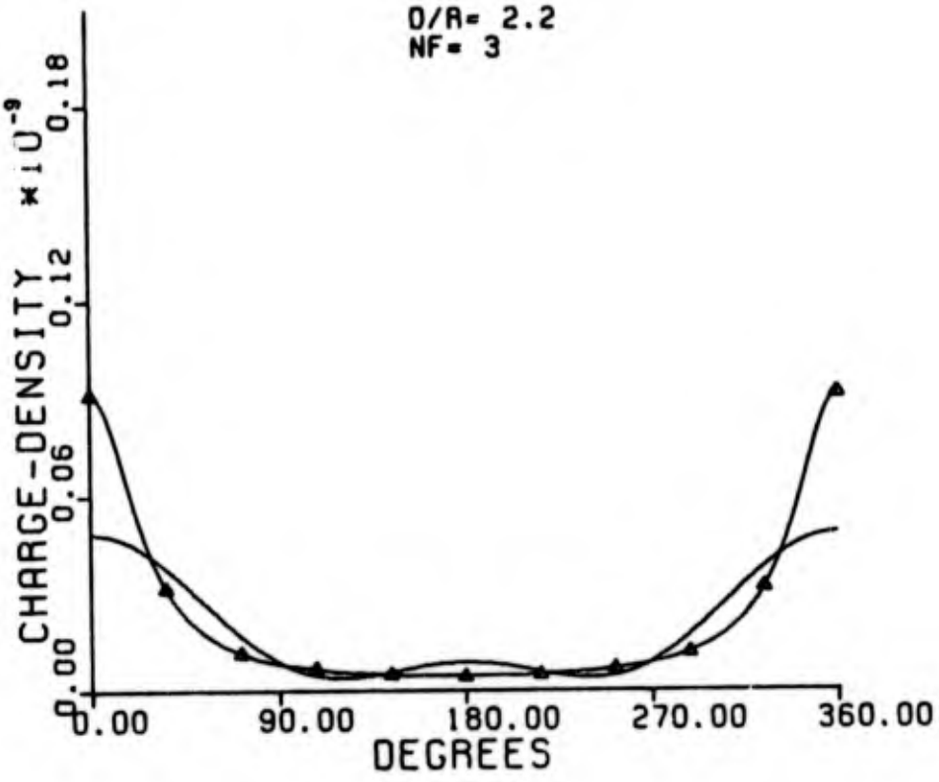
O/R= 2.2
NF= 3
CHARGE-DENSITY *10^-9
0.00
0.06
0.12
0.18
0.00
90.00
180.00
270.00
360.00
DEGREES

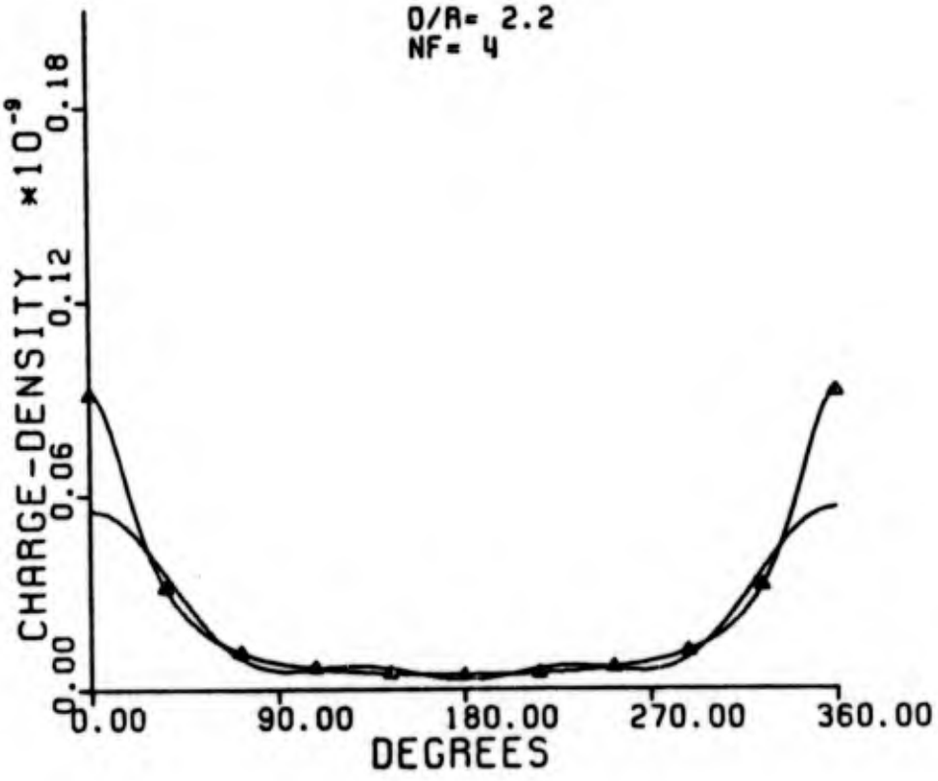
O/R= 2.2
NF= 4
CHARGE-DENSITY *10^-9
0.00
0.06
0.12
0.18
0.00
90.00
180.00
270.00
360.00
DEGREES

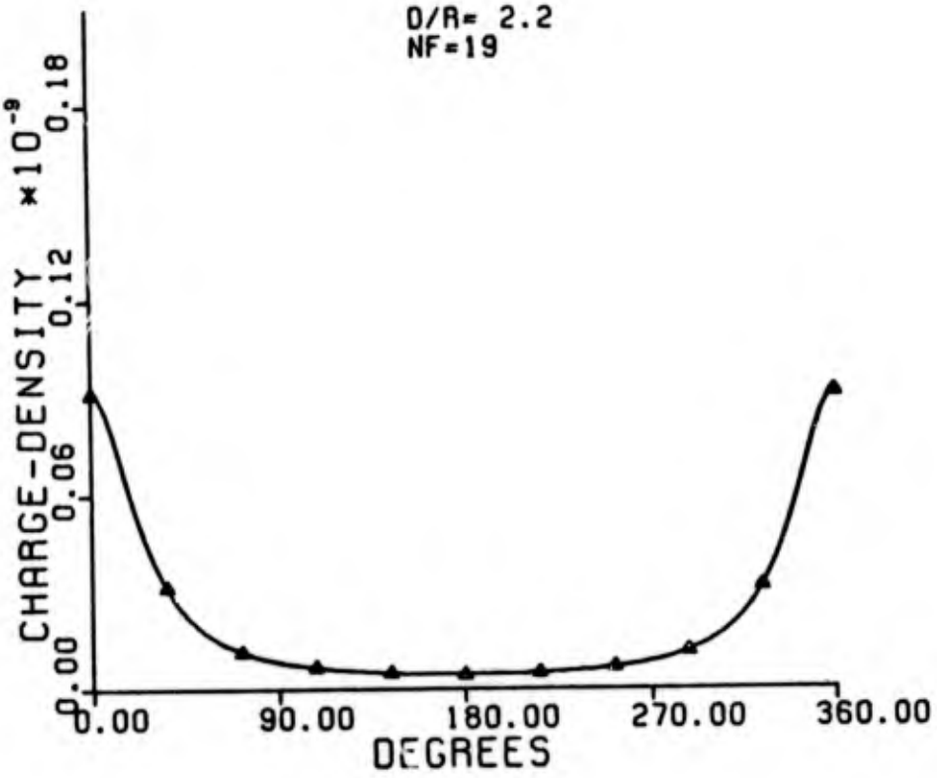
D/R= 2.2
NF=19
CHARGE-DENSITY *10^-9
0.00
0.06
0.12
0.18
0.00
90.00
180.00
270.00
360.00
DEGREES

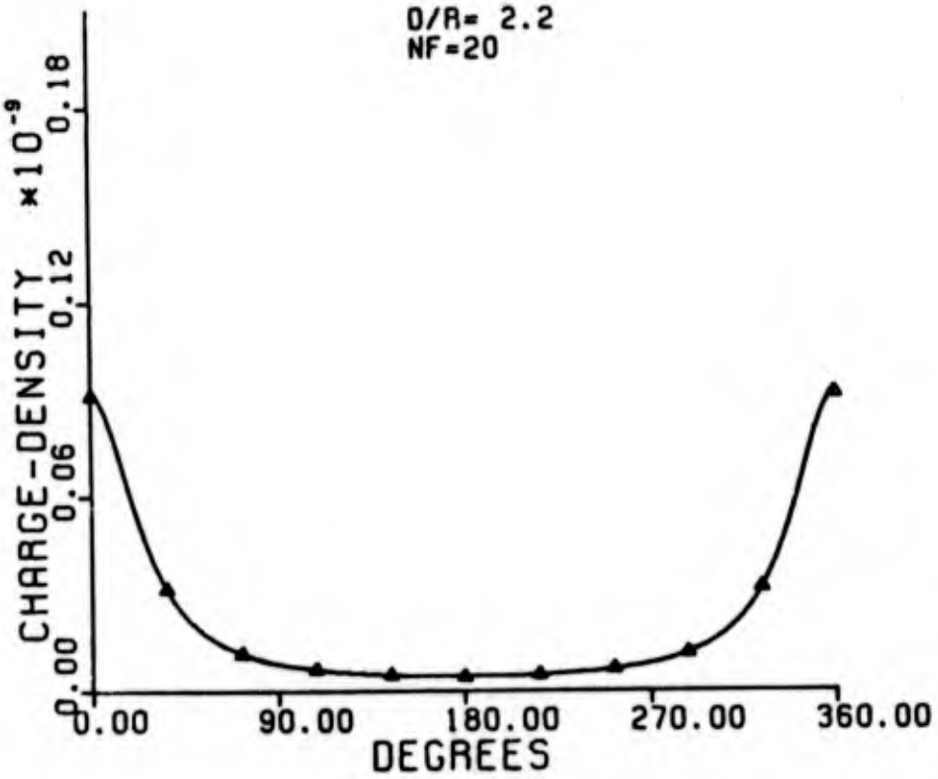
D/R= 2.2
NF=20
CHARGE-DENSITY *10^-9
0.00
0.06
0.12
0.18
0.00
90.00
180.00
270.00
360.00
DEGREES

FOURIER SERIES

D/R=2.3. The exact capacitance = $0.5133601 \times 10^{-10}$
Δ-Odd values of NF. *-Even values of NF.

| NF | Approx.*Capac. | NF | Approx. Capac. |
|---|---|---|---|
| 1 | 0.3021029 | 11 | 0.5134190 |
| 2 | 0.3894184 | 12 | 0.5131394 |
| 3 | 0.5018097 | 13 | 0.5133777 |
| 4 | 0.4774476 | 14 | 0.5132949 |
| 5 | 0.5138287 | 15 | 0.5133654 |
| 6 | 0.5035773 | 16 | 0.5133405 |
| 7 | 0.5138780 | 17 | 0.5133617 |
| 8 | 0.5106671 | 18 | 0.5133541 |
| 9 | 0.5135492 | 19 | 0.5133606 |
| 10 | 0.5125987 | 20 | 0.5133583 |

*Capacitance values are multiplied by $10^{-10}$.

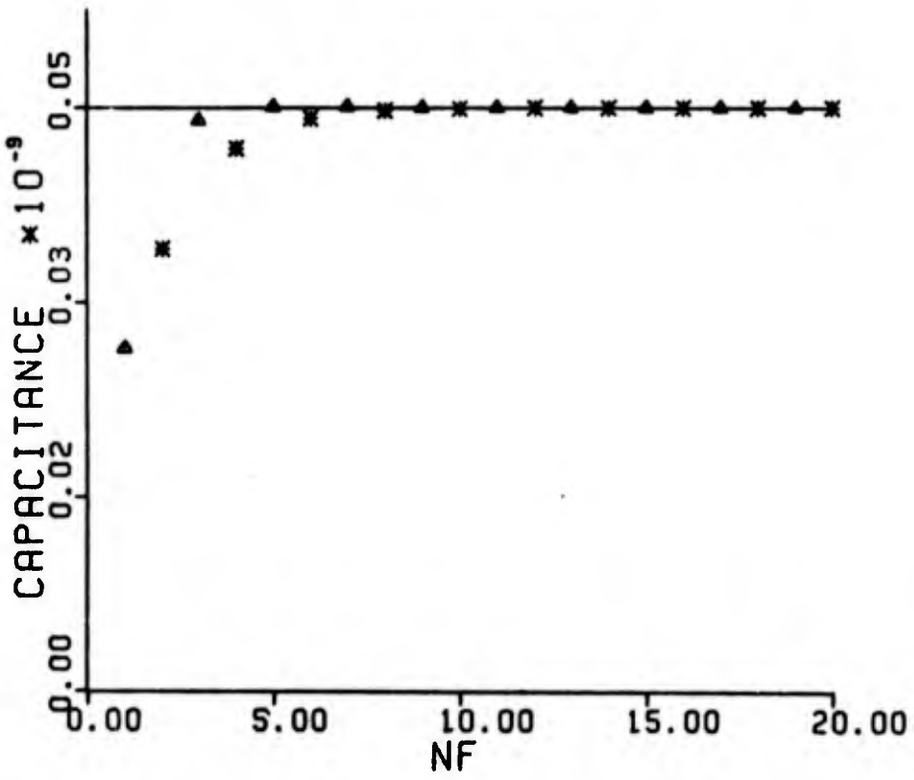

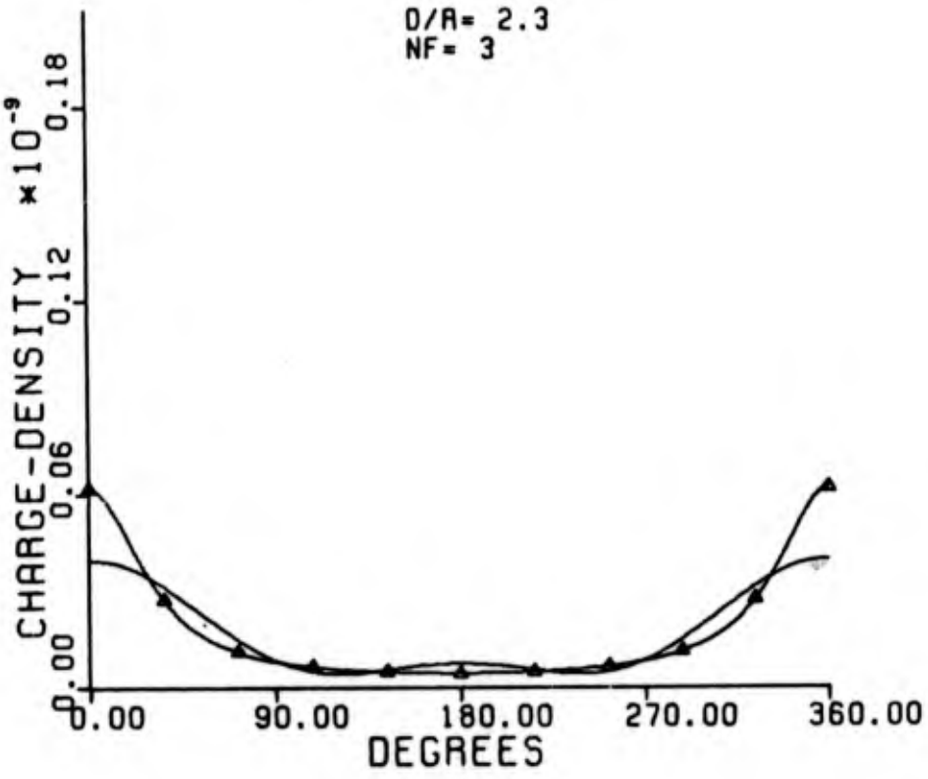
D/R= 2.3
NF= 3
CHARGE-DENSITY *10^-9
0.00
0.06
0.12
0.18
0.00
90.00
180.00
270.00
360.00
DEGREES

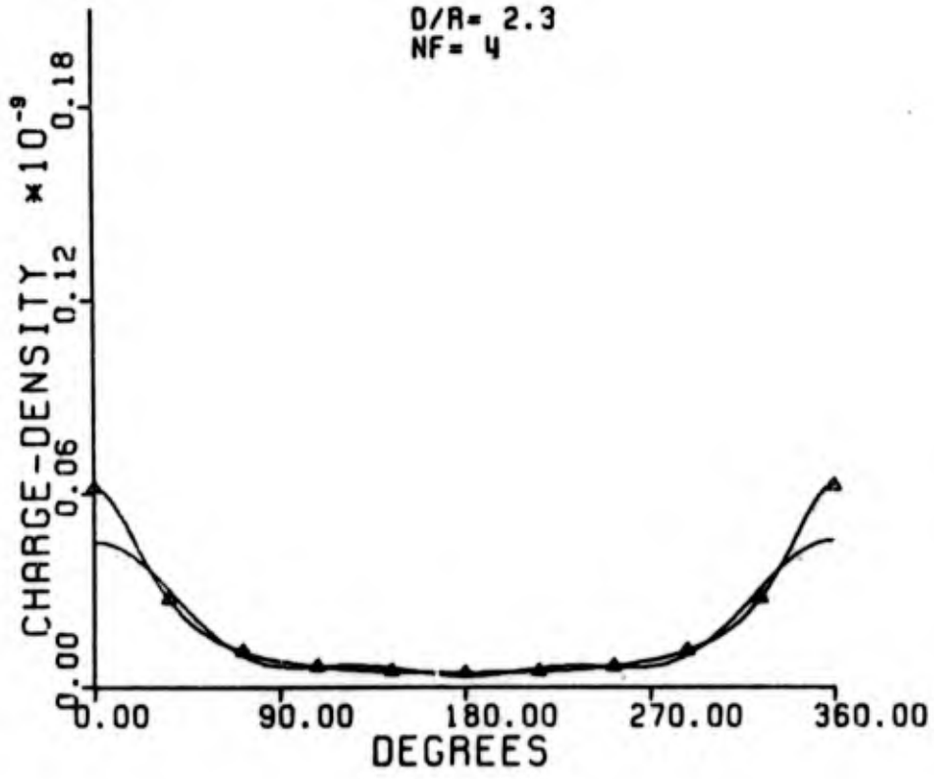
D/R= 2.3
NF= 4
CHARGE-DENSITY *10^-9
0.00
0.06
0.12
0.18
0.00
90.00
180.00
270.00
360.00
DEGREES

FOURIER SERIES

D/R=3.0. The exact capacitance = $0.2886231835048649 \times 10^{10}$
Δ-Odd values of NF. *-Even values of NF.

| NF | Approx.* Capac. | NF | Approx. Capac. |
|---|---|---|---|
| 1 | 0.2412747121684733 | 11 | 0.2886235924344002 |
| 2 | 0.2719488136671805 | 12 | 0.2886228765366393 |
| 3 | 0.2904101192191045 | 13 | 0.2886232342549118 |
| 4 | 0.2869302227645756 | 14 | 0.2886231447174977 |
| 5 | 0.2888755056932352 | 15 | 0.2886231899399235 |
| 6 | 0.2884418942160559 | 16 | 0.2886231785174214 |
| 7 | 0.2886521827296925 | 17 | 0.2886231843345695 |
| 8 | 0.2886024264216044 | 18 | 0.2886231828546509 |
| 9 | 0.2886265711256679 | 19 | 0.2886231836132704 |
| 10 | 0.2886206980858796 | 20 | 0.2886231834191468 |

*Capacitance values are multiplied by $10^{-10}$.

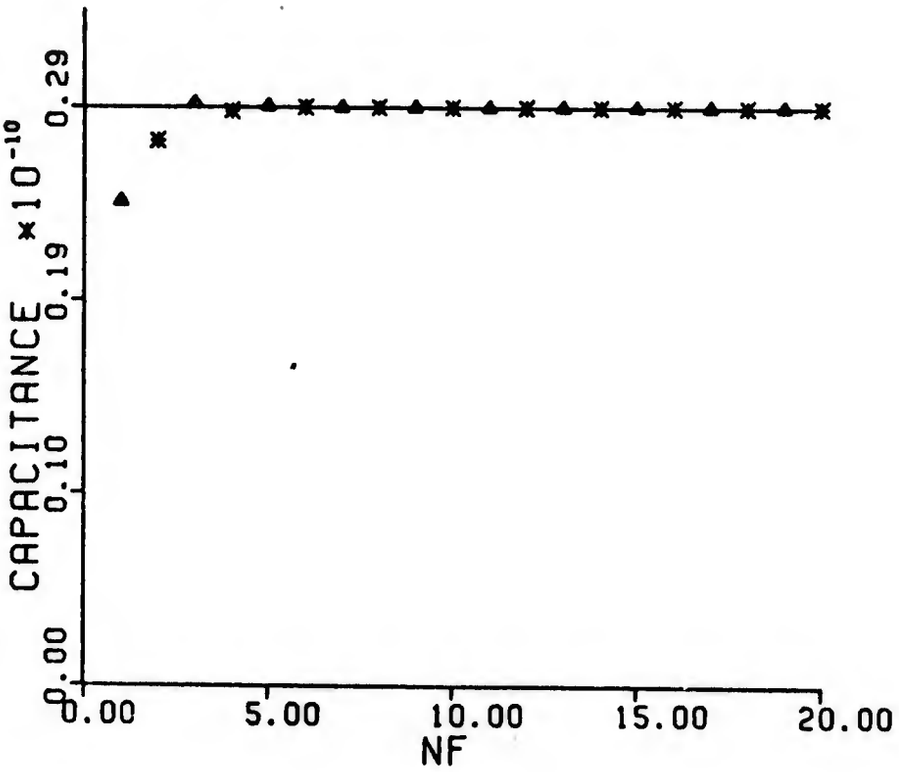

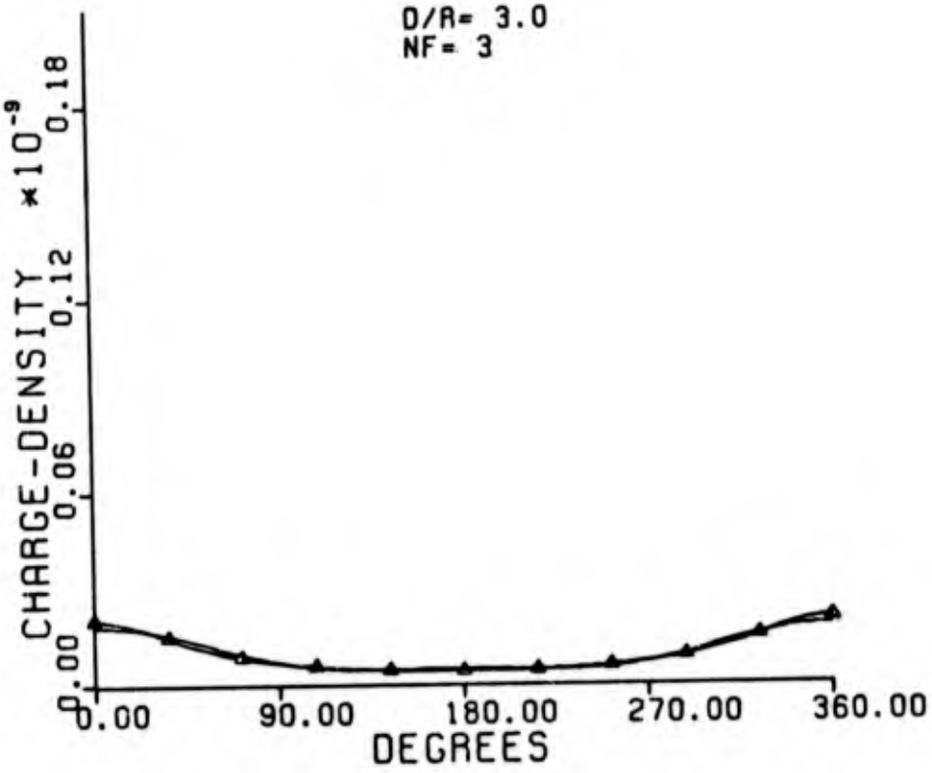
D/R= 3.0
NF= 3
CHARGE-DENSITY *10^-9
0.18
0.12
0.06
0.00
0.00
90.00
180.00
270.00
360.00
DEGREES

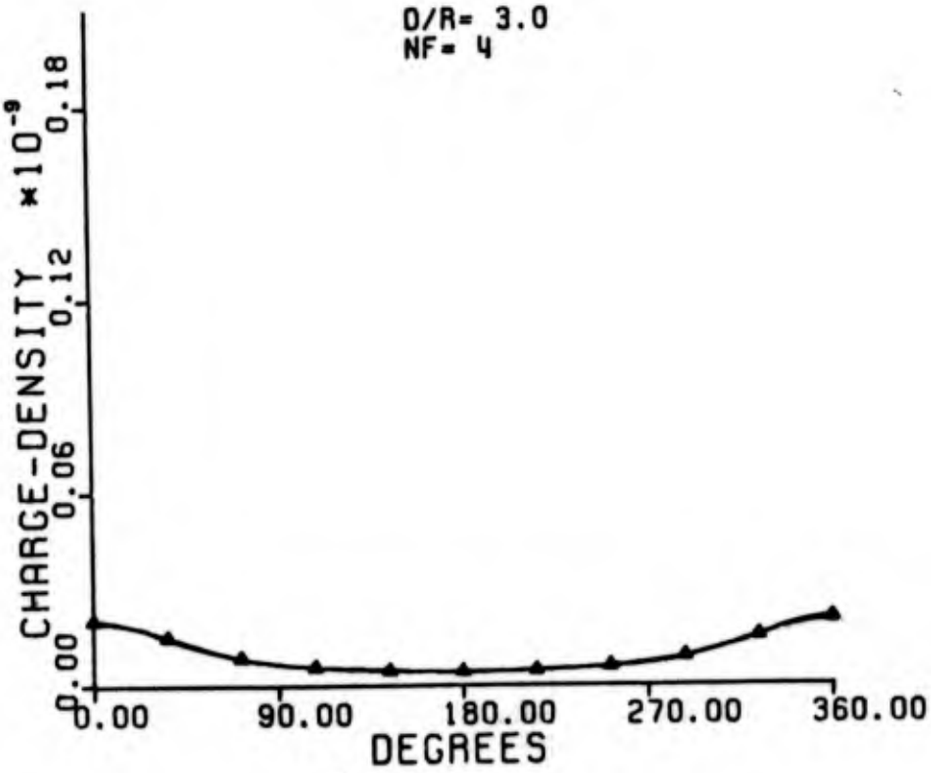
D/R= 3.0
NF= 4
CHARGE-DENSITY *10^-9
0.18
0.12
0.06
0.00
0.00
90.00
180.00
270.00
360.00
DEGREES

FOURIER SERIES

D/R=10.0. The exact capacitance = $0.121171671751922 \times 10^{-10}$
Δ-Odd values of NF. *-Even values of NF.

| NF | Approx.* Capac. | NF | Approx. Capac. |
|---|---|---|---|
| 1 | 0.1203772585197398 | 11 | 0.1211716717519726 |
| 2 | 0.1210299396876566 | 12 | 0.1211716717519171 |
| 3 | 0.1211841683799823 | 13 | 0.1211716717519225 |
| 4 | 0.1211705396429918 | 14 | 0.1211716717519220 |
| 5 | 0.1211717656245885 | 15 | 0.1211716717519220 |
| 6 | 0.1211716631672821 | 16 | 0.1211716717519220 |
| 7 | 0.1211716724813113 | 17 | 0.1211716717519220 |
| 8 | 0.1211716716833484 | 18 | 0.1211716717519220 |
| 9 | 0.1211716717578787 | 19 | 0.1211716717519220 |
| 10 | 0.1211716717513502 | 20 | 0.1211716717519220 |

*Capacitance values are multiplied by $10^{-10}$.

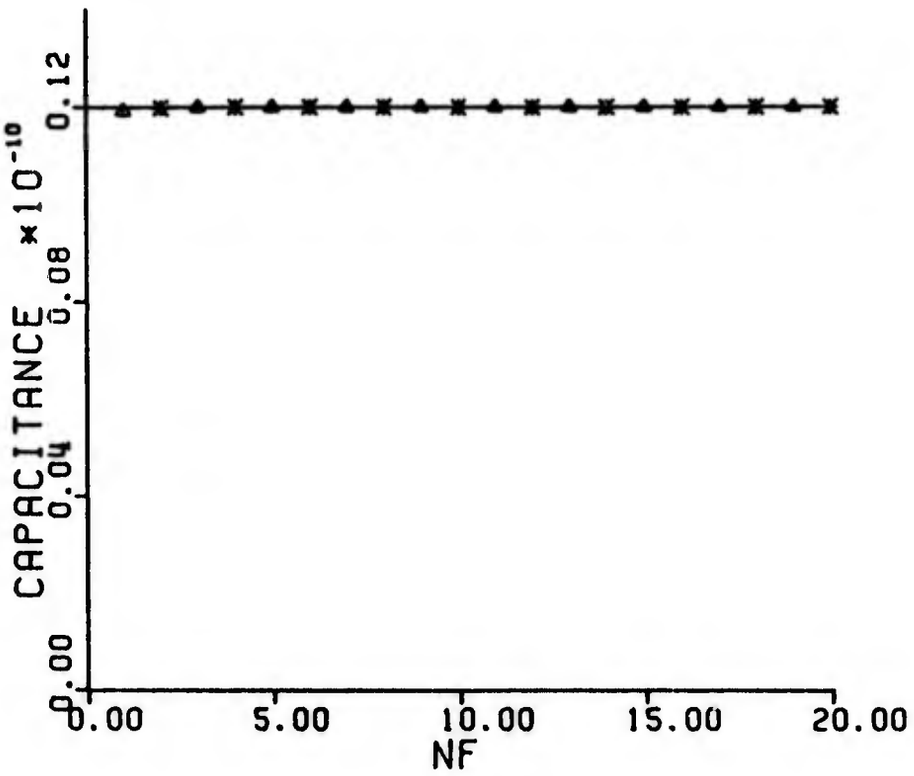

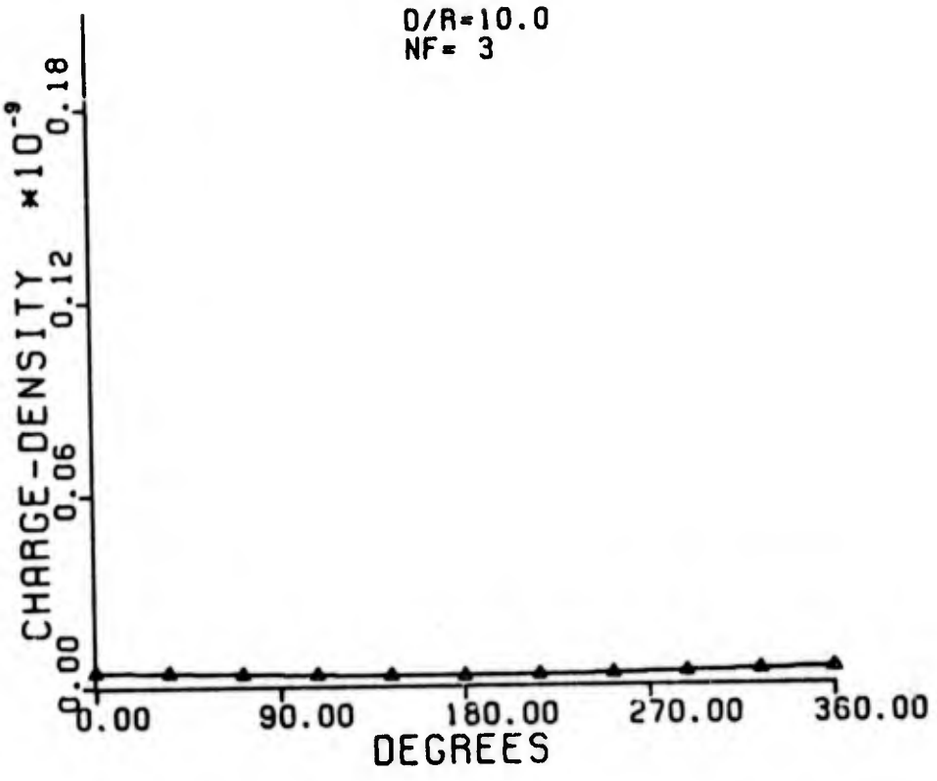
D/R=10.0
NF= 3
CHARGE-DENSITY *10^-9
0.00
0.06
0.12
0.18
0.00
90.00
180.00
270.00
360.00
DEGREES

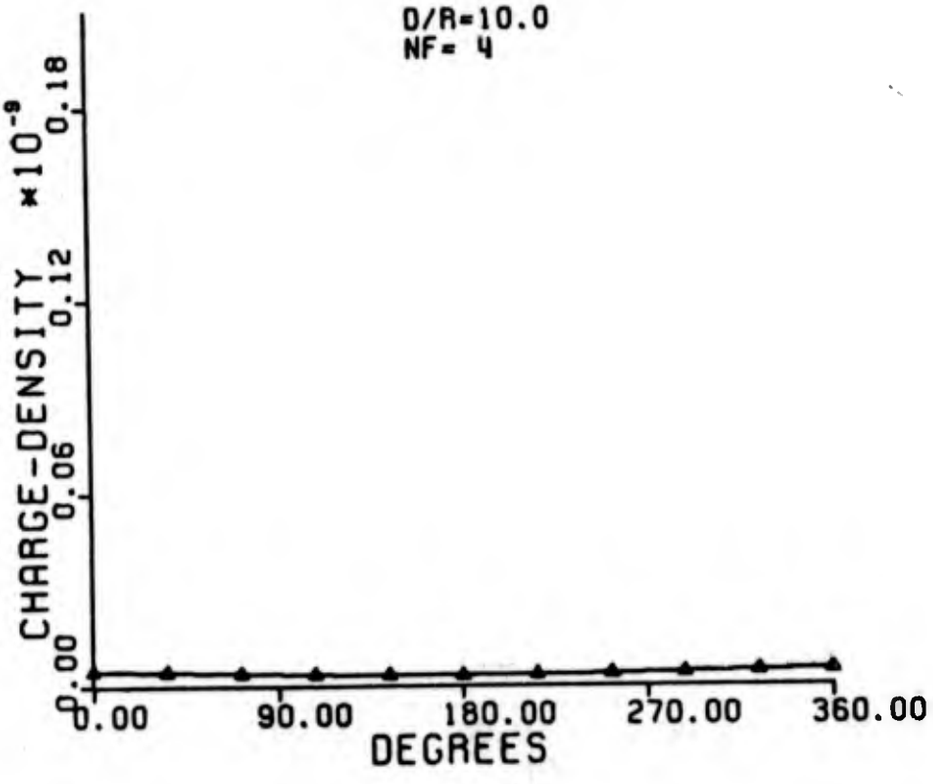
D/R=10.0
NF= 4
CHARGE-DENSITY *10^-9
0.00
0.06
0.12
0.18
0.00
90.00
180.00
270.00
360.00
DEGREES

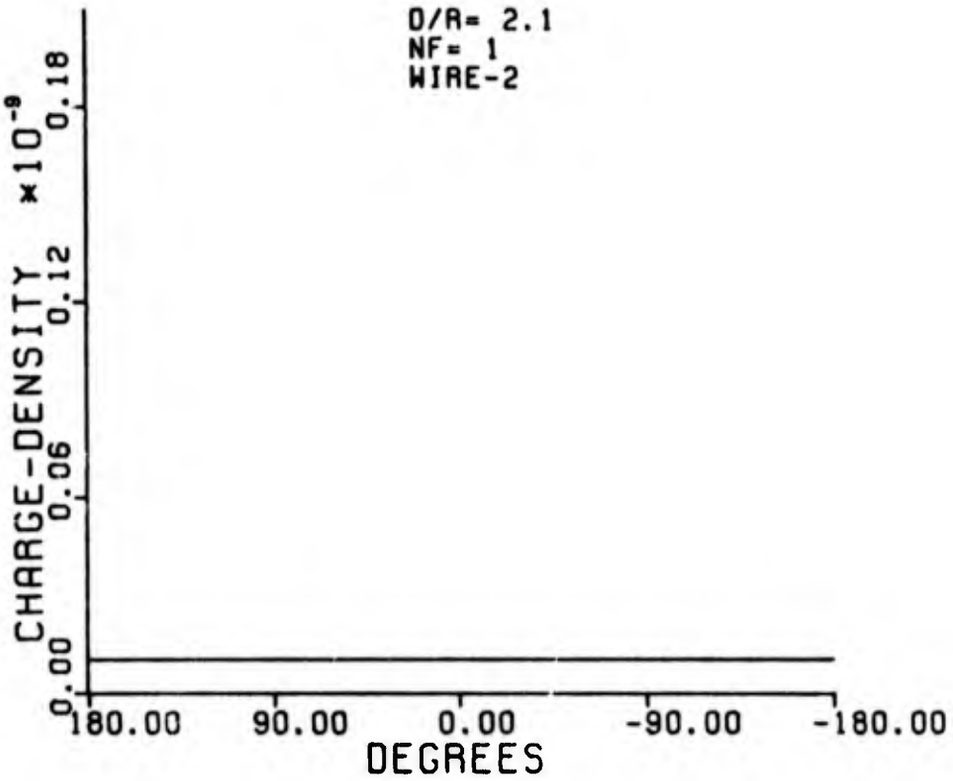
D/R= 2.1
NF= 1
WIRE-2
CHARGE-DENSITY ×10⁻⁹
0.18
0.12
0.06
0.00
180.00
90.00
0.00
-90.00
-180.00
DEGREES

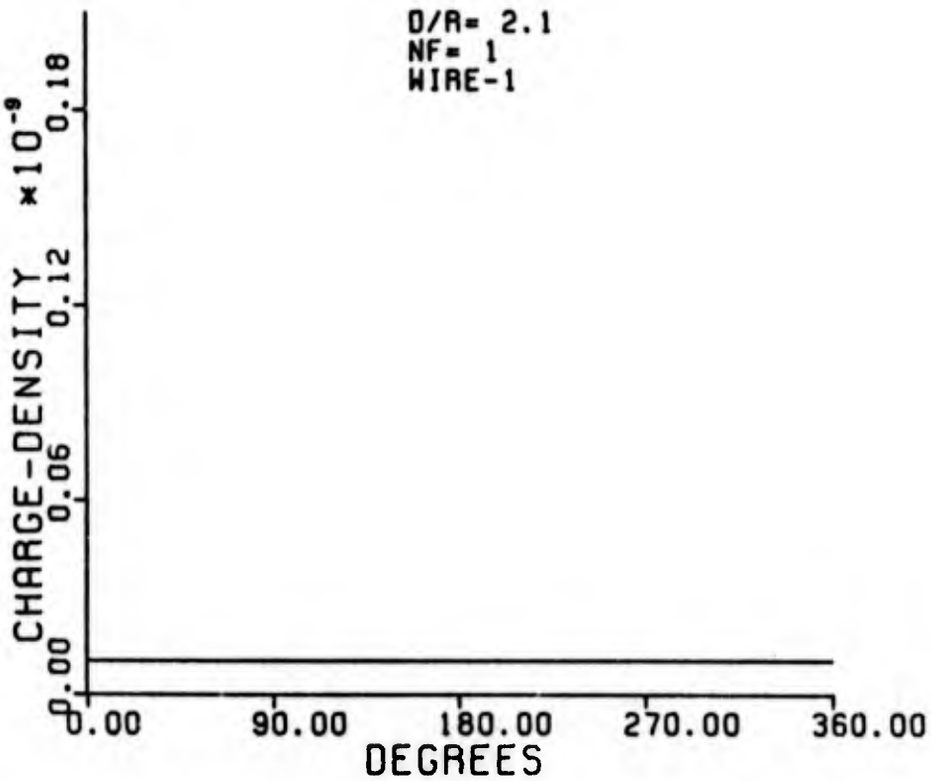
D/R= 2.1
NF= 1
WIRE-1
CHARGE-DENSITY ×10⁻⁹
0.18
0.12
0.06
0.00
0.00
90.00
180.00
270.00
360.00
DEGREES

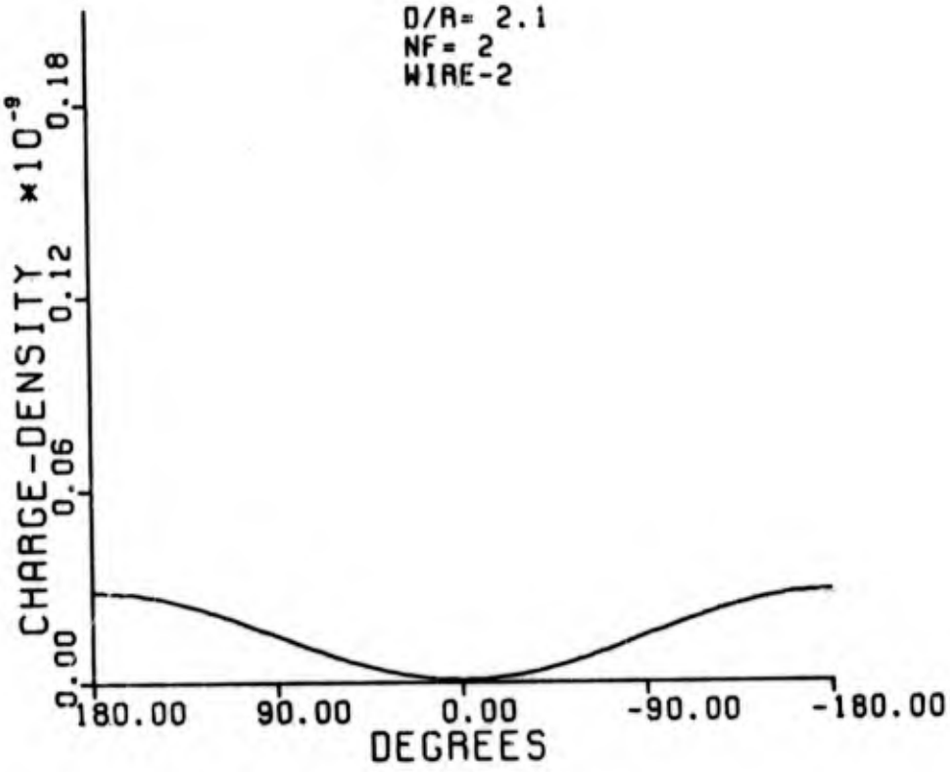
D/R= 2.1
NF= 2
WIRE-2
CHARGE-DENSITY ×10⁻⁹
0.00
0.06
0.12
0.18
180.00
90.00
0.00
-90.00
-180.00
DEGREES

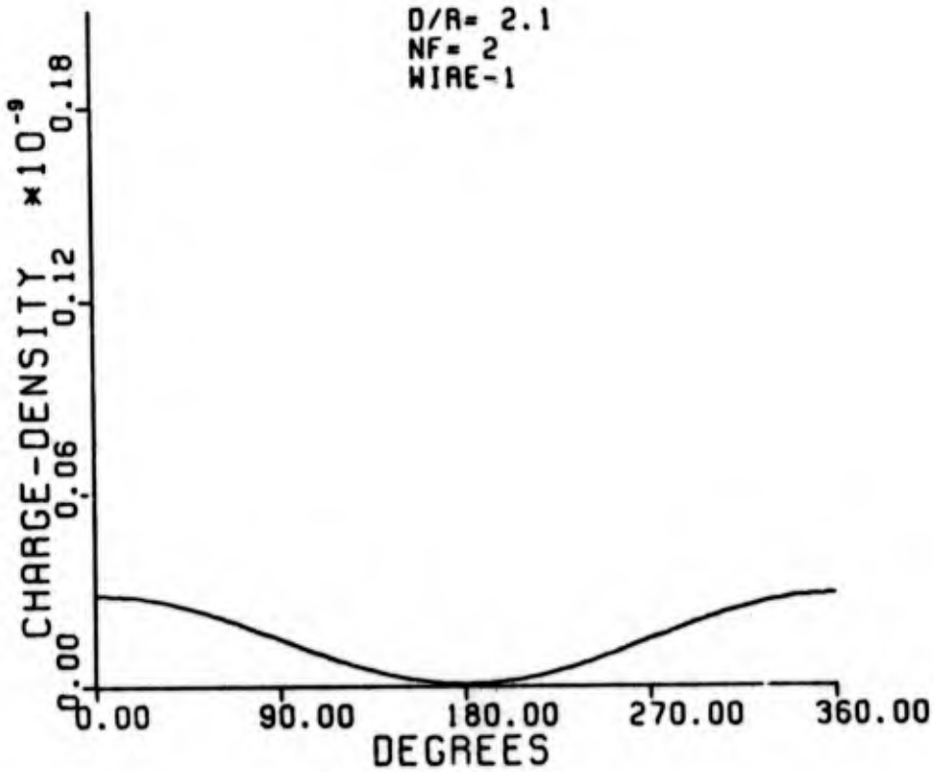
D/R= 2.1
NF= 2
WIRE-1
CHARGE-DENSITY ×10⁻⁹
0.00
0.06
0.12
0.18
0.00
90.00
180.00
270.00
360.00
DEGREES

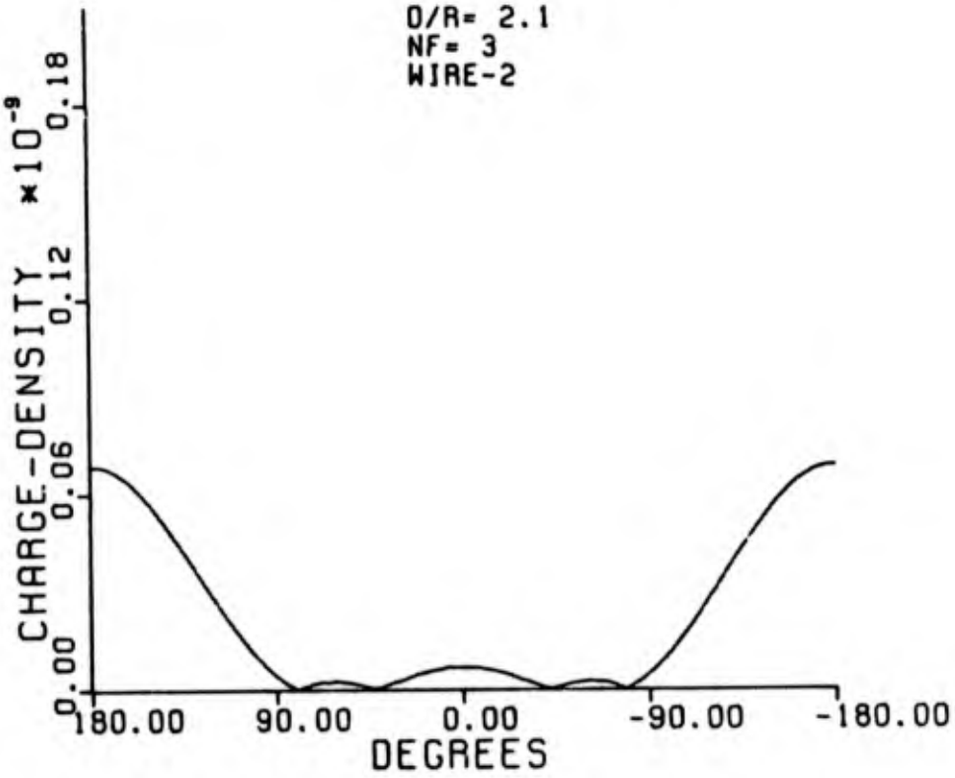
D/R= 2.1
NF= 3
WIRE-2
CHARGE-DENSITY ×10⁻⁹
0.00
0.06
0.12
0.18
180.00
90.00
0.00
-90.00
-180.00
DEGREES

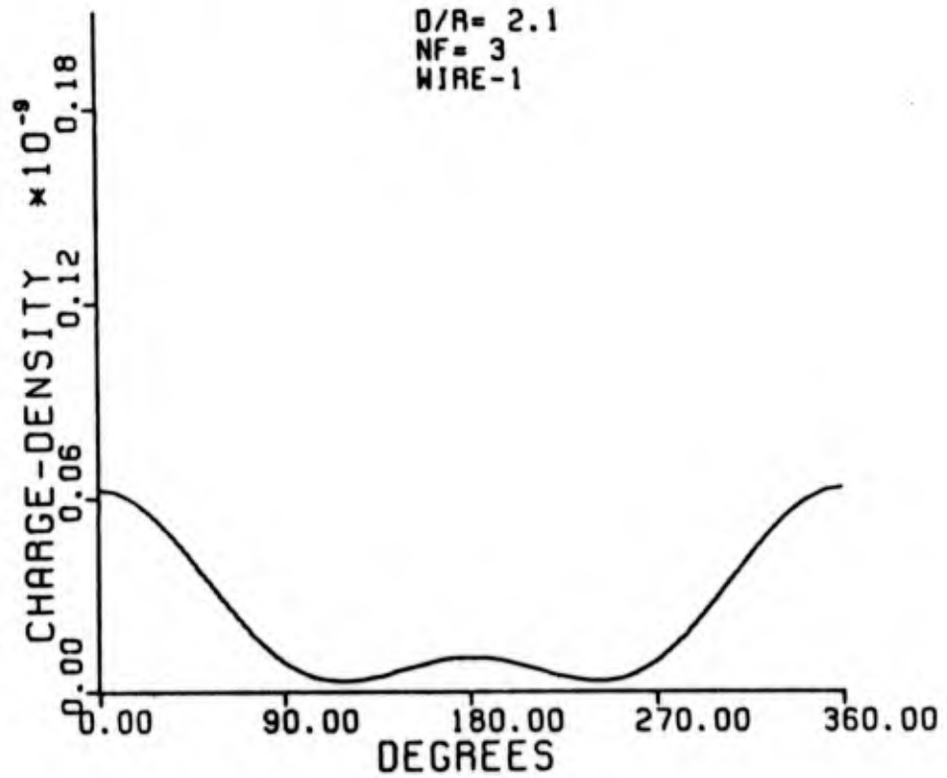
D/R= 2.1
NF= 3
WIRE-1
CHARGE-DENSITY ×10⁻⁹
0.00
0.06
0.12
0.18
0.00
90.00
180.00
270.00
360.00
DEGREES

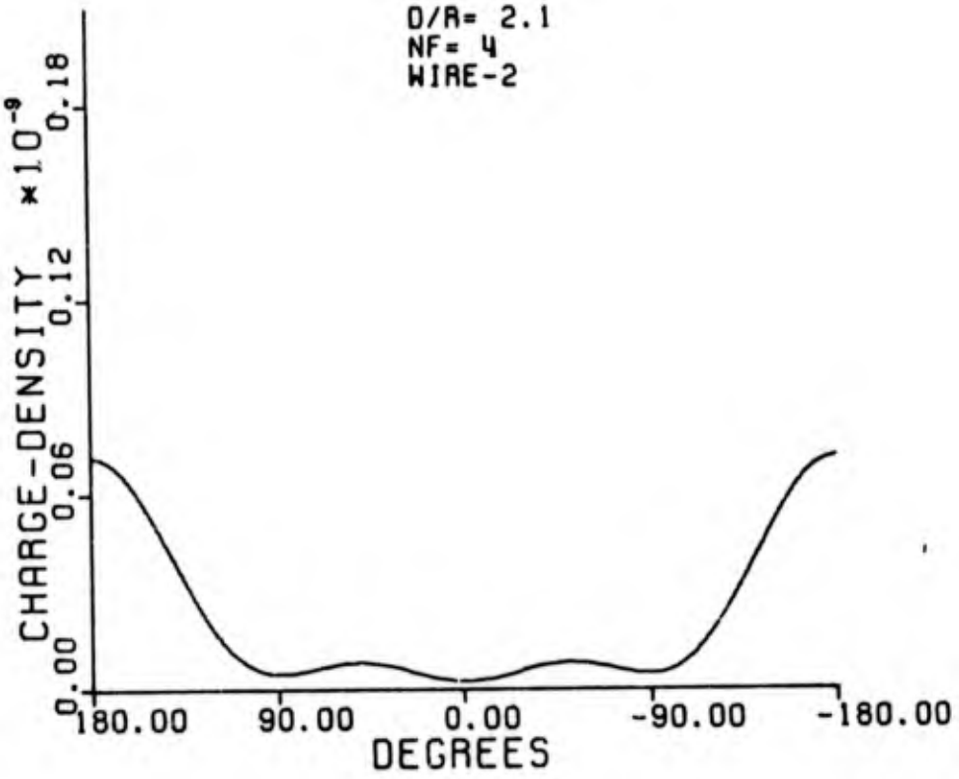
D/R= 2.1
NF= 4
WIRE-2
CHARGE-DENSITY *10^-9
0.00
0.06
0.12
0.18
180.00
90.00
0.00
-90.00
-180.00
DEGREES

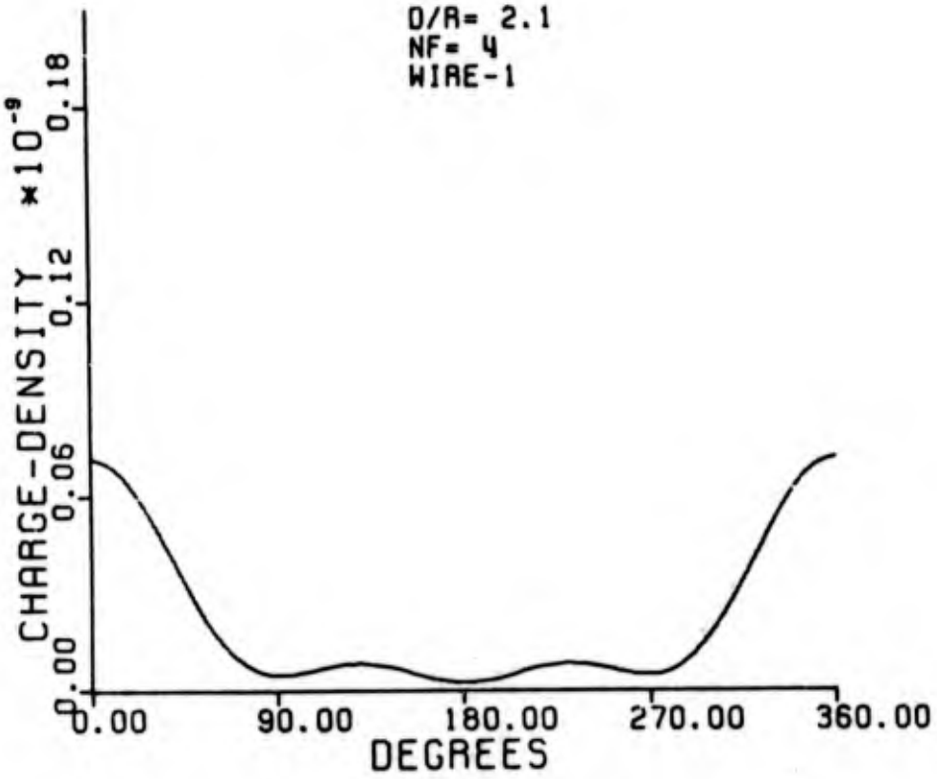
D/R= 2.1
NF= 4
WIRE-1
CHARGE-DENSITY *10^-9
0.00
0.06
0.12
0.18
0.00
90.00
180.00
270.00
360.00
DEGREES

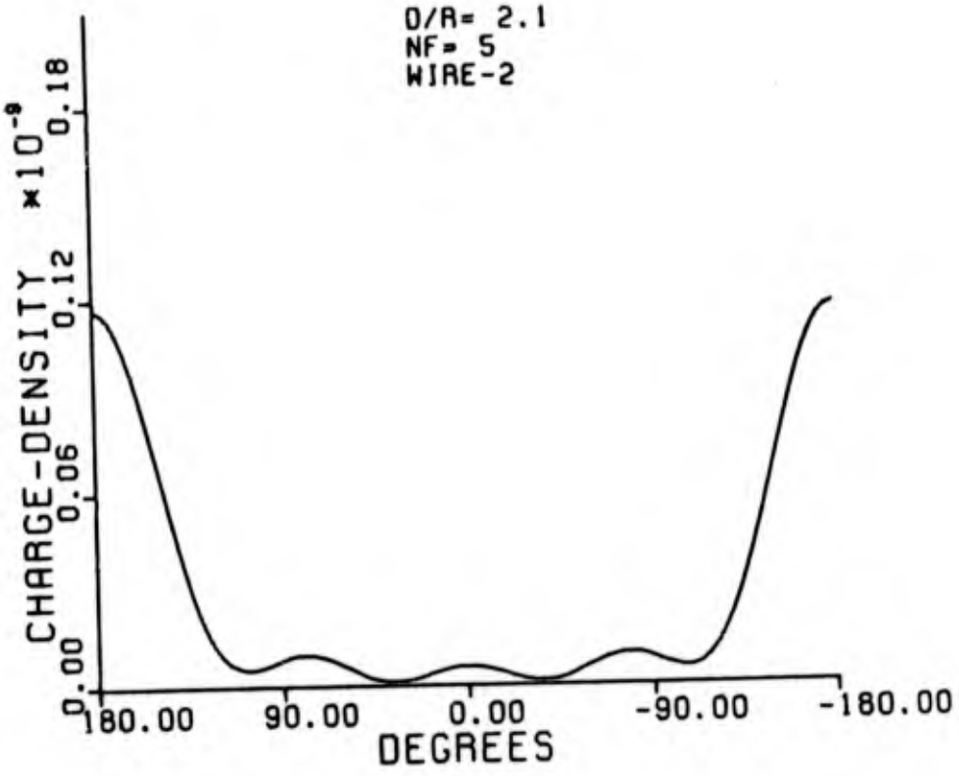
D/R= 2.1
NF= 5
WIRE-2
CHARGE-DENSITY ×10⁻⁹
0.18
0.12
0.06
0.00
180.00
90.00
0.00
-90.00
-180.00
DEGREES

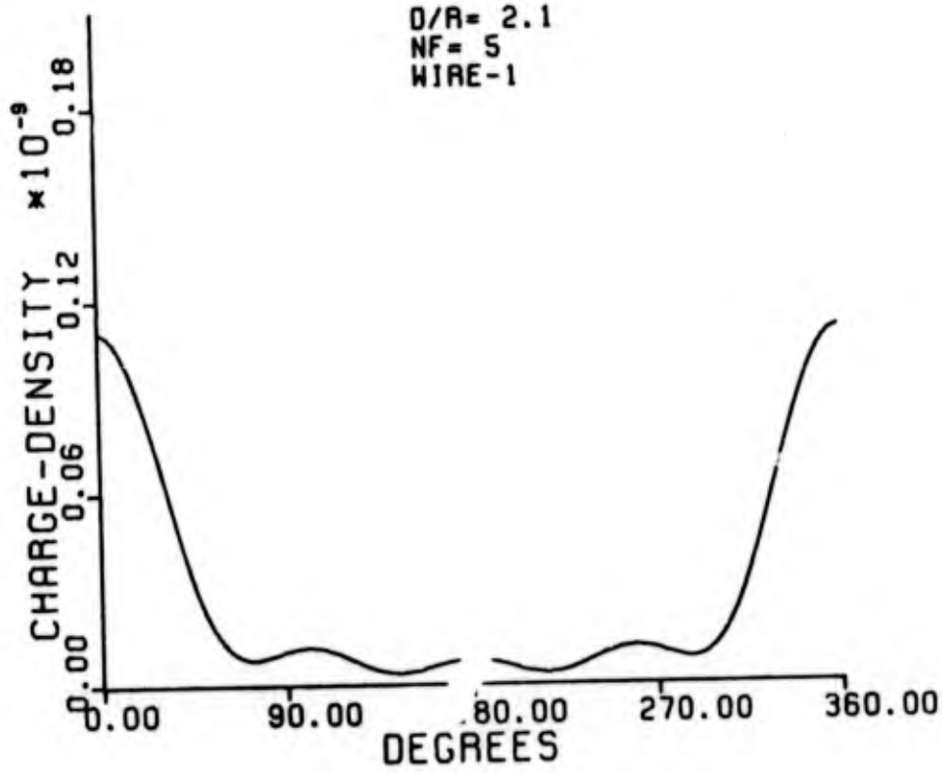
D/R= 2.1
NF= 5
WIRE-1
CHARGE-DENSITY ×10⁻⁹
0.18
0.12
0.06
0.00
0.00
90.00
180.00
270.00
360.00
DEGREES

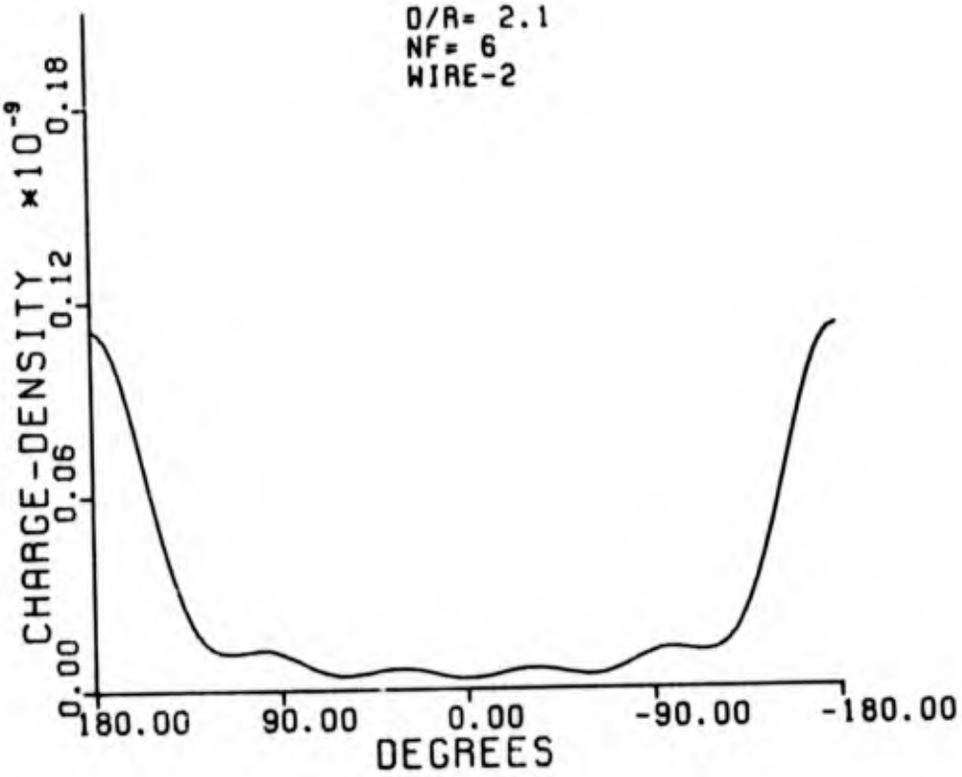
D/R= 2.1
NF= 6
WIRE-2
CHARGE-DENSITY ×10⁻⁹
0.18
0.12
0.06
0.00
180.00
90.00
0.00
-90.00
-180.00
DEGREES

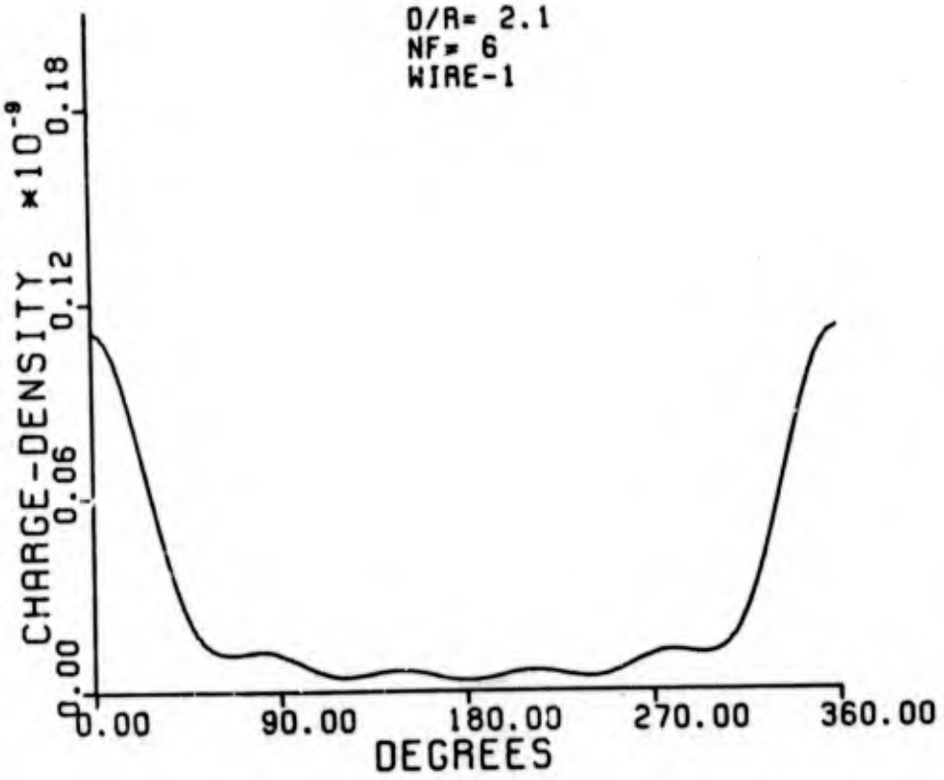
D/R= 2.1
NF= 6
WIRE-1
CHARGE-DENSITY ×10⁻⁹
0.18
0.12
0.06
0.00
0.00
90.00
180.00
270.00
360.00
DEGREES

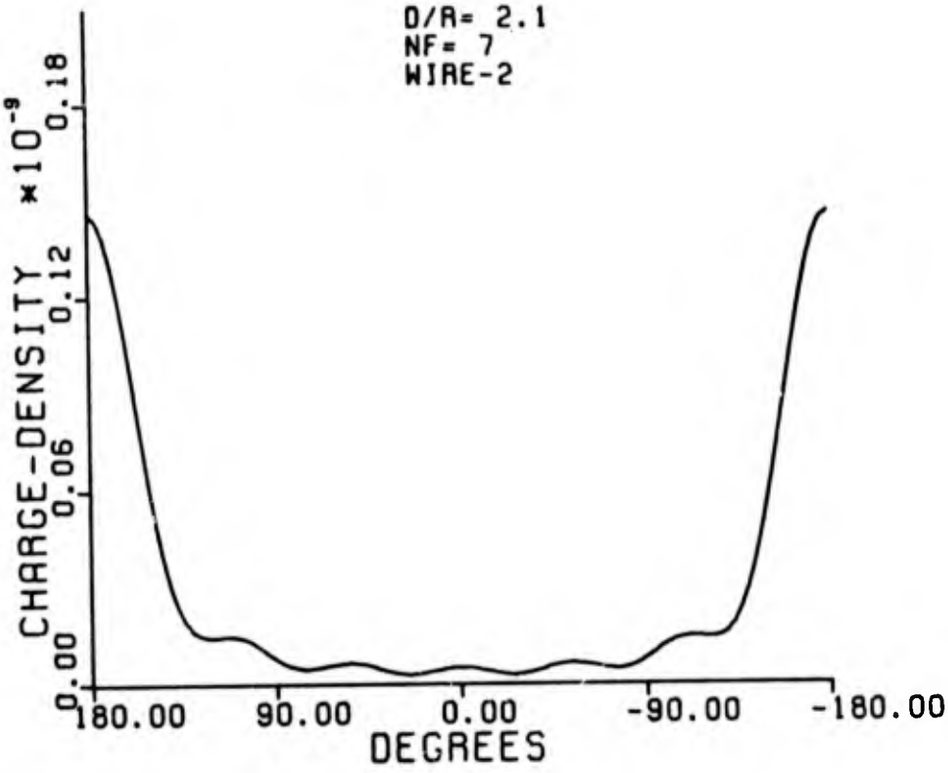
D/R= 2.1
NF= 7
WIRE-2
CHARGE-DENSITY ×10⁻⁹
0.00
0.06
0.12
0.18
180.00
90.00
0.00
-90.00
-180.00
DEGREES

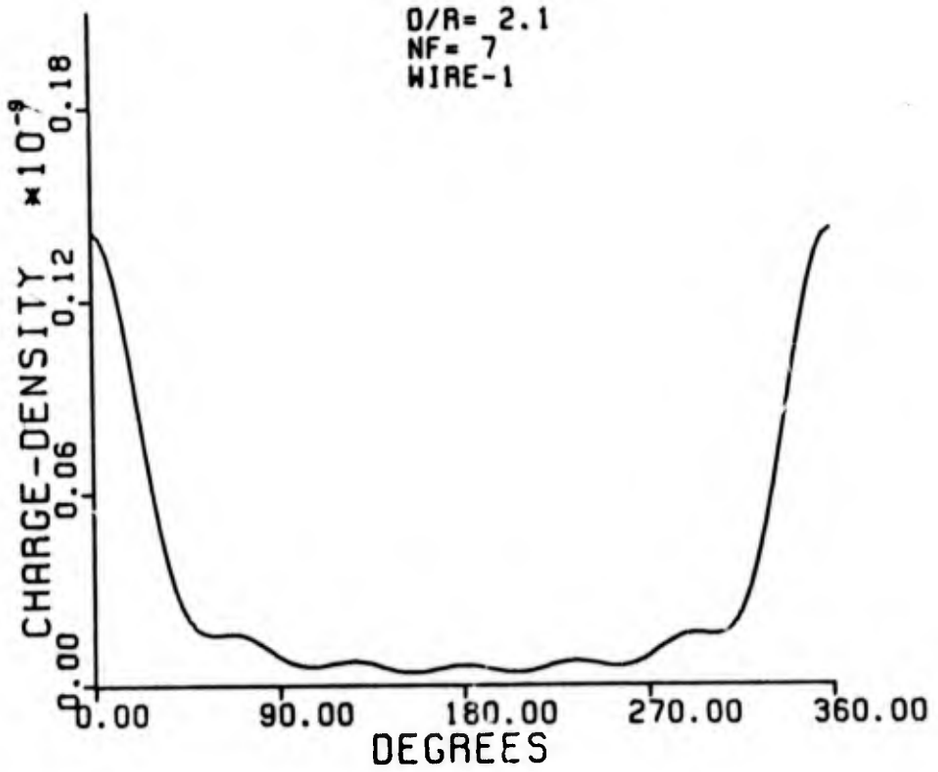
D/R= 2.1
NF= 7
WIRE-1
CHARGE-DENSITY ×10⁻⁹
0.00
0.06
0.12
0.18
0.00
90.00
180.00
270.00
360.00
DEGREES

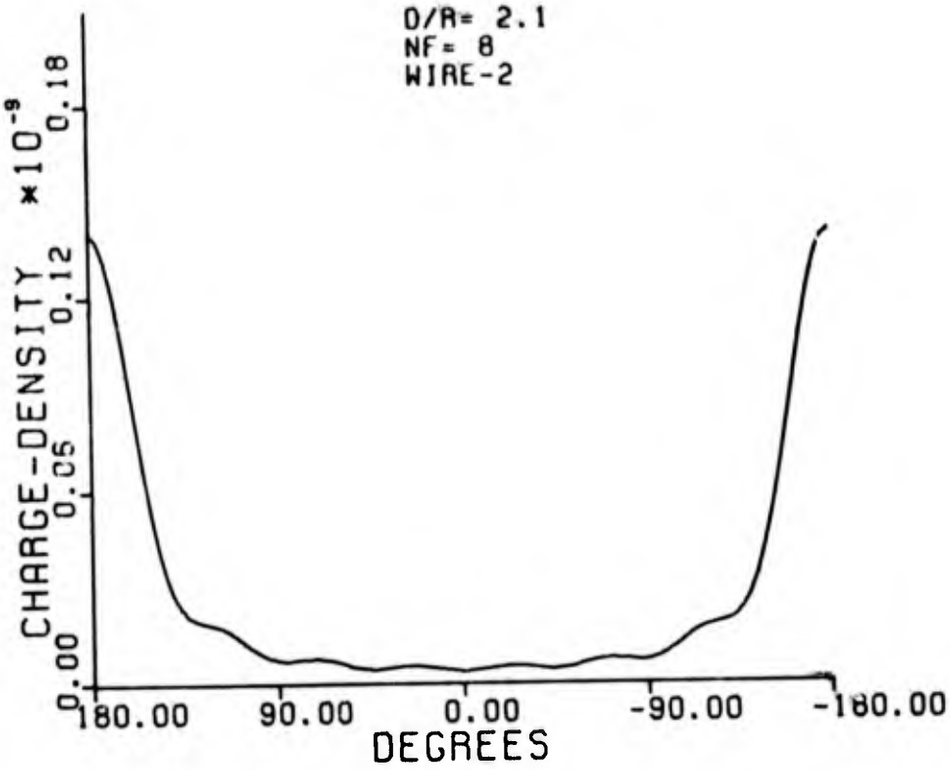
D/R= 2.1
NF= 8
WIRE-2
CHARGE-DENSITY *10^-9
0.18
0.12
0.05
0.00
180.00
90.00
0.00
-90.00
-180.00
DEGREES

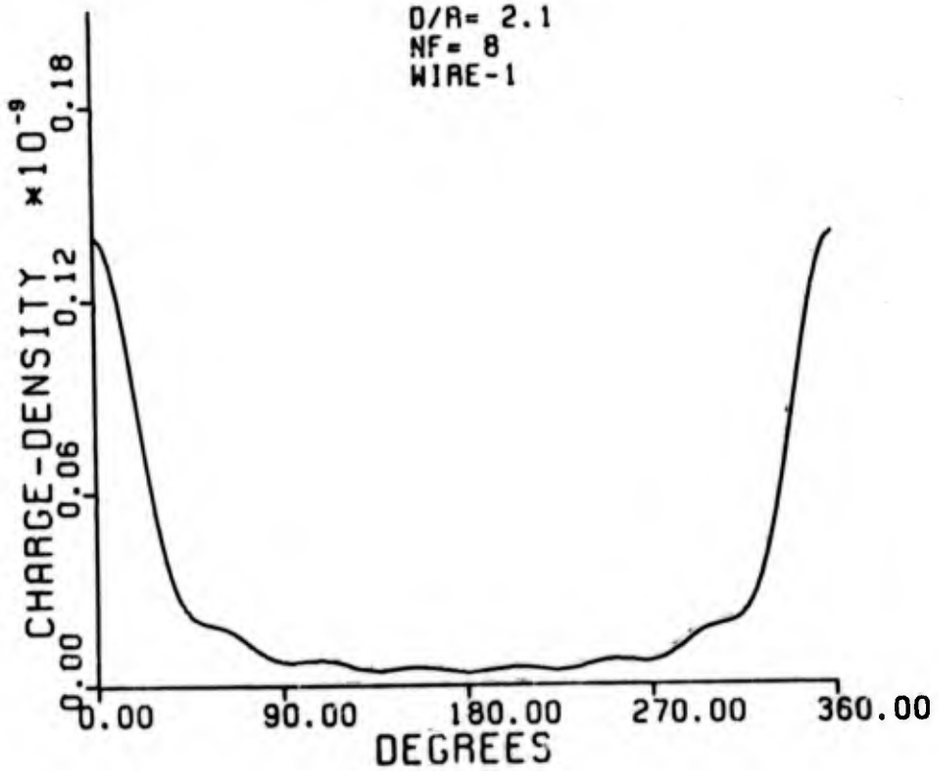
D/R= 2.1
NF= 8
WIRE-1
CHARGE-DENSITY *10^-9
0.18
0.12
0.06
0.00
0.00
90.00
180.00
270.00
360.00
DEGREES

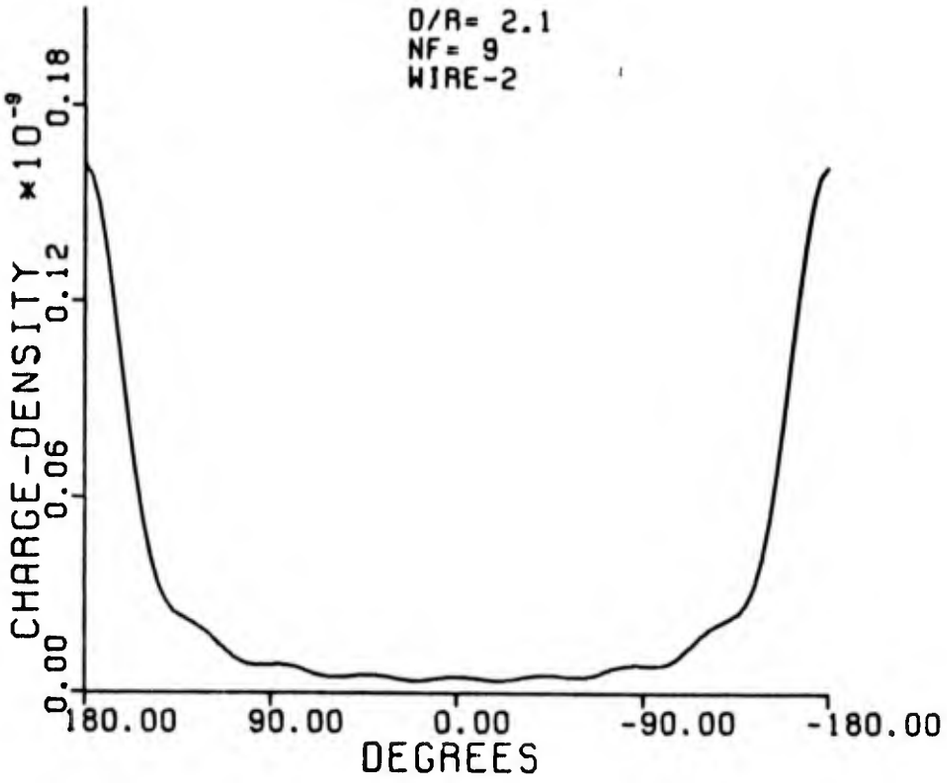
D/R= 2.1
NF= 9
WIRE-2
CHARGE-DENSITY ×10⁻⁹
0.00
0.06
0.12
0.18
180.00
90.00
0.00
-90.00
-180.00
DEGREES

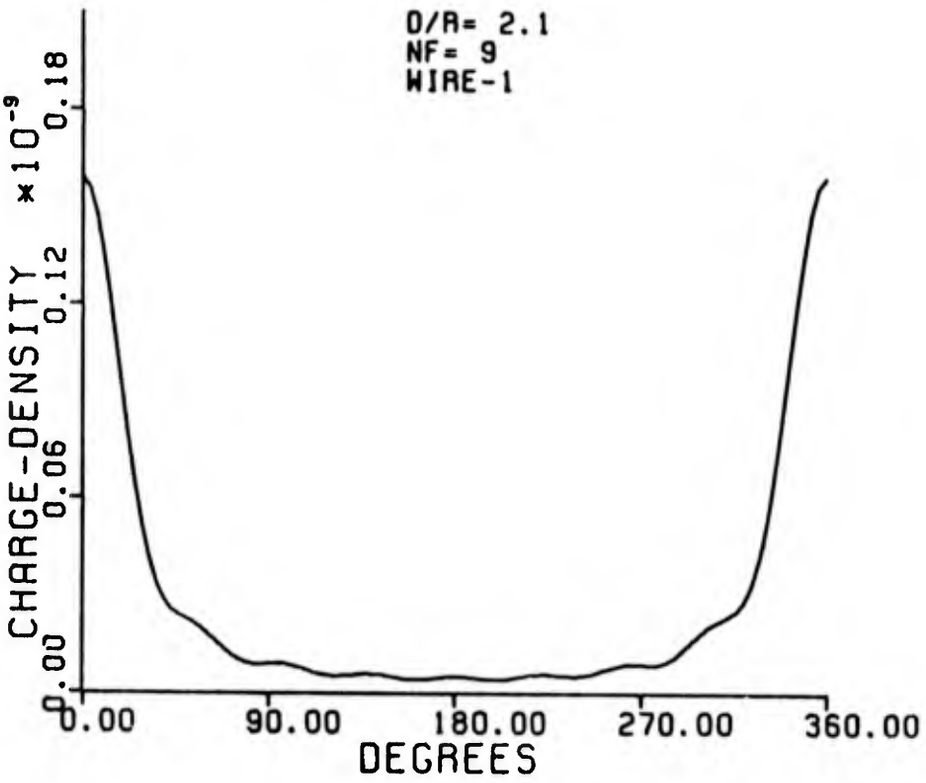
D/R= 2.1
NF= 9
WIRE-1
CHARGE-DENSITY ×10⁻⁹
0.00
0.06
0.12
0.18
0.00
90.00
180.00
270.00
360.00
DEGREES

APPENDIX E

TWO DIELECTRIC-COATED WIRES
D=4.0. Rw=1.0. ER=3.0. RD=2.0.

| NF | Capac* | Capac. Without Dielectric |
|---|---|---|
| 1 | 0.2653264896459874 | 0.1960867354804229 |
| 2 | 0.3108506305227654 | 0.2071380629272396 |
| 3 | 0.3393609436687546 | 0.2100767569534968 |
| 4 | 0.3584912360384726 | 0.2107338195732281 |
| 5 | 0.3720153065688648 | 0.2108804221423331 |
| 6 | 0.3818456597652442 | 0.2109137271295523 |
| 7 | 0.3891344456080068 | 0.2109214318604873 |
| 8 | 0.3946295718522494 | 0.2109232422462171 |
| 9 | 0.3988341472703791 | 0.2109236732499677 |
| 10 | 0.4020940875094267 | 0.2109237770025262 |
| 11 | 0.4046513532521321 | 0.2109238022139820 |
| 12 | 0.4066779808931132 | 0.2109238083896527 |
| 13 | 0.4082983337761532 | 0.2109238099128993 |
| 14 | 0.4096038066487121 | 0.2109238102908678 |
| 15 | 0.4106626268763988 | 0.2109238103851455 |
| 16 | 0.4115264599525303 | 0.2109238104087696 |
| 17 | 0.4122349259783496 | 0.2109238104147134 |
| 18 | 0.4128187408064898 | 0.2109238104162142 |
| 19 | 0.4133019407684728 | 0.2109238104165944 |
| 20 | 0.4137034869082607 | 0.2109238104166910 |

*Capacitance values are multiplied by $10^{-10}$.

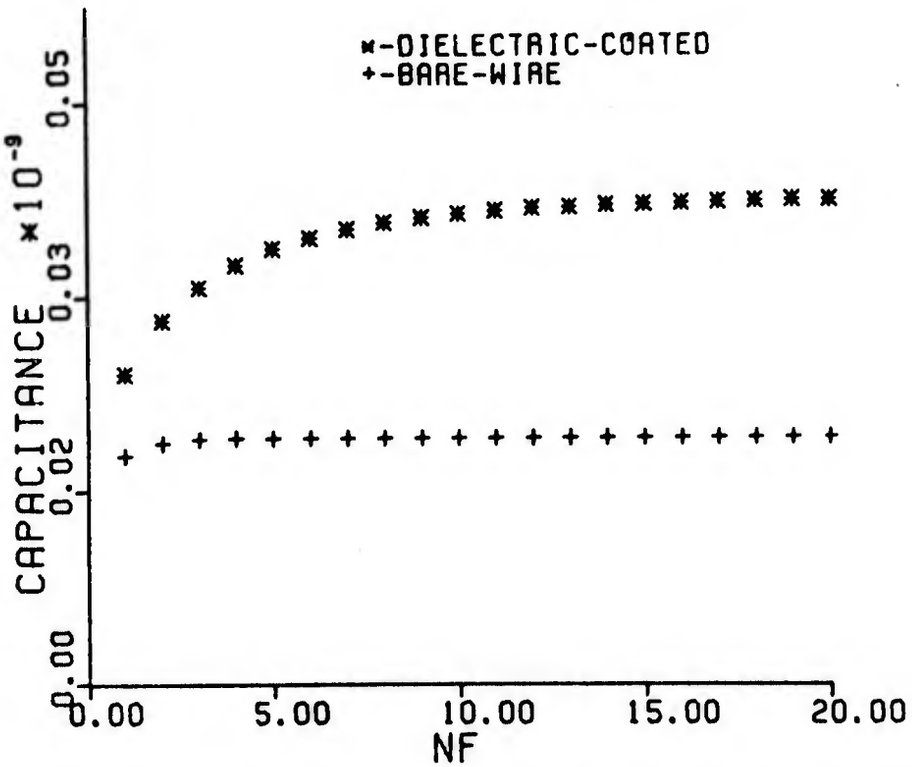

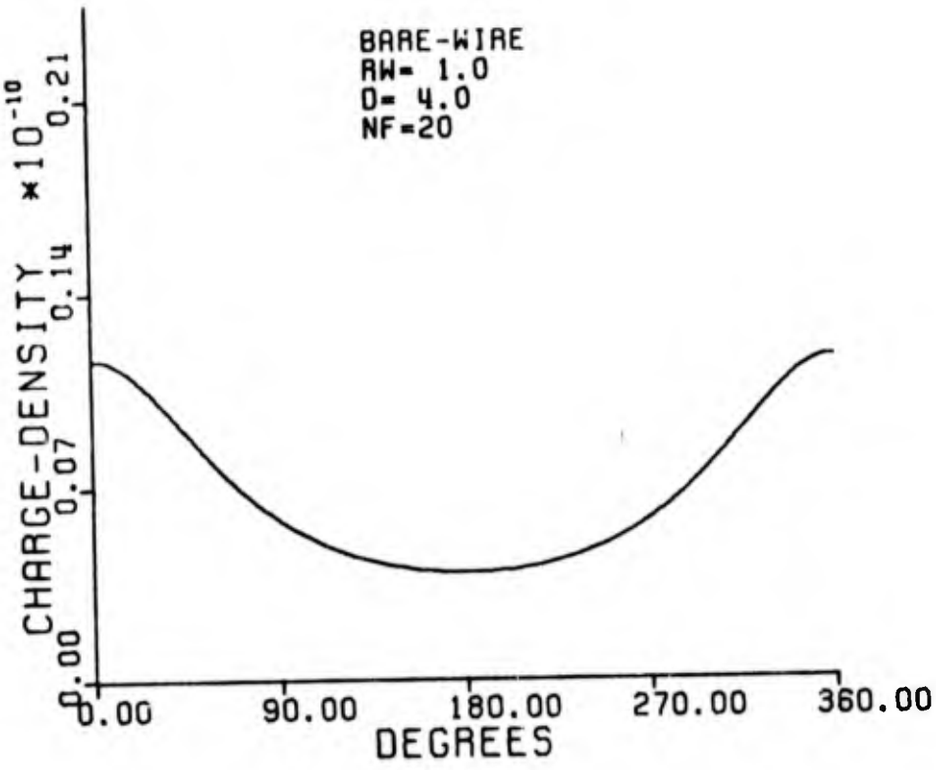
BARE-WIRE
RW= 1.0
D= 4.0
NF=20
CHARGE-DENSITY *10^-10
0.00
0.07
0.14
0.21
0.00
90.00
180.00
270.00
360.00
DEGREES

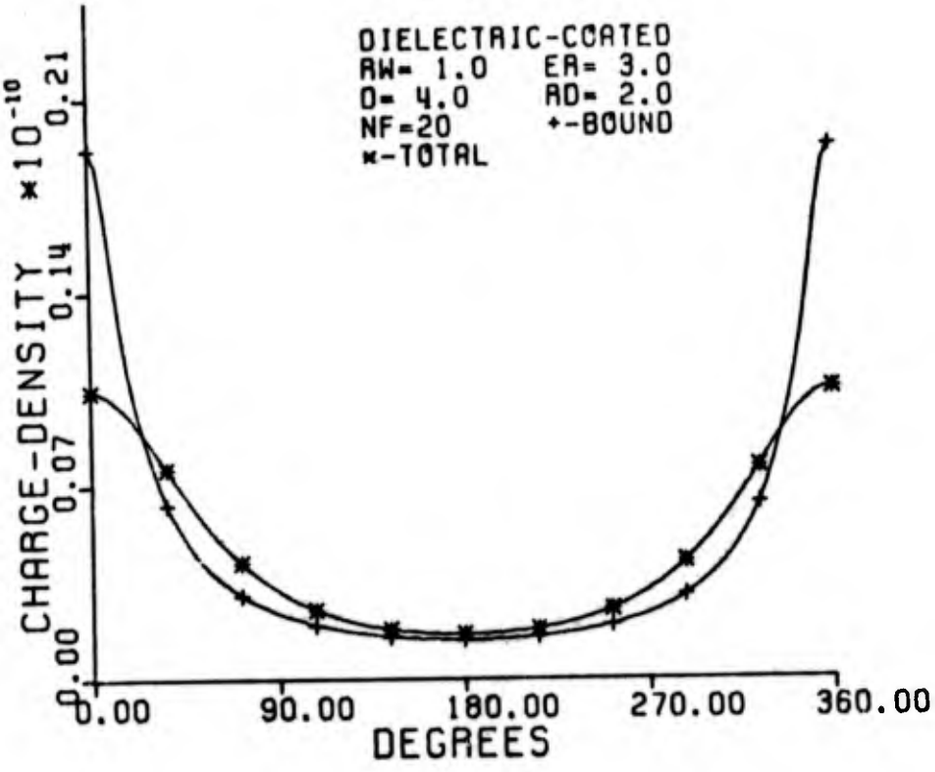
DIELECTRIC-COATED
RW= 1.0 ER= 3.0
D= 4.0 RD= 2.0
NF=20 +-BOUND
*-TOTAL
CHARGE-DENSITY *10^-10
0.00
0.07
0.14
0.21
0.00
90.00
180.00
270.00
360.00
DEGREES

TWO DIELECTRIC-COATED WIRES
D=4.1. Rw=1.0. ER=3.0. RD=2.0.

| NF | Capac.* | Capac. Without Dielectric |
|---|---|---|
| 1 | 0.2604319063960941 | 0.1929173044921796 |
| 2 | 0.3028769038550849 | 0.2030825115569347 |
| 3 | 0.3289748694412965 | 0.2057327456875594 |
| 4 | 0.3460954632999954 | 0.2063103162395421 |
| 5 | 0.3579070700053849 | 0.2064357703678684 |
| 6 | 0.3662586222351133 | 0.2064634942344962 |
| 7 | 0.3722511534286733 | 0.2064697303587507 |
| 8 | 0.3765954732933833 | 0.2064711548373961 |
| 9 | 0.3797696962114337 | 0.2064714844922656 |
| 10 | 0.3821033761841270 | 0.2064715616285173 |
| 11 | 0.3838275925609864 | 0.2064715798479409 |
| 12 | 0.3851065822548474 | 0.2064715841860081 |
| 13 | 0.3860583821732247 | 0.2064715852260650 |
| 14 | 0.3867686001727846 | 0.2064715854769164 |
| 15 | 0.3872997761397828 | 0.2064715855377361 |
| 16 | 0.3876978575787908 | 0.2064715855525498 |
| 17 | 0.3879967507554561 | 0.2064715855561725 |
| 18 | 0.3882215630012440 | 0.2064715855570617 |
| 19 | 0.3883909380417583 | 0.2064715855572806 |
| 20 | 0.3885187523763949 | 0.2064715855573347 |

*Capacitance values are multiplied by $10^{-10}$.

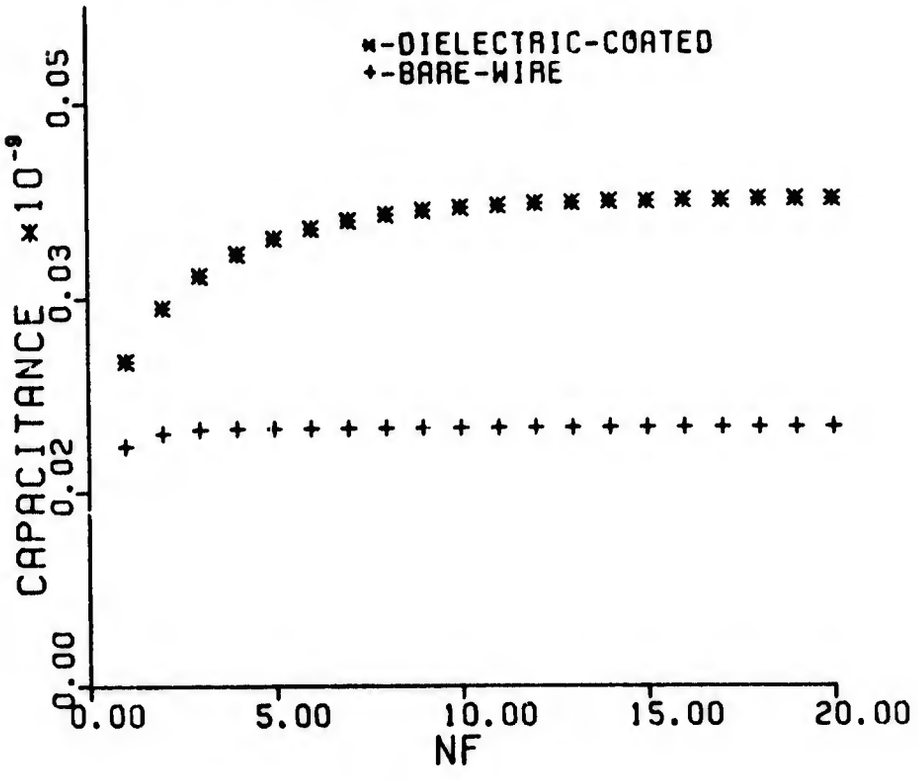

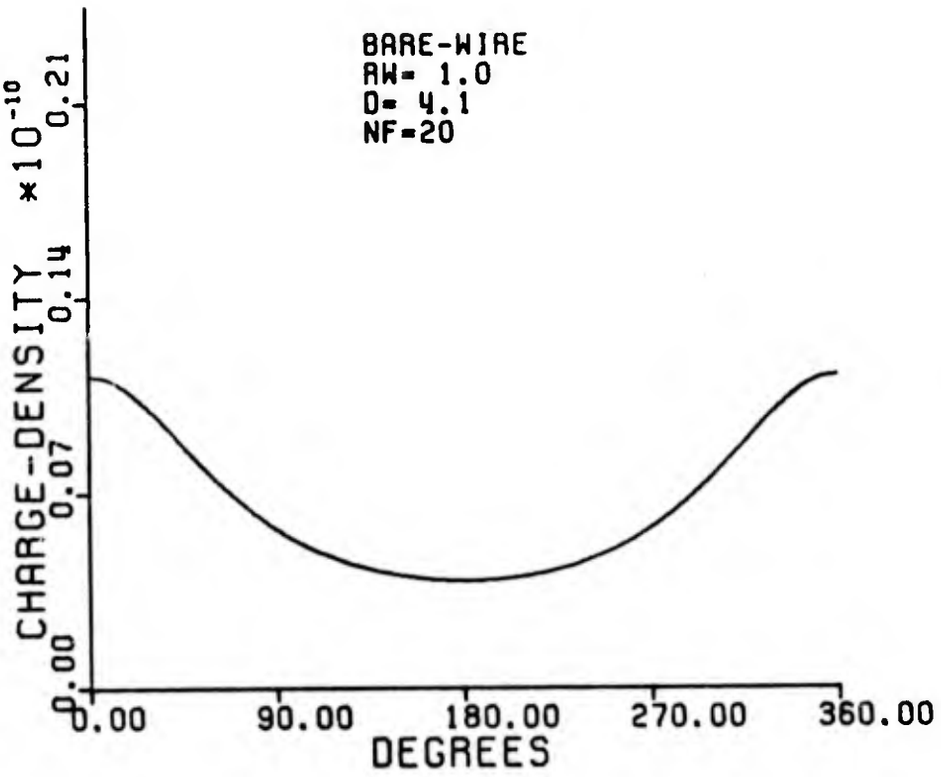
BARE-WIRE
AW= 1.0
D= 4.1
NF=20
CHARGE-DENSITY *10^-10
0.21
0.14
0.07
0.00
0.00
90.00
180.00
270.00
360.00
DEGREES

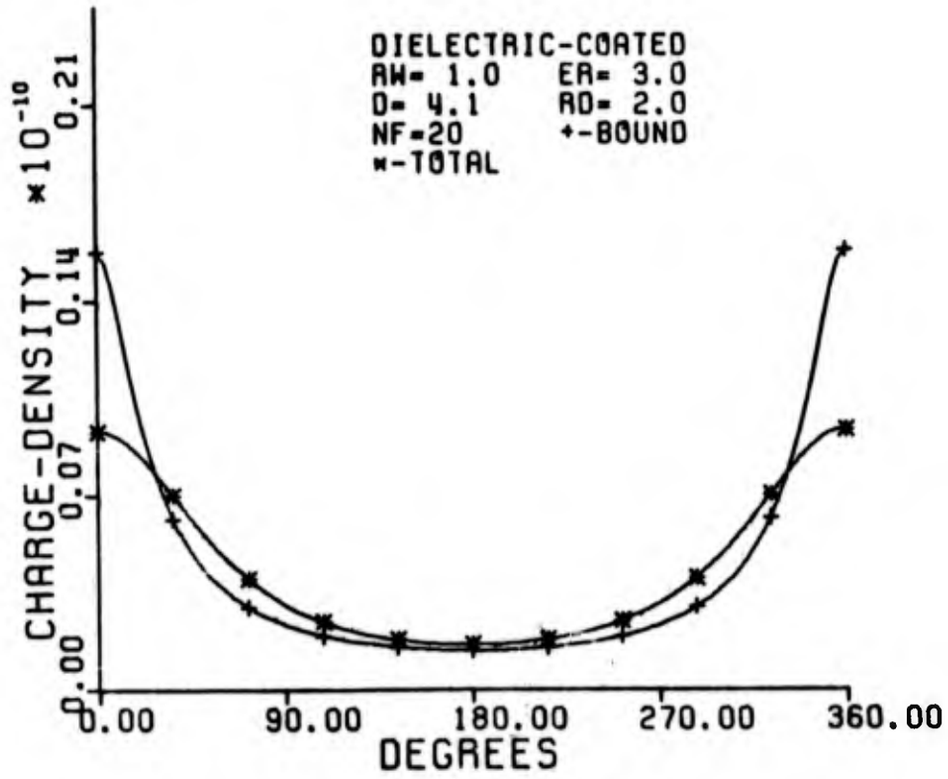
DIELECTRIC-COATED
AW= 1.0
D= 4.1
NF=20
*-TOTAL
ER= 3.0
RO= 2.0
+-BOUND
CHARGE-DENSITY *10^-10
0.21
0.14
0.07
0.00
0.00
90.00
180.00
270.00
360.00
DEGREES

TWO DIELECTRIC-COATED WIRES
D=4.2. Rw=1.0. ER=3.0. RD=2.0.

| NF | Capac.* | Capac Without Dielectric |
|---|---|---|
| 1 | 0.2557871588972137 | 0.1899134080764515 |
| 2 | 0.2954031675125870 | 0.1992873566770083 |
| 3 | 0.3192843847738925 | 0.2016871791799262 |
| 4 | 0.3345521956226898 | 0.2021974603456526 |
| 5 | 0.3447751549652867 | 0.2023054546120705 |
| 6 | 0.3517506926792652 | 0.2023286889879440 |
| 7 | 0.3565470897415853 | 0.2023337749808398 |
| 8 | 0.3598550040632434 | 0.2023349053607118 |
| 9 | 0.3621388193464109 | 0.2023351598716085 |
| 10 | 0.3637162231777009 | 0.2023352178109649 |
| 11 | 0.3648060323998851 | 0.2023352311251508 |
| 12 | 0.3655592762927137 | 0.2023352342093318 |
| 13 | 0.3660802110488975 | 0.2023352349287207 |
| 14 | 0.3664407727055842 | 0.2023352350975258 |
| 15 | 0.3666905755216971 | 0.2023352351373434 |
| 16 | 0.3668638333063562 | 0.2023352351467787 |
| 17 | 0.3669841442734397 | 0.2023352351490236 |
| 18 | 0.3670677930755379 | 0.2023352351495596 |
| 19 | 0.3671260261458896 | 0.2023352351496880 |
| 20 | 0.3671666180597795 | 0.2023352351497189 |

*Capacitance values are multiplied by $10^{-10}$.

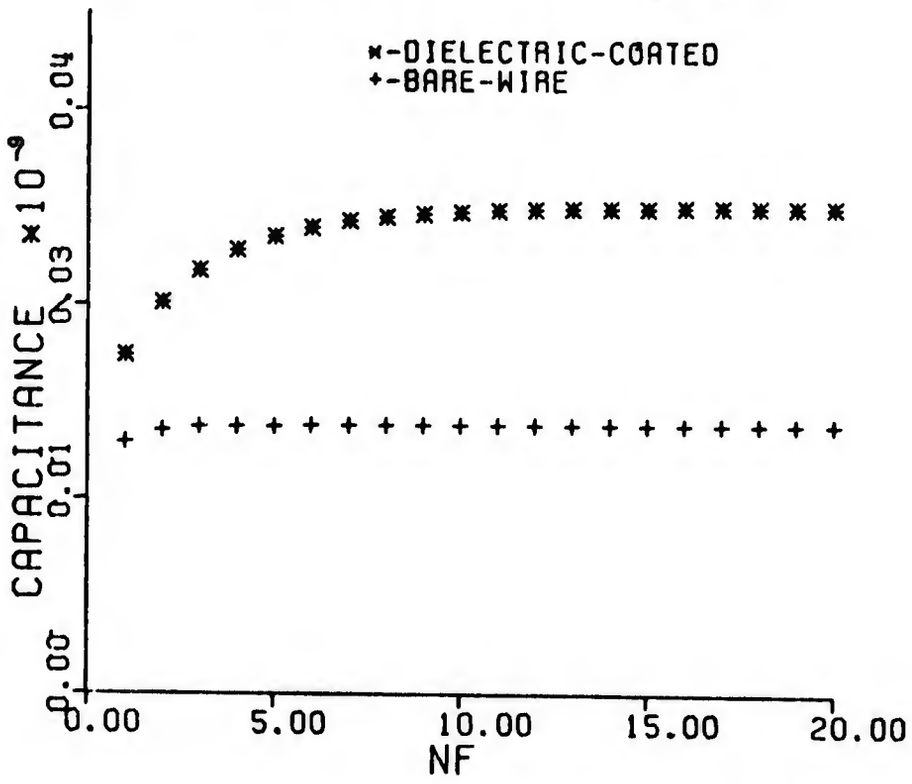

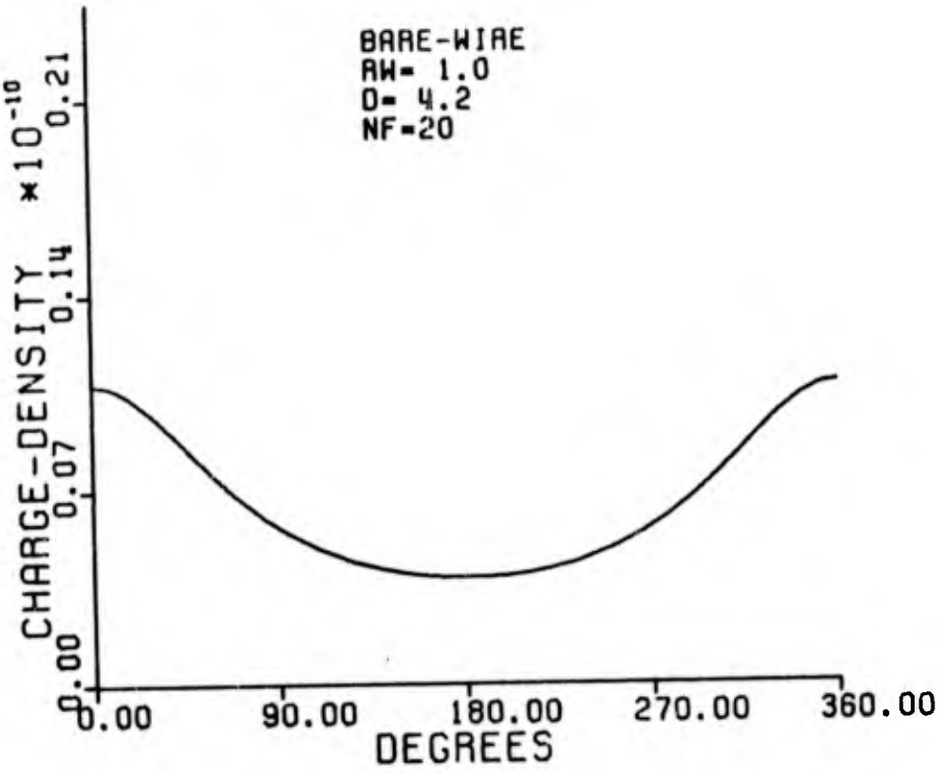
BARE-WIRE
RW= 1.0
O= 4.2
NF=20
CHARGE-DENSITY *10^-10
0.21
0.14
0.07
0.00
0.00
90.00
180.00
270.00
360.00
DEGREES

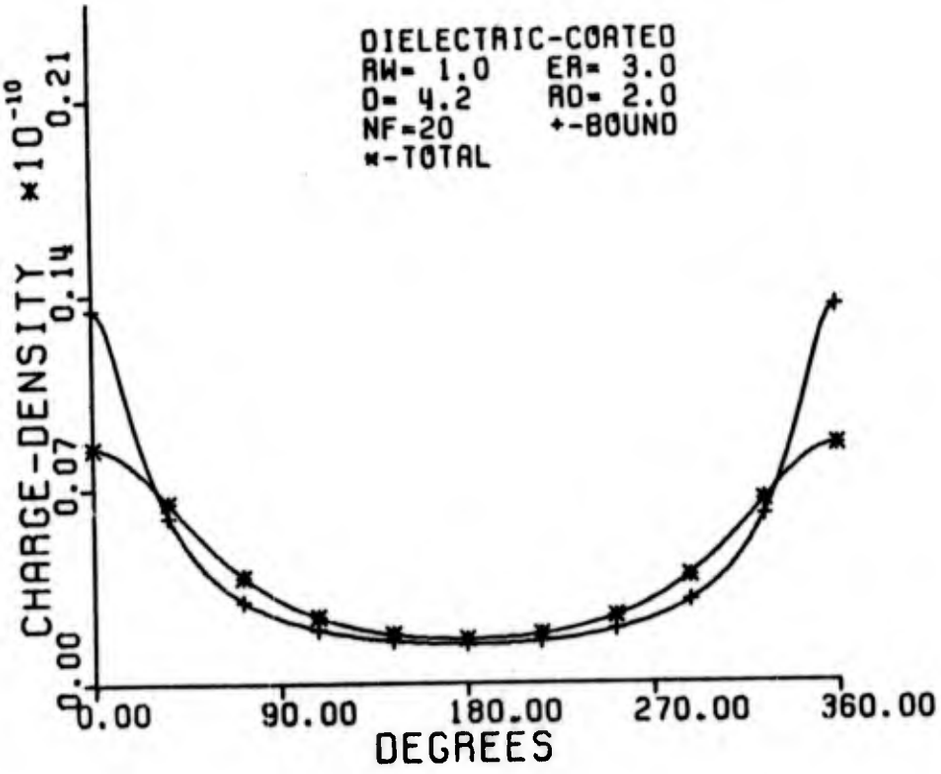
DIELECTRIC-COATED
RW= 1.0 ER= 3.0
O= 4.2 RO= 2.0
NF=20 +-BOUND
*-TOTAL
CHARGE-DENSITY *10^-10
0.21
0.14
0.07
0.00
0.00
90.00
180.00
270.00
360.00
DEGREES

TWO DIELECTRIC-COATED WIRES
D=5.0. Rw=1.0. ER=3.0. RD=2.0.

| NF | Capac.* | Capac. Without Dielectric |
|---|---|---|
| 1 | 0.2257093741973848 | 0.1705153757945194 |
| 2 | 0.2494256881887268 | 0.1758055244407856 |
| 3 | 0.2614712295113060 | 0.1770245327472820 |
| 4 | 0.2675604417395873 | 0.1772431255450668 |
| 5 | 0.2700608535507242 | 0.1772816035066989 |
| 6 | 0.2722173639390625 | 0.1772884483574665 |
| 7 | 0.2729859037772993 | 0.1772896842792562 |
| 8 | 0.2733606744470815 | 0.1772899106629535 |
| 9 | 0.2735420620000049 | 0.1772899526590334 |
| 10 | 0.2736295188553207 | 0.1772899605352879 |
| 11 | 0.2736716293216173 | 0.1772899620263389 |
| 12 | 0.2736919084473859 | 0.1772899623108797 |
| 13 | 0.2737016841820507 | 0.1772899623655550 |
| 14 | 0.2737064036607244 | 0.1772899623761239 |
| 15 | 0.2737086859912218 | 0.1772899623781777 |
| 16 | 0.2737097916793498 | 0.1772899623785786 |
| 17 | 0.2737103282746830 | 0.1772899623786571 |
| 18 | 0.2737105891236849 | 0.1772899623786726 |
| 19 | 0.2737107161270438 | 0.1772899623786757 |
| 20 | 0.2737107780533231 | 0.1772899623786762 |

* Capacitance values are multiplied by $10^{-10}$.

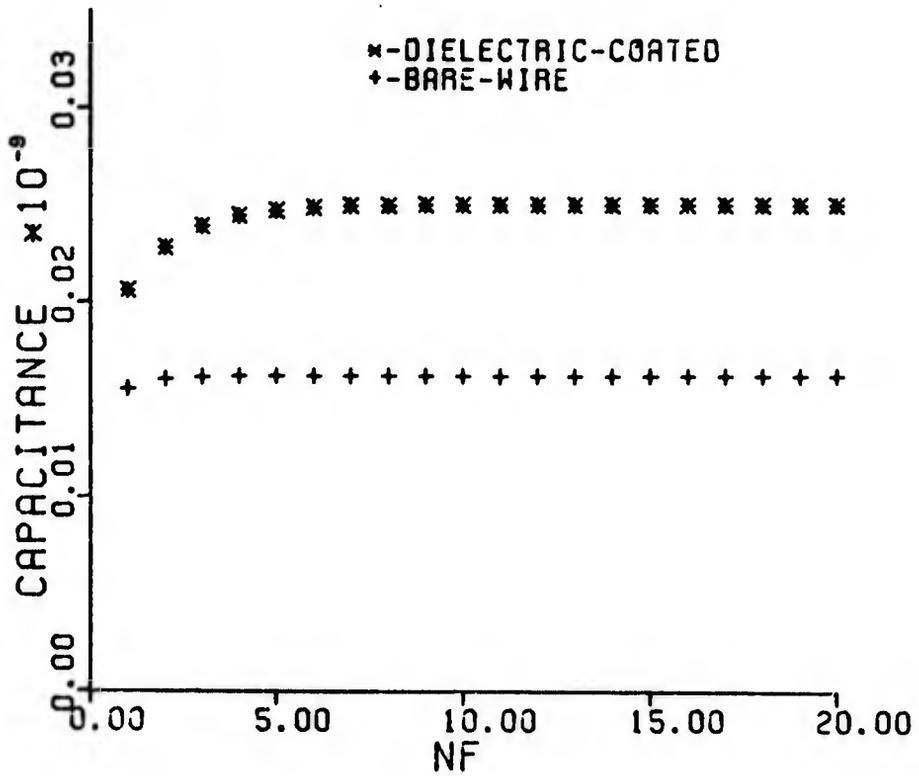

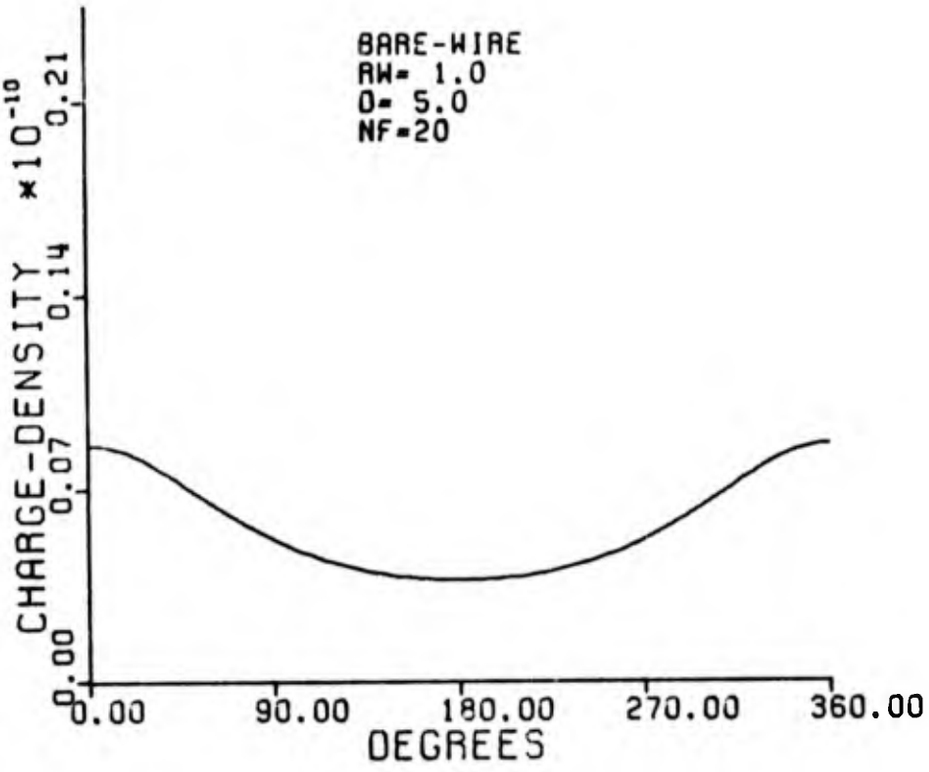
BARE-WIRE
RW= 1.0
D= 5.0
NF=20
CHARGE-DENSITY *10^-10
0.21
0.14
0.07
0.00
0.00
90.00
180.00
270.00
360.00
DEGREES

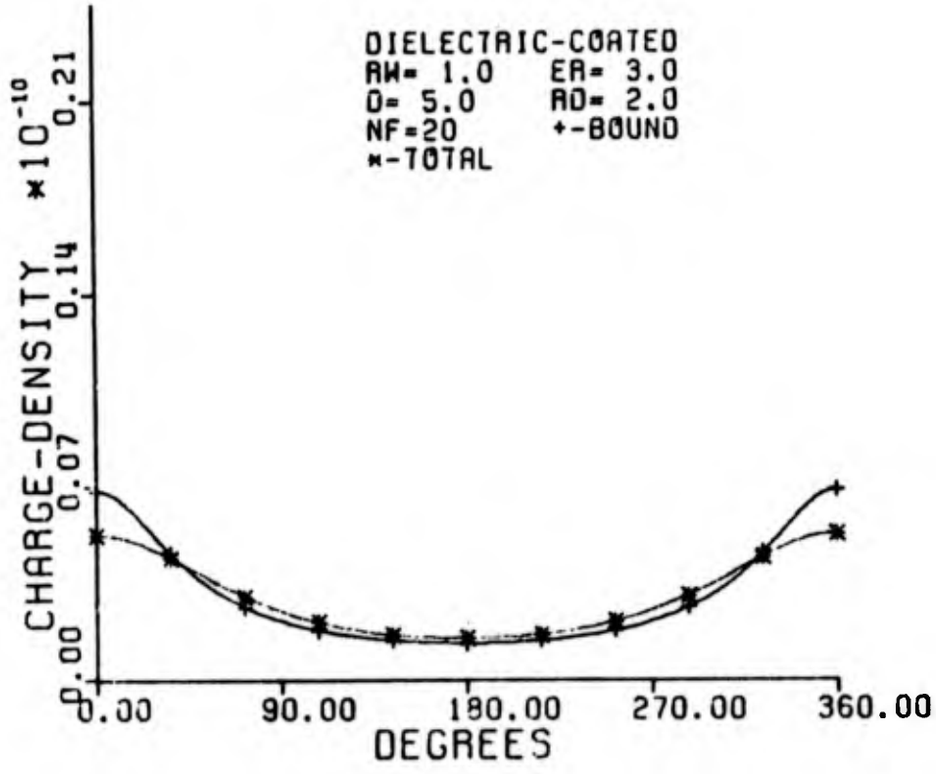
DIELECTRIC-COATED
RW= 1.0
D= 5.0
NF=20
ER= 3.0
RD= 2.0
+-BOUND
*-TOTAL
CHARGE-DENSITY *10^-10
0.21
0.14
0.07
0.00
0.00
90.00
180.00
270.00
360.00
DEGREES

TWO DIELECTRIC-COATED WIRES
D=10.0. Rw=1.0. ER=3.0. RD=2.0.

| NF | Capac.* | Capac. Without Dielectric |
|---|---|---|
| 1 | 0.1490835886151976 | 0.1203772585197398 |
| 2 | 0.1520330278488584 | 0.1210299396876566 |
| 3 | 0.1529676017807938 | 0.1211585873313780 |
| 4 | 0.1531868413628555 | 0.1211705396429918 |
| 5 | 0.1532356907958095 | 0.1211715737759614 |
| 6 | 0.1532462747689041 | 0.1211716631672821 |
| 7 | 0.1532485295649667 | 0.1211716709894101 |
| 8 | 0.1532490049178664 | 0.1211716716833484 |
| 9 | 0.1532491044639186 | 0.1211716717456885 |
| 10 | 0.1532491252195867 | 0.1211716717513502 |
| 11 | 0.1532491295346320 | 0.1211716717518692 |
| 12 | 0.1532491304299485 | 0.1211716717519171 |
| 13 | 0.1532491306154635 | 0.1211716717519216 |
| 14 | 0.1532491306538672 | 0.1211716717519220 |
| 15 | 0.1532491306618121 | 0.1211716717519220 |
| 16 | 0.1532491306634549 | 0.1211716717519220 |
| 17 | 0.1532491306637945 | 0.1211716717519220 |
| 18 | 0.1532491306638647 | 0.1211716717519220 |
| 19 | 0.1532491306638792 | 0.1211716717519220 |
| 20 | 0.1532491306638821 | 0.1211716717519220 |

*Capacitance values are multiplied by $10^{-10}$.

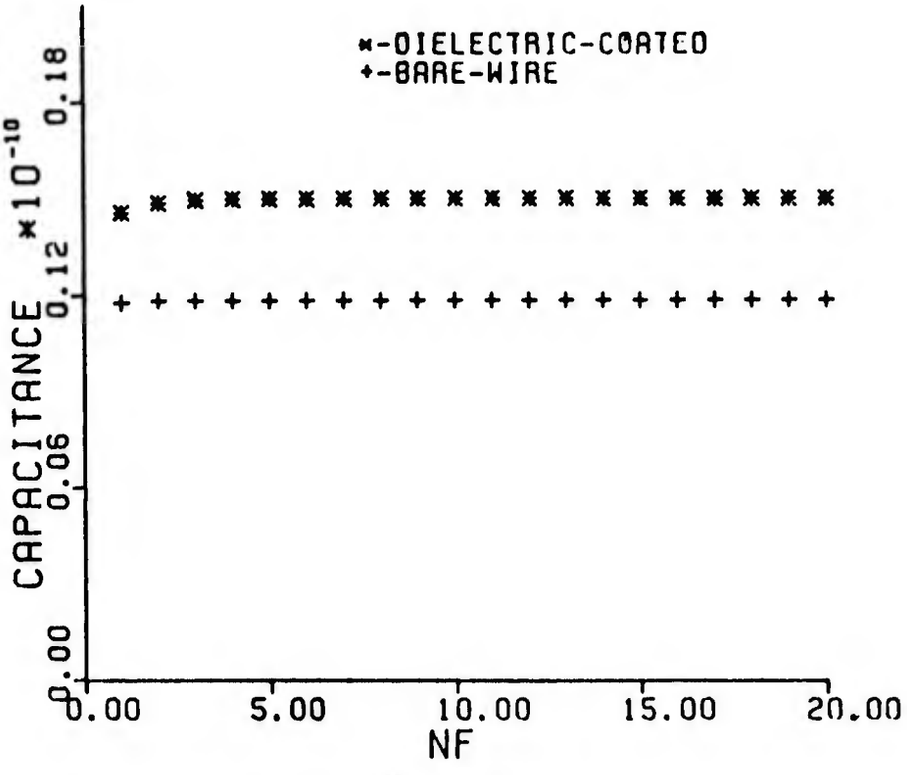

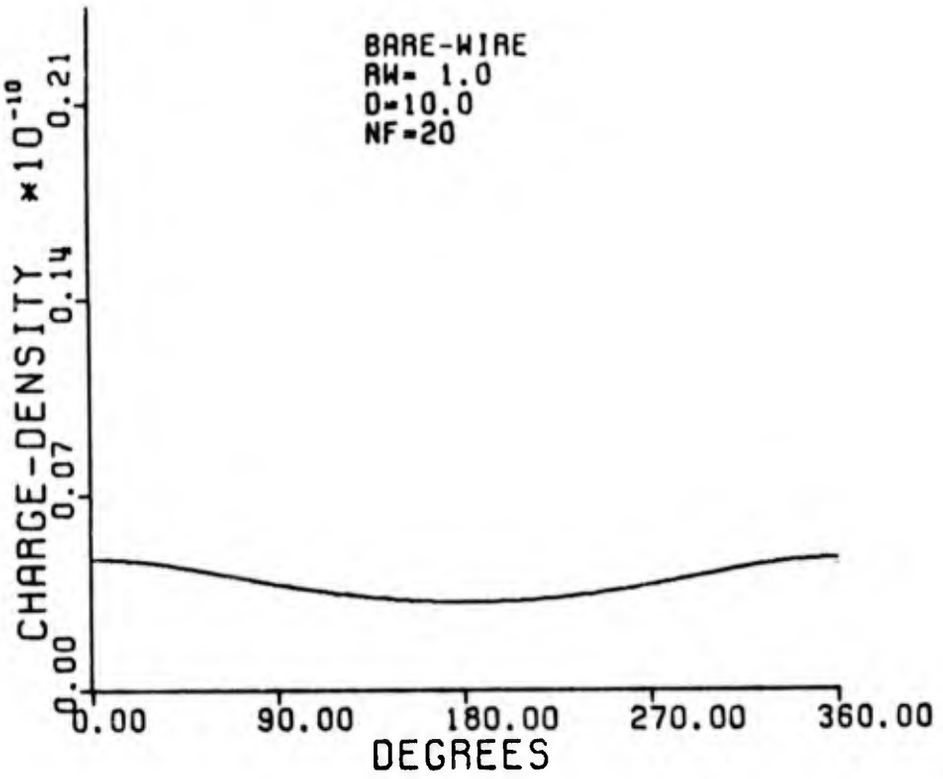
BARE-WIRE
RW= 1.0
D=10.0
NF=20
CHARGE-DENSITY *10^-10
0.21
0.14
0.07
0.00
0.00
90.00
180.00
270.00
360.00
DEGREES

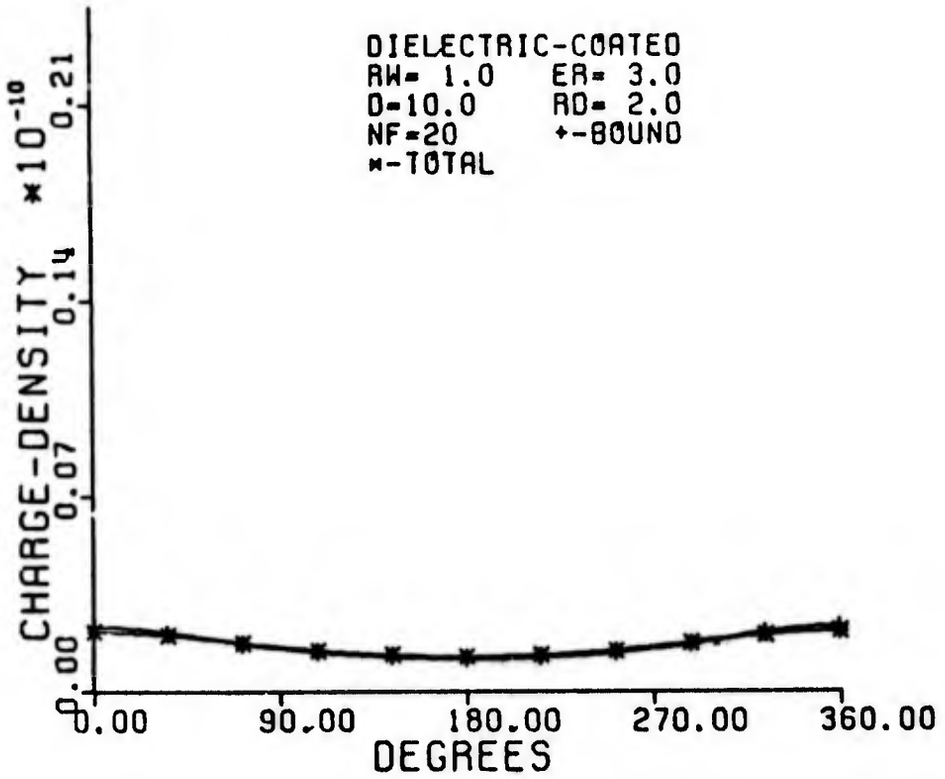
DIELECTRIC-COATED
RW= 1.0 ER= 3.0
D=10.0 RD= 2.0
NF=20 +-BOUND
*-TOTAL
CHARGE-DENSITY *10^-10
0.21
0.14
0.07
0.00
0.00
90.00
180.00
270.00
360.00
DEGREES

# *MISSION*
# *of*
# *Rome Air Development Center*

*RADC is the principal AFSC organization charged with planning and executing the USAF exploratory and advanced development programs for electromagnetic intelligence techniques, reliability and compatibility techniques for electronic systems, electromagnetic transmission and reception, ground based surveillance, ground communications, information displays and information processing. This Center provides technical or management assistance in support of studies, analyses, development planning activities, acquisition, test, evaluation, modification, and operation of aerospace systems and related equipment.*